UNIVERSITY OF SOUTHAMPTON
FACULTY OF ENGINEERING AND THE ENVIRONMENT

Modelling of food waste digestion using ADM1 integrated with Aspen Plus

by

Hoa Huu Nguyen

Supervisors: **Prof Charles Banks and Dr Sonia Heaven**

Thesis for the degree of Doctor of Philosophy

June 2014

This thesis is dedicated to my beloved Dad!

UNIVERSITY OF SOUTHAMPTON

ABSTRACT

Doctor of Philosophy

MODELLING OF FOOD WASTE DIGESTION USING ADM1 INTEGRATED WITH ASPEN PLUS

by Hoa Huu Nguyen

The aim of this research was to produce an integrated modelling platform in which an anaerobic digester could be linked to the other unit operations which serve it, both in maintaining the physical–chemical conditions in the digester and in transforming the digestion products to useful fuel and nutrient sources. Within these system boundaries an accurate mass and energy balance could be determined and further optimised, particularly where the desired energy products are a mix of heat, power, and biomethane. The anaerobic digestion of food waste was choosen as the subject of the research because of its growing popularity and the availability of validation data.

Like many other organic substrates, food waste is potentially a good source of renewable energy in the form of biogas through anaerobic digestion. A number of experimental studies have, however, reported difficulties in the digestion of this material which may limit the applicability of the process. These arise from the complexity of the biochemical processes and the interaction between the microbial groups that make up the anaerobic community. When using food waste there is a tendency to accumulate intermediate volatile fatty acid products, and in particular propionic acid, which eventually causes the pH to drop and the digester to fail. Two factors are important in understanding and explaining the changes in the biochemical process that leads to this condition. The first is due to the differential in sensitivity to free ammonia of the two biochemical pathways that lead to methane formation. The acetoclastic methanogenic route is inhibited at a lower concentration than the hydrogenotrophic route, and methane formation therefore occurs almost exclusively via acetate oxidation to CO_2 and H_2 at high free ammonia concentrations. The accumulation of propionic acid is thought to be because formate, a product of its degradation, cannot be converted to CO_2 and H_2 as the necessary trace elements to build a formate dehydrogenase enzyme complex are missing.

The Anaerobic Digestion Model No. 1 (ADM1) was modified to reflect ammonia inhibition of acertoclastic methanogenesis and an acetate oxidation pathway was added. A further modification was included which allowed a

'*metabolic switch*' to operate in the model based on the availability of key trace elements. This operated through the H_2 feedback inhibition route rather than creating a new set of equations to consider formate oxidation in its own right: the end result is, however, identical in modelling terms. With these two modifications ADM1 could simulate experimental observations from food waste digesters where the total ammoniacal nitrogen(TAN) concentration exceeded 4 gN l^{-1}. Under these conditions acetate accumulation is first seen, followed by proprionate accumulation, but with the subsequent decrease in acetate until a critical pH is reached. The ADM1 model was implemented in MATLAB with these modifications incorporated.

The second part of the research developed an energy model which linked ADM1 to the mechanical processes for biogas upgrading, Combined Heat and Power (CHP) production, and the digester mixing system. The energy model components were developed in the framework of the Aspen Plus modelling platform, with sub–units for processes not available in the standard Aspen Package being developed in Fortran, MS Excel or using the Aspen Simulation Workbook (ASW). This integration of the process components allows accurate sizing of the CHP and direct heating units required for an anaerobic digestion plant designed for fuel–grade methane production.

Based on the established model and its sub–modules, a number of case studies were developed. To this end the modified ADM1 was applied to mesophilic digestion of Sugar Beet Pulp to observe how the modified ADM1 responded to different substrate types. Secondly, to assess the capability of adding further mechanical processes the model was used to integrate and optimise single stage biogas upgrading. Finally, the digestion of food waste in the municipal solid waste stream of urban areas in Vietnam was considered.

Keywords: Anaerobic digestion, modelling, food waste, ADM1, Aspen Plus, biogas, water scrubbing, acetate oxidation, trace elements, ammonia removal.

.

Contents

List of Tables

List of Figures

Acknowledgements

Firstly, I would like to send my thanks for financial support from Vietnamese Government, the University of Southampton and VALORGAS project.

I owe my deepest gratitude to my supervisors Professor Charles Banks and Dr. Sonia Heaven for their endless supply of guidance and support throughout my thesis. Further to this, I will never forget Sonia's kind words of encouragement that got me through the tough time. I would never forget those intensive weeks working with them in their office from dawn till dusk to solve out the problems. Especially, during the very last weeks before submission, they have dedicated their precious time to reading and giving valuable feedback without which, this study would hardly have been completed.

My genuine thanks are also due to Dr. Ludwig Gredmainer, who was my co-supervisor during the first year of my PhD with his technical support.

Many thanks go to Dr. Yue Zhang. I have benefited so much from her ingenious ideas towards my model.

Also many thanks go to Mr. Stephen Robertson, Dr Alba Serna–Maza, Dr. Sri Suhartini for their contribution to my work.

I am also indebted to my friends in Southampton who have enthusiastically assisted me with this PhD. I would like to thank Dr Nguyen Thanh An for his useful explanation on mathematical aspects of my model. My appreciation also goes to Dr. Nguyen Tri Dung for his willingness in exchanging ideas and discussing related issues. I must also add further thanks to Dr William Nock for his continuous assistance in proofreading my writing although he has been extremely busy with his own in China.

I would never forget my Vietnamese friends who shared their thoughts at lunch time with me for years, and those who enjoyed playing sports with me in our free time. These made my student life colourful and enjoyable.

My family have been both an inspiration and constant source of support throughout the thesis. I owe a great debt of gratitude to my parents, my brothers and sisters, my parents in law whose encouragement, especially during difficult times, have strengthened my will and determination.

I would like to express appreciation to my beloved wife who spent sleepless nights to take care of my son and helped me to achieve this work. I owe so much to her for encouragement and for her endless love. Last, but by no means least, I also would like to dedicate this work to my little son Nguyen Bui Nam Anh who has always been my strong motivation.

Declaration of Authorship

I, Hoa Huu Nguyen, declare that the thesis entitled:

MODELLING OF FOOD WASTE DIGESTION USING ADM1 INTEGRATED WITH ASPEN PLUS

and the work presented in the thesis is both my own, and has been generated by me as the result of my own original research. I confirm that:

- this work was done wholly or mainly while in candidature for a research degree at this University;
- where any part of this thesis has previously been submitted for a degree or any other qualification at this University or any other institution, this has been clearly stated;
- where I have consulted the published work of others, this is always clearly attributed;
- where I have quoted from the work of others, the source is always given.
- With the exception of such quotations, this thesis is entirely my own work;
- I have acknowledged all main sources of help;
- where the thesis is based on work done by myself jointly with others, I have made clearly what was done by others and what I have contributed myself;
- parts of this work have been published:
  a. (**Journal**) Hoa H. Nguyen, Sonia Heaven, Charles Banks (2014). Energy potential from the anaerobic digestion of food waste in municipal solid waste stream of urban areas in Vietnam. *Int J Energy Environ Eng (2014) 5:365–374.* (DOI: 10.1007/s40095-014-0133-1).
  b. (**International Conference poster**) Hoa H. Nguyen, Rimika Kapoor, Sonia Heaven, Charles Banks and Virendra K. Vijay (2014). Simulation and optimisation of single stage biogas upgrading and bottling system using Aspen Plant. *International Conference on Anaerobic Digestion - Biogas Science 2014.* Vienna, Austria.
  c. (**Presentation**) Modelling of food waste digestion using ADM1 integrated with Aspen Plus (2014). *3rd Annual Early Career Biomass Network Symposium.* Southampton.
  d. (**Conference poster**) Energy model of anaerobic digestion plant (2014). *Theme conferences.* University of Southampton.

Signed: .....

Date: .....

Abbreviations and Nomenclature

AC	Acetoclastic
AD	Anaerobic Digestion
ADM1	Anaerobic Digestion Model No. 1
AO	Acetate Oxidation
ASW	Aspen Simulation Workbook
CHP	Combined Heat and Power
COD	Chemical Oxigen Demand
CODp	Chemical Oxigen Demand particulate
CODs	Chemical Oxigen Demand soluble
CSTR	Continuously Stirred Tank Ractor
DE	Differential Equations
EU	European Union
FS	Fixed Solids
HRT	Hydraulic Retention Time
LCFA	Long-chain Fatty Acids
Norg	Total Organic Nitrogen
ODE	Ordinary Differential Equations
OLR	Organic Loading Rates
PSA	Pressure Swing Adsorption
SAO	Syntrophic Acetate Oxidation
SBP	Sugar Beet Pulp
SRT	Solids Retention Time
STP	Standard Temperature and Pressure
TA	Total Alkalinity
TAN	Total Ammonia Nitrogen
TC	Total Carbon
TE	Trace Element
TIC	Total Inorganic Carbon
TKN	Total Kjedhal Nitrogen
TN	Total Nitrogen
TOC	Total Organic Carbon
TP	Total Phosphorus
TS	Total Solids
VFA	Volatile Fatty Acid
VS	Volatile Solids
WW	Wet Weight

Chapter 1

Introduction

This chapter briefly introduces the development of anaerobic digestion technology, its benefits and recent research trends. It then highlights the need for establishing a new model for food waste digestion plants, and concludes with the aims and objectives of the work.

1.1 Background

Anaerobic digestion (AD) is a series of natural processes in which microorganisms break down biodegradable material (organic matter) in the absence of oxygen, producing biogas and a stabilised digestate. This process is widely applied as an effective option for renewable energy because under controlled conditions the biogas produced (consisting mainly of methane and carbon dioxide) can be used for energy production, helping to replace fossil fuels. The nitrogen content and minerals in the digestate make it potentially useful for agricultural application as a soil conditioner or bio–fertiliser with associated economic, energy and carbon gains from offsetting the requirement for artificial fertilisers.

According to He (2010), there is historical evidence that the anaerobic digestion process was used in China and India about 2000–3000 years ago. The history of scientific interest in anaerobic digestion perhaps dates back to 1776 when Volta made an estimate of the amount of flammable gas produced by decaying organic materials (Fujishima *et al.*, 2000). This was later assessed and corrected by Dalton, Henry and Davy during 1801 to 1810 (Gunnerson & Stuckey, 1986; Appels *et al.*, 2011). The past few decades have seen increasing interest in both research and real–life applications of AD. From the 1990s to the present, research on anaerobic digestion has developed rapidly, with one driving force being the desire of many governments to address both rising energy demands and the need for renewable energy sources. Moreover, from the ecological and economic points of view AD is a better option for management of biodegradable wastes when compared to conventional methods *e.g.* landfilling and composting (Edelmann *et al.*, 2000). The European Commission (2010) stated that proper handling of biowastes, such as the use of AD technology, is often the best and most cost–effective means of addressing a range of other problems from nutrient management to greenhouse gas emissions.

Food waste is a typical form of organic matter with a high potential for energy production through anaerobic degradation. Studies have shown that the methane yield from anaerobic digestion is in the range of 350 to 435 mL g^{-1} VS_{added} depending upon operational conditions, reactor types, and composition of the input food waste (Cho *et al.*, 1995; Zhang *et al.*, 2007; Demirel *et al.*, 2010; Banks, Chesshire, *et al.*, 2011). Finnveden *et al.* (2005) analysed data obtained from LCA scenarios and concluded that with food waste substrate, in general, anaerobic digestion is preferable to composting and landfilling regarding energy use and emissions of greenhouse gases. Because of the benefits

in terms of energy saving, waste management and environmental aspects, biogas production from food waste together with other renewable organic sources *i.e.* agricultural waste has been suggested as a means of meeting one–third of renewable energy demand in transport by 2020 in the EU (COM, 2010).

The benefits of anaerobic digestion can be categorised under four major aspects: energy, environmental, waste treatment, and economic, as summarised in Table 1.1.

Table 1.1 Benefits of AD (gathered from Stuckey (1986) Fulford (1988), Maier *et al.* (2000), Spellman (2007), Deublein and Steinhauser (2008a), Wall *et al.* (2008), Sivanagaraju (2010) and Conly (2011)

Energy benefits	Produces a renewable fuel that is flexible and can be used to generate heat and power.
	Biogas can be used on site, or upgraded to biomethane for use as a vehicle fuel, or transported to where energy is demanded *e.g.* by injection into the gas grid.
	Removing the wet fraction from waste improve the calorific value of the residual waste stream.
Environmental benefits	Reduction of greenhouse gas emissions by capture and use of methane that might otherwise leak into the atmosphere and increase the greenhouse effect.
	Can reduce emissions of nitrous oxide (a strong greenhouse gas) compared to composting or landfill.
	Can contribute to improved nutrient management creating a closed cycle of nutrients (N, P, K).
	Plant fertiliser quality is improved compared to raw agricultural waste
	Good pathogen removal depending on temperature.
Waste treatment benefits	Allows wastes to be treated locally and at small scale, adhering to the proximity principle.
	Potential for co-digestion with other organic waste streams (industrial wastes *e*.g. food processing waste and agricultural wastes e.g. manure)
Economic benefits	No supply costs in the case of waste products utilisation
	Substantial reduction of the disposal costs of organic wastes, even including meaningful re–use (*e.g.* as fertilisers), because the quantity of biomass decreases so significantly
	Digested residues and fibre can potentially be used or sold.

Although AD can potentially offer many benefits as shown, its application to certain types of organic waste has been difficult to implement because it is a complex system of biochemical and physical processes. Therefore this requires a detailed understanding for design, control, operation and maintenance to ensure high efficiency. For instance, the system can become unstable or even fail due to feed overload, accumulation of intermediate products, unsteady pH, lack of nutrients or key trace elements, *etc.* (Graef & Andrews, 1974; Costello *et al.*, 1991; Gavala *et al.*, 2003; Banks *et al.*, 2012). Food waste, like many other waste types, presents its own problems for anaerobic digestion. For example, the high protein content in food waste leads to high ammonia concentrations, which can be inhibitory to microorganisms involved in the process, especially the acetoclastic methanogens. Further, propionic acid can accumulate in the digester due to inadequate removal of formic acid or hydrogen as an intermediate. With certain types of feedstock foaming problems can occur, which in severe cases may even cause digester failure (Murto *et al.*, 2004; Banks & Zhang, 2010; Moeller *et al.*, 2012; Suhartini, 2014). These factors can limit the applicability of anaerobic digestion of organic wastes in general, and food waste in particular.

To address these issues, large numbers of studies have been undertaken on the anaerobic digestion of solid wastes. These have mainly adopted two approaches: experimental trials, and modelling to optimise factors that contribute to the efficiency of the process.

On the laboratory–based side, digester performance, process enhancement, inhibition factors, co–digestion, digestate dewatering and one or two–phase systems are among the most popular themes (Mata-Alvarez *et al.*, 2000). To date, a wide range of studies has focused on different aspects of the anaerobic digestion process with the aim of further optimisation, including: (*i*) assessment of the microbial community composition and its evolution during digestion, (*ii*) minimisation of capital cost and energy ultilisation, (*iii*) further improvement and optimisation of pre–treatment methods to improve the degradability of the feedstock and (*iv*) upgrading and refining of the obtained biogas (Appels *et al.*, 2011). In order to achieve these goals, experiments have traditionally been carried out based on experience or trial–and–error methods (Amon *et al.*, 2006; Sreela-or *et al.*, 2011; Banks *et al.*, 2012; Maria *et al.*, 2012; Zhang & Jahng, 2012; Lim & Wang, 2013; Zahedi *et al.*, 2013). However, experimental systems and pilot models are usually expensive to establish and very time-consuming and labour intensive to operate until the point where stable conditions are achieved (Vavilin *et al.*, 1994). Furthermore, efforts to improve and optimise the performance of digesters have often been obliged to treat the AD system as

a complex black box in which some of the the interactions between different factors and processes are not yet fully understood.

In these circumstances, as knowledge and understanding of the system develops, modelling approaches have something to offer in supporting laboratory–based studies and overcoming some of the associated problems. Although it can never replace experimental work, modelling is an efficient aid in research as it helps the researcher to ask relevant questions by structuring present knowledge, and allows logical selection of the most promising experimental strategy through consideration of the results from multiple scenarios. Modelling can also help to optimise the overall performance of anaerobic systems with respect to mass and energy balances, or for design and control purposes. Especially in environmental systems, which are normally complex, flowsheet simulation models are enormously useful because it becomes feasible to work with a substitute rather than with the real process plants. Generally, the three most popular objectives of using a model could be highlighted as: understanding the system's behaviour and the interaction of its components; quantitatively expressing or verifying hypotheses; and predicting the behaviour of the system in the future or under similar conditions (Donoso-Bravo *et al.*, 2011). Once a model of anaerobic digestion is developed and validated, it can bring the following benefits:

- It can be used to look at effect on operational performance of changes in conditions (substrate, temperature, loading, *etc.*);
- It can help in testing the limits of operation, providing real–time management or identifying the most promising set–up;
- researchers can use the model for "*what–if*" scenarios, *e.g.* what will happen to the energy routes if waste input or environmental conditions are changed?
- generated data and forensic simulations after failure can be post–processed (*i.e.* statistical analysis or visualisation) for better understanding and dissemination of information.

Reviews of anaerobic digestion modelling at both digester unit process and biogas plant level show that, although a number of models have been developed for one or more components of biogas systems, until now there is no appropriate model dedicated to food waste digestion, especially at a system level. Therefore, a new model needs to be proposed that can offer sub–units in so–called plant–wide models rather than focusing on parts of the digestion process only.

The model developed should also take advantage of existing models, data from previous experimental investigations and from real anaerobic digestion plants, and advanced software packages, in order to provide enhanced productivity, reliability, decision-making and profitability of the plant life cycle. Based on this point of view, two powerful tools were employed in this study: the Anaerobic Digestion Model No. 1 (ADM1) (Batstone *et al.*, 2002) and the Aspen Plus simulation V7.3 (AspenTech, 2011). ADM1 is widely used and considered as the most complete model, with high accuracy in terms of data, reactions and kinetics calculations. It can therefore be regarded as a trustworthy platform for a food waste digestion model. Aspen Plus provides flexible methods for exchanging data to other software such as Microsoft Excel, Matlab, *etc.* For example, spreadsheets can be linked to Aspen process flowsheets directly or via an Aspen Simulation Workbook (ASW). Moreover, Aspen Plus performs rigorous material and energy balance calculations, using detailed equipment models, to determine the flow rates, composition and energy flow for all streams involved in the process. Therefore, Aspen Plus was chosen for this study. This approach brings advantages since, on the one hand, a tool–independent modelling representation can be developed to facilitate information exchange between the heterogeneous tools (Li & Lam, 2004); and on the other, it follows the current modelling trend which encourages users to incorporate external models into an overall flowsheet (Tolsma & Barton, 2001).

1.2 Aim and structure of the thesis

1.2.1 Aim of the research

The aim of this research was to produce an integrated modelling platform in which anaerobic digestion can be combined with other unit operations to provide accurate mass and energy balances prediction.

1.2.2 Structure of the thesis

The thesis consists of 8 chapters:

The current chapter firstly provides a basic background to anaerobic digestion technology, its benefits in food waste applications and recent research trends. Secondly, it highlights the need for establishing a new model for food waste digestion AD plants. Finally it presents the aims and objectives of the work.

Chapter 2 gives a critical review and assessment of problems relating to the research aims, including food waste digestion, biogas plant configurations, existing anaerobic digestion models, and flowsheeting simulation software. The chapter ends with a short conclusions section identifying gaps in our current knowledge and objectives of the work.

Chapter 3 addresses tools and systematic procedures for modelling components of the whole system such as the anaerobic digester, biogas upgrading unit, Combined Heat and Power (CHP) unit *etc.*, with emphasis on methods used to implement a modified ADM1 model.

Chapter 4 describes the construction and modifications of ADM1 with an acetate oxidation pathway and trace elements switches.

Once the modified ADM1 model was developed, it was then integrated with an energy model established in Aspen Plus to enable this model to estimate accurate mass and energy balances for biogas system. Details and formulation of the energy model as well as an indication of how to include the modified ADM1 as a part of the energy are covered in Chapter 5.

Chapter 6 presents the ammonia stripping model developed by the combination of the modified ADM1 model, Aspen Simulation Workbook (ASW) and Aspen Plus.

Chapter 7 presents case studies that uses the developed tools to simulate the mesophilic digestion of Sugar Beet Pulp, to size CHP and direct heating units in an anaerobic digestion plant for fuel–grade methane production, and to estimate the energy potential from anaerobic digestion of food waste in MSW stream in urban areas in Vietnam.

Chapter 8 consists of brief conclusions and suggestions for future work.

This page is intentionally left blank

Chapter 2

Literature review

This chapter starts by giving an overview of food waste in the UK and the energy potential from food waste through several well–known technologies. There is then a brief background to the anaerobic digestion process, followed by some key points for food waste digestion including emphasis on acetate oxidation, trace elements and ammonia issues. The configurations of popular digesters and biogas systems are also presented. A review of biogas upgrading methods is carried out to find an appropriate method for modelling in the current work. Modelling of anaerobic digestion at both process and plant level is reviewed to support the choice of an appropriate modelling platform. The chosen model is then described and its shortcomings considered in order to clarify the problems that need to be addressed in this study. The chapter concludes with an evaluation of software packages for flowsheet simulation to bring together these components.

2.1 Food waste

According to the legal definition by the EU Commission, food waste is any food substance, raw or cooked, which is discarded, or intended or required to be discarded (Lal & Stewart, 2012). Food waste mainly consists of organic residues including fruits, vegetables, meat, poultry, seafood, shellfish, bones, rice, beans, pasta, bakery items, cheese, eggshells, and coffee grounds.

In the UK, there is increasing interest in anaerobic digestion of both domestic and commercial and industrial food. The amount of food waste produced by a household and its occupants is affected by several factors such as the household size, the age of the individual occupants and affluence (Ventour, 2008). Some other sources of food waste are the food industry, supermarkets, and educational and other institutions.

According to Ventour (2008), it is estimated that about 5.6 million tonnes of domestic food waste is produced each year in England, 0.3 million tonnes in Wales, and in Scotland and Northern Ireland 0.6 and 0.2 million tonnes, respectively. In other words, every year there is about 6.7 million tonnes of food waste generated in the UK.

Food waste like any other organic matter contains the potential to produce energy *e.g.* heat and electricity. Assuming that approximately 255 kWh of exportable electricity could be achieved from each tonne of food waste generated (Stuart, 2009), this corresponds to about 1,708 GWh of electricity each year or enough to meet the needs of about 340,000 households in the UK (DEFRA, 2010). Because of the benefits in terms of energy saving, environmental aspects and waste management, AD from food waste has been identified as an optimum solution for waste management strategy in England (DEFRA, 2011).

2.2 Overview of Anaerobic Digestion process

2.2.1 Microbial aspects of the anaerobic digestion process

Anaerobic digestion occurs in environments depleted of oxygen, and involves the breakdown of organic matter into biogas and other trace gases, as well as a residual effluent or digestate. There are four main steps in the anaerobic digestion process: hydrolysis, acidogenesis, acetogenesis and methanogenesis. In the first process, hydrolysis, complex materials are converted into less complex and soluble compounds. In the acidogenesis phase, volatile fatty acids (VFAs) are generated alongside alcohols, lactic acid, CO_2,

H_2, NH_3, H_2S and new cell material. Acetogenesis is the third step with the production of acetate and molecular hydrogen via the anaerobic oxidation of higher fatty acids and the conversion of propionate, butyrate and valerate to acetate and hydrogen (acetogenesis process). Methanogenesis, the final stage, involves the production of methane from the materials produced in previous stages. A schematic outline of the digestion process is presented in Figure 2.1.

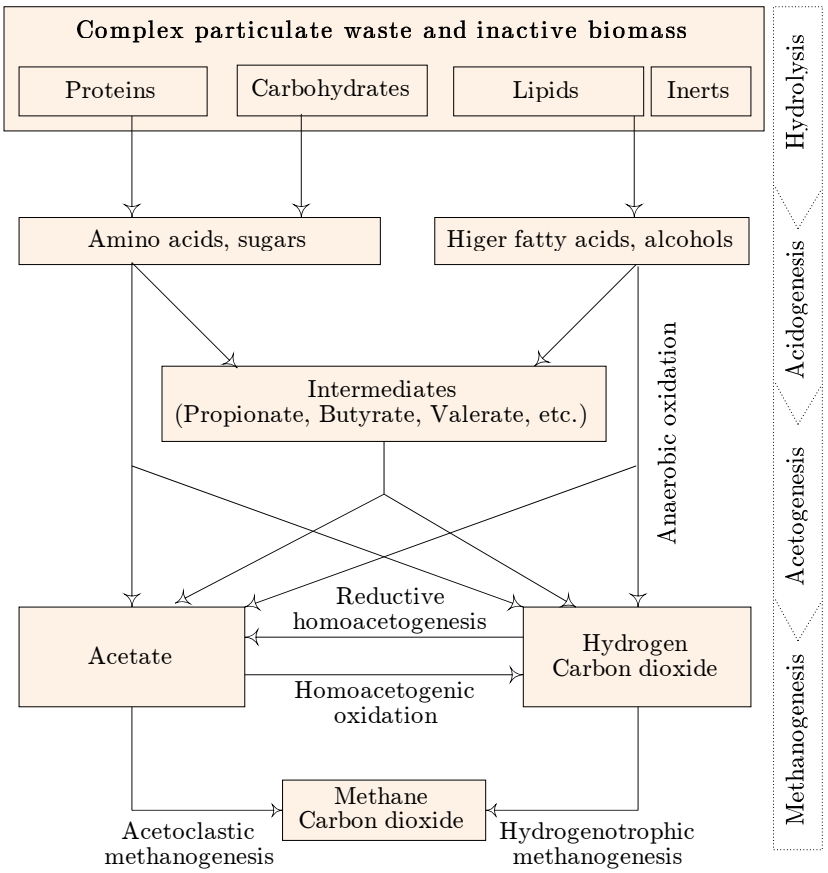

Figure 2.1 A schematic pathway of anaerobic conversion from biomass to methane. Adapted from Batstone *et al.* (2002); Lier *et al.* (2008); Demirel and Scherer (2008)

2.2.1.1. Hydrolysis

During the hydrolysis process, proteins are hydrolysed to amino acids, polysaccharides to simple sugars and lipids to long chain fatty acids by the action of exo–enzymes produced by hydrolytic bacteria. These products are monomeric and dimeric compounds which are readily accessible for acidogenic bacteria in the next stage. Anaerobic digesters often contain between 10^8–10^9 hydrolytic bacteria per ml comprising both obligate and facultative anaerobes.

On the whole, the more that organic substances are solubilised, the more their volatile solids become biodegradable. Hence, the efficiency of anaerobic digestion can be increased by using physical or chemical pretreatment processes to enhance the rate of hydrolysis (Eastman & Ferguson, 1981). For example, Yang *et al.* (2010) used additional enzymes to enhance hydrolysis efficiency and consequently improved the anaerobic digestion process; by combining two different hydrolysis processes (thermochemical and biological hydrolysis), Park *et al.* (2005) also reported that hydrolysis was enhanced, leading to better digestion efficiency.

Hydrolysis is considered by most authors as a rate–limiting step in the anaerobic digestion of organic particulates such as food waste (Eastman & Ferguson, 1981; Vavilin *et al.*, 1996; Miron *et al.*, 2000). The rate–limiting step is defined by Lawrence (1971) as that which will cause process failure to occur under imposed conditions of kinetic stress. However, this step may differ for different types of waste (Parkin & Owen, 1986).

Many studies have attempted to model substrate hydrolysis rates during the anaerobic digestion process. In most cases, the evidence suggests that the rate of hydrolysis is influenced by many factors *e.g.* pH, temperature, substrate composition, VFAs, hydraulic retention time (HRT) and particle size (Veeken & Hamelers, 1999; Miron *et al.*, 2000; Veeken *et al.*, 2000; Zhang *et al.*, 2005; Chen *et al.*, 2007; Feng *et al.*, 2009; Xu *et al.*, 2011). Generally, four approaches have been proposed to model hydrolysis rate: first–order kinetics, the Monod equation, two–phase Monod equations and Contois kinetics (Vavilin *et al.*, 1996). Of these, the first–order hydrolysis function, an empirical expression that reflects the cumulative effect of all the microbially–mediated processes occurring, is the simplest and can successfully describe hydrolysis in many cases; however, the drawback of this method is that it is not directly coupled to microbial growth which obviously may affect the overall hydrolysis rate (Vavilin *et al.*, 2008). Several authors have attempted to revise the simple first–order kinetics *e.g.* Llabres-Luengo and Mata-Alvarez (1988), McCarty and Mosey (1991). Nevertheless, it has been reported that a first–order function may be most appropriate for complex, heterogeneous substrates such as food waste, while other hydrolysis functions may be more appropriate for single homogeneous substrates (Eastman & Ferguson, 1981).

The first–order kinetic equation for hydrolysis can be expressed as:

$$r_{hyd} = -k_{hyd} X_S \tag{2.1}$$

where X_S is the substrate concentration, kg m^{-3}; k_{hyd} is the first-order hydrolysis constant (maximum specific rate), day^{-1}.

Literature values for the coefficient (K_{hyd}) of the first–order equation for several substrates are shown in Table 2.1. As can be seen, the hydrolysis rate for carbohydrates is faster than that for proteins and lipids.

Table 2.1 Kinetic constants (day^{-1}) for carbohydrate, protein and lipid hydrolysis

Substrate	Reference		
	[1]	[2]	[3]
Carbohydrates	0.5–2	5.22	0.025–0.2
Proteins	0.1–0.7	1.86	0.015–0.075
lipid	0.25–0.8	1.24	0.005–0.01

[1] (Garcia-Heras, 2003)

[2] (Zaher, Li, *et al.*, 2009)

[3] (Christ *et al.*, 2000)

The rate of hydrolysis varies depending upon types of solid wastes (Trzcinski & Stuckey, 2012). It can be affected by the accumulation of amino acids and sugar, pH, and un–ionised VFAs (Garcia-Heras, 2003).

2.2.1.2. Acidogenesis

Acidogenesis is generally considered to be the fastest step in the anaerobic digestion process. Growth rates of acidogenic bacteria are ten to twenty–fold higher than those of methanogens, and bacterial yields and conversion rates are five–fold higher. Therefore, anaerobic reactors can be subject to souring, *i.e.* a sudden pH drop when reactors are overloaded, leading to a higher concentration of non–dissociated VFAs (Lier *et al.*, 2008). Products from this stage cannot be used directly by the methanogens and must be degraded further in a subsequent process, namely, acetogenesis (Bjornsson, 2000).

2.2.1.3. Acetogenesis

In the acetogenesis stage, which is carried out mainly by obligate hydrogen producing acetogens (OHPA), VFAs and LCFAs are syntrophically oxidised to produce acetate, carbon dioxide and hydrogen. These are the only substrates that can be metabolised efficiently by the methanogens in the final stage of anaerobic digestion (Anderson *et al.*, 2003). New cell materials also are created in the acetogenesis process (Lier *et al.*, 2008).

During degradation, fatty acids act as electron donors in producing CO_2, along with electron acceptors in transforming H^+ ions into H_2.

2.2.1.4. Methanogenesis

The methanogenic step is the final stage of the conversion process of organic matter, with the two important products being methane and carbon dioxide. Methanogenic archaea accomplish this stage and for engineering purposes, they are categorised into two main groups, *i.e.* acetate converting or acetoclastic methanogens, and hydrogen–utilising or hydrogenotrophic methanogens. Accordingly, there are two routes of methane formation. In the first route, acetate is cleaved to form carbon dioxide and methane (acetoclastic methanogenesis). In the second route, acetate is oxidised to H_2 and CO_2, then CO_2 is reduced with H_2 to yield CH_4 and H_2O (the syntrophic acetate oxidation pathway).

Because hydrogen is an electron donor, whereas carbon dioxide is an electron acceptor, both of them are converted to methane by hydrogenotrophic methanogenic bacteria. These bacteria grow in syntrophic co–culture, together with the acetogenic OHPA bacteria. Therefore, hydrogenotrophic methanogenesis must be considered jointly with acetogenesis in the formation of methane (Harper & Pohland, 1986; Boone *et al.*, 1989). The syntrophic acetate oxidation pathway is described more extensively in section 2.3.2.

Although it is often stated that acetoclastic methanogenesis is the most important pathway for methane production accounting for about 70% of methane evolved in a digester (Valcke & Verstraete, 1983), and that the SAO pathway is only observed under thermophilic condition (Zinder & Koch, 1984), this view is no longer entirely valid. In mesophilic high ammonia environments, the syntrophic acetate oxidation pathway has been observed (Schnurer *et al.*, 1994; Schnurer *et al.*, 1999; Banks *et al.*, 2012), suggesting that the dominance of the acetate oxidation pathway can be shifted under such conditions. This is discussed more thoroughly in section 2.3.2.

2.2.2 Factors affecting the anaerobic digestion process

In the anaerobic digestion system, a healthy population of the relevant groups of microorganisms is a very important factor for effective degradation. A large number of studies have been carried out on factors affecting the anaerobic digestion process, and some key points are summarised below.

2.2.2.1. Substrate, nutrients and trace elements

Organisms need certain essential ingredients for their growth (Pazdernik & Clark, 2012). If this condition is not met, growth will not proceed satisfactorily. However, many essential nutrients can become toxic when present in high

concentrations (Gunnerson & Stuckey, 1986). Nitrogen (N) and phosphorus (P) are building blocks for cell synthesis, and their requirements are directly related to microbial growth in an anaerobic digester (Wall *et al.*, 2008). The amounts of nutrients that are required in digesters can be derived from the elemental composition of microbial cells within the digestate (Lettinga, 1995).

Nitrogen can occur in a wide variety of inorganic forms, the most common being ammonia (NH_3), nitrate (NO_3^-), nitrite (NO_2^-), and nitrogen gas (N_2). The COD:N ratio most commonly recommended for anaerobic digestion is 100:2.5 (Anderson *et al.*, 2003).

Several values for phosphorus requirement have been reported, with a COD:P ratio varying from 80:1 to 200:1 (Anderson *et al.*, 2003). The usual forms taken by phosphorus in aqueous solution include orthophosphate, polyphosphate, and organic phosphate. The orthophosphates, for example PO_4^-, HPO_4^{2-}, $H_2PO_4^-$, H_3PO_4, are immediately available for biological metabolism without further modification. Organic phosphates must generally be hydrolysed by the cell to release inorganic phosphate before use.

In addition to the two main macronutrients above, trace elements also play an important role in stabilising digestion process since they are crucial for microorganism metabolism and growth. For instance, sulphide is necessary for building up cell structures, while methanogens have a requirement for Nickel (Ni), Cobalt (Co), Molybdenum (Mo) (Schonheit *et al.*, 1979; Pesta, 2007). Other micronutrients necessary for anaerobic digestion have been identified, including Iron (Fe), Copper (Cu), Manganese (Mn), Zinc (Zn), and Vanadium (V) (Wilkie *et al.*, 1986; Speece, 1996). The role of trace elements is as metallic enzyme activators and for electron transfer in oxidation–reduction reactions (Wood & Tchobanoglous, 1975; Banks *et al.*, 2013).

In a recent batch study of the effects of eight trace elements (Ca, K, Cr, Ni, Zn, Co, Mo and W) on mesophilic digestion of OFMSW (Lo *et al.*, 2012), it was concluded that metals concentrations higher than threshold values could result in unfavourable effects, leading to the inhibition of biogas production. The solutions suggested were maintaining a reasonable concentration of these metals or diluting to secure a suitable value.

The specific trace element requirements in the case of food waste are discussed in more detail in section 2.3.3.

2.2.2.2. Temperature

Temperature is one of the most influential environmental factors as it controls the activity of all microorganisms through two contrasting effects. Microbial activity and growth decrease by one half for every 10°C decrease in temperature below 35°C (Kashyap *et al.*, 2003). A rise in temperature leads to an increase in the rate of biochemical and enzymatic reactions within cells, causing increased growth rates. Above a specific temperature, however, the microbial growth rate will decline exponentially (Figure 2.2).

Generally, digester operating temperatures can be divided into three broad ranges: psychrophilic (< 20°C), mesophilic (> 20°C and < 45°C) and thermophilic (> 45°C) (Evans, 2001). Martin (1998) found that the methane production rate increased with temperature: for example, methane production at 25°C was 25% lower than that at 60°C. In terms of energy efficiency and economics, however, this result does not necessarily mean the higher temperature is the more optimal, since higher digestion temperatures require more energy to achieve and maintain (Chae *et al.*, 2008).

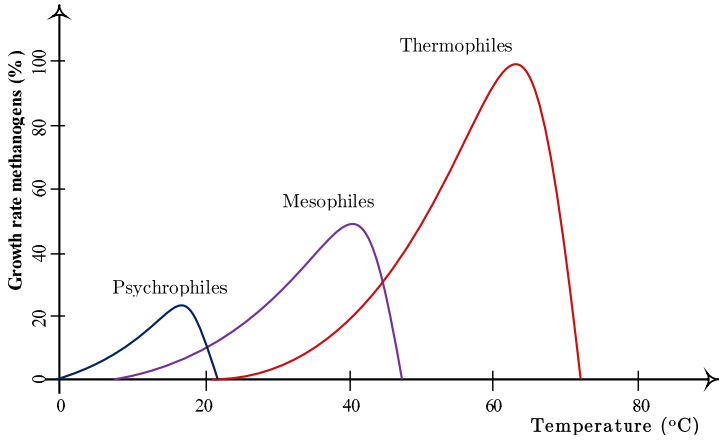

Figure 2.2 Relative growth rate of psychrophilic, mesophili, and thermophilic methanogens. Redrawn from (Lier *et al.*, 1997)

2.2.2.3. pH and Alkalinity

Anaerobic microorganisms, especially methanogens, are sensitive to extremes of pH. Many species can grow effectively in a pH range between 6 and 9 (Swamy, 2008; Ivanov, 2009; Lyberatos & Pullammanappallil, 2010), but methanogenesis works best when the pH is near its neutral value of 7. A number of studies have suggested that the optimum pH range for anaerobic

digestion in mesophilic conditions is 6.5–7.5 (Ishida *et al.*, 1982; Seely, 1985; Anderson & Yang, 1992; Van Ginkel *et al.*, 2001; Cecchi *et al.*, 2003; Khalid *et al.*, 2011). In thermophilic conditions, the optimum pH value for the highest methane production is a little higher than in mesophilic operation (Liu *et al.*, 2008).

Alkalinity is attributed mainly to HCO_3^- ions (bicarbonate alkalinity) derived from the evolution of CO_2 during the biodegradation of organics. When the digester works under normal conditions, pH is decreased by HCO_3^-. Under unfavourable conditions (*e.g.* inhibition of methanogenesis followed by VFA accumulation), pH may also drop if the system has a small buffering capacity (low alkalinity), which can lead to further inhibition and bioreactor failure (Lyberatos & Pullammanappallil, 2010). Equation (2.2) shows that the partial pressure of CO_2, pH, and alkalinity are directly related:

$$pH = pK_{al} + \log\left(\frac{alkalinity(bicarbonate) \,/\, 50000}{CO_2(g) \,/\, K_H}\right) \tag{2.2}$$

where pK_{al} = 5–10^{-7} (35°C) is the dissociation constant for carbonic acid; K_H = 38 atm $mole^{-1}$ (35°C) is Henry's constant for CO_2.

2.2.2.4. Mixing

In order to achieve optimal anaerobic digestion performance, proper mixing is required (McFarland, 2001; Karim *et al.*, 2005; Borole *et al.*, 2006; Elnekave *et al.*, 2006). Mixing has also been widely considered as one of the most important factors determining the rate of biogas production (Stafford, 1982; Kaparaju *et al.*, 2008). The key purposes of mixing in an anaerobic digestion system are: (*i*) providing contact between the active biomass and new substrate; (*ii*) providing physical, chemical and biological uniformity within the digester; (*iii*) distribution of organics and dilution of inhibitory substances within the digester; (*iv*) avoiding hydraulic dead zones which can have damaging effects on the process reaction kinetics; (*v*) preventing stratification and temperature gradients; and (*vi*) minimising the formation of a scum layer and the deposition of solids (Verhoff *et al.*, 1974; EPA, 1979; Burton & Turner, 2003).

Generally, methods of mixing can be categorised into three groups: gas mixing systems, mechanical mixing systems and mechanical pumping systems (Qasim, 1998; Tiehm *et al.*, 2001). Gas mixing systems often involve the

recirculation of biogas and are classified as unconfined and confined (Rundle *et al.*, 1981; Garber, 1982; Lee *et al.*, 1995; Appels *et al.*, 2008). Unconfined gas mixing systems are designed to collect biogas at the top of the digester, which is then compressed and released through a series of bottom diffusers or top–mounted lances. In confined gas mixing systems, biogas is collected at the top of the digester, compressed, and then discharged through confined tubes. Mechanical mixing systems use low–speed turbine impellers: mixers can be installed through the digester cover or through the walls of the tank, and the digestate is transported by the rotating impeller(s). In mechanical pumping systems, mixing is achieved by circulation of the anaerobic liquor either by propeller–type pumps mounted in internal or external draft tubes, or by an axial or centrifugal pump installed externally.

The degree and type of mixing also affects the growth rate and distribution of microorganisms within the digestate, the substrate availability and utilisation rates, granule formation, and gas production. Therefore, it may be used as an operational tool to stabilise unstable digesters (Stroot *et al.*, 2001).

Mechanical mixing and gas recirculation are the most common methods of digester mixing and have been successfully applied in many studies (Lee *et al.*, 1995; Reinhold & Markl, 1997; Wellinger, 1999; Borole *et al.*, 2006). This study, hence, considers both of these two popular mixing methods.

2.2.2.5. Toxicity and inhibition

Speece (1983) defined toxicity as an adverse effect (not necessarily lethal) on microbial metabolism, while inhibition is an impairment of microbial function. Anaerobic digestion feedstock or the by–products of anaerobic metabolism can contain substances that may be toxic to anaerobic populations (McCarty & McKinney, 1961b, 1961a; Chynoweth *et al.*, 2001; Chen *et al.*, 2008). Many potentially toxic substances that can slow down the rate of digestion (toxicity) or cause process failure (inhibition) may be present, either as components in a reactor feed or as by–products of anaerobic metabolism. Common examples include heavy metals, alkali and alkaline earth metals, VFAs, oxygen, ammonia and sulphide (McCarty, 1964; Mehrotra *et al.*, 1987; Hickey *et al.*, 1989; Lin, 1993; Steffen *et al.*, 1998; Anderson *et al.*, 2003; Chen *et al.*, 2008).

The above sections have briefly reviewed the fundamentals of the anaerobic digestion process. This knowledge is essential not only for understanding the theoretical background, but also for assessing the strengths and weaknesses of the anaerobic digestion models to be reviewed. Moreover, it provides substantial help for validation of kinetic factors in model building.

2.3 Anaerobic digestion of food waste

Food waste, although it shares many properties with other organic substrates such as animal manure, sewage sludge, agricultural residues, *etc.*, also has some specific features. Therefore, it is important to consider the specific characteristics of food waste and their influence on the anaerobic digestion process.

2.3.1 Waste stream and current knowledge

Source segregated food wastes are very high in energy potential but due to their high moisture content and high biodegradability, bioconversion technologies (*e.g.* anaerobic digestion) are the most effective way to gain energy from them (Zhang *et al.*, 2007). Recent studies have confirmed the high energy content of food waste (about 0.435 mL CH_4 g^{-1} VS_{added}), equivalent to approximately 100 m^3 of methane for each tonne of wet food waste (Cho *et al.*, 1995; Demirel *et al.*, 2010; Banks, Chesshire, *et al.*, 2011; Zhang & Jahng, 2012).

A common problem that has been repeatedly reported in the long–term operation of food waste digesters is instability, when the process suffers from high VFA concentrations. Food wastes contain large amounts of soluble organics that can be easily converted to VFAs. Consequently, excessive conversion to intermediate VFA without a corresponding conversion of these to methane and carbon dioxide may cause microbial stress, resulting in severe falls in pH and inhibition of the methanogenesis process (Li *et al.*, 2011). Banks *et al.* (2008) operated a technical–scale trial using kitchen waste collected weekly from domestic properties in the UK and found that VFA accumulation was connected with failure of the autotrophic methanogens. Similar problems were also encountered in other studies (Wang & Banks, 2003; Murto *et al.*, 2004; Climenhaga & Banks, 2008; Banks & Zhang, 2010).

Food waste, with its recognised high protein content, is easily degraded anaerobically to produce a considerable amount of ammonia. The ammonia concentration in food waste digestate is thus higher than for many other waste types (Banks *et al.*, 2008). A number of reports have found a link between high ammonia concentrations and the failure of food waste digesters (McCarty, 1964; Wiegant & Zeeman, 1986; Angelidaki & Ahring, 1993). At the same time, when the ammonia concentration reaches a threshold value, an alternative metabolic route may become dominant in methane formation *i.e.* the hydrogenotrophic methanogenesis pathway (Angelidaki & Ahring, 1993; Karakashev *et al.*, 2006; Schnurer & Nordberg, 2008; Banks *et al.*, 2012).

2.3.2 The role of acetate oxidation pathway of methane generation

For a long time, the acetoclastic pathway was thought of as the dominant route for methane generation. Much evidence has confirmed, however, that syntrophic acetate oxidation, can contribute to methane formation and even, in some cases, become more important than acetoclastic methanogenesis. This alternative pathway plays a role in ensuring the proper functioning of anaerobic digestion by preventing acetate accumulation, and therefore it is very important in maintaining the stability of AD systems (Angenent & Scott, 2010). The two reactions in the process are expressed by Thauer (1977):

$$(1)\ CH_3COO^- + 4H_2O \rightarrow 4H_2 + 2HCO_3^- + H^+ \quad (\Delta G^{o'} = +104.6\ \text{kJ/reaction})$$
$$(2)\ 4H_2 + HCO_3^- + H^+ \rightarrow CH_4 + 3H_2O \quad (\Delta G^{o'} = -135.6\ \text{kJ/reaction})$$

The methanogens and the SAO bacteria are interactively influenced by each other to perform these metabolic processes. The acetate oxidation (reaction 1) can only proceed if the concentration of hydrogen and formate are kept low by the methanogens (reaction 2). Energetically, the oxidation of acetate to hydrogen and carbon dioxide is unfavourable in standard conditions due to the high Gibbs free energy ($\Delta G^{o'}$= +104.6 kJ mol^{-1}), though it can proceed when hydrogenotrophic methanogens consume the hydrogen to keep hydrogen partial pressures low (Stams, 1994; Hattori, 2008). Reaction (2) is an exergonic reaction ($\Delta G^{o'}$= –135.6 kJ mol^{-1}); therefore by combining the two reactions, the overall Gibbs free energy is $\Delta G^{o'}$= –31 kJ mol^{-1}. In other words, the overall reaction becomes exergonic, with the same stoichiometry as acetoclastic methanogenesis (Hattori, 2008). The free energy budget is low, and the co–operating organisms have to share this small amount of energy for their sustenance (Schink, 2002). Additionally, although low concentrations of hydrogen and formate are essential for the two reactions, previous investigations have stated that a sufficient concentration must be available to favour hydrogen–consuming methanogenesis (Stams, 1994). Because of these restricted conditions, syntrophic acetate oxidation had long been considered as an extremely difficult or even impossible pathway. Hattori (2008) concluded that this may explain why, although the process was initially described by Barker (1936) it was largely ignored for about a half a century until the confirmation by Zinder and Koch (1984). Thereafter, evidence derived from studying anaerobic digesters confirmed that SAO could play a substantial role in methanogenesis in certain circumstances.

Shigematsu *et al.* (2004) used the dilution method to operate two anaerobic chemostats for over two years and showed that in acetate–fed chemostats, the dilution rate could cause a shift in the primary pathway of conversion to methane. At a lower dilution rate (0.025 day^{-1}), the acetate–oxidising syntrophs, coupled with hydrogen–consuming methanogens, could metabolically out–compete the acetoclastic methanogens and play a crucial role in the conversion of acetate to methane, whereas the acetoclastic pathway dominated at a higher dilution rate (0.6 day^{-1}).

Thermodynamically, the SAO process becomes energetically more favourable at high temperatures. Hence, many studies have been carried out in thermophilic conditions to confirm the proportions of acetotrophic and hydrogenotrophic methanogens during anaerobic conversion of biomass to methane, such as in work by Zinder and Koch (1984), Lee and Zinder (1988), Petersen and Ahring (1991), Ahring (1995), Shigematsu *et al.* (2004), Karakashev *et al.* (2006), Hori *et al.* (2006), Krakat *et al.* (2010), Ryan *et al.* (2010), Hao *et al.* (2010), Mayumi *et al.* (2011), Sasaki *et al.* (2011).

Although it was believed for a long time that the process could only occur in enhanced temperature environments, more recent investigations have shown that acetate oxidation can also be found in mesophilic digesters. Schnurer *et al.* (1994) grew a triculture in a mesophilic digester (37°C) with a high ammonium concentration at pH 8. The results indicated that SAO in a mesophilic culture is clearly possible; however, the growth rate was very low. This agrees with the theory that the energy yield is much lower at 37°C than at 60°C. Thereafter, Schnurer and Nordberg (2008) continued their work and explored how the dominant CH_4 generation pathway shifts from acetoclastic methanogenesis to syntrophic acetate oxidation under elevated ammonia concentrations. Recently, acetate oxidation was concluded to be the main route of methane formation in research conducted by Banks *et al.* (2012) when investigating anaerobic digestion of food waste at a mesophilic temperature.

As mentioned previously, an elevated concentration of ammonia, *i.e.* total free ammonia and ammonium, could contribute to the shift in the dominant methanogenic pathway from acetoclastic to hydrogenotrophic. When the ammonia concentration reaches a threshold value, and the shift occurs. Hydrogenotrophic methanogens are commonly agreed to be less sensitive to high free ammonia concentrations than are the acetoclastic methanogens (Sprott & Patel, 1986; Angelidaki & Ahring, 1993; Karakashev *et al.*, 2006; Schnurer & Nordberg, 2008). Therefore, it is not surprising that under high ammonia concentrations, methane is formed via acetate oxidation by bacteria and subsequent hydrogen utilisation by methanogens without the need for

acetoclastic methanogens (Angenent *et al.*, 2002; Banks *et al.*, 2012). Research conducted by Angelidaki and Ahring (1993) indicated that the specific growth rate for the acetoclastic methanogens decreased by 50% at ammonia concentrations of 3.5 g N L^{-1}, compared to 7 g N L^{-1} for the hydrogenotrophic methanogens.The threshold value of ammonia concentration appears to be difficult to generalise since anaerobic reactors used in ammonia toxicity trials have been operated under various conditions *e.g.* different types of feedstocks, inoculum, temperature, pH values. In most reactor studies, however, inhibitory concentrations are in the range 1.7–6 g total ammonia–N L^{-1}, corresponding to 0.4–1.1 g NH_3–ammonia L^{-1} (Angelidaki & Ahring, 1993; Borja *et al.*, 1996; Hansen *et al.*, 1999; Banks *et al.*, 2012). Observing the anaerobic digestion of food wastes, which are rich in organic nitrogen compared to many other waste types, from the published literature and current work at the University of Southampton, it can be seen that at elevated ammonia concentrations (*e.g.* around 5 g ammonia–N L^{-1}) in mesophilic conditions both acetoclastic and acetate oxidation pathways contribute to methane formation (Feng *et al.*, 2010; Banks *et al.*, 2012).

In the reports reviewed, the hydraulic retention time has been noted to influence the conversion of acetate to methane. It is essential that HRT should exceed the microbial doubling time in order to avoid washout of the microbial population (Weiland, 2010). Westerholm (2012) reviewed the literature and concluded that whilst it is problematic to predict the HRT needed to maintain syntrophic acetate oxidation in a continuously stirred tank reactor (CSTR), around 64 days could be suitable.

The relationship between acetate concentration and SAO has also been investigated. For the most part, it is suggested that when the concentration of acetate is low, the SAO pathway is the major process for acetate conversion (Petersen & Ahring, 1991; Ahring, 1995). Nevertheless, information about the acetate concentration controlling the development of SAO is conflicting. For example, in thermophilic digesters, previous studies proposed SAO as the predominant pathway at either a low range of 0.1–1.2 mM (Zinder & Koch, 1984; Ahring, 1995; Hori *et al.*, 2006) or a high (*e.g.* 100 mM) acetate concentration (Hao *et al.*, 2010). Under mesophilic conditions, however, Shigematsu *et al.* (2004) reported that a low acetate concentration (*e.g.* 0.2 mM) causes dominance of syntrophic acetate oxidation, whereas the pattern is reversed at a higher concentration (*e.g.* 4 mM).

Overall, it can be concluded that SAO can contribute to the conversion process of methanogenesis from organic matter, including food waste. Furthermore, in favourable conditions of substrate and working environment, SAO can be the dominant pathway.

2.3.3 Trace elements in anaerobic digestion of food waste

Because of their important role in enhancing stability, trace elements have been widely used to improve the performance of anaerobic digesters. Moreover, this method of digestion optimisation has recently been attracting great attention from many researchers.

Nutrient content analysis of typical food waste showed that although it contained well balanced macro–nutrients for anaerobic microorganisms, it often lacks trace elements to perform successfully (Zhang *et al.*, 2007). Facchin *et al.* (2012) found that in the mesophilic anaerobic digestion of food waste, the addition of trace metals (Co, Mo, Ni, Se and W) could improve methane production. Banks *et al.* (2012) noted that although mesophilic digesters can operate on food waste over extended periods at high concentrations of VFA and ammonia without a great loss in biogas production, there is a risk that these conditions could result in sudden failure. They concluded that the deficiency of Se, crucial for both syntrophic hydrogenotrophic methanogenesis and propionate oxidation, leads to the problem. The study also suggested that the problem can be overcome by adding appropriate trace elements. For instance, a digester with Se and Co supplemented shows an improvement in performance (*i.e.* a higher specific methane yield) and a reduced risk of process failure due to accumulation of VFA. Zhang and Jahng (2012) operated a single–stage food waste digester and reported that without extra trace elements the digestion ended in failure. In contrast, in a digester supplemented with trace metals, methane production and pH are maintained nearly constantly, and the VFA concentration remained low. Similar evidence of the specific role of trace elements in anaerobic reactors digesting food waste can be found in investigations conducted by Murray and Van Den Berg (1981), Climenhaga and Banks (2008), Feng *et al.* (2010), Zhang *et al.* (2011).

2.3.4 Ammonia removal from food waste digestate

2.3.4.1. Introduction

In the anaerobic digestion process, ammonia is generated mainly from the fermentation of proteins, amino acids and the breakdown of methylamine and

other nitrogenous compounds (Anderson & Yang, 1992; Omil *et al.*, 1995; Gallert *et al.*, 1998). Although it is essential for bacterial growth (Parkin & Owen, 1986), at elevated concentrations (*e.g.* 3.0–6.0g NH_4^+–N L^{-1}), it is harmful to the bacteria community. The problem is that ammonium (NH_4^+) is not broken down or removed during anaerobic digestion (Rousseau *et al.*, 2008). This can result in a high concentration of ammonia in the digestate which may cause failure as indicated by a decrease or cessation in biogas and methane production (Angelidaki & Ahring, 1993; Hansen *et al.*, 1998; Sung & Liu, 2003; Fricke *et al.*, 2007). Moreover, it can lead to ammonia emissions when applying digestate to land (Gustin & Marinsek-Logar, 2011). As yet knowledge of the mechanisms of ammonia inhibition is limited and it has been suggested that until this changes, researchers must focus on methods to reduce the concentration of ammonia in digestate (Kayhanian, 1999). This is the reason why removal of ammonia from anaerobic by–products is valuable, and has been attracting attention from investigators, especially for food waste digestion applications. This study therefore considers ammonia removal from digestate with the aim of keeping a safe ammonia concentration in the digester for stable operation, while also recovering a valuable fertiliser product in a potentially more useful form.

Methods that have so far been used for ammonia removal include biological ammonia oxidation and denitrification (Wett & Rauch, 2003; Kim *et al.*, 2004; Deng *et al.*, 2006), electrochemical conversion (Lei & Maekawa, 2007), physiochemical processes such as struvite precipitation (Turker & Celen, 2007), microwave radiation (Lin *et al.*, 2009), ultrasound treatment (Wang *et al.*, 2008), membrane filtration (Bodalo *et al.*, 2005), and air stripping (Bonmati & Flotats, 2003; Lei *et al.*, 2007; Rubia *et al.*, 2010; Walker *et al.*, 2011). Among these, ammonia stripping is the most feasible due to the low investment required, the basic pH of anaerobically digested effluent and the potential availability of a source of heat from biogas combustion (Bonmati & Flotats, 2003); and the fact that it does not increase the volume of digestate for disposal (Zhang, Lee, *et al.*, 2012). Successful studies using this method have been rported for different substrates, *e.g.* pig slurry (Liao *et al.*, 1995; Bonmati & Flotats, 2003; Zhang, Lee, *et al.*, 2012), landfill leachate (Cheung *et al.*, 1997; Calli *et al.*, 2005), urea fertilizer plant wastes (Minocha & Rao, 1988), and food waste (Rubia *et al.*, 2010; Walker *et al.*, 2011; Yabu *et al.*, 2011). The University of Southampton has been conducting experimental work on an ammonia stripping system removing ammonia from food waste digestate (VALORGAS, 2013). Results of this study are a good source of data for ammonia stripping model validation.

2.3.4.2. Theory of ammonia stripping

In anaerobic digesters, nitrogen is mostly in the form of ammonium (NH_4^+) and is dissolved in water (Deublein & Steinhauser, 2011). Ammonia stripping is based on the transformation of the ammonium ion to ammonia gas. Lei *et al.* (2007) based on study of Srinath and Loehr (1974) suggested the following process equations (2.3) and (2.4).

$$NH_4^+ \longleftrightarrow NH_3 + H^+ \tag{2.3}$$

$$[NH_3] = \frac{[NH_3] + [NH_4^+]}{1 + [H^+] / K_a} \tag{2.4}$$

$$K_a = \frac{[NH_3][H^+]}{[NH_4^+]} \tag{2.5}$$

where $[NH_3]$ is the free ammonia concentration, mol L^{-1}; $[NH_4^+]$ is the ammonium concentration, mol L^{-1}; $[H^+]$ is the hydrogen ion concentration, mol L^{-1}; $[NH_3] + [NH_4^+]$ is total ammonia concentration, mol L^{-1}; K_a is the acid ionization constant of ammonia, mol L^{-1}.

Ammonia is transferred from the solid–liquid phase to the gas phase, then absorbed from the gas into a strong acid solution (*e.g.* sulphuric acid) (Bonmati & Flotats, 2003). Figure 2.3 describes a possible system of ammonia removal from food waste digestate called '*side–stream*' where the stripping reactor and pasteuriser are separate. This ammonia stripping method was modelled in this study.

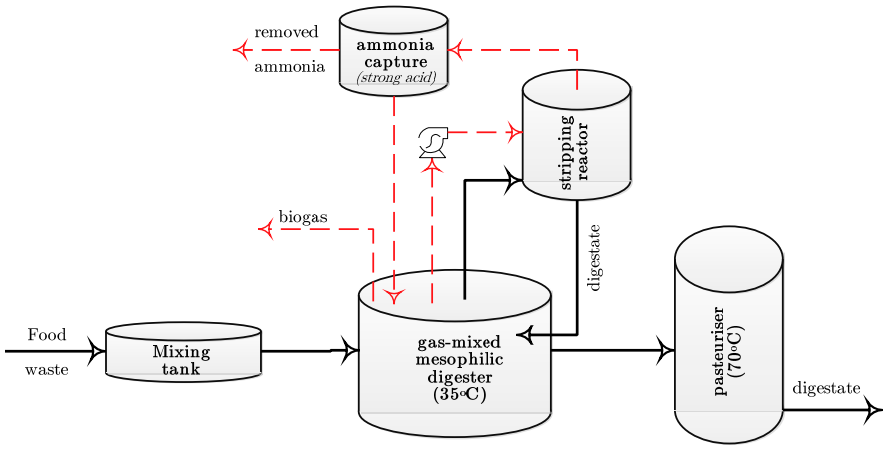

Figure 2.3 *Side–stream* ammonia removal used. Adapted from (Walker *et al.*, 2011).

2.3.5 Conclusions on AD of food waste

Food waste, as a typical form of organic matter, contains the potential to produce energy *e.g.* heat and electricity. The well–known and most appropriate method for conversion food waste to energy is anaerobic digestion. Practical experience with food waste digesters shows, however, that in order to operate successfully, it is necessary to take the waste characteristics into account based on state–of–the–art work carried out on this waste. There appear to be three important issues that need to be considered in modelling the process. Firstly, there is the presence of an alternative pathway for methanogenesis shifted from the conventional acetoclastic route under certain conditions (*i.e.* the acetate oxidation pathway). Second, the role of trace elements in nurturing stability during the digestion process. Lastly, the benefit of removing ammonia from digestate as an important area in which modelling may provide valuable guidance for research on and operation of anaerobic digesters treating food waste.

2.4 Anaerobic digester configurations

In practice, digesters of many configurations have been used to treat a wide range of feedstocks such as residues from agricultural products, food processing industries, organic waste, and wastewater treatment biosolids.

Regarding process management of anaerobic digesters, three types can be distinguished: batch (discontinuous processes), semi–continuous and continuous. Batch reactors are the simplest: in this type of process, feedstock is added to the reactor in a single batch and left to degrade. On completion, the digesters are emptied or left about 10–15% full to provide an inoculum for fresh input waste, then recharged with a new batch of feed and the cycle is repeated (Evans, 2001). In order to produce biogas at a constant rate, it is necessary to have different digesters at different stages of the process, operating in parallel. In continuous systems substrate is added continuously, and a similar amount of digestate is usually removed at the same time in order to maintain a constant level in the digester. Continuous–load digesters are especially efficient when raw materials consist of a regular supply of easily digestible wastes from nearby or persistent sources. Semi–continuous digesters are similar in concept but are fed semi–continuously *e.g.* one or multiple times per day (Deutsche & Ecofys, 2005).

Anaerobic digesters also can be categorised according to the operating temperature. In psychrophilic systems, methane production occurs at a relatively

low temperature range (5–20°C). This is not an optimal condition for microorganisms, so the system is most often applied in small–scale operation at ambient temperature with relatively low efficiency and for quite long retention times (*e.g.* 100 days). By contrast, thermophilic systems operate at a high temperature (50–60°C) which makes digestion and methane production occur quickly, while pathogens elimination rates are high. In the mesophilic process, temperature is maintained at a moderate range (30–35°C). Compared to both psychrophilic and thermophilic systems, mesophilic systems have two benefits: there are more anaerobic mesophiles in nature than psychrophiles and thermophiles, and the operating costs are lower than for thermophilic systems. Therefore, the number of mesophilic anaerobic digesters exceeds that of psychrophilic and thermophilic digesters (Gerardi, 2003).

Anaerobic digestion systems can also be divided into single–stage or those with two (or occasionally more) stages. In the single system, all microbial activities take place in one digester, whilst in a dual system the activities take place sequentially in two digesters. Compared to multiple–stage, single–stage has a simpler design, meaning it is less likely to suffer technical failures and has smaller investment costs (Mata-Alvarez, 2001). This probably explains why the large majority of industrial applications use single–stage systems (Lissens *et al.*, 2001).

Based on the means of transport of material and homogenisation in reactor, anaerobic digesters can also be classified as continuous stirred–tank reactors (CSTR), plug flow reactors (PFR), and sequencing batch reactors (SBR). In a CSTR, the composition, temperature and degree of mixing are the same at any point in the reactor and consistent inputs are an an important factor. In PFRs, all the particles pass through the reactor with no mixing and have the same residence times at a given cross section. In SBR systems, receiving, treating and discharging substrate are accomplished step–by–step in a single tank. Among these reactor types, the CSTR is the most common and widely applied in both laboratory–scale and plant–scale systems (Lyberatos & Skiadas, 1999; Ramasamy & Abbasi, 2001; Antonelli & Astolfi, 2003). On the modelling side, literature sources show that the CSTR has also found extensive use with a large number of current models implementing CSTR .

Overall, a number of digestion systems are available for treatment of organic residues in general and for food waste in particular. Among them, the CSTR system appears to be the most appropriate type because of its flexibility and its widespread use.

2.5 Biogas utilisation and biogas upgrading

2.5.1 Biogas utilisation

There are four basic ways in which biogas can be utilised: for production of heat and steam, electricity production/co–generation, vehicle fuel and production of chemicals. Of these, the two most common applications for biogas are heating and power generation. Using biogas as a vehicle fuel and injecting the upgraded gas into the gas grid are applications that have been attracting more and more interest.

Various options for biogas utilisation are summarised and presented in Figure 2.4.

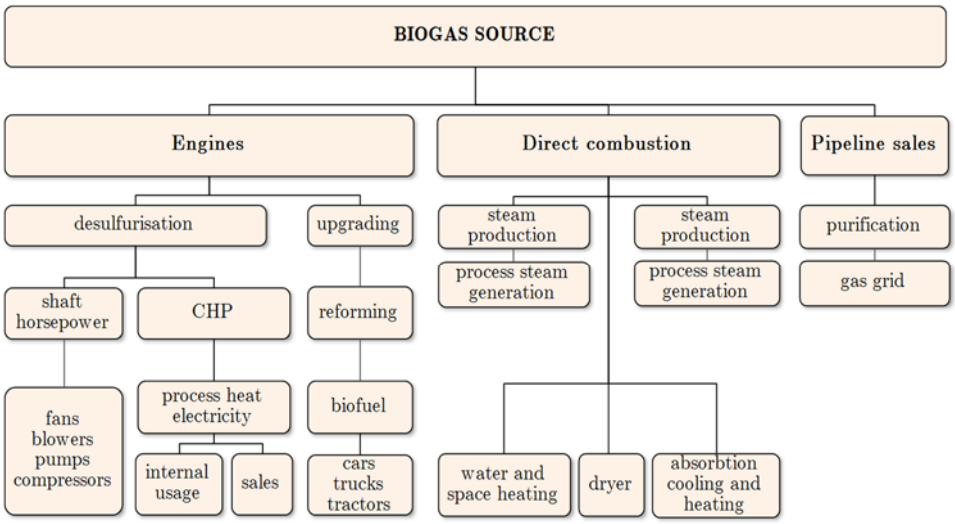

Figure 2.4 Biogas utilisation options. Adapted from (Walsh *et al.*, 1988; Nijaguna, 2006; Persson & Wellinger, 2006; Deublein & Steinhauser, 2011)

2.5.1.1. Biogas for heating

Burning biogas in a boiler to produce heat is an established and reliable technology. Boilers do not have a high gas quality requirement and normally operate at pressures of around 8 to 25 mbar. It is recommended to reduce the hydrogen sulphide concentration in the biogas to below 1000 ppm, to maintain the dew point around 150°C (Persson & Wellinger, 2006). Biogas from small–scale plants in developing countries is often used directly for cooking and lighting, whereas in industrialised countries biogas is often used for steam production. In these countries, boilers are present only in a small number of plants where biogas is used as fuel only without additional CHP generation (Kapoor & Vijay, 2013).

2.5.1.2. CHP–engines

CHP units are very common in biogas plants and have been studied elsewhere (Nilsson *et al.*, 2004; McCormick & Kaberger, 2005; Tomescu, 2005). In parallel with the generation of electricity, a more or less high percentage of heat is developed in CHP units, depending on the power generator technology.

Approximately 50% of the CHP units installed in biogas plants in Europe run with four–stroke engines, and about 50% with ignition oil Diesel engines. The total efficiency, *i.e.* the sum of the electrical and thermal efficiencies, of modern CHP engines is within the range 85–90%. This means only 10–15% of the energy of the biogas is wasted, but the electrical efficiency is still very low (about 40%): from 1 m^3 biogas only 2.4 kWh electric current can be produced (Deublein & Steinhauser, 2011).

2.5.1.3. Biogas for injection into the natural gas network

After upgrading and adjustment of some properties *i.e.* pressure, density, total sulphur, oxygen and humidity content and Wobbe index, biogas can be fed into the natural gas network (Deublein & Steinhauser, 2011).

There are several advantages of using biogas in the gas grid. Firstly, it enables the gas to reach new customers by using the grid connection in densely populated areas. Secondly, injecting biogas into the gas grid improves the local security of supply since most countries consume more gas than they produce.

2.5.1.4. Biogas as fuel for vehicles

With respect to economy and technology, the utilisation of biogas as fuel looks interesting, since compressors are already integrated in service stations and the ecological aspect could be marketed. In comparison with feeding the biogas into the natural gas network, utilisation as vehicle fuel is generally less problematic and can be achieved much more cheaply (Deublein & Steinhauser, 2011). To use biogas for this purpose, it has to be upgraded. By doing this, a gas can be obtained that:

- has a higher calorific value in order to allow long driving distances;
- has a regular/constant gas quality to ensure safe driving;
- does not cause corrosion due to high levels of hydrogen sulphide, ammonia and water;
- does not contain mechanically damaging particles;
- does not give ice–clogging due to a high water content;
- has a declared and assured quality.

In practice, a methane concentration of above 97 vol. % is required. One cubic metre of "green" gas is approximately the same as one litre of gasoline. Different countries require different quality specifications for vehicle fuel (Wheeler *et al.*, 2000).

2.5.1.5. Fuel cells

A fuel cell is an electrochemical cell that converts chemical energy from a fuel into electricity. Electricity is generated from the reaction between a fuel *e.g.* hydrogen and an oxidising agent *e.g.* oxygen (Breverton, 2012).

Fuel cells are different from conventional electrochemical cell batteries in that they consume reactant from an external source, which must be replenished (Barsukov, 2006). Fuel cells have extremely low emissions because there is no conversion from fuel into mechanical energy and heat by the intermediate process.

Among the options considered, biogas upgrading to produce biofuel for transportation and gas for natural gas system is currently raising interest throughout the world as it is the most promising technology that could support rapid expansion of energy utilisation (Weiland, 2003; Poeschl *et al.*, 2010; JyU, 2013).

2.5.2 Biogas upgrading

As noted, biogas is a good source of energy that can be used for all applications that are designed for natural gas. Only methane contributes to the energy potential of biogas, however. Other components including about 35% of carbon dioxide and unwanted substances (*i.e.* hydrogen sulphide, nitrogen, oxygen, ammonia, siloxanes, moisture and particles) are useless, and need to be removed to enhance the energy value of gas, to fulfil the requirements of gas appliances (*i.e.* gas engines, boilers, fuel cells, vehicles, *etc.*) or to meet natural gas standards (Wellinger & Lindberg, 1999; Hagen, 2001; Wheless & Pierce, 2004; Persson *et al.*, 2006; Popat & Deshusses, 2008; Ryckebosch *et al.*, 2011).

The most noticeable contaminants in biogas are H_2S and other malodorous sulphur–containing compounds *e.g.* CH_3SH coming from the anaerobic fermentation of S–bearing organic molecules *i.e.* proteins (Abatzoglou & Boivin, 2009). H_2S concentration in biogas typically ranges from 10–30 to 1000–2000 ppm (Cosoli *et al.*, 2008). Besides its bad smell, this contaminant can be converted to highly corrosive, unhealthy and environmentally hazardous sulphur dioxide (SO_2) and sulphuric acid H_2SO_4 (Jensen & Webb, 1995; Kohl &

Nielsen, 1997; Smet *et al.*, 1998; Fischer, 2010). Other contaminants also found in biogas include halogenated compounds, moisture and siloxanes, ammonia, dust and particles (Persson & Wellinger, 2006; Francis, 2008; El-Mashad & Zhang, 2010; Khanal, 2011). Some of these contaminants can destroy internal fittings in machinery and corrode pipework (Gadre, 1989).

Among other components, ammonia (NH_3) comes second to H_2S in terms of its corrosion and health risk problems. Combustion of biogas containing NH_3 can slightly increase nitrogen oxide (NO_x) emissions (Abatzoglou & Boivin, 2009), which can adversely affect the environment (Ash *et al.*, 2010). Other substances in biogas (CO_2, H_2O, O_2, N_2, H_2, *etc.*) are generally considered to be harmless or sometimes useful. For example, O_2 is useful in H_2S–removal processes that use oxidation to convert S^{2-} to elemental sulphur (S^0). Siloxanes, a group of silicon (Si)–bearing molecules, are also sometimes present in biogas. While there have been quite a number of investigations of this contaminant in biogas from landfill or sewage sludge digesters (Huppmann *et al.*, 1996; Schweigkofler & Niessner, 2001; Hagmann *et al.*, 2002; Dewil *et al.*, 2006; Dewil *et al.*, 2007; Matteson & Jenkins, 2007; Rasi *et al.*, 2007; McBean, 2008), no studies appear to mention whether siloxanes occur in biogas from anaerobic digestion of food waste.

For the above reasons, removal of unwanted components in biogas is essential for eventual utilisation.

'Upgrading' means removal of carbon dioxide to enhance the calorific value of the gas, which increases the energy content for a specific volume of gas, and also removal of other undesirable contaminant compounds. When toxic contaminants are present and cannot be reduced to the required concentration, they must be removed before upgrading in order to prevent corrosion and mechanical wear of the upgrading equipment itself.

Several biogas upgrading technologies are commercially available, including: physical absorption (*e.g.* water scrubbing, pressure swing absorption), chemical and physical absorption (*e.g.* amine scrubbing), membrane and cryogenic methods (Persson *et al.*, 2006; Vijay *et al.*, 2006; Petersson & Wellinger, 2009; Patterson *et al.*, 2011; Ryckebosch *et al.*, 2011). Other techniques are at the pilot or demonstration phase: new developments, both for new and more traditional techniques, may reduce investment and operational costs.

Upgrading adds to the cost of biogas production, and emissions of methane from the upgrading process can have negative effects on the environment. Therefore, it is important to have an optimised upgrading process in terms of low energy consumption and high efficiency giving high methane content in the upgraded gas (Petersson & Wellinger, 2009). It is also very important to

minimise, or if possible avoid, emissions of methane from the upgrading process, since methane has a greenhouse gas effect 20–30 times greater than that of carbon dioxide (Schneider, 1989; Su & Agnew, 2006; Dawson & Spannagle, 2009). This means that the methane content in the reject gas from upgrading units should be minimised.

The following sections briefly present information on the state of the art in biogas upgrading technologies.

2.5.2.1. Pressure swing adsorption

Pressure swing adsorption (PSA) is a technique for upgrading biogas in which CO_2, nitrogen, oxygen and water are separated from the raw biogas stream by adsorbing gases at high pressure and desorbing them at low pressure as waste.

The advantages of the PSA–process are the high CH_4–enrichment of more than 97%, the low power demand and the low level of emissions (Kaparaju *et al.*, 2013). The main disadvantage of PSA technology is the requirement for pre–treatment of H_2S since it may harm the adsorbent at such high pressure (Lopez *et al.*, 2012). Also, the tail gases from PSA still need to be treated (Petersson & Wellinger, 2009). PSA technology is also considered to be flexible due to the wide range of adsorbent materials available to separate the components of various gases and liquids.

2.5.2.2. Water scrubbing

The principle of this method is that carbon dioxide and hydrogen sulphide both have a higher solubility in water than methane, and they will therefore dissolve to a greater extent than methane, particularly at lower temperatures, *e.g.* the solubility of CO_2 at 10°C and 1 bar is about 61 times higher than that of methane (Geankoplis, 1993). The raw gas is often pressurised (around 4 or 10 bar depending upon whether low or high pressure is used, respectively) and introduced to the bottom of the scrubbing tower whilst water is flushed into the top of the tower. Upgraded gas leaves the top of the column. The water that exits the tower with absorbed CO_2 and/or H_2S can be regenerated and re–circulated back to the absorption column. Regeneration is accomplished by de–pressuring or by stripping with air in a similar tower. For energy recovery purposes, any CH_4 dissolved within the water is usually captured by depressurising the water to 2–4 bar within a flash tank. Gases released are then returned to the bottom of the column (Hakansson, 2006). The CH_4 purity

obtained using this process can reach 98% and yields of up to 94% can be achieved (Hullu *et al.*, 2008).

Of the existing technologies, water scrubbing is considered the simplest method and the most cost–effective and appropriate for small–scale use (Kapdi *et al.*, 2005; Hullu *et al.*, 2008; Abatzoglou & Boivin, 2009; Basu *et al.*, 2010). This technique is a fully physical process and therefore no special chemicals are required. Another positive aspect of the technique is that both CO_2 and H_2S can be removed at the same time (Zhao *et al.*, 2010).

The disadvantages of water scrubbing are that it requires a lot of water even with regeneration, and there are limitations on H_2S removal, because the CO_2 decreases the pH of the solution and H_2S can cause corrosion of the equipment (Hullu *et al.*, 2008; Kaparaju *et al.*, 2013).

2.5.2.3. Organic physical scrubbing

Organic physical scrubbing is very similar to water scrubbing but the water is replaced by an organic solvent such as polyethylene glycol. Carbon dioxide is more soluble in polyethylene glycol than in water and for the same upgrading capacity the flow of the liquid phase can be lower and so the plant can be smaller. The polyethylene glycol solution is regenerated by heating and/or depressurising. Hydrogen sulphide, water, oxygen and nitrogen may be removed together with carbon dioxide (Petersson & Wellinger, 2009). The energy required to regenerate the solution after adsorbing H_2S is high, however, so H_2S needs to be removed before the process.

2.5.2.4. Chemical absorption

In the chemical absorption process, unwanted compounds in the gas stream are dissolved into a solvent. The chemical reactions can be reversible or irreversible (Kohl & Nielsen, 1997). Chemical solvents used can be in aqueous solutions of amines (*i.e.* mono–, di– or tri–ethanolamine) or aqueous solutions of alkaline salts (*i.e.* sodium, potassium and calcium hydroxides) (Kapdi *et al.*, 2005).

Compared to physical absoption (*i.e.* water scrubbing), chemical absorption has higher efficiency and reaction rates, and the ability to work at low pressure and to remove H_2S. Because of these advantages, chemical absorption is usually applied for large–scale industrial applications, including natural gas purification (Palmeri *et al.*, 2008). However,

disadvantages of this technique are the additional chemical requirements and the need to treat waste chemicals from the process.

2.5.2.5. Membrane separation

Membrane separation is another common technique for separation of CO_2 from CH_4. In this method, because of the difference in particle size or affinity, some components of a gas mixture pass through the membrane, while others are retained.

In biogas upgrading applications the membrane sepration technique has a number of advantages, including low energy requirements, safety and simplicity of operation and maintenance without hazardous compounds (Spillman, 1989; Baker & Lokhandwala, 2008; Badenes *et al.*, 2013). According to Baker and Lokhandwala (2008), the membrane method is advantageous economically if the gas volume flow is relatively low and the content of CO_2 is relatively high.

2.5.2.6. Cryogenic separation

Cryogenic separation makes use of relatively low temperatures, close to –90°C, and high pressure, approximately 40 bar (Rajaram *et al.*, 2011). This method is based on differences in the physical properties of methane and carbon dioxide. Methane has a boiling point of –160°C at atmospheric pressure whereas the boiling point of CO_2 is –78 °C (Zhao et al., 2010). Therefore, carbon dioxide can be liquefied and then separated from the remaining gas by cooling the biogas mixture at elevated pressure. Methane can be separated from biogas in the gas or liquid phase, depending on the type of cryogenic system (Kaparaju et al., 2013).

The cryogenic separation technique can achieve a high purity of the upgraded biogas (>97%) together with removal of siloxanes without an additional removal stage (Zhao *et al.*, 2010; Deublein & Steinhauser, 2011). However, this process requires complex equipment *i.e.* compressors, turbines and heat exchangers as well as having a high energy demand (Zhao *et al.*, 2010; Kaparaju *et al.*, 2013). Of the existing techniques being used for biogas upgrading, cryogenic separation is still in the early stages of research and development (Rajaram *et al.*, 2011).

A comparison of some of the most popular biogas upgrading methods taken from various literature sources is summarised in Table 2.2.

Table 2.2 Comparison of various biogas upgrading processes

Techniques	Max. achievable yield (%)	Max. achievable purity (%)	Advantages	Disadvantages
Chemical absorption	90	98	Almost complete H_2S removal	• Only removal of one component in column • Expensive catalyst
High pressure water scrubbing	94	98	• Removes gases and particulates • High purity, good yield • Simple technique, no special chemicals or equipment required • Neutralization of corrosive gases	• Limitation of H2S absorption due to changing pH, • H2S damages equipment • Requires a lot of water, even with the regenerative process
Pressure swing adsorption	91	98	• More than 97% CH_4 enrichment • Low power demand • Low level of emissions • Adsorption of N_2 and O_2	• Additional complex H2S removal step needed
Cryogenic separation	98	91	• Can produce large quantities with high purity • Easy scaling up • No chemicals used in the process	• A lot of equipment is required
Membrane separation	78	89.5	• Compact and light weight • Low maintenance • Low energy requirements • Easy process	• Relatively low CH_4 yield • H_2S removal step needed • Membranes can be expensive

2.5.3 Conclusions on biogas utilisation and upgrading

Biogas from anaerobic digestion has a high potential energy content which can be used in different ways. One effective option is to use biogas as a source of vehicle fuel. In order to do so, however, raw biogas needs to be upgraded to meet the biofuel quality requirements. This is achieved by removing carbon dioxide from the gas, hence increasing the methane concentration.

At present, there are several different upgrading techniques such as pressure swing adsorption, water scrubbing, physical scrubbing, chemical absorption, membrane separation, *etc.* Among them, water scrubbing appears

to be a low–cost and widely used method. In this study, the water scrubbing method was modelled for upgrading of biogas from food waste digestion to produce vehicle fuel.

2.6 Anaerobic digestion modelling

2.6.1 Modelling of the anaerobic digestion process

In order to choose an appropriate anaerobic digestion model for implementation with food waste as a substrate, it is necessary briefly to review the development of modelling, existing relevant models and their applicability to anaerobic digestion.

Modelling of anaerobic digestion has expanded noticeably in recent decades, with a movement towards more complicated biochemical structures. Several anaerobic process models have been developed in the last 40 years including very simple kinetic models used to determine anaerobic rates of degradation of long chain fatty acids as found in (Novak & Carlson, 1970; Graef & Andrews, 1974); and more complex structured models such as Anaerobic Digestion Model No. 1 (ADM1) which has now become a standard model for anaerobic digestion (Batstone *et al.*, 2002). While early models used single stage kinetics to calculate biodegradability and gas flow at steady state, recent models have been implemented to simulate the more complex biodegradation of organic matter under sophisticated anaerobic processes.

In the early studies on anaerobic process modelling carried out by Novak and Carlson (1970) and a few years later by Graef and Andrews (1973), attention was given to the final stage of the anaerobic digestion (methanogenesis) as it was considered rate–limiting, and therefore the most important step of the overall process. Inhibition factors were used in these models to simulate the failure of digestion at high volatile solids concentrations or low pH (Andrews, 1974). Although it was claimed by Graef and Andrews that their model could be used for simulating digester start–up and the response of the digester to organic and hydraulic overloading or entry of an inhibitor, no experimental verification of this model has been made (Lyberatos & Skiadas, 1999).

Later models often built upon prior knowledge, previous models and experimental data collected from real plants, driven by the need to model more complex aspects of the anaerobic degradation process. For example, the process of converting soluble substrate into acetic acid was included in a dynamic model for animal waste digestion (Hill & Barth, 1977), in addition to the methanogenesis process. The problem in this model, however, is that both

hydrolysis and acidogenesis steps were supposed to be inhibited by un–ionised VFAs, whereas these only inhibit the methanogens. The same shortcoming was found in a two–step model of an anaerobic CSTR introduced by Moletta *et al.* (1986), which involved an acidogenesis step that forms acetate from glucose, and has both acidogenic and methanogenic microorganisms inhibited by undissociated acetic acid. Heyes and Hall (1981) considered the dynamics of hydrogen partial pressure and the higher volatile acids (propionate and butyrate) in anaerobic digesters undergoing loading changes. In this model, however, un–ionised VFAs are not considered toxic. Failure was caused by the accumulation of hydrogen, resulting in propionate accumulation and pH drop. While all the models described so far do not take into account the complexity of anaerobic substrates, Bryers (1985) initially proposed a structured model that considers the complex biodegradable organic particulates of wastewater. The model predictions compared well with data from two independent experimental studies. Due to a lack of data, however, the particulate matter, proteins, carbohydrates and lipids are regarded as a single component. This consequently leads to insufficient estimation of hydrolysed products (Gupta *et al.*, 1994; Gavala *et al.*, 2003).

Although the above models were simple and easy to use, their shortcomings made them unable to describe process performance accurately, especially under transient conditions (Donoso-Bravo *et al.*, 2011). Therefore, they are inadequate for further development in this study.

Further microbiological studies led to the emergence of more sophisticated models fulfilling the need to describe more complex aspects of the anaerobic degradation process. These complex models have generally used a structured approach and been orientated towards specific applications.

Angelidaki *et al.* (1993) introduced a model in which the hydrolysis, acidogenesis, acetogenesis and methanogenesis phases occurred in conjunction with four microbial groups: the glucose fermenting acidogens, the propionate degrading acetogens, the butyrate degrading acetogens and the acetoclastic methanogens. Unlike previous models, this proposed free ammonia as an additional factor causing failure of the anaerobic system, besides the two other well–accepted factors of VFA and acetate inhibition. Another advantage of this model was that it allowed the reproduction of empirically–observed behaviour on a computer, in clear and quantifiable mathematical equations. In this model, however, apart from intermediates, all substrate fed to the process were considered as glucose units with associated ammonia. Clearly, this assumption is only acceptable to describe simple wastes such as manure, and could not describe important aspects of more complex wastes containing identified lipids and proteins, such as organic industrial waste, food waste, *etc.* This weakness was

well recognised by the authors and mentioned in an extended model (Angelidaki *et al.*, 1999). The newer model still appears limited, however, as separate hydrogen and glycerol kinetics have been omitted, and the estimation of model parameters was reported as unpredictable (Angelidaki *et al.*, 1999). Despite this, several recent studies have used Angelidaki's model to simulate other anaerobic digestion substrates (Lopez & Borzacconi, 2010; Moya *et al.*, 2012).

Siegrist *et al.* (1993) developed a slightly more complex model for mesophilic sewage sludge treatment. Special emphasis was given to acetate degradation kinetics as the step that determines the stability of anaerobic digestion. The model also considered the involvement of hydrogen–utilising methanogens in hydrogen conversion to methane. Later on, the model was expanded to apply to two–stage thermophilic processes (Siegrist *et al.*, 2002). The order of steps was fixed, however, with the main process mesophilic, and the thermophilic process modelled as a preliminary step. In addition, it seems that using only one set of parameters for both mesophilic and thermophilic conditions in the model may lead to inaccurate results (Siegrist *et al.*, 2002).

A four–step pathway model for the co–digestion of piggery, olive–mill and dairy wastewaters in a CSTR was developed by Gavala *et al.* (1996). The model considers four steps (*i.e.* hydrolysis, acidogenesis, acetogenesis, and methanogenesis) and three bacterial groups (acidogens, acetogens and acetoclastic methanogens). This seems to cover the main developments in microbiological studies; however, the composition of combined wastes was simplified as carbohydrates, proteins and VFA. It was also not able to describe the pH and the biogas composition, and the inhibitory effect of low pH values, while high VFA or ammonia concentrations were neglected (Fezzani & Cheikh, 2008).

All of the models described so far have made significant contributions to the development of anaerobic digestion modelling. Despite the fact that these models were simple and readily usable, they tended to be limited in use due to their adoption of specific substrates and oversimplification of the microbiological mechanisms. Several successful attempts were made to elucidate the mechanisms of biodegradation of complex organic matter, but no appropriate kinetic modelling framework was available (Lyberatos & Skiadas, 1999).

In order to overcome the limitations of previous models, the IWA Anaerobic Digestion Model No. 1 was developed through an international collaboration between leading researchers from multiple anaerobic process technology disciplines. The structure of the model was based on the published IWA activated sludge models (ASMs) that have achieved widespread acceptance by practitioners. Specificities or peculiarities of certain processes were omitted from the model to make it more generic and usable. Since its publication, the model has been widely accepted as a standard platform and

extensively used, analysed, and extended in both academic and practical applications (Batstone & Keller, 2003; Fedorovich *et al.*, 2003; Batstone & Keller, 2006; Lubken *et al.*, 2007; Ramirez & Steyer, 2008; Fezzani & Cheikh, 2009; Gali *et al.*, 2009; Ramirez *et al.*, 2009; Shimada *et al.*, 2011).

A summary of the strengths and weaknesses of the ADM1 model, as reviewed in the literature are summarised in Table 2.3.

Table 2.3. Main strength and weakness of the ADM1 model

	Strengths and weakness	Reference
Strength	It has been accepted as the standard platform for anaerobic digestion of sludge and solid waste in terms of process design and dynamic simulation	(Donoso-Bravo *et al.*, 2011)
	Its mechanisms are well expressed, readily extendible, and give a common basis for further model development and validation studies to make outcomes more comparable and compatible and to assist technology transfer from research to industry.	(Batstone *et al.*, 2002; Freudenthal *et al.*, 2005; Jeong *et al.*, 2005; Batstone & Keller, 2006; Varma *et al.*, 2007; Mata-Alvarez *et al.*, 2011)
	There have been successful models combining ADM1 with other parts of the wastewater treatment plant to simulate the whole system operation.	(Gernaey *et al.*, 2006; Jeppsson *et al.*, 2006; Nopens *et al.*, 2009)
	It can be applied to a range of feedstocks, operating conditions and reactor configurations.	(Batstone *et al.*, 2002)
	A number of researchers have successfully used ADM1 for specific aims. Their findings are useful for reference.	(Batstone *et al.*, 2006; Derbal *et al.*, 2009; Donoso-Bravo *et al.*, 2011)
Weakness	It requires a lot of effort and knowledge to understand and implement.	
	It requires an appropriate and detailed characterisation of the substrate for correct implementation. However, this is a difficult task.	(Huete *et al.*, 2006)
	Some simplifications in reactions are inadequate. For example first–order kinetics may not be suitable to describe the hydrolysis phase since it has been suggested that biomass concentration, substrate and types of material should be taken into account.	(Fernandez *et al.*, 2001; Yasui *et al.*, 2008)
	The original version of ADM1 appeared to contain some discrepancies in carbon and nitrogen balances.	(Blumensaat & Keller, 2005; Rosen *et al.*, 2006)
	It left out some mechanisms or intermediate products such as: nitrate reduction, biomineralisation, H_2S, Phosphorus, *etc.*	(Batstone & Keller, 2006)

Because of the predominant advantages of the ADM1 compared to the disadvantages, as well as its applicability, this model was chosen to modify and implement in this thesis. A conceptual description of the ADM1 model and its problems/shortcomings is presented in section 2.7.

2.6.2 Modelling of anaerobic digestion systems

At the system level, several models have been developed in order to provide tools for design, operation and optimisation of anaerobic digestion systems. They deal not only with the digestion process as a core component, but also with other components of the biogas plant. Some of these also cover the whole waste management system, including waste collection, waste treatment, by–product utilisation and life cycle assessment. The following paragraphs briefly outline some of these models.

A generic model called ORWARE (ORganic WAste REsearch) was developed by Dalemo *et al.* (1997). It consists of several sub–models of the solid management system such as waste collection, a sewage treatment plant, incineration plant, landfill, composting plant, anaerobic digestion plant, truck transport, and transport by sewers. The model was stated to be a tool for organic solid waste management with emissions and energy aspects (Sonesson *et al.*, 1997; Dalemo, 1999; Sundqvist, 2004). Although the model has been considered as a framework for several studies (Dalemo *et al.*, 1997; Sonesson *et al.*, 1997; Dalemo *et al.*, 1998; Bjorklund *et al.*, 1999; Eriksson *et al.*, 2005; Eriksson *et al.*, 2007), it still appears to have drawbacks. For instance, the digestion process sub–component uses an empirical relation to calculate degradation rate from a rate constant (k) and the retention time (R). The value of k is independent of operational conditions such as loading rate, temperature, pH, *etc.* This leads to inadequate values for methane generation in certain conditions. Electricity and heat used in the plant are also assumed to be based on the produced gas and the digester size and retention time. This leads to inaccurate results in terms of energy balance. A report from (Bjorklund, 2000) also revealed several more limitations of the model *e.g.* data for model validation are limited, certain organic substance groups are missing, season–based runs are impossible, *etc.*

A farm–based anaerobic digestion tool was developed at the University of Southampton (Salter *et al.*, 2007; Salter & Banks, 2009; Banks, Salter, *et al.*, 2011; Jain *et al.*, 2011; Jones & Salter, 2013). The tool was designed for analysing the mass and energy balance of anaerobic digestion systems. It addresses some aspects of transportation, digestion, dewatering, upgrading processes, embodied energy and CO_2 emissions in order to achieve a usable

model for mass and energy prediction (Salter *et al.*, 2007; Salter & Banks, 2009). A new waste–based version of the model was recently released (Salter *et al.*, 2013). Although the tool is quite simple and implemented in MS Excel which is easily accessible for users, it is a static spreadsheet. Therefore, while it can provide the ultimate results, it does not represent intermediate products or even final results under transition conditions.

Another model called the '*Methane Energy Value Model*' (MEVM) was introduced by Amon et al. (2007). Its aim was to optimise biogas production by estimating the methane yield of different agricultural substrates (*e.g.* maize, cereals, grass), the nutrient requirement for anaerobic digestion, electricity used and generated, harvesting energy consumption, *etc.* The model is rather simple, however, as it mainly estimates methane production from Buswell's equation (Symons & Buswell, 1933) with some validation from crops, and its statistical analysis of methane yields is currently only relevant to maize and cereals.

A computer–based life cycle assessment model called EASEWASTE was developed at the Technical University of Denmark for evaluating the overall resource consumption and environmental impacts of municipal solid waste management systems (Kirkeby *et al.*, 2006a). The model considers environmental impacts from waste generation, collection, treatment and disposal. According to the developers, the model is suitable for evaluating the overall environmental consequences of different waste management strategies and technologies, and can be used for most waste material fractions in household waste (Kirkeby *et al.*, 2006b). While the aim of this thesis is to focus on biogas plant systems, the anaerobic digestion treatment process implemented in EASEWASTE has been described as a black box with no supporting information (Hansen *et al.*, 2006). This makes it on the one hand difficult to understand, and on the other hand unverifiable.

In order to simulate the interaction of the different processes involved in the biogas plant system (*i.e.* biogas generation, energy conversion, residual digestate and energy requirement, *etc.*), an integrated model has been developed at the University of Kassel. The model combines separate modules programmed in Excel, VBA, LandSHIFT, Umberto and MapPoint to cover different parts of the agricultural waste system including cultivation of energy crops, the biochemical process of biogas generation and the utilisation of digestate. The model and its subsystems simulate different stages of the biogas system to get data and provide evaluation (Schaldach *et al.*, 2010). However, the model development adhered to the German biogas system and may not share the same configurations with biogas system world wide. Additionally, the

model's components are closed and no information can be found relating to the biogas generation prediction. Hence, this model appears to be inaccessible.

As a part of the of LCA series, the Integrated Waste Management (IWM) model was developed by McDougall and White (2001) to apply in the assessment of environmental and economic impacts from changes in waste systems. In this model the whole waste system was considered, from collection, sorting, treatment method *e.g.* composting and anaerobic digestion, nutrient content as commercial fertilisers (N, P_2O_5 and K_2O), and air emissions from the fertiliser–to–land process. The model is based on summing up farm–based inventories to get the data, however, and it does not include biochemical and physical processes or equipments in the biogas plant.

Overall, although the models described are proposed as LCA tools, none of them looks in detail at the biogas plant or the important component of the anaerobic digester. Moreover, it may appear to users that they are tools that can accomplish '*everything*' with regard to environmental assessment; but because they attempt to include the whole life cycle, and all environmental issues, they cannot deal with each unit comprehensively. Moreover, many of these systems' boundaries are far beyond the proposed boundary in this study (Figure 3.1) and therefore, none of them are appropriate for application.

2.6.3 Conclusions on modelling

A review of anaerobic digestion modelling at both process and system level shows that a number of models have been developed in order to represent effectively one or more components of the biogas systems. Nonetheless, to date, not many of them are relevant or worthwhile to apply to anaerobic digestion of food waste without major modifications and extension, especially at a system level. It appears, however, that the ADM1 platform can be used as a sensible choice for the food waste digestion model.

2.7 ADM1 model

As mentioned previously, the ADM1 model was developed by the IWA task force for Anaerobic Digestion Modelling. Its goal was to provide a generic and widely applicable mathematical description of the anaerobic digestion of organic substrates. The following is a brief description of how the model works and a review of its applications to date.

2.7.1 Conceptual modelling of ADM1

Originally, the ADM1 model consisted of descriptions of 7 groups of bacteria and archaea, 19 biochemical process rates, 24 components (12 soluble & 12 particulate elements), 3 gas–liquid transfer kinetic processes, and 6 acid–base kinetic processes together with a set of 105 kinetic and stoichiometric parameters/variables (Batstone *et al.*, 2002; Kleerebezem & Loosdrecht, 2006).

2.7.1.1. Conversion processes

As noted in section 2.2.1, the anaerobic digestion process is commonly described as consisting of four stages: hydrolysis, acidogenesis, acetogenesis and methanogenesis. It was thought, however, that a disintegration phase should precede the more complex hydrolysis steps, and also generally be used when the primary substrate can be represented with lumped rate and biodegradability constants. Hence, the disintegration step is intentionally included in the model as well as the four others. These physico–chemical and biochemical conversions are summarised in Figure 2.5 which is adapted from various sources, with the intended modifications for this study.

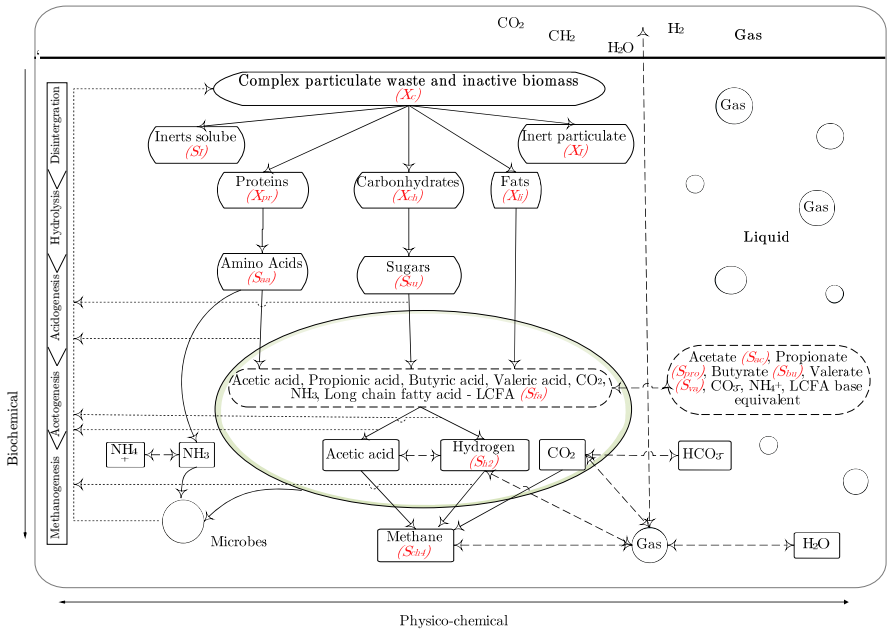

Figure 2.5 Biochemical and Physicochemical conversion processes adopted in ADM1. Adapted from (Batstone *et al.*, 2002; Parker, 2005; Demirel & Scherer, 2008; Lier *et al.*, 2008)

Note that the physicochemical reactions are reversible, whereas the biochemical reactions are not; this is indicated by two–way and one–way arrows, respectively. The model includes acid based equilibrium reactions and gas–liquid mass transfer.

Disintegration is taken as the first step of the anaerobic digestion conversion from biomass to methane. It provides the substrates for hydrolysis. Unlike the other steps, disintegration is an extracellular biological and non–biological processes mediating the breakdown and solubilisation of complex organic matter (Batstone *et al.*, 2002). Investigations showed that the rate of this process varies and depends on the feedstock characteristics and the condition of the inoculum. The first–order kinetic equation has been widely accepted for describing the process. This is rational since first–order kinetics have been established by observation, and because the diversity of disintegration processes cannot support a different, more fundamental approach (Batstone *et al.*, 2002). For solid waste, a disintegration constant (k_{dis}) of about 0.5 day^{-1} is suggested (Mata-Alvarez, 2001).

The first–order kinetics of organic material disintegration are expressed in ADM1 as follows:

$$r_{dis} = -k_{dis} X_C \tag{2.6}$$

Where X_C is complex particulate organics, kgCOD m^{-3}; k_{dis} is the first–order disintegration constant, day^{-1}.

Overall, processes in ADM1 can be grouped into three types: biochemical, physico–chemical, and mass transfer processes. The biochemical series are catalysed by intra– or extracellular enzymes produced by microorganisms which degrade stepwise soluble and particulate substrates for digestion, and finally produce carbon dioxide and methane. The decay of biomass and hydrolysis of particulates are processes of this type. Physico–chemical reactions mainly refer to the acid–base equilibrium (ion associations/dissociations). The mass transfer process refers to the transfer between gas and liquid phases.

In the ADM1 model, COD (kgCOD m^{-3}) was defined as the chemical component base unit. As exceptions, inorganic carbon (HCO_3^- and CO_2), and nitrogen (NH_4^+ and NH_3) were designated in kmoleC m^{-3} and kmoleN m^{-3}, respectively.

2.7.1.2. Process matrix (Petersen matrix)

The Petersen matrix has been used successfully in developing the ADM1 model. Components presented in ADM1 are broadly classified into two categories: soluble components and particulate components. Behaviour of components in the model are represented by defined state variables. The ADM1 model makes use of chemical oxygen demand (COD) balance for

describing all organic species and molecular hydrogen. However, nitrogenous and inorganic carbon groups are described as their molar concentrations (Lier *et al.*, 2008).

In the model, soluble components are assumed to be monomers of complex polymers (amino acids, long chain fatty acids, sugars), volatile organic acids (propionate, butyrate, valerate, acetate), hydrogen and methane and carbon dioxide. Whereas biomass and particulate substances include sugar fermenters, amino acid fermenters, LCFA oxidisers, butyrate and valerate oxidisers, propionate oxidisers, acetoclastic methanogens and hydrogenotrophic methanogens. Non–microbial particulate components are presumed to be composites including: carbohydrates, proteins and LCFAs from disintegration process, organics matter from influent flows or the death and decay of microbial species. (Batstone *et al.*, 2002; Parker, 2005).

In the model, a particulate component is denoted by X, whereas a soluble component is denoted by S. In this way, the components are separated into two main groups: particulate components (Xi) and soluble components (Si). Components are assigned the index i, while the processes are assigned the index j; kinetic expressions for each process (ρ_j) are described in the right–hand side. The mass relationship between the system components in each process is specified by stoichiometric coefficients (v_{ij}). For example, uptake of acetate (–1) results in the growth of acetate consumers (Y_{ac}) and production of methane ($1-Y_{ac}$). Obviously, all elements in each process are expressed in the same unit (kgCOD), and the sum of the stoichiometric coefficients in each row is zero. In other words, the COD balance is maintained for all processes.

The Petersen matrix of the processes and components in ADM1 model with extensions developed in this study is shown in Appendix A.

2.7.2 Current application, problems/shortcomings of ADM1

Because the ADM1 model is quite complex, it requires considerable manual effort and extensive expertise to implement. For instance, to find the best set of kinetic parameters for anaerobic digestion of food waste or to determine which parameters are the key ones controlling each process are not easy tasks. Published investigations can help in dealing with these difficulties and decrease the implementation workload: a review of previous work was therefore conducted.

2.7.2.1. Process mechanisms and inhibition factors

The ADM1 model purposely excludes various mechanisms or intermediate products which may be important in some scenarios. For example, although phosphorus is critical in simulating wastewater treatment, this component is not included in the model. Likewise, inhibition by H_2S, nitrate reduction, inhibition by LCFAs, and competition between homoacetogens and autotrophs have been omitted. These omissions were made for several reasons: some intermediates can either be lumped with other stage variables, as in the case of lactate; or deemed of little significance under normal conditions *e.g.* ethanol which occurs in very low concentrations at typical operating pH. Others were neglected purely to simplify the complexity of the model.

Currently, ADM1 has no hydrogen regulation to influence the fraction of VFAs from sugars, and instead this is implemented only by fixed stoichiometry. This is inadequate to the actual acidogenic processes in most systems, since it is known that the stoichiometry of glucose fermentation is a function of pH, concentration products and other environmental conditions (Batstone & Keller, 2006; Rodriguez *et al.*, 2006).

The presence of the acetate oxidation pathway in conjunction with the competition between two groups of methanogens (*i.e. Methanosaeta sp* and *Methanosarcina sp*) was reported in an investigation of the effects of acetoclastic methanogen population dynamics on mesophilic digester stability using the ADM1 model (Straub *et al.*, 2006). This was confirmed later by Shimada *et al.* (2011) with a modified version of ADM1 with extensions for syntrophic acetate oxidation to describe the reduction in acetoclastic methanogens and the dominance of hydrogen–utilising methanogens. This study used sludge as a substrate, however, and only focused on two–phase (acid–phase) anaerobic digesters to confirm the shift between acetoclastic and hydrogenotrophic methanogenesis in the digester.

Some modified versions of ADM1 have introduced inhibition factors to the model as recommended by the original authors (Batstone *et al.*, 2006). Derbal *et al.* (2009) added an inhibition process to account for the toxic effects of cyanide on acetate concentration. Boubaker and Ridha (2008) changed the rate of acetate uptake from the original ADM1 model by adding an inhibition equation representing the effect of the total VFA inhibition constant on methanogenesis. It was stated that without adding this inhibition term, the original ADM1 model could not predict reactor failure at short HRT. Likewise, Fedorovich *et al.* (2003) included an inhibition term for undissociated H_2S in their modified ADM1 model.

2.7.2.2. Adapting parameter values to experimental data

A common practice in implementation of ADM1 is to change default kinetic parameters to give the best fit to experiments with different substrates. Parker (2005) ran the original ADM1 model using data from a mesophilic single–stage reactor study conducted by Rivero *et al.* (2002) and found that in conditions where there is substantial solids destruction the model under–estimated ammonium–nitrogen concentration. It was suggested that the lack of a nitrogen mass balance in the ADM1 model or inadequate assumptions on the actual protein content of the substrate might cause the differences. Also, it was recommended that the model does not incorporate a pH function for the disintegration and hydrolysis processes. The ammonia and TKN concentrations in the feedstock need to be well characterised because of their impact on pH buffering and inhibition functions. Analysis in this study showed that with its default parameters, ADM1 clearly over–predicted the concentration of acetate while under–predicting the concentrations of propionate, butyrate and valerate. Parker suggested that this may have resulted from under–estimation of the substrate consumption coefficients for acetoclastic methanogenesis or overestimation of the inhibition of this activity by ammonia. This could be corrected by two modifications: (*i*) reduce the half saturation coefficient of acetate ($K_{S,ac}$) and increase the half saturation coefficient of propionate/butyrate ($K_{S,pro}$, $K_{S,c4}$), (*ii*) increase the ammonia inhibition constant and decrease the hydrogen inhibition constant. Regarding half saturation coefficient values, Batstone and Keller (2006) reviewed several studies and suggested that adapted parameters may be necessary in some applications. In addition, it was suggested that it is feasible to increase the decay rate while simultaneously increasing the uptake rate to gain the expected outputs.

Other similar studies can be found in the literature (Blumensaat & Keller, 2005; Lee *et al.*, 2009; Zaher, Buffiere, *et al.*, 2009; Kerroum *et al.*, 2010; Astals *et al.*, 2011).

2.7.2.3. Feedstock characterisation

The complexity of the ADM1 feedstock characterisation and the general lack of information on methods of characterisation made feedstock fractionation problematic (Huete *et al.*, 2006; Johnson & Shang, 2006). Many authors have complained that the feedstock characterisation in ADM1 required far more information than is commonly available, and therefore estimation of feedstock parameters is often challenging (Parker, 2005; Johnson & Shang, 2006; Lubken *et al.*, 2007; Fezzani & Cheikh, 2009). While the ADM1 model takes input values in terms of CODs, solid wastes are often characterised by volatile solids

content (VS). Hence, there is clearly a need for a standardised protocol for characterising the influent substrates, since inadequate estimation of inputs could result in incorrect predictions of outputs (Parker, 2005).

In response to these criticisms, there have been various attempts to address this problem. Angelidaki and Sanders (2004) suggested equations to determine the relation between COD and VS content based on the stoichiometric relationships between completely oxidized waste molecules and the oxygen necessary for complete oxidation. Nopens *et al.* (2009) developed a tool based on concepts proposed previously by Copp *et al.* (2003) for estimation of secondary components (carbohydrates, proteins and lipids) from composite particulates. This tool was stated to be suitable for a range of wastewater biosolids, resulting in realistic gas production without the need for extensive parameter calibration.

Kleerebezem and Loosdrecht (2006) suggested a method for generating ADM1 input for wastewater characteristics using a limited set of measurements including COD, TOC, organic nitrogen (*i.e.* Kjeldahl nitrogen corrected for ammonium) and total alkalinity. An elemental balance was then computed using stoichiometry, electron balancing and carbon valence balancing, and used to derive a substrate characterisation that can be employed in ADM1.

Huete *et al.* (2006) described a systematic methodology to characterise the influent sludge components from the experimental parameters traditionally used in wastewater for the ADM1 model. Their report indicated that some components are inadequately defined in ADM1 and can be optimised by using the proposed mathematical algorithms.

Several other methods of substrate characterisation can be found in the literature (Lubken *et al.*, 2007; Wichern *et al.*, 2009; Koch *et al.*, 2010; Rojas *et al.*, 2011; Zhou *et al.*, 2011; Girault *et al.*, 2012).

To date, the most complicated model for solid waste characterisation was developed by Zaher and Chen (2006). It is based on the Continuity–Based Interfacing Method (CBIM) proposed by Vanrolleghem *et al.* (2005) to determine ADM1 inputs in terms of carbohydrates, proteins and lipids. This tool was later improved (Zaher, Buffiere, *et al.*, 2009), and became popular under the name '*Transformer*' (Zaher *et al.*, 2007). Manure and different food waste types were used to test the model scenarios. The results showed that applying food waste characteristics generated from the *transformer* to ADM1 can lead to better results and accuracy compared to other characterisation methods.

The *transformer* allows generation of 32 required input parameters for ADM1 from complex substrates such as food wastes. These parameters are estimated through the input of 11 key parameters. This development helps to reinforce the link between ADM1 and the commonly measured characteristics of solid wastes. The transformer was programmed in C and incorporated into a General Integrated Solid Waste Co–Digestion model (GISCOD) which runs in Matlab–Simulink (Zaher, Li, *et al.*, 2009). The transformer itself is quite easy and straightforward to use: it originated in Microsoft Excel and users simply need to input the 11 required elements into a spreadsheet. Another good aspect of the transformer is that it maintains the mass balance and COD balance according to a predefined, ordered maximisation procedure.

In order to make use of the transformer for food waste digestion, the 11 following characteristics are required: Particulate COD (CODp), Soluble COD (CODs), Volatile Fatty Acids (VFA), Total Organic Carbon (TOC), Total Organic Nitrogen (Norg), Total Ammonia Nitrogen (TAN), Organic Phosphorus (TP–OrthoP), Ortho–Phosphate (orthoP), Total Inorganic Carbon (TIC), Total Alkalinity (Scat) and Fixed Solids (FS).

So far, this tool has been successfully used by several authors to produce influent substrate characteristics for ADM1 implementation. Curry and Pillay (2012) applied the transformer for biogas prediction and design of a food–waste–to–energy system, and confirmed that this tool allows ADM1 to give more accurate biogas estimates. Ozkan-Yucel and Gokcay (2010) used the transformer for a model of a full-scale anaerobic digester under dynamic organic loading conditions.

Based on the above, the *transformer* was used in the current work to generate the concentration of soluble/particulate components in food waste substrate.

2.7.2.4. Carbon and Nitrogen balance

The problem of the nitrogen and carbon balance in the original ADM1 model has been well recognised by many authors (Blumensaat & Keller, 2005; Rosen & Jeppsson, 2005; Batstone & Keller, 2006; Kleerebezem & Loosdrecht, 2006; Ozkan-Yucel & Gokcay, 2010). The nitrogen content of particulate composites in the original ADM1 was not consistent with the nitrogen content of the degradation products, resulting in a surplus of 0.1 moles of nitrogen for every kgCOD disintegrated (Rosen & Jeppsson, 2005). Subsequently, this

required an adjustment of the nitrogen content of composites (N_{xc}) to prevent surplus nitrogen from being formed.

The uptake of sugars, amino acids, propionate, acetate and hydrogen all consume or produce inorganic carbon. This is reflected for all state variables in the original version of ADM1 in the following equation:

$$\nu_{10,j} = \sum_{i=1-9,11-24} C_i \nu_{10,j} \tag{2.7}$$

Where C_i represents the carbon content of component i, kmoleC kgCOD^{-1}; $\nu_{10,j}$ is the inorganic carbon coefficient for process j.

When biomass decays, it is presumably converted into particulate composites (see Figure 2.5). However, the carbon released from the decay of biomass is lost due to a discrepancy between the carbon content of biomass C_{bac} (0.0313 kmoleC kgCOD^{-1}), and of influent particulate composites C_{xc} (0.03 kmoleC kgCOD^{-1}). Similarly, a discrepancy can be found in the nitrogen content of biomass and particulate composites, which is 0.00625 kmoleN kgCOD^{-1} and 0.002 kmoleN kgCOD^{-1}, respectively. This requires an adjustment to the inorganic carbon and inorganic nitrogen entries of the rate coefficient matrix in order to achieve more accurate results. The method for carbon and nitrogen balance is presented in Chapter 3.

2.7.2.5. Heterogeneity and flocculation

In digesters, both solid substrates and microbial distribution are heterogeneous (Batstone *et al.*, 2002; Holm-Nielsen *et al.*, 2006; Picioreanu *et al.*, 2008; Zaher, Buffiere, *et al.*, 2009). This raises a number of issues. On the one hand, differences at a very small scale in parameters such as pH, gas concentrations etc., may be highly significant for the microbial syntrophy that is essential for effective digestion. On the other hand, values for these and other parameters measured at specific positions in a digester may not be representative of the whole digester contents for modelling purposes. Consequently, a model using these monitored parameters for validation may not replicate correctly the real process, especially in large-scale digesters. Ideally, therefore, it is preferable to take into consideration the heterogeneity of the system, at least at the medium scale. In practice, however, this is presents considerable difficulties. Firstly, from a modelling point of view, when considering the digester there is a requirement to increase significantly the number of sampling points and thus the amount of analytical data required to set up and validate the model (Zaher, Buffiere, *et al.*, 2009; Fdez.-

Guelfo *et al.*, 2011). Moreover, consideration of the heterogeneity of substrates leads to difficulties in defining their characteristics, and hence in specifying the kinetics of hydrolysis of their components in terms of carbohydrates, proteins and lipids (Blumensaat & Keller, 2005). Heterogeneity may also affect the diffusion resistance involved in transport phenomena among different phases (Tomei *et al.*, 2009). To date, however, no comprehensive studies have been carried out that fully quantify the impact of heterogeneity on the anaerobic digestion process, either in terms of empirically-determined performance or through quantitative modelling. For these reasons, in the ADM1 model, complex particulate waste is assumed to be a homogeneous mass which disintegrates to carbohydrate, protein and lipid particulate substrate, and the heterogeneity of the medium is not considered (Batstone *et al.*, 2002). This assumption is a shortcoming in the ADM1 model; but in the current work, as in previous studies by Fdez.-Guelfo *et al.* (2011) and Palanichamy and Palani (2014), no attempt was made to incorporate the concept of heterogeneity due to the difficulties in validating such an approach.

Heterogeneity and mass transfer also need to be considered in flocculated or granular biomass. Flocculation is the process of forming larger composite particles from smaller particles via various physical, chemical, and biological interactions (Liss *et al.*, 2004). Microorganisms such as bacteria, algae, fungi and actinomyces have been identified as capable of producing bioflocs (Subramanian *et al.*, 2009). Typically, bioflocs are formed in different shapes and sizes depending upon temperature, pH, solid retention time, initial total solids, mixing, concentration of organic and inorganic substances, metals and the presence of divalent cations (Subramanian *et al.*, 2009; Siles *et al.*, 2010). Floc formation in conjunction with the immobilisation of bacteria in bioflocs influences the COD removal efficiency in digesters (Pant & Adholeya, 2007), depending on the digester configuration (Snape *et al.*, 2008).

Within digesters, reaction rates are subject to mass transfer limitations which are dependent on the size and characteristics of the bioflocs. Substrates are conveyed by convection from the liquid phase to the exterior diffusion layer, followed by external mass transfer from the diffusion film to the surface of the biofloc. Finally, due to the concentration gradients in flocs, internal mass transfer is required to diffuse the substrates (Snape *et al.*, 2008). The mass transfer mechanism for substrates into bioflocs is presented in Figure 2.6.

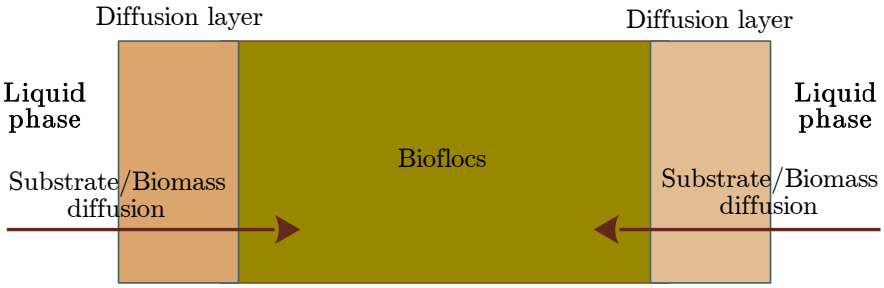

Figure 2.6. Mass transfer for substrates into bioflocs.
Adapted from (Snape *et al.*, 2008)

Mass transfer of substrates into biological flocs within anaerobic digesters may be an important factor which should be included in advanced modelling of digestion processes. It has, however, been omitted not only from the original ADM1 but also from subsequent modified versions of the model. The reason for this is again probably due to the lack of adequate validation data and limitations in the underlying knowledge of the causes and functionality of flocculation and bioflocs in anaerobic digestion. Therefore, although this phenomenon may have an impact on modelling outcomes, especially in dynamic simulations, it has not been taken into account in the current study.

2.8 Software evaluation

For modelling of a complex system, a single piece of software may be insufficient and different components may need to be combined to create a powerful interoperable tool (Gosling, 2005). Although the ADM1 model is the best modelling tool to describe anaerobic digestion, it is only a theoretical platform without any capacity for biogas plant simulation. Hence, it is necessary to integrate ADM1 into other simulation software to simulate a biogas plant.

Before commencing on the development of a tool for simulation of biogas systems and assessment of energy balances, it is worth evaluating the potential suitability of commercially available software packages. Some purpose–built software was assessed as it has been suggested that this may be a good solution for flowsheet simulation (Gosling, 2005).

Although various modelling tools are available from the flowsheeting simulation market, only five of the most relevant packages were evaluated: UniSim, gPROMS, CHEMCAD, SuperPro Designer and Aspen Plus. The aim was to choose the most appropriate tool for process simulation. The choice of

the software was based on the required details for process equipment, thermodynamic package, capabilities, previous research in pertinent topics, and cost.

2.8.1 UniSim

UniSim Design Suite is provided by Honeywell. The providers say it is an intuitive and interactive process modelling software that enables engineers to create steady–state and dynamic models for plant design, performance monitoring, troubleshooting, operational improvement, business planning, and asset management (Honeywell, 2011). A noticeable feature of UniSim is its interoperability, in other words, it can be integrated with other tools (Ramachandran, 2008). However, the unit operation models it offers are mainly from the oil and gas, refining, chemical and petrochemical process industries (Coker, 2010).

In the field of anaerobic digestion, only a few UniSim design applications have been reported: optimal design and operation of a gas–to–liquid process (Rafiee & Hillestad, 2010), and operation of solid oxide fuel cells on anaerobically–derived wastewater treatment plant biogas (Lackey, 2012). Milledge (2013) used UniSim and an excel spreadsheet to build a tool for assessment of the energy balance of an algal biofuel production system. After reviewing the literature and communication with Honeywell's staff, however, he concluded that UniSim does not have all of the unit operations required for simulation of anaerobic digestion. Although users can create custom unit operations, property packages and kinetic reactions to meet their purposes, this could take a significant amount of effort and time.

2.8.2 gPROMS

gPROMS is a general process modelling system for simulation, optimisation and control (both steady state and dynamic) of highly complex processes (PSe, 2011). It is described by mixed systems of integral, partial differential, and algebraic equations (IPDAEs). gPROMS defines a dual description for processes as MODELs and TASKs. The former contain IPDAEs which allows users to represent the physical, chemical and biological behaviour of the process and the later operate on MODELs and represent the operating procedures that are used to run the simulation (Mujtaba, 2012).

One interesting feature of gPROMS is that it offers extensive methods for linking to external software platforms *e.g.* Aspen Plus flowsheet (Gosling,

2005). Furthermore, a significant advantage of gPROMS is that its libraries of common process models can be extended and customised to ensure applicability to the specific requirements through gPROMS ModelBuilder environment (Leineweber *et al.*, 2003; Klemes, 2011; Lam *et al.*, 2011). Despite the fact that this component can be a flexible tool for engineers to generate optimised models (Lam *et al.*, 2011), the manual code for flexible equation–based units in gPROMS comes with little or no guidance or help, is time consuming to use and errors are easy to make (Clark *et al.*, 2000). In addition, previous research by Oddone and Iribarren (2002) noted that implementation of the modular structure in gPROMS caused problems since variables and parameters must be defined in a global way, *i.e.* it does not allow re–definition of the type of variables in blocks independently. They also mentioned that the scheduling is a result of the optimisation and cannot be handled from outside. Another drawback of gPROMS is that it does not provide a mass and energy balance feature (Gosling, 2005). Additionally, it requires customisation for unit operation models for bioprocess applications which brings many explicit problems, as already mentioned.

Within the literature several attempts have been made to use gPROMS in anaerobic digestion applications. For instance, a dynamic model of real biological reactors for the treatment of complex substrates (Mussati *et al.*, 1998); modelling of soluble microbial products in anaerobic digestion to measure the effect of feed strength and composition (Barker & Stuckey, 2001); energy efficiency in wastewater treatment plants through an activated sludge process coupled with anaerobic digestion (Descoins *et al.*, 2012). Similarly, Fuentes *et al.* (2013) used gPROMS to perform the dynamic optimisation of bio–hydrogen production and C–N removal in combined anaerobic–aerobic systems: in this study, however, ADM1–based and ASM3–based kinetics models had to be integrated into the gPROMS platform to simulate anaerobic and aerobic reactors, respectively.

2.8.3 CHEMCAD

CHEMCAD is a software tool provided by Chemstations. It is capable of modelling continuous, batch and semi–batch processes, and can simulate both steady–state and dynamic systems (Chemstations, 2011). In addition, the application of CHEMCAD for gas refining has attracted attention from users. Besides, its interactive interface allows unit operations run individually to produce a flowsheet for quick "*what–if*" scenarios.

CHEMCAD, unlike other software like Aspen Plus and gPROMS, does not support an optimisation capability using SQP based algorithms, instead leaving users to examine the potential solutions (Bogle & Cameron, 2002).

Several applications have been reported using CHEMCAD for anaerobic digestion and biogas purification *e.g.* H_2S removal using Biofiltration (Fischer, 2010), flowsheet simulation of biogas upgrading via a membrane process (Molino *et al.*, 2013), purification of biogas using aqueous amine solutions (Gawel, 2012), and conceptual design of a hydrogen production process from bioethanol reforming (Cormos *et al.*, 2013). Beam (2011) used CHEMCAD to estimate the concentration of CO_2 dissolved in the liquid phase in an anaerobic digester during methane production which was then used for AD process optimisation. Thus, while some models of a digester simulated in Aspen Plus were found in the literature, none have been carried out in CHEMCAD.

For gas process applications, CHEMCAD has been described as the most accurate tool as it employs electrolyte reactions together with thermodynamic models (Andersson & Johnsson, 2006). Noticeable drawbacks of CHEMCAD, however, are that it omits economic analysis and lacks an expert guidance system (Spooner, 1994).

2.8.4 SuperPro Designer

SuperPro Designer is a flowsheet modelling software that is stated by the manufacturer Intelligen to facilitate modelling, evaluation and optimisation of integrated processes in a wide range of industries including water and wastewater treatment, waste management and environmental impact assessment (Intelligen, 2011). The software allows the study of various process configurations by providing different types of bioreaction kinetics and removal mechanisms. It is also noted that common types of anaerobic digester *e.g.* CSTR, Batch, Plug–flow, equilibrium reactors, and absorber/stripper reactors are available for simulation (Flora *et al.*, 1998).

SuperPro has been reported to give successful process simulation in fuel ethanol production (Kwiatkowski *et al.*, 2006); analysis of biodiesel production costs (Haas *et al.*, 2006); and waste–to–energy bioreactors (Malakahmad *et al.*, 2012).

Generally, SuperPro appears to be versatile but some drawbacks should not be ignored. Although SuperPro includes an economic analysis feature, sufficient and relevant information to nourish its databank library from proper estimation models and actual equipment manufacture is required (Meireles, 2009); this may result in uncertainty (Heinzle, 2006). Additionally, although

the software can produce material and energy balances for both continuous and batch systems, it is incapable of simulating a dynamic system (Gosling, 2005; Julien & Whitford, 2007). Therefore, further investigation of SuperPro software was terminated.

2.8.5 Aspen Plus

Aspen Plus is an interactive and flexible process modelling tool for conceptual design, optimisation, process operational improvement and asset management for the chemical, polymer, specialty chemical, metals and minerals, and coal power industries. It belongs to the sequential modular class of simulators with a loop analyser to handle recycle streams. The Aspen system has a library of various common industrial operations which are called built–in modules. By interconnecting the modules using material, work and heat streams, process flowsheets can be constructed. Each module in Aspen provides an integrated FORTRAN and Excel environment for calculation or customisation. Unlike the UniSim software which offers a simple spreadsheet calculation, the spreadsheet environment in Aspen is more functional and can link to a simulation via a user model (denoted as a "USER2" block) to deal with more complicated spreadsheet models.

Aspen Plus also includes a large database of pure components and phase equilibrium data for conventional chemicals, electrolytes, solids and polymers. This database is updated regularly by the US National Institute of Standards and Technology.

Aspen Plus has some drawbacks: it is complicated and requires considerable effort to handle, it does not contain biological components/database therefore users have to program their own components/models; however, many advantages of the software should be taken into account. It:

- provides a wide range of built–in models for instant use: pumps, compressors, mixers, separators, reactors, heat exchangers, *etc.;*
- can be enhanced through a number of optional add–on applications such as Aspen Plus Dynamic, Aspen Energy Analyzer, Aspen Custom Modeler, *etc.*;
- offers the option of using other programs or programming languages such as Excel, Fortran, Visual Basic, Matlab to expand Aspen's features;
- allows building up large flowsheets a few blocks at a time;

- has the world's most extensive property database and powerful flexibility in handling solid, fluid and gas phase processes;
- provides a high level of adjustment options by means of parameterisation, and the level of detail can be chosen easily;
- has an integrated Activated Economics tool allowing insight into capital and operating expenses directly from the flowsheet;
- has been widely applied in industrial and academic process simulation and design. For example, simulation of cogeneration plants (Zheng & Furimsky, 2003), biomass gasification systems (Nikoo & Mahinpey, 2008; Paviet *et al.*, 2009), a waste incineration process with flue gas cleaning and heat recovery sections (Cimini et al., 2005), and thermodynamic simulation and evaluation of a steam CHP plant using Aspen Plus (Ong'iro et al., 1996).

Although it is difficult to model a complex AD process in Aspen Plus, as biological processes are not integrated in the Aspen system, to date several attempts have been made to simulate biogas plants or their components such as the AD process, gas upgrading process, or CHP units.

Loeser and Redfern (2010) used Aspen Plus for steady–state modelling and simulation of a biomass generation plant at micro–scale level. The main intention of the model was to investigate the thermal optimisation of the energy demands of a real digester. In this study, instead of modelling all occurring reactions, the author neglected microbial reactions and used performance data available in the literature to simulate the digester with the assumption that a certain amount of biomass intake is converted into biogas.

Hoffmann *et al.* (2013) used Aspen Plus to simulate an integrated hydrothermal liquefaction and biogas plant for bioenergy production from manure. In this study Aspen models were used to simulate a digester, CHP and upgrading processes. Although this study tried to build some of the main components of biogas plant, it had many limitations: *e.g.* the whole system is a steady–state process without the potentially complex considerations of dynamics; the digester model was based on stoichiometric reactions; and in the upgrading unit only three oxygen–eliminating reactions for the fatty acid model compound have been taken into account.

Recently, Rajendran *et al.* (2014) used Aspen Plus to simulate the anaerobic digestion process for prediction of biogas production with various substrates in given process conditions. This model is able to act as a library package with intermediary reactions, inhibitions, and kinetics for further AD

simulation. It has not been developed to predict and understand the mechanism of AD, however, and ignores other components of the process such as pH, alkalinity, nitrogen concentration, VFA, *etc.*

Aspen proposes a modular modelling approach and allows users to choose models from fixed black box units in a library. Code is generated automatically, therefore the system can give increased confidence in the design without mistakes from programmers (Clark *et al.*, 2000).

Hence, compared to the other flowsheet simulation tools reviewed, Aspen Plus was chosen because of its explicit advantages, frequency of use and as it provides a large number of built–in models that are beneficial for creating a realistic system.

2.8.6 Conclusions from software evaluation

Evaluation of some of the most well–known models showed that the three models UniSim, gPROMS and Aspen Plus seem to be capable of producing a dynamic model of an anaerobic digestion system. For mass and energy balance purposes, however, only UniSim and Aspen Plus meet the aim. Even so, both of these require customisation in order to model bio–processes in reactors. Although UniSim could be capable of dealing with this problem, a very considerable amount of time and effort could be needed. Moreover, guidance material for building up user–created units in UniSim is limited; whereas many documents and examples for modelling user–models in Aspen Plus are available and free for access. This can obviously save time and effort. Moreover, Aspen Plus provides flexible methods to exchange data with other software such as Microsoft Excel, Matlab, *etc.* For example, an Excel spreadsheet can link directly to Aspen process flowsheet or via Aspen Simulation Workbook (ASW). Therefore, Aspen Plus was chosen for the current study.

2.9 Conclusions from literature review

World–wide energy demand coupled with concerns about greenhouse gas emissions has stimulated international interest in untapped sourxes of renewable energy such as degradable organic materials. In this context, anaerobic digestion offers a useful energy production technology. Food waste, a substrate with high energy potential, can be converted successfully by this technology to produce biogas. In an AD plant, biogas from the digestion process can be used in different ways such as: generating heat and electricity by

CHP unit, producing heat from a boiler unit, cleaning for fuel–grade methane production. Several of these methods can be combined and work simultaneously in biogas plants. If heat and electricity are generated they can be used not only for internal purposes such as to heat the digesters and pasteurisers, to run mixing systems, compressors, pumps, fans, *etc.*, but also for external utilisation. Enhanced biogas with a high methane content achieved by means of an upgrading process can be used for gas–grid injection or vehicle fuel.

For high efficiency in operating a biogas plant treating food waste substrate, an adequate knowledge of the options for design, control and operation of the system is essential. This could be achieved by using appropriate models that can deal with elements of the system individually and in combination. Nonetheless, to date, there is no satisfactory model which can simulate the anaerobic digestion of food waste adequately at an AD plant level. This is probably due to the fact that for a complex system, a single type of software may be insufficient and therefore, a combination is needed to bring together interoperable features of different software and create a powerful simulation tool. Hence, in the current research a simulation model of a biogas plant which focuses on the most important component (*i.e.* the digester unit) was developed by combining two existing tools: the standardised ADM1 platform and Aspen Plus software.

The ADM1 model was chosen to simulate anaerobic digestion with relevant modifications and improvements to fit real food waste digester results. While ADM1 brings together the key concepts in anaerobic digestion of wastes, its previous focus has basically been on digestion of sewage sludge. Other residues like food waste and MSW have not been studied in the same detail (Gali *et al.*, 2009). For example, in order to maintain successful digestion of food waste, VFAs, ammonia concentration and trace elements are among important issues that need to be controlled. Furthermore, when simulating methane production, either acetoclastic methanogenesis or syntrophic acetate oxidation methanogenesis can become predominant depending upon certain conditions. The acetate oxidation pathway has not been included in the original ADM1, on the assumption that the majority of hydrogen and acetate would continue to pass through the acetoclastic pathway (Batstone *et al.*, 2002). This may lead to inadequate results, especially in the specific circumstances mentioned. It is, accordingly, worth adding the acetate oxidation pathway into the original ADM1 model to acquire a more accurate simulation including biogas production and other by–products *i.e.* VFA, pH, ammonia concentration, *etc.*, and to describe more closely the way the system behaves. This would,

consequently, bring a lot of benefits when using the model for future work, especially optimisation and flowsheet simulation.

Successful operation of food waste digesters with consideration of both the acetoclastic and syntrophic acetate oxidation pathways and with the addition of trace elements leads to the need for an accurate model for anaerobic degradation of food waste. Nonetheless, not only the original ADM1 version, but also all other extended versions with modifications have omitted trace element issues. Therefore, it is worth including trace elements into an anaerobic digester model in order to optimise the conversion process by controlling these factors. This, eventually, will not only help to improve the simulation of the food waste digestion system, and find the necessary adjustments to guarantee proper functioning of the system, but also provide extra options for model users.

The extended version of ADM1 can then be integrated with Aspen Plus, which performs rigorous material and energy balance calculations, using detailed equipment models, to determine the flow rates, composition and energy flow for all streams involved in the process. Ammonia removal from digestate can also be included in the generic model of ADM1 and Aspen Plus with the aim of keeping a suitable concentration of ammonia in the digester to maintain the stability of the anaerobic treatment process.

Finally, after the creation of an improved digester model, it can be integrated with Aspen Plus to simulate a biogas plant in which water scrubbing is used to model the biogas upgrading.

2.10 Objectives

Based on the results of the literature review, and in order to achieve the overall aim of the research as defined in Chapter 1, a number of objectives were set as below:

- To develop a core anaerobic process model based on ADM1 that could accurately predict the biochemical transformations and pathways seen in food waste digestion and the resulting methane output from a digester.
- To develop a process flowsheet model based on Aspen Plus that links the physico–chemical and mechanical unit processes and operations used in the treatment of food waste and upgrading of biogas with the core anaerobic digestion model.
- To use the integrated models to predict the maximum energy that can be produced from anaerobic digestion of food waste in the form of heat,

electricity and biofuel, taking into account the energy consumption required for plant operation.

- To develop an ammonia removal tool integrated with developed ADM1 model for optimisation/control of ammonia concentration in food waste digesters and quantification by–product streams and nutrient balances.
- To deliver a modelling platform that is flexible and adjustable and could also be applied to the anaerobic digestion of other types of organic substrates.

This page is intentionally left blank

Chapter 3

Methods and tools

This chapter addresses firstly the work programme for modelling the whole system, followed by a methods section which indicates: research boundaries, scope of the work, selection of component models, unit processes considered and factors taken into consideration, model verification, calibration and validation. As the digester unit was stated to be the core component in this study, a section of the ADM1 model for a digester unit is presented. Methods used during modelling ADM1 are described with emphasis on extensions added to its original version. Finally, tools employed and integration procedures of ADM1 and Aspen Plus are outlined.

3.1 Work programme

Prior to determining the appropriate methods and tools applied throughout this work, a detailed work programme was formulated to assist in the selection of these methods and tools (Table 3.1).

Table 3.1. Work programme

A	**A core anaerobic process model based on ADM1**	
A1	Identify the specific problems encountered in treating food waste	
A2	Carry out a critical review of existing models by identifying their strengths and weakness as well as their capabilities in dealing with the problems specified	
A3	Review the ADM1 model to understand its conceptual design and current applications as well as its critical problems and any shortcomings in food waste digestion applications. This helps to point out aspects of ADM1 that need to be modified/extended	
A4	Develop a platform to run the ADM1 model for a CSTR system	
	A4.1	*Program code to enable simulation under continuous feeding regime*
	A4.2	*Compare model with published journals using ADM1 for verification*
	A4.3	*Validate the model with independent sources of full data conducted by the BORRG at University of Southampton*
A5	Optimise ADM1 to the food waste substrate	
	A5.1	*Characterise food waste in terms of elemental components, Total Solids, Volatile Solids, etc*
	A5.2	*Amend parameter set in terms of kinetic factors, biochemical coefficient, etc. that are adequate for food waste based on data acquired from digestion of source–segregated food waste*
A6	Simulate, without modification, the ADM1 to assess the suitability of ADM1 model to represent food waste digestion with elevated ammonia concentration and the system failure without trace elements	
A7	Modify the ADM1 to include the pathway selection based on ammonia concentration and trace elements	
	A7.1	*Modify the structure of ADM1 matrix to include the syntrophic acetate oxidation pathway in methane formation process and revise the program codes at the same time*
	A7.2	*Modify the inhibition factors in conjunction with its concentration and trace elements*
	A7.3	*Test the revised model and parameters*
B	**A process flowsheet model based on Aspen Plus**	
B1	Establish a biogas system in Aspen Plus	
	B1.1	*Create main components of a biogas plant in Aspen Plus. Each of these units would come with relevant validation or assumptions*
	B1.2	*Adding necessary calculation to count the energy balance such as heat loss, digester mixing, etc.*
	B1.3	*Integrate the modified ADM1 as the digester unit in the system*
B2	Carry out case studies for simulation of a biogas plant using the model developed (modified ADM1 integrated with Aspen Plus)	
C	**An ammonia removal tool**	
C1	Establish an ammonia stripping model in Aspen Plus which integrates the modified ADM1 model and the Aspen Simulation Workbook (ASW) tool	
C2	Calibrate the model using experimental data acquired by BORGG group at the University of Southampton to determine the appropriate efficiency of stripping column	
C3	Simulation run	

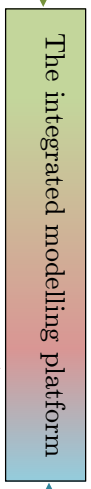

3.2 Method

3.2.1 Scope of work and method objectives

The simulation was developed specifically to address the anaerobic digestion of food waste in which the biogas produced is upgraded to biomethane. The process flow schematic (Figure 3.1) interlinks the five main components which consist of the digester, CHP, Boiler, Upgrading unit and Ammonia removal stage.

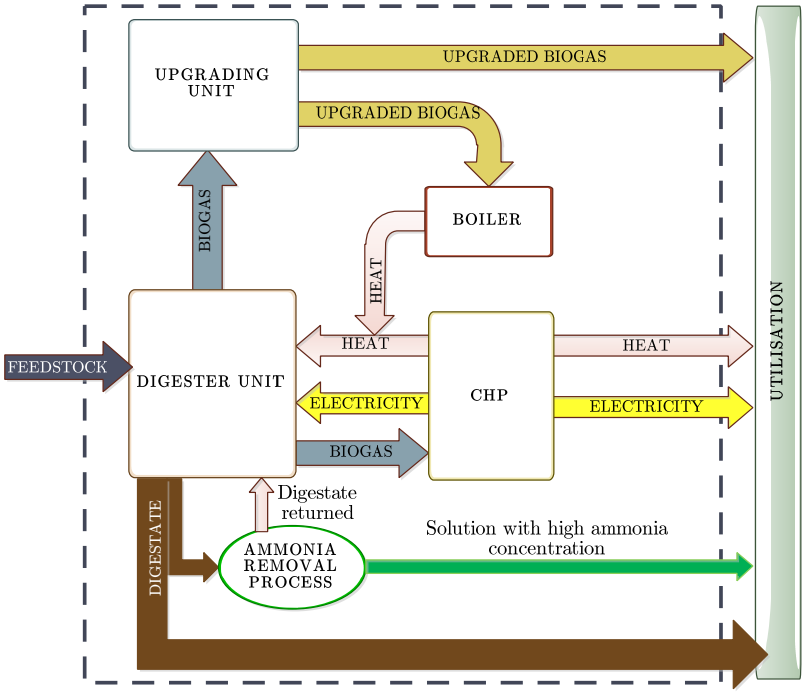

Figure 3.1 System boundaries (inside the dashed line - - - - - - -)

The methodology developed had the following objectives:

- To have a core anaerobic process model that could accurately predict the biochemical transformations and pathways seen in food waste digestion.
- To use the core anaerobic digestion model to predict the methane output from the digester.
- To integrate the core anaerobic digestion model with process models and simulations to allow prediction of the maximum energy that can be generated in the form of heat, electricity and biofuel, taking into account the energy consumption required for plant operation.

- To provide more detailed information on mass and energy balances for each stage in the whole system.
- To provide a modelling platform which is flexible and adjustable and could also be applied to the anaerobic digestion of other types of organic substrates.
- For the model to predict within ±10% in comparison to real data. From a modelling point of view this value is considered a desired accuracy (Hangos & Cameron, 2001; Smith & Smith, 2007; Ford, 2010; Pistikopoulos *et al.*, 2010). However, because of the complexity of the developed generic model, a lower accuracy could be acceptable.

3.2.2 Selection of component models

The component models needed to describe the different unit operations considered in the simulation, *i.e.* anaerobic reactor (digester) using a mathematical model (ADM1), ancillary equipment, including the biogas upgrading unit, CHP unit, Boiler unit, with Aspen Plus were selected.

This was followed by selection of suitable programming languages/tools to allow seamless communication between the component parts of the simulation. The ADM1 model was programmed in MATLAB/Simulink®, and all flowsheeting was carried out using Aspen Plus®. To allow this model to tackle functions, processes and equipment not available in the Aspen Plus suite, new modules were written in Fortran, Microsoft Excel and using the Aspen Simulation Workbook (ASW).

Different model components were calibrated separately for each part of the system. The simulation was verified and validated from laboratory data taken from digesters running under a variety of different conditions within the defined system boundaries.

3.2.3 Unit processes considered and factors taken into consideration

Each of the unit processes is controlled or influenced by a number of factors, which in some cases are independent, or more commonly influenced through interaction of one unit process with another. The controlling factors identified as relevant to the modelling of individual components of the system and to the final process integration and process simulation are given in Table 3.2.

Table 3.2 Controlling factors associated with unit processes

Components	Controlling factors
Digester	• Biochemical pathways leading to methane production; type of reactor configuration, mode of mixing and temperature control. • Operational parameters affecting the efficiency of biochemical conversion process from food waste to methane such as pH, COD concentration, temperature, etc.
CHP unit	• Efficiency of the engine and its components *e.g.* compressors, turbines, heat recovery units, *etc.* • Quality of air fed to the combustion vessel
Boiler unit	• Efficiency of the burners, hot steam recovery equipment • Quality of fuel and air fed to the combustion vessels
Upgrading unit	• Efficiency of the equipment *i.e.* compressors, pumps, heaters, *etc.*, • Temperature, pressure of the performance
Ammonia removal unit	• Characteristics of digestate • Efficiency of the equipment *i.e.* stripping tower, pumps, etc.

All of the controlling factors mentioned above have been taken into account and are discussed in more detail in the next chapter.

3.2.4 Validating data sets

Data were available from various sources, including laboratory and pilot–scale experimental work conducted by the University of Southampton; from the literature; and from the existing databank incorporated in the Aspen Plus software. For the present purposes default precision values were imposed as follows unless specified (Hangos & Cameron, 2001):

- Industrial measured data is ±10% to ±30%.
- Estimated parameters from laboratory or pilot–plant data is ±5% to ±25%.

3.2.5 Models used in the simulation

The objective was not to develop new models, but wherever possible to expand those already available and to construct bridges between them so as to give an integrated process simulation that could be run in a dynamic mode. A step–by–step explanation about how each of these models was formulated, modified and used is given in Chapter 4 and 5.

3.2.6 Model verification calibration, and validation

Verification, calibration, and validation of the overall simulation is required and is an essential prerequisite to the credible and reliable use of this and of the results it generates (Sokolowski, 2009).

Verification determines whether the program is giving an output in line with expectations, and the code is free from errors that could give rise numerical inaccuracies. In the verification step, the correctness of the formal representation of the model is assessed using data from experiments and literature sources. To achieve this, output data from the model was considered against what was expected from the input data. The accuracy of the programme code ADM1 was also checked against data from two published journals, one with a steady–state simulation and one with a dynamic profile (Rosen & Jeppsson, 2005; Boubaker & Ridha, 2008). Comparison of the results generated from the coding of ADM1 in this study was in agreement with the output from these two sets of published data.

Each of the models used was calibrated by comparison between experimental results and the model output. To calibrate the Aspen Plus components of the energy model, data were taken from the literature and from experimental work carried out on full–scale digesters as part of the VALORGAS project (2010-2013). Coefficients within the model were selectively adjusted so that the Aspen Plus model simulated these full–scale operational systems.

ADM1 as originally published incorporates kinetic data for specific purposes, and coefficient values are also given. These kinetic parameters need to be altered depending on process type and feed material. This is achieved by (*a*) sensitivity analysis of the most appropriate parameters to each controlled processes and (*b*) adjustment of the coefficients based on literature values and in–depth knowledge of the reaction routes and rates, applying curve fitting techniques where appropriate. To achieve this a group of experts (Professor Charles Banks, Dr Yue Zhang, Dr Sonia Heaven and Mr Stephen Robertson) held regular meetings with the author to determine and set appropriate model parameters as part of the calibration process.

Validation involves a direct comparison between the model output and real data from the process that it represents. If the results from the validation do not match the process, then the whole sequence has to be re–examined to assess where any discrepancies arise. To some extent this is usually necessary, as a fully representative model is more or less impossible to achieve at a first attempt

(Hangos & Cameron, 2001). Anaerobic digestion was modelled in Aspen Plus using a stoichiometric approach and also modelled using ADM1, then outputs from the steady–state condition were compared. Experimental results (published and not yet published) from both laboratory–scale and pilot–scale digesters run at the University of Southampton were also used in the validation.

3.2.7 Running scenarios and case studies

The built model was used to run different scenarios: these were of the "*what–if*" principle *i.e.* what will happen to the energy routes if waste input and environmental conditions are changed? To test the established model and its sub–modules, case studies were carried out.

3.2.8 ADM1 model for digester unit

3.2.8.1. Assumptions and boundaries

ADM1 was only used to model the processes in a CSTR reactor design. Solids Retention Time (SRT) and hydraulic retention time (HRT) in completely–mixed reactors can be assumed to have the same value (Zeeman & Kujawa, 2013). SRT is the conventional parameter relating an operational parameter to the growth rate of microorganisms, whereas HRT describes the statistical average residence time of a defined amount of matter inside the reactor (Busch, 2013). It was also assumed that the heterogeneity and flocculation in digesters can be omitted.

The volume of the liquid phase was assumed to be constant: in other words, input flow rate (q_{in}) and output flow rate (q_{out}) are constant ($q_{in} = q_{out} = q$). The mass balance of inflow (wet input material) and the outflow (digestate, gases) were derived from the input and output data from ADM1. ADM1 was not, however, used to assess energy use for mixing or heat balances, which were calculated using Aspen Plus.

3.2.8.2. Mathematical implementation of ADM1

Ordinary Differential Equations (ODEs) were implemented in MATLAB/Simulink® and solved with the Euler method solver (*ode15s*) for stiff differential equation systems for a variable time step. The original published version of ADM1 has 36 state variables corresponding to 36 ODEs, and an additional one was added as part of this research to represent the syntrophic acetate oxidation pathway.

The rate of change of any soluble or particulate substances (S_i or X_i) in the liquid volume of the digester is given by the following:

$$\text{Total} = \text{inf low} - \text{outflow} + \text{accumulation}$$

That is:

$$\frac{dS_{liq,i}}{dt} = \frac{q_{in}S_{in,i}}{V_{liq}} - \frac{q_{out}S_{liq,i}}{V_{liq}} + \sum_{j=1-19} \rho_j \upsilon_{i,j} \tag{3.1}$$

$$or\ \frac{dS_{liq,i}}{dt} = \frac{q}{V_{liq}}(S_{in,i} - S_{liq,i}) + \sum_{j=1-19} \rho_j \upsilon_{i,j}\ \text{because}\ q_{in} = q_{out} = q \tag{3.2}$$

Where ρ_j is the kinetic rate for process j, kgCOD m^{-3} day^{-1}; $\upsilon_{i,j}$ is the stoichiometric coefficient of component i at process j; S_i is the concentration of component i, kgCOD m^{-3}; q_{in}, q_{out} are the inflow and outflow, m^3 day^{-1}; V_{liq} is the volume of the reactor, m^3.

The gas phase rate equations are described as in equation (3.1), with only dynamic state components (assuming a constant gas volume).

$$\frac{dS_{gas,i}}{dt} = -\frac{q_{gas}S_{gas,i}}{V_{gas}} + \rho_{T,i}\frac{V_{liq}}{V_{gas}} \tag{3.3}$$

Where $S_{gas,i}$ is the gas concentration of gas i, kmole m^{-3}; q_{gas} is the gas flow, m^3 day^{-1}; V_{liq} and V_{gas} are the volumes of reactor and headspace, m^3, respectively; $\rho_{T,i}$ is the transfer rate of gas i, kmole m^{-3} day^{-1}, to the gas headspace.

All differential and algebraic equations are shown in Chapter 4.

3.2.8.3. Inhibition factors

Inhibition is reflected by a reduction in microbial growth as a result of a decrease in the number of organisms present or of alterations in the microbial environment (Madigan *et al.*, 2012). Inhibition factors incorporated in ADM1 are in the form:

$$\rho_j = k_m \frac{S}{K_S + S} X \cdot I_j \tag{3.4}$$

$$I_j = I_1 \cdot I_2 \cdot I_3 \cdots I_n \tag{3.5}$$

Where the first part of the equation (3.4) is an uninhibited Monod–type uptake, and $I_j = f(S_{I,1\ldots n})$ is the inhibition function of n inhibition factors to the process j, S_I is the inhibitory compound for that inhibition function and

process. Values of I_j range from 1 to 0, reflecting no inhibition and complete inhibition, respectively.

It can be seen from equation 3.5 that the inhibition function of each process is very easy to adjust by altering the inhibition expression. In the current work the inhibition function was generally used to switch on or off specific biochemical pathways in the processes.

3.2.8.4. Waste characterisation

In order to generate initial inputs for ADM1 from food waste, the *transformer* tool (Zaher, Buffiere, *et al.*, 2009) was used. Table 3.3 shows the 11 input parameters required for the *transformer* to work. These were embedded in an Excel file which was readable using a MATLAB script and placed in the MATLAB workspace. The output from the *transformer* process gives the input parameters for ADM1 in the format required; these input values are held in the MATLAB workspace and can be pasted back into Excel for reference or printing. It was also noted that the set of outputs derived from the *transformer* includes a certain amount of phosphorus. For the mass balance, it was assumed in this work that phosphorus is included in particulate inerts.

Since the characteristics of food waste presented here were taken from a '*typical*' food waste used in many studies at the University of Southampton, for simplication purposes, all verification and validation procedures in this study applied the data as given in Table 3.3.

Table 3.3 Typical food waste characteristics for *transformer* input

Components	Unit	Values	Explanations
Total Solids	%WW	21.3	
Volatile Solids	%WW	19	
Density of wet food waste	kg m^{-3}	1000	assumed
(1) Particulate COD (COD_p)	g m^{-3}	264600	= CODt – CODs
(2) CODs–VFA	g m^{-3}	2700	
(3) Volatile Fatty Acids (VFA)	g m^{-3}	2700	1% of CODt
(4) Total Organic Carbon (TOC)	gC m^{-3}	99360	= TC – TIC
(5) Total Organic Nitrogen (Norg)	g m^{-3}	7243	(TS/VS) % TKN
(6) Total Ammonia Nitrogen	g m^{-3}	877	= TKN – Norg
(7) Organic Phosphorus (TP–orthoP)	gP m^{-3}	1028	(TS/VS) % of TP
(8) Ortho–Phosphate (orthoP)	gP m^{-3}	124	= TP – TP–orthoP
(9) Total Inorganic Carbon (TIC)	moleHCO_3^- m^{-3}	169	= (TC – TOC)/12
(10) Total Alkalinity (S_{cat})	equ m^{-3}	25	assumed
(11) Fixed Solids (FS)	g m^{-3}	23000	= TS – VS

Where COD_t estimated 270 g kg^{-1} WW, TC is 47.6% TS (Zhang, Banks, *et al.*, 2012b)

3.2.8.5. Balancing carbon and nitrogen contents

As mentioned in Chapter 2, obtaining a carbon and nitrogen balance is one of the problematic aspects of ADM1 as the model does not take into account the inorganic carbon and inorganic nitrogen originating from biomass decay. The method used for balancing the carbon and nitrogen content was that previously suggested (Batstone *et al.*, 2002; Rosen *et al.*, 2006) and defines the carbon content C_i and nitrogen content N_i of all model components and closes the carbon balance for each reaction with the inorganic carbon (S_{IC}) and inorganic nitrogen (S_{IN}). Thus, the stoichiometry of S_{IC} and S_{IN} are defined by (3.6) and (3.7) for all reactions.

$$\nu_{10,j} = -\sum_{\substack{i=1-9,11-25 \\ j=1-19}} C_i \nu_{i,j} \tag{3.6}$$

$$\nu_{11,j} = -\sum_{\substack{i=1-10,12-25 \\ j=1-19}} N_i \nu_{i,j} \tag{3.7}$$

Where $\nu_{10,j}$ and $\nu_{11,j}$ are the coefficients for processes 10 and 11 for inorganic carbon and inorganic nitrogen in a Petersen matrix; $\nu_{i,j}$ is the coefficient of processes j for component i; $C_i = (C_{bac} - C_{xc})$ and $N_i = (N_{bac} - N_{xc})$ is the stoichiometric term added, representing the carbon content and nitrogen content of component i in kmoleC kgCOD^{-1} and kmoleN kgCOD^{-1}, respectively.

This ensures that within each biochemical step, the difference in carbon and nitrogen content between all components was eventually compensated by inorganic carbon and inorganic nitrogen.

After defining the carbon and nitrogen content as above, they are updated in column 10 and 11 in the Petersen matrix of ADM1. The updated matrix with extensions can be found in Appendix A.

3.3 Simulation tools and integration procedures

3.3.1 Simulation tools

The model uses Aspen Plus® as a platform for modelling ancillary processes and also as the basis for the energy model. In general, pre–built models in Aspen such as splitters, pumps, compressors, absorbers, strippers, flashtanks, fans, heat exchangers, etc. were used directly. When these built–in models did

not meet simulation expectations, the additional subroutines required for the simulation were created using FORTRAN subroutines in calculator blocks and Excel models.

3.3.2 Integration of ADM1 with Aspen Plus

The procedures for integration of ADM1 with Aspen Plus are shown in Figure 3.2, for the process flow of food waste as the input material and biomethane, recovered ammonia, and digestate as the product streams.

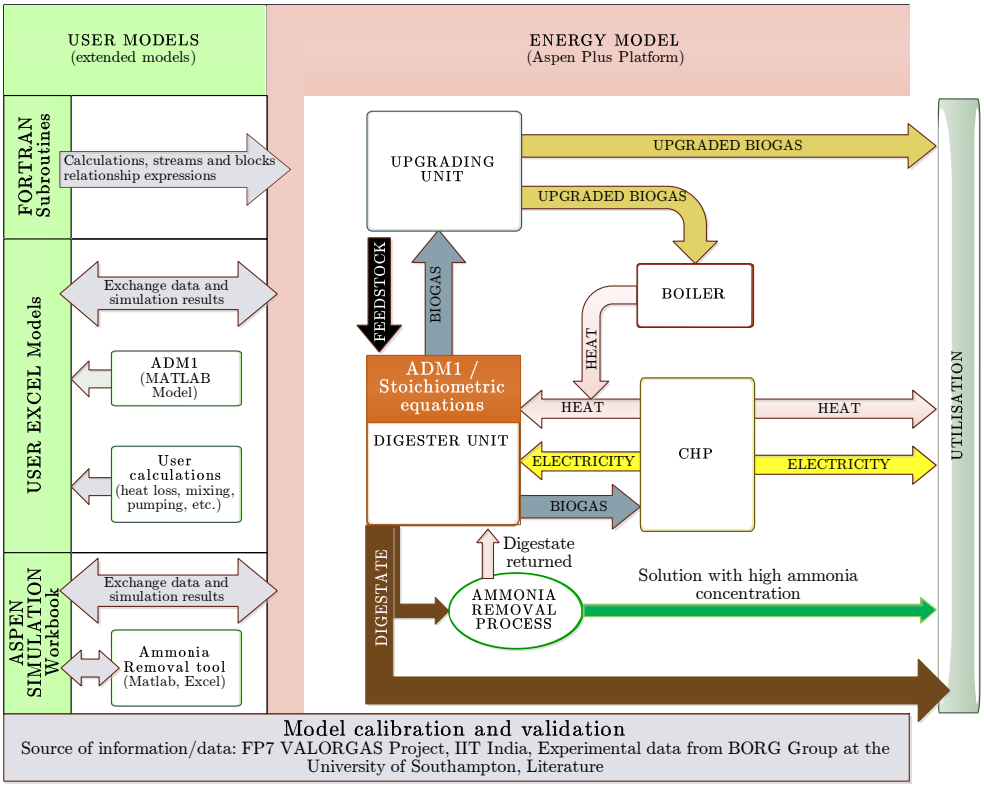

Figure 3.2 Systematic integration of sub–models with Aspen Plus

Aspen Plus acts as a platform connecting the essential unit processes *i.e.* digester, CHP unit, biogas upgrading unit, boiler unit and ammonia removal unit. The digester as an Aspen plus unit can exchange data with ADM1 (implemented in MATLAB) through an Excel user model. This Excel model imports the outputs from the ADM1 simulation and sends them to the digester model in Aspen Plus. Subsequently, this information is used for simulation of the energy requirements of the system and the energy output. The energy model can use one of two stoichiometric–based digester models written for

Aspen plus, or take the input data from ADM1, depending upon the accuracy required, and the availability of input waste characterisation data.

The ammonia removal unit was constructed as an Aspen Simulation Workbook which can directly exchange data with both the MATLAB model of ADM1 and the Aspen Plus energy model.

Chapter 4

ADM1 model and modifications with acetate oxidation pathway and trace element switches

This chapter presents the systematic equations which were implemented in MATLAB to represent the original ADM1 model. It then assesses the suitability of the original ADM1 model for simulation of food waste digestion at elevated ammonia concentrations. Modification of the ADM1 model for accurate prediction of the behaviour of food waste digesters is described in the following section. Finally, the chapter ends with model validation.

4.1 ADM1 model

Before expanding the ADM1 model for the purposes of this study, a platform ADM1 for CSTR simulation was developed using the assumptions, tools and methods proposed in Chapter 3. In this section, if not specified otherwise the term ADM1 refers to the original version of the model, with no additions.

4.1.1 ADM1 implementation

4.1.1.1.ADM1 components, parameters and variables

ADM1 consists of 24 components which are presented in Table 4.1 together with their units (Batstone *et al.*, 2002).

Table 4.1 ADM1 components and units

No	Model components	Descriptions	Unit
1	S_{su}	Monochaccharides (sugars)	kgCOD m^{-3}
2	S_{aa}	Amino acids	kgCOD m^{-3}
3	S_{fa}	Fatty acids	kgCOD m^{-3}
4	S_{va}	Total valerates	kgCOD m^{-3}
5	S_{bu}	Total butyrates	kgCOD m^{-3}
6	S_{pro}	Total propionates	kgCOD m^{-3}
7	S_{ac}	Total acetate	kgCOD m^{-3}
8	S_{h2}	Hydrogen gas	kgCOD m^{-3}
9	S_{ch4}	Methane gas	kgCOD m^{-3}
10	S_{IC}	Inorganic carbon	kmoleC m^{-3}
11	S_{IN}	Inorganic nitrogen	kmoleN m^{-3}
12	S_I	Soluble inerts	kgCOD m^{-3}
13	X_c	Composites	kgCOD m^{-3}
14	X_{ch}	Carbohydrates	kgCOD m^{-3}
15	X_{pr}	Protein	kgCOD m^{-3}
16	X_{li}	Lipid	kgCOD m^{-3}
17	X_{su}	Sugar degraders	kgCOD m^{-3}
18	X_{aa}	Amino acids degraders	kgCOD m^{-3}
19	X_{fa}	Fatty acids degraders	kgCOD m^{-3}
20	X_{c4}	Valerate and Butyrate degraders	kgCOD m^{-3}
21	X_{pro}	Propionate degraders	kgCOD m^{-3}
22	X_{ac}	Acetate degraders	kgCOD m^{-3}
23	X_{h2}	Hydrogen degraders	kgCOD m^{-3}
24	X_I	Particulate inerts	kgCOD m^{-3}

ADM1 parameter and variable notations are given in Table 4.2 (Batstone *et al.*, 2002).

Table 4.2 ADM1 parameter and variable notations

Notation	Expression	Unit
Stoichiometric and kinetic coefficients		
$f_{i,j}$	Yield of product i in component j	kgCOD kgCOD^{-1}
C_i	Carbon content of component i	kmoleC kgCOD^{-1}
N_i	Nitrogen content of component i	kmoleN kgCOD^{-1}
ρ_j	Reaction rate of process j	varies
$\upsilon_{i,j}$	Coefficient of component i on process j in the matrix	–
Y_i	Yield of biomass on component i	kgCOD kgCOD^{-1}
k_{dis}	Disintegration rate (first–order)	day^{-1}
$k_{hyd,i}$	Hydrolysis rate of component i	day^{-1}
$k_{m,j}$	Maximum uptake rate of process j	day^{-1}
$K_{S,i}$	Half saturation coefficient of component i	kgCOD m^{-3}
$k_{dec,i}$	Biomass decay rate of degrader i	day^{-1}
$K_{Ii,j}$	50% inhibitory coefficient of inhibitor i on process j	kgCOD m^{-3}
$I_{i,j}$	Inhibition function of inhibitor i on process j	–
Physico–chemical processes		
$K_{a,i}$	Acid dissociation constant of acid i	mole m^{-3}
$pK_{a,i}$	Acid–base equilibrium constant of acid i	–
$k_{A,Bi}$	Acid–base kinetic constant of acid i	m^3 mole^{-1} day^{-1}
$K_{H,i}$	Henry's law coefficient of gas i	mole m^{-3} bar^{-1}
K_w	Ion constant for water	M
k_La	overall gas–liquid mass transfer coefficient	day^{-1}
k_P	pipe resistance coefficient	m^3 day^{-1} bar^{-1}
R	universal gas constant	bar m^3 mole^{-1} K^{-1}
$pH_{UL,i}$	Upper pH limit for uptake component i	–
$pH_{LL,i}$	Lower pH limit for uptake component i	–
Variables		
S_i	concentration of soluble component i	kgCOD m^{-3}
X_i	concentration of particulate component i	kgCOD m^{-3}
$P_{gas,i}$	pressure of gas i	bar
P_{atm}	external (atmospheric) pressure	bar
T_{op}	absolute temperature in digester	K
T_{base}	absolute temperature in standard condition	K

Originally, there are 19 bioconverison processes in ADM1. These and their conversion rates are presented in Table 4.3 (Batstone *et al.*, 2002).

Table 4.3 Kinetic expressions of bioconversions in ADM1

No	Process name	Converison rate (kgCOD m^{-3})
1	Disintegration	$\rho_1 = k_{dis} X_c$
2	Hydrolysis of carbohydrates	$\rho_2 = k_{hyd,ch} X_{ch}$
3	Hydrolysis of proteins	$\rho_3 = k_{hyd,pr} X_{pr}$
4	Hydrolysis of lipids	$\rho_4 = k_{hyd,li} X_{li}$
5	Uptake of sugars	$\rho_5 = k_{m,su} \frac{S_{su}}{K_{S,su} + S_{su}} X_{su} I_{5,6}$
6	Uptake of amino acids	$\rho_6 = k_{m,aa} \frac{S_{aa}}{K_{S,aa} + S_{aa}} X_{aa} I_{5,6}$
7	Uptake of fatty acids	$\rho_7 = k_{m,fa} \frac{S_{fa}}{K_{S,fa} + S_{fa}} X_{fa} I_7$
8	Uptake of valerate	$\rho_8 = k_{m,c4} \frac{S_{va}}{K_{S,c4} + S_{va}} X_{c4} \frac{S_{va}}{S_{bu} + S_{va}} I_{8,9}$
9	Uptake of butyrate	$\rho_9 = k_{m,c4} \frac{S_{bu}}{K_{S,c4} + S_{bu}} X_{c4} \frac{S_{va}}{S_{va} + S_{bu}} I_{8,9}$
10	Uptake of propionate	$\rho_{10} = k_{m,pro} \frac{S_{pro}}{K_{S,pro} + S_{pro}} X_{pro} I_{10}$
11	Uptake of acetate	$\rho_{11} = k_{m,ac} \frac{S_{ac}}{K_{S,ac} + S_{ac}} X_{ac} I_{11}$
12	Uptake of hydrogen	$\rho_{12} = k_{m,h2} \frac{S_{h2}}{K_{S,h2} + S_{h2}} X_{h2} I_{12}$
13	Decay of sugar consumers	$\rho_{13} = k_{dec,Xsu} X_{su}$
14	Decay of amino acid consumers	$\rho_{14} = k_{dec,Xaa} X_{aa}$
15	Decay of fatty acid consumers	$\rho_{15} = k_{dec,Xfa} X_{fa}$
16	Decay of valerate and butyrate consumers	$\rho_{16} = k_{dec,Xc4} X_{c4}$
17	Decay of propionate consumers	$\rho_{17} = k_{dec,Xpro} X_{pro}$
18	Decay of acetate consumers	$\rho_{18} = k_{dec,Xac} X_{ac}$
19	Decay of hydrogen consumers	$\rho_{19} = k_{dec,Xh2} X_{h2}$

Inhibition functions as shown in Table 4.3 are demonstrated in Table 4.4 (Batstone *et al.*, 2002; Rosen *et al.*, 2006).

Table 4.4 Process inhibition expressions in ADM1

Inhibition function	Expression
$I_{5,6} = I_{pH,aa} I_{IN,\mathrm{lim}}$	Inhibition function of pH and inorganic nitrogen to uptake of sugars and uptake of amino acids
$I_7 = I_{pH,aa} I_{IN,\mathrm{lim}} I_{h2,fa}$	Inhibition function of pH, inorganic nitrogen and hydrogen to uptake of fatty acids
$I_{8,9} = I_{pH,aa} I_{IN,\mathrm{lim}} I_{h2,c4}$	Inhibition function of pH, inorganic nitrogen and hydrogen to uptake of valerate and uptake of butyrate
$I_{10} = I_{pH,aa} I_{IN,\mathrm{lim}} I_{h2,\mathrm{pro}}$	Inhibition function of pH, inorganic nitrogen and hydrogen to uptake of propionate
$I_{11} = I_{pH,ac} I_{IN,\mathrm{lim}} I_{\mathrm{nh}\,3}$	Inhibition function of pH, inorganic nitrogen and free ammonia uptake of acetate
$I_{12} = I_{pH,\mathrm{h}\,2} I_{IN,\mathrm{lim}}$	Inhibition function of pH and inorganic nitrogen to uptake of hydrogen
$I_{IN,\mathrm{lim}} = \frac{1}{1+\frac{K_{S,IN}}{S_{IN}}}$	Inhibition function of inorganic nitrogen
$I_{h2,fa} = \frac{1}{1+\frac{S_{h2}}{K_{Ih2,fa}}}$	Inhibition function of hydrogen to uptake of fatty acids
$I_{h2,c4} = \frac{1}{1+\frac{S_{h2}}{K_{Ih2,c4}}}$	Inhibition function of hydrogen to uptake of valerate and butyrate
$I_{h2,pro} = \frac{1}{1+\frac{S_{h2}}{K_{Ih2,pro}}}$	Inhibition function of hydrogen to uptake of propionate
$I_{nh3} = \frac{1}{1+\frac{S_{nh3}}{K_{I,nh3}}}$	Inhibition function of free ammonia
$I_{pH,aa}, I_{pH,ac}, I_{pH,h2}$	Inhibition function of pH to uptake of amino acids, uptakeof acetate and uptake of hydrogen. These are demonstrated in more detailed in section *4.1.1.4*

The original ADM1 contains 35 differential equations and a set of algebraic equations (Thamsiriroj & Murphy, 2011), as given in (Batstone *et al.*, 2002). For ease of reference and to show the modifications clearly, the original equations are presented here. For the purposes of this model they were implemented in MATLAB/Simulink.

Equations (4.1)–(4.36) represent these 35 differential equations together with another differential equation suggested by Thamsiriroj and Murphy (2011) for pH.

4.1.1.2. Differential equations

Water phase equations:

$$\frac{d_{S_{su}}}{dt} = \frac{q}{V_{liq}}\left(S_{su,in} - S_{su}\right) + \rho_2 + \left(1 - f_{fa,li}\right)\rho_4 - \rho_5 \tag{4.1}$$

$$\frac{d_{S_{aa}}}{dt} = \frac{q}{V_{liq}}\left(S_{\mathrm{aa},in} - S_{aa}\right) + \rho_3 - \rho_6 \tag{4.2}$$

$$\frac{d_{S_{fa}}}{dt} = \frac{q}{V_{liq}}\left(S_{fa,in} - S_{fa}\right) + f_{fa,li}\rho_4 - \rho_7 \tag{4.3}$$

$$\frac{d_{S_{va}}}{dt} = \frac{q}{V_{liq}}\left(S_{va,in} - S_{va}\right) + \left(1 - Y_{aa}\right)f_{va,aa}\rho_6 - \rho_8 \tag{4.4}$$

$$\frac{d_{S_{bu}}}{dt} = \frac{q}{V_{liq}}\left(S_{bu,in} - S_{bu}\right) + \left(1 - Y_{su}\right)f_{bu,\mathrm{su}}\rho_5 + \left(1 - Y_{aa}\right)f_{bu,aa}\rho_6 - \rho_9 \tag{4.5}$$

$$\frac{d_{S_{pro}}}{dt} = \frac{q}{V_{liq}}\left(S_{pro,in} - S_{pro}\right) + \left(1 - Y_{su}\right)f_{\mathrm{pro,su}}\rho_5 + \left(1 - Y_{aa}\right)f_{\mathrm{pro},aa}\rho_6 + \left(1 - Y_{c4}\right)0.54\rho_8 - \rho_{10} \tag{4.6}$$

$$\frac{d_{S_{ac}}}{dt} = \frac{q}{V_{liq}}\left(S_{ac,in} - S_{ac}\right) + \left(1 - Y_{su}\right)f_{\mathrm{ac,su}}\rho_5 + \left(1 - Y_{aa}\right)f_{\mathrm{ac},aa}\rho_6 + \left(1 - Y_{fa}\right)0.7\rho_7 + \left(1 - Y_{c4}\right)0.31\rho_8 + \left(1 - Y_{c4}\right)0.8\rho_9 + \left(1 - Y_{pro}\right)0.57\rho_{10} - \rho_{11} \tag{4.7}$$

$$\frac{d_{S_{h2}}}{dt} = \frac{q}{V_{liq}}\left(S_{h2,in} - S_{h2}\right) + \left(1 - Y_{su}\right)f_{\mathrm{h\,2,su}}\rho_5 + \left(1 - Y_{aa}\right)f_{\mathrm{h\,2},aa}\rho_6 + \left(1 - Y_{fa}\right)0.3\rho_7 + \left(1 - Y_{c4}\right)0.15\rho_8 + \left(1 - Y_{c4}\right)0.2\rho_9 + \left(1 - Y_{pro}\right)0.43\rho_{10} - \rho_{12} - \rho_{T,8} \tag{4.8}$$

$$\frac{d_{S_{ch4}}}{dt} = \frac{q}{V_{liq}}\left(S_{ch4,in} - S_{ch4}\right) + \left(1 - Y_{ac}\right)\rho_{11} + \left(1 - Y_{h2}\right)\rho_{12} - \rho_{T,9} \tag{4.9}$$

$$\frac{d_{S_{IC}}}{dt} = \frac{q}{V_{liq}}\left(S_{IC,in} - S_{IC}\right) - \sum_{j=1}^{19}\left(\sum_{i=1-9,11-24} C_i \upsilon_{i,j}\rho_j\right) - \rho_{T,10} \tag{4.10}$$

More specifically, the sum in equation (4.10) is calculated as:

$$\sum_{j=1}^{19}\left(\sum_{i=1-9,11-24} C_i \upsilon_{i,j}\rho_j\right)$$
$$= \sum_{k=1}^{12} stoich_k\rho_k + stoich_{13}\left(\rho_{13}+\rho_{14}+\rho_{15}+\rho_{16}+\rho_{17}+\rho_{18}+\rho_{19}\right)$$

Where:

$$stoich_1 = -C_{xc} + f_{sI,xc}C_{sI} + f_{ch,xc}C_{ch} + f_{pr,xc}C_{pr} + f_{li,xc}C_{li} + f_{xI,xc}C_{xI}$$
$$stoich_2 = -C_{ch} + C_{su}$$
$$stoich_3 = -C_{pr} + C_{aa}$$
$$stoich_4 = -C_{li} + \left(1-f_{fa,li}\right)C_{su} + f_{fa,li}C_{fa}$$
$$stoich_5 = -C_{su} + \left(1-Y_{su}\right)\left(f_{bu,su}C_{bu} + f_{pro,su}C_{pro} + f_{ac,su}C_{ac}\right) + Y_{su}C_{bac}$$
$$stoich_6 = -C_{aa} + \left(1-Y_{aa}\right)\left(f_{va,\mathrm{aa}}C_{va} + f_{bu,\mathrm{aa}}C_{bu} + f_{pro,\mathrm{aa}}C_{pro} + f_{ac,\mathrm{aa}}C_{ac}\right) + Y_{aa}C_{bac}$$
$$stoich_7 = -C_{fa} + \left(1-Y_{fa}\right)0.7C_{ac} + Y_{fa}C_{bac}$$
$$stoich_8 = -C_{va} + \left(1-Y_{c4}\right)0.54\,\mathrm{C}_{pro} + \left(1-Y_{c4}\right)0.31\,\mathrm{C}_{ac} + Y_{c4}C_{bac}$$
$$stoich_9 = -C_{bu} + \left(1-Y_{c4}\right)0.8\,\mathrm{C}_{ac} + Y_{c4}C_{bac}$$
$$stoich_{10} = -C_{pro} + \left(1-Y_{pro}\right)0.57\,\mathrm{C}_{ac} + Y_{pro}C_{bac}$$
$$stoich_{11} = -C_{ac} + \left(1-Y_{ac}\right)C_{ch4} + Y_{ac}C_{bac}$$
$$stoich_{12} = \left(1-Y_{h2}\right)\mathrm{C}_{ch4} + Y_{h2}C_{bac}$$
$$stoich_{13} = -C_{bac} + C_{xc}$$

$$\begin{aligned}\frac{d_{S_{IN}}}{dt} &= \frac{q}{V_{liq}}\left(S_{IN,in} - S_{IN}\right) - Y_{su}N_{bac}\rho_5 + \left(N_{aa} - Y_{aa}N_{bac}\right)\rho_6 - \\ &Y_{fa}N_{bac}\rho_7 - Y_{c4}N_{bac}\rho_8 - Y_{c4}N_{bac}\rho_9 - Y_{pro}N_{bac}\rho_{10} - Y_{ac}N_{bac}\rho_{11} - \\ &Y_{h2}N_{bac}\rho_{12} + \left(N_{bac} - N_{xc}\right)\sum_{i=13}^{19}\rho_i + \\ &\left(N_{xc} - f_{xI,xc}N_I - f_{sI,xc}N_I - f_{pr,xc}N_{aa}\right)\rho_1\end{aligned} \tag{4.11}$$

$$\frac{d_{S_I}}{dt} = \frac{q}{V_{liq}}\left(S_{I,in} - S_I\right) + f_{sI,xc}\rho_1 \tag{4.12}$$

Differential equations for particulate components:

$$\frac{dX_c}{dt} = \frac{q}{V_{liq}}\left(X_{c,in} - X_c\right) - \rho_1 + \sum_{i=13}^{19} \rho_i \tag{4.13}$$

$$\frac{dX_{ch}}{dt} = \frac{q}{V_{liq}}\left(X_{ch,in} - X_{ch}\right) + f_{ch,xc}\rho_1 - \rho_2 \tag{4.14}$$

$$\frac{dX_{pr}}{dt} = \frac{q}{V_{liq}}\left(X_{pr,in} - X_{pr}\right) + f_{pr,xc}\rho_1 - \rho_3 \tag{4.15}$$

$$\frac{dX_{li}}{dt} = \frac{q}{V_{liq}}\left(X_{li,in} - X_{li}\right) + f_{li,xc}\rho_1 - \rho_4 \tag{4.16}$$

$$\frac{dX_{su}}{dt} = \frac{q}{V_{liq}}\left(X_{su,in} - X_{su}\right) + Y_{su}\rho_5 - \rho_{13} \tag{4.17}$$

$$\frac{dX_{aa}}{dt} = \frac{q}{V_{liq}}\left(X_{aa,in} - X_{aa}\right) + Y_{aa}\rho_6 - \rho_{14} \tag{4.18}$$

$$\frac{dX_{fa}}{dt} = \frac{q}{V_{liq}}\left(X_{fa,in} - X_{fa}\right) + Y_{fa}\rho_7 - \rho_{15} \tag{4.19}$$

$$\frac{dX_{c4}}{dt} = \frac{q}{V_{liq}}\left(X_{c4,in} - X_{c4}\right) + Y_{c4}\rho_8 + Y_{c4}\rho_9 - \rho_{16} \tag{4.20}$$

$$\frac{dX_{pro}}{dt} = \frac{q}{V_{liq}}\left(X_{pro,in} - X_{pro}\right) + Y_{pro}\rho_{10} - \rho_{17} \tag{4.21}$$

$$\frac{dX_{ac}}{dt} = \frac{q}{V_{liq}}\left(X_{ac,in} - X_{ac}\right) + Y_{ac}\rho_{11} - \rho_{18} \tag{4.22}$$

$$\frac{dX_{h2}}{dt} = \frac{q}{V_{liq}}\left(X_{h2,in} - X_{h2}\right) + Y_{h2}\rho_{12} - \rho_{19} \tag{4.23}$$

$$\frac{dX_I}{dt} = \frac{q}{V_{liq}}\left(X_{I,in} - X_I\right) + f_{xI,xc}\rho_1 \tag{4.24}$$

Differential equations for cations and anions:

$$\frac{d_{cat^+}}{dt} = \frac{q}{V_{liq}}\left(S_{cat_f^+} - S_{cat^+}\right) \tag{4.25}$$

$$\frac{d_{an^-}}{dt} = \frac{q}{V_{liq}}\left(S_{an_f^-} - S_{an^-}\right) \tag{4.26}$$

Differential equations of ion states:

$$\frac{dS_{va^-}}{dt} = -\rho_{A,4} \tag{4.27}$$

$$\frac{dS_{bu^-}}{dt} = -\rho_{A,5} \tag{4.28}$$

$$\frac{dS_{pro^-}}{dt} = -\rho_{A,6} \tag{4.29}$$

$$\frac{dS_{ac^-}}{dt} = -\rho_{A,7} \tag{4.30}$$

$$\frac{dS_{hco3^-}}{dt} = -\rho_{A,10} \tag{4.31}$$

$$\frac{dS_{nh3}}{dt} = -\rho_{A,11} \tag{4.32}$$

The pH of the digester can be determined by various methods such as those proposed in (Volcke *et al.*, 2005; Rosen *et al.*, 2006). However, in order to reduce the complexity of implementing the model using differential equation systems, this study uses the differential equation based on the concentration of the H^+ ion introduced by Thamsiriroj and Murphy (2011):

$$\begin{aligned}
&\frac{dS_{H^+}}{dt} = \frac{A}{B} \; with \\
&A = \frac{dS_{an^-}}{dt} + \frac{K_{a,IN}}{K_{a,IN} + S_{H^+}}\frac{dS_{IN}}{dt} + \frac{K_{a,co2}}{K_{a,co2} + S_{H^+}}\frac{dS_{IC}}{dt} + \\
&\left(\frac{1}{64}\right)\frac{K_{a,ac}}{K_{a,ac} + S_{H^+}}\frac{dS_{ac}}{dt} + \left(\frac{1}{112}\right)\frac{K_{a_{pro}}}{K_{a_{pro}} + S_{H^+}}\frac{dS_{pro}}{dt} + \\
&\left(\frac{1}{160}\right)\frac{K_{a,bu}}{K_{a,bu} + S_{H^+}}\frac{dS_{bu}}{dt} + \left(\frac{1}{208}\right)\frac{K_{a,va}}{K_{a,va} + S_{H^+}}\frac{dS_{va}}{dt} - \frac{dS_{IN}}{dt} - \frac{dS_{cat^+}}{dt} \\
&B = 1 + \frac{K_{a,IN}S_{IN}}{\left(K_{a,IN} + S_{H^+}\right)^2} + \frac{K_{a,co2}S_{IC}}{\left(K_{a,co2} + S_{H^+}\right)^2} + \left(\frac{1}{64}\right)\frac{K_{a_{ac}}S_{ac}}{\left(K_{a,ac} + S_{H^+}\right)^2} \\
&+\left(\frac{1}{112}\right)\frac{K_{a,pro}S_{pro}}{\left(K_{a,pro} + S_{H^+}\right)^2} + \left(\frac{1}{160}\right)\frac{K_{a,bu}S_{bu}}{\left(K_{a,bu} + S_{H^+}\right)^2} \\
&+\left(\frac{1}{208}\right)\frac{K_{a,va}S_{va}}{\left(K_{a,va} + S_{H^+}\right)^2} + \frac{K_w}{\left(S_{H^+}\right)^2}
\end{aligned} \tag{4.33}$$

Differential equations for gas phase equations:

$$\frac{dS_{gas,h2}}{dt} = -\frac{q_{gas}}{V_{gas}} S_{gas,h2} + \rho_{T,h2} \frac{V_{liq}}{V_{gas}} \tag{4.34}$$

$$\frac{dS_{gas,ch4}}{dt} = -\frac{q_{gas}}{V_{gas}} S_{gas,ch4} + \rho_{T,ch4} \frac{V_{liq}}{V_{gas}} \tag{4.35}$$

$$\frac{dS_{gas,co2}}{dt} = -\frac{q_{gas}}{V_{gas}} S_{gas,co2} + \rho_{T,co2} \frac{V_{liq}}{V_{gas}} \tag{4.36}$$

4.1.1.3. Acid–base and gas transfer rate equations

Acid–base rates were calculated according to the method suggested in (Batstone *et al.*, 2002) with modifications from (Rosen *et al.*, 2006) for ODE implementation:

$$\rho_{A,4} = k_{A,Bva}\left[S_{va^-}\left(K_{a,va} + S_{H^+}\right) - K_{a,va}S_{va}\right] \tag{4.37}$$

$$\rho_{A,5} = k_{A,Bbu}\left[S_{bu^-}\left(K_{a,bu} + S_{H^+}\right) - K_{a,bu}S_{bu}\right] \tag{4.38}$$

$$\rho_{A,6} = k_{A,Bpro}\left[S_{pro^-}\left(K_{a,pro} + S_{H^+}\right) - K_{a,pro}S_{pro}\right] \tag{4.39}$$

$$\rho_{A,7} = k_{A,Bac}\left[S_{ac^-}\left(K_{a,ac} + S_{H^+}\right) - K_{a,ac}S_{ac}\right] \tag{4.40}$$

$$\rho_{A,10} = k_{A,Bco2}\left[S_{hco3^-}\left(K_{a,co2} + S_{H^+}\right) - K_{a,co2}S_{IC}\right] \tag{4.41}$$

$$\rho_{A,11} = k_{A,BIN}\left[S_{nh3}\left(K_{a,IN} + S_{H^+}\right) - K_{a,IN}S_{IN}\right] \tag{4.42}$$

Gas transfer rates for hydrogen, methane and carbon dioxide from the liquid phase to the gas phase were calculated as in (Tchobanoglous *et al.*, 2003):

$$\rho_{T,8} = \rho_{T,h2} = k_L a_{h2}\left(S_{h2} - 16K_{H,h2}p_{gas,h2}\right) \tag{4.43}$$

$$\rho_{T,9} = \rho_{T,ch4} = k_L a_{ch4}\left(S_{ch4} - 64K_{H,\mathrm{ch}\,4}p_{gas,\mathrm{ch}\,4}\right) \tag{4.44}$$

$$\rho_{T,10} = \rho_{T,co2} = k_L a_{co2}\left(S_{co2} - K_{H,\mathrm{co}\,2}p_{gas,\mathrm{co}\,2}\right) \tag{4.45}$$

Where $k_L a_i$ is the overall transfer coefficient multiplied by specific transfer area of gas i, day^{-1}. Since digesters are often operated under well controlled conditions and the diffusion coefficients are similar, to reduce complexity $k_L a_i$ was assumed to be the same for all the gases (Batstone *et al.*, 2002).

The Henry equilibrium constants (acid–base dissociation constants) are calculated by:

$$K_{a,i} = 10^{(-pKa,i)} \tag{4.46}$$

Where pKa,i is the acid equilibrium constant of each of the components. For some elements, when the heat of dissolution for Henry's Law coefficients (ΔH^0) is available, temperature compensation needs to be included by using the Van't Hoff equation.

$$K_{a,Top} = K_{a,Tstd} \exp\left[\frac{\Delta H^0}{R}\left(\frac{1}{T_{std}} - \frac{1}{T_{op}}\right)\right] \tag{4.47}$$

Where $K_{a,Top}$ is the acid–base equilibrium constant at operation temperature; $K_{a,Tstd}$ is the acid–base equilibrium constant at 298.15K; ΔH^0 is the heat of dissolution for Henry's Law coefficients.

4.1.1.4.pH inhibition equations

For calculation of pH inhibition in continuous systems, Rosen *et al.* (2006) suggested that the Hill inhibition functions should be used instead of the switch functions from Batstone *et al.* (2002) to avoid numerical instabilities. Similar pH inhibition calculation methods were also applied successfully in (Siegrist *et al.*, 2002). Hence, Hill functions were employed here.

$$I_{pH,aa} = \frac{\left(pH_{Lim,aa}\right)^{k_{aa}}}{\left(S_{H^+}\right)^{k_{aa}} + \left(pH_{Lim,aa}\right)^{k_{aa}}} \tag{4.48}$$

$$I_{pH,ac} = \frac{\left(pH_{Lim,ac}\right)^{k_{ac}}}{\left(S_{H^+}\right)^{k_{ac}} + \left(pH_{Lim,ac}\right)^{k_{ac}}} \tag{4.49}$$

$$I_{pH,\mathrm{h2}} = \frac{\left(pH_{Lim,\mathrm{h2}}\right)^{k_{h2}}}{\left(S_{H^+}\right)^{k_{h2}} + \left(pH_{Lim,\mathrm{h2}}\right)^{k_{h2}}} \tag{4.50}$$

Where $pH_{Lim,i}$ is the inhibition constant of component i, which can be calculated as:

$$pH_{Lim,i} = 10^{-\frac{pH_{LL,i}+pH_{UL,i}}{2}}$$

and coefficients k_{aa}, k_{ac}, k_{h2} can be calculated as:

$$k_{aa} = \frac{24}{pH_{UL,aa} - pH_{LL,aa}}$$

$$k_{ac} = \frac{45}{pH_{UL,ac} - pH_{LL,ac}}$$

$$k_{h2} = \frac{3}{pH_{UL,\mathrm{h2}} - pH_{LL,\mathrm{h2}}}$$

Where pH_{LL} to pH_{UL} is the range of pH inhibiton with a value of one at the upper pH limit and a value of zero at the lower pH limit.

4.1.1.5. Algebraic equations

Algebraic equations of ion states:

$$S_{nh4^+} = S_{IN} - S_{nh3} \tag{4.51}$$

$$S_{co2} = S_{IC} - S_{hco3^-} \tag{4.52}$$

Pressure of an individual gas in the gas phase and total pressure of the gas phase in the digester can be calculated from:

$$p_{gas,h2} = S_{gas,h2}\frac{RT_{op}}{16} \tag{4.53}$$

$$p_{gas,ch4} = S_{gas,ch4}\frac{RT_{op}}{64} \tag{4.54}$$

$$p_{gas,co2} = S_{gas,co2} R T_{op} \tag{4.55}$$

$$P_{gas} = p_{gas,h2} + p_{gas,ch4} + p_{gas,co2} + p_{gas,H_2O} \tag{4.56}$$

The gas flow rate in the digester can be estimated according to Rosen *et al.* (2006), modified from Batstone *et al.* (2002):

$$q_{gas} = k_p \left(P_{gas} - P_{atm} \right) \frac{P_{gas}}{P_{atm}} \tag{4.57}$$

4.1.2 Model verification

In order to verify the model, data were used from two published journal papers, one giving a steady–state simulation and one a dynamic simulation. Selected relevant parameters *e.g.* biogas production, VFA, *etc.* from the publications and the model simulation were compared after implementing the same inputs with the same kinetic coefficients.

4.1.2.1. Steady–state simulation

The ADM1 benchmark model for a mesophilic digester presented in (Rosen & Jeppsson, 2005) was used:

- Volume of digester: 3700 m^3 (V_{liq} = 3400 m^3, V_{gas} = 300 m^3);
- Working temperature: 35^{o}C;
- Flow rate q = 170.0 m^3 day^{-1}.

Model parameters and simulation inputs are shown in Appendix C (Tables C1, C2, C3, C4). Results of the benchmarking exercise and outputs derived from simulation with the ADM1 model used in this study for the same input values are presented in Table 4.5.

As can be seen from the comparison between the benchmark data and steady–state results derived from the model simulation, there was a very close agreement for all values. Only minor errors were encountered *i.e.* largest relative errors in the range of 10^{-7}. Reasons for the differences between the two simulations could be discrepancies in the inoculum condition and the duration of the simulation (t_{span}) used to obtain final values at steady–state conditions (t_{span} used for steady–state simulation was 1000 days). Hence, it can be concluded that the developed model was correctly implemented and can give accurate steady–state results.

Table 4.5 Model simulation againsts benchmark model

Stage	Variable	Unit	Benchmark simulation	This study model simulation
1	S_{su}	kgCOD m^{-3}	0.0119548297170	0.0119548297170
2	S_{aa}	kgCOD m^{-3}	0.0053147401716	0.0053147401716
3	S_{fa}	kgCOD m^{-3}	0.0986214009308	0.0986214011770
4	S_{va}	kgCOD m^{-3}	0.0116250064639	0.0116250064639
5	S_{bu}	kgCOD m^{-3}	0.0132507296663	0.0132507296664
6	S_{pro}	kgCOD m^{-3}	0.0157836662845	0.0157836666433
7	S_{ac}	kgCOD m^{-3}	0.1976297169375	0.1976297052214
8	S_{h2}	kgCOD m^{-3}	0.0000002359451	0.0000002359451
9	S_{ch4}	kgCOD m^{-3}	0.0550887764460	0.0550887761805
10	S_{IC}	kmoleC m^{-3}	0.1526778706263	0.1526778668546
11	S_{IN}	kmoleN m^{-3}	0.1302298158037	0.1302298158009
12	S_{I}	kgCOD m^{-3}	0.3286976637215	0.3286976637260
13	X_{xc}	kgCOD m^{-3}	0.3086976637215	0.3086976637360
14	X_{ch}	kgCOD m^{-3}	0.0279472404350	0.0279472404352
15	X_{pr}	kgCOD m^{-3}	0.1025741061067	0.1025741061068
16	X_{li}	kgCOD m^{-3}	0.0294830497073	0.0294830497075
17	X_{su}	kgCOD m^{-3}	0.4201659824546	0.4201659824566
18	X_{aa}	kgCOD m^{-3}	1.1791717989237	1.1791717989257
19	X_{fa}	kgCOD m^{-3}	0.2430353447194	0.2430353447200
20	X_{c4}	kgCOD m^{-3}	0.4319211056360	0.4319211056358
21	X_{pro}	kgCOD m^{-3}	0.1373059089340	0.1373059089263
22	X_{ac}	kgCOD m^{-3}	0.7605626583132	0.7605626587478
23	X_{h2}	kgCOD m^{-3}	0.3170229533613	0.3170229533502
24	X_{I}	kgCOD m^{-3}	25.6173953274430	25.6173953274542
25	S_{cat}	kmole m^{-3}	0.0400000000000	0.0400000000000
26	S_{an}	kmole m^{-3}	0.0200000000000	0.0200000000000
27	S_{va^-}	kgCOD m^{-3}	0.0115962470726	0.0115962470714
28	S_{bu^-}	kgCOD m^{-3}	0.0132208262485	0.0132208262474
29	S_{pro^-}	kgCOD m^{-3}	0.0157427831916	0.0157427835470
30	S_{ac^-}	kgCOD m^{-3}	0.1972411554365	0.1972411437287
31	S_{hco3^-}	kmoleC m^{-3}	0.1427774793921	0.1427774755120
32	S_{nh3}	kmoleN m^{-3}	0.0040909284584	0.0040909283065
33	$S_{gas,h2}$	kgCOD m^{-3}	0.0000102410356	0.0000102410356
34	$S_{gas,ch4}$	kgCOD m^{-3}	1.6256072099814	1.6256072009496
35	$S_{gas,co2}$	kmoleC m^{-3}	0.0141505346784	0.0141505348328
36	$S_{H^+}{}^{(*)}$	kmoleH^+ m^{-3}	0.0000000342344	0.0000000342344

Note: $^{(*)}$ As the objective was to check for bugs and errors in the MATLAB ADM1 platform developed, in this simulation the concentration of ion H^+ was calculated using the original method in (Rosen & Jeppsson, 2005).

4.1.2.2.Dynamic simulation

To verify the implementation of the model under dynamic conditions, and with the further aim of checking the suitability of applying ADM1 to specific solid substrates, information from the study by (Thamsiriroj & Murphy, 2011) was selected. The reason for choosing this study for comparison is that the journal paper was well presented and came with a comprehensive list of information that was often not given in other publications.

Three parameter profiles were compared: biogas yield, methane yield and VFAs. It should be noted, however, that only information relating to vessel 1 (the first stage) was used.

Results of measured and simulated biogas production, total VFAs from benchmark study and from this study model are presented in Figures 4.1, 4.2.

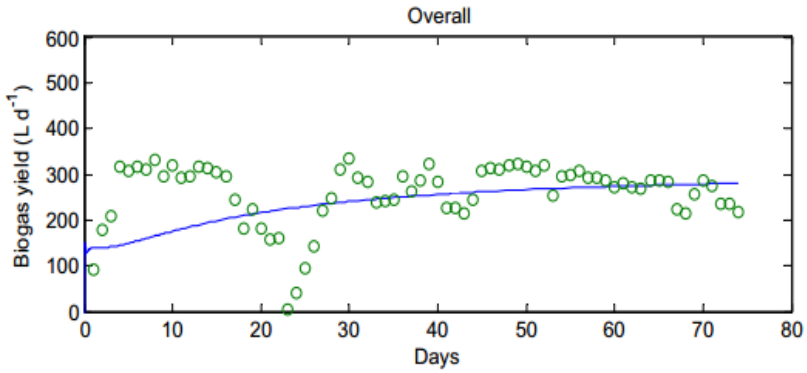

(a)

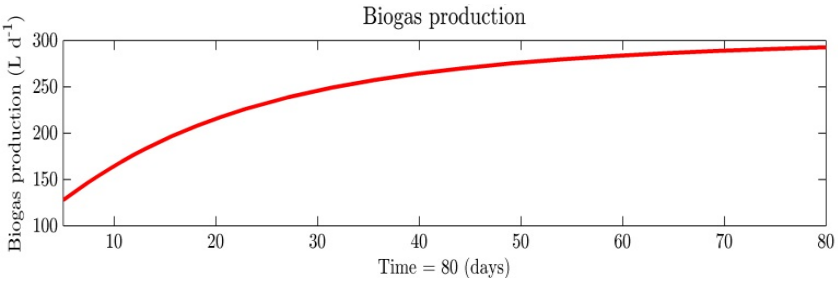

(b)

Figure 4.1 Biogas production comparison: (*a*) and (*b*) show simulated results from benchmark study and from this study model, respectively.

ooo : Experimental data

— : Benchmark simulation

— : This model simulation

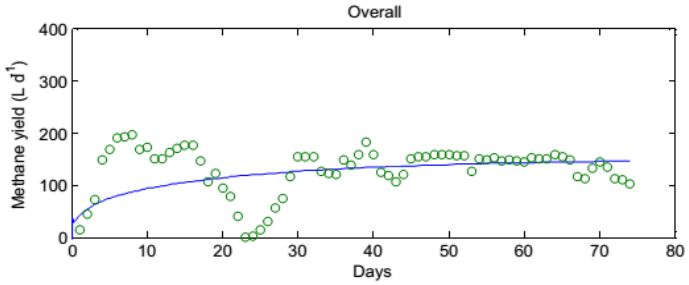

(a)

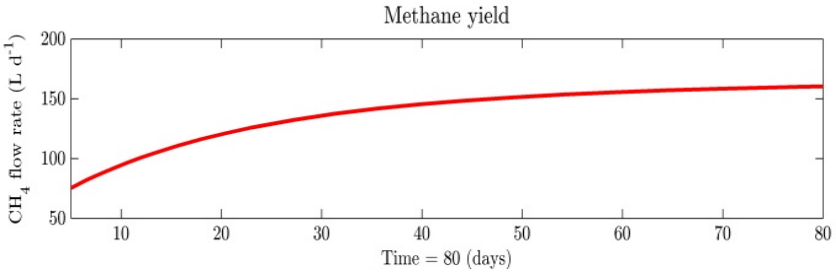

(b)

Figure 4.2 Methane production comparison: (*a*) and (*b*) is simulated results from the benchmark study and from the model used in this study, respectively.

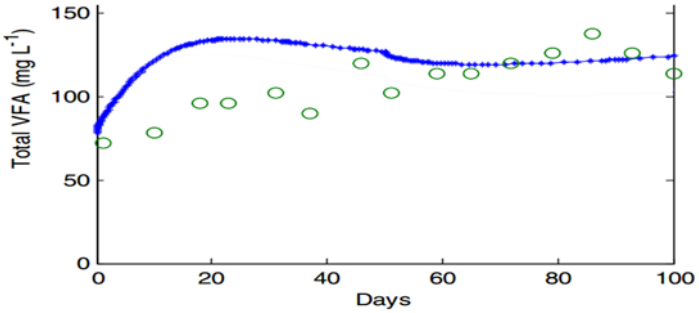

(a)

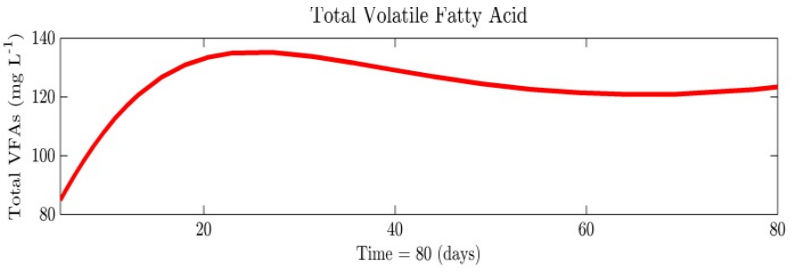

(b)

Figure 4.3 Total VFAs comparison: (*a*) and (*b*) is simulated results from benchmark study and from this study model, respectively.

In both Figure 4.2, 4.3 : ooo : Experimental data
— : Benchmark simulation
— : This model simulation

The results from the comparisons show good agreement between the two simulations in terms of gas production and VFAs. Likewise, these two simulations also give a good fit to the experimental data from the benchmark study.

4.1.2.3. Conclusions from ADM1 verification

In this verification step, it was clearly seen that output data from the model conformed to what was expected from the input data. Additionally, comparison of the results generated from the coding of ADM1 in this study was in agreement with the output from the two benchmarking studies. Therefore, it was concluded that the implemented model and its codes were satisfactory for further tasks.

4.2 Original ADM1 model to replicate the AD of food waste

Although ADM1 has recently been applied for various types of substrates (Shang *et al.*, 2005; Kalfas *et al.*, 2006; Boubaker & Ridha, 2008; Wichern *et al.*, 2009; Koch *et al.*, 2010; Mairet *et al.*, 2011; Thamsiriroj & Murphy, 2011), no studies to date appear to have carried out a satisfactory implementation of ADM1 for food waste. Hence, before commencing any significant modifications, it was worth testing ADM1, without modification, to assess its suitability for representing food waste digestion, especially at high ammonia concentrations.

4.2.1 Specifications for trial simulation

4.2.1.1. Disintegration and hydrolysis rates

Many authors have previously suggested that the disintegration and hydrolysis rates proposed in the original ADM1 are too high and are more likely to be appropriate for activated sludge substrate (Feng *et al.*, 2006; Vavilin *et al.*, 2008; Zaher, Li, *et al.*, 2009; Souza *et al.*, 2013). These rates were adapted as seen in Table 4.6 before applying them to food waste substrate. Other kinetic parameters were taken from the original ADM1 (Batstone *et al.*, 2002).

Table 4.6 Disintegration and hydrolysis rates for food waste

Parameters	Expressions	Unit	Default	Used	Souce
K_{dis}	Disintegration rate of composit	day^{-1}	5	0.55	(Vavilin *et al.*, 2004)
$K_{hyd,ch}$	Hydrolysis rate of carbohydrates	day^{-1}	10	5.22	(Zaher, Li, *et al.*, 2009)
$K_{hyd,pr}$	Hydrolysis rate of proteins	day^{-1}	10	1.86	(Zaher, Li, *et al.*, 2009)
$K_{hyd,li}$	Hydrolysis rate of lipds	day^{-1}	10	1.24	(Zaher, Li, *et al.*, 2009)

4.2.1.2. Adjustment factor (a_f) to concentration output of the ADM1 model

In practice, there is a complicating factor that may cause a discrepancy between experimental and model results. From the mass balance point of view, solid balances for a digester can be simplified as in Figure 4.4.

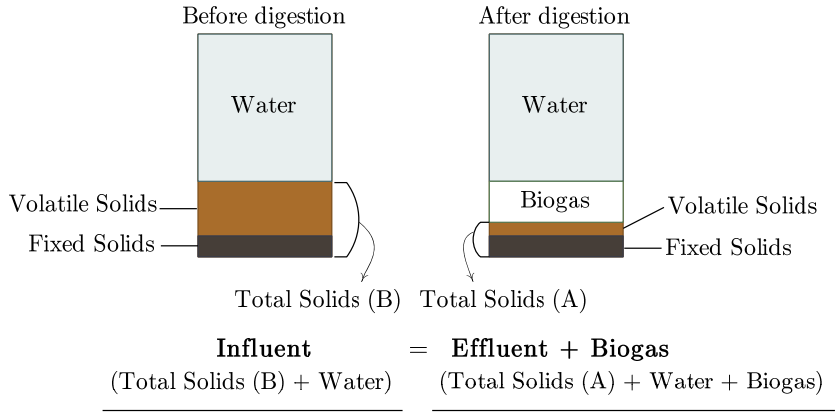

Figure 4.4 Solid balance of a digester

As can be seen from Figure 4.4, a certain amounts of VS in the digester is converted into biogas which goes to the gas phase, resulting in a reduction in volume of the liquid phase and a corresponding increase in the concentration of any conserved compounds. However, as noted in section *3.2.8.1*, the implemented ADM1 model assumed that the volumes of both the liquid phase and gas phase are constant. This obviously led to a problem that the concentrations of components in the liquid phase estimated from the model were lower than that of real experimental data. Hence, an adjustment factor (a_f) was made and applied to the ADM1 model to gain accurate concentration predictions.

Several studies on food waste digestion have indicated that the efficiency of converting VS to biogas is about 70–95% depending upon operational conditions (Cho *et al.*, 1995; Chu *et al.*, 2008; Liu *et al.*, 2009). Therefore, this study assumed that 85% of VS in '*typical*' food waste substrate is converted into biogas. Since the substrate contains 19% VS (see Table 3.3), the mass of digestate could be reduced by 16.15%. Assuming that the specific gravity of digestate is about 1 kg m^{-3}, this meant a reduction in volume of the liquid phase of 16.15%. Accordingly, $a_f = 1/(1–0.1615) = 1.2$ was used as a concentration adjustment factor. However, it should be noted that this is only an issue for high solids substrates that are highly degradable, like food waste, since in dilute substrates or those with low degradability the volume change and thus the effect on concentration is relatively small.

4.2.1.3. Ammonia inhibitory parameter

As described in the literature review, observation of food waste digesters has shown that at elevated ammonia concentrations VFA accumulation can occur, resulting in a fall in pH and failure of the digestion. On the other hand this process may take a long time before signs of failure appear and in that period the digester can operate at high VFA concentrations (initially consisting mainly of acetate, and buffered by the ammonia) with continuing healthy gas production. As can be seen from the Petersen matrix in Appendix A, two processes that generate methane are the uptake of acetate and the uptake of hydrogen. Of these, the process of acetate uptake is controlled by the accumulation rate ρ_{11} which is inhibited by TAN concentration (indicated by 50% inhibitory concentration of free ammonia to acetate uptake $K_{I,nh3}$), as seen in the Table 4.3. Recently, Wett *et al.* (2014) stated that once acetoclastic methanogenesis is affected by $K_{I,nh3}$, a metabolic side–route over acetate oxidation to hydrogen can be dominant, which in turn affects the methane generation. Therefore, this inhibitory parameter was selected for adjustment for the attempt at replicating the dynamic behaviour of food waste digesters.

4.2.1.4. Inoculum conditions an model inputs

The inoculum conditions for this simulation were assumed as in Table 4.7.

Table 4.7 Inoculum (initial) conditions for testing ADM1 model

No	Component	Value	Unit	No	Component	Value	Unit
1	$S_{su,ini}$	0.005	kgCOD m^{-3}	19	$X_{fa,ini}$	0.079	kgCOD m^{-3}
2	$S_{aa,ini}$	0.002	kgCOD m^{-3}	20	$X_{c4,ini}$	0.089	kgCOD m^{-3}
3	$S_{fa,ini}$	0.041	kgCOD m^{-3}	21	$X_{pro,ini}$	0.072	kgCOD m^{-3}
4	$S_{va,ini}$	0.105	kgCOD m^{-3}	22	$X_{ac,ini}$	2.960	kgCOD m^{-3}
5	$S_{bu,ini}$	0.173	kgCOD m^{-3}	23	$X_{h2,ini}$	1.609	kgCOD m^{-3}
6	$S_{pro,ini}$	0.054	kgCOD m^{-3}	24	$X_{I,ini}$	25.018	kgCOD m^{-3}
7	$S_{ac,ini}$	0.210	kgCOD m^{-3}	25	$S_{cat,ion,ini}$	1.0E–5	kmole m^{-3}
8	$S_{h2,ini}$	4.2E–7	kgCOD m^{-3}	26	$S_{an,ion,ini}$	1.0E–5	kmole m^{-3}
9	$S_{ch4,ini}$	0.051	kgCOD m^{-3}	27	$S_{va,ion,ini}$	0.008	kgCOD m^{-3}
10	$S_{IC,ini}$	0.720	kmoleC m^{-3}	28	$S_{bu,ion,ini}$	0.017	kgCOD m^{-3}
11	$S_{IN,ini}$	0.140	kmoleN m^{-3}	29	$S_{pro,ion,ini}$	0.073	kgCOD m^{-3}
12	$S_{I,ini}$	9.882	kgCOD m^{-3}	30	$S_{ac,ion,ini}$	1.129	kgCOD m^{-3}
13	$X_{c,ini}$	1.004	kgCOD m^{-3}	31	$S_{hco3,ion,ini}$	0.616	kmole m^{-3}
14	$X_{ch,ini}$	9.943	kgCOD m^{-3}	32	$S_{nh3,ion,ini}$	0.012	kmoleN m^{-3}
15	$X_{pr,ini}$	1.395	kgCOD m^{-3}	33	$S_{gas,h2,ini}$	1.55E–5	kgCOD m^{-3}
16	$X_{li,ini}$	0.004	kgCOD m^{-3}	34	$S_{gas,ch4,ini}$	1.298	kgCOD m^{-3}
17	$X_{su,ini}$	3.264	kgCOD m^{-3}	35	$S_{gas,co2,ini}$	0.017	kmoleC m^{-3}
18	$X_{aa,ini}$	0.015	kgCOD m^{-3}	36	$S_{h,ion,ini}$	1.26E–8	kmoleH^{+} m^{-3}

As noted in section *3.2.8.4*, the food waste characteristics in this test were assumed to be the same as in Table 3.3. Input data for the ADM1 run, derived from the *transformer* tool, are shown in Table 4.8.

Table 4.8 Input data for testing ADM1 model (output of *transformer* tool)

No	Component	Value	Unit	No	Component	Value	Unit
1	$S_{su,f}$	2.9	kgCOD m^{-3}	19	$X_{fa,f}$	205.31	kgCOD m^{-3}
2	$S_{aa,f}$	0	kgCOD m^{-3}	20	$X_{c4,f}$	47.76	kgCOD m^{-3}
3	$S_{fa,f}$	0	kgCOD m^{-3}	21	$X_{pro,f}$	6.922	kgCOD m^{-3}
4	$S_{va,f}$	0	kgCOD m^{-3}	22	$X_{ac,f}$	0	kgCOD m^{-3}
5	$S_{bu,f}$	0	kgCOD m^{-3}	23	$X_{h2,f}$	0	kgCOD m^{-3}
6	$S_{pro,f}$	0	kgCOD m^{-3}	24	$X_{I,f}$	19.023	kgCOD m^{-3}
7	$S_{ac,f}$	5.8	kgCOD m^{-3}	25	$S_{cat,ion,f}$	0.025	kmole m^{-3}
8	$S_{h2,f}$	0	kgCOD m^{-3}	26	$S_{an,ion,f}$	0.216	kmole m^{-3}
9	$S_{ch4,f}$	0	kgCOD m^{-3}	27	$S_{va,ion,f}$	0	kgCOD m^{-3}
10	$S_{IC,f}$	0.097	kmoleC m^{-3}	28	$S_{bu,ion,f}$	0	kgCOD m^{-3}
11	$S_{IN,f}$	0.006	kmoleN m^{-3}	29	$S_{pro,ion,f}$	0	kgCOD m^{-3}
12	$S_{I,f}$	2.288	kgCOD m^{-3}	30	$S_{ac,ion,f}$	0	kgCOD m^{-3}
13	$X_{c,f}$	0	kgCOD m^{-3}	31	$S_{hco3,ion,f}$	0	kmole m^{-3}
14	$X_{ch,f}$	205.31	kgCOD m^{-3}	32	$S_{nh3,ion,f}$	0	kmoleN m^{-3}
15	$X_{pr,f}$	47.76	kgCOD m^{-3}	33	$S_{gas,h2,f}$	0	kgCOD m^{-3}
16	$X_{li,f}$	6.922	kgCOD m^{-3}	34	$S_{gas,ch4,f}$	0	kgCOD m^{-3}
17	$X_{su,f}$	0	kgCOD m^{-3}	35	$S_{gas,co2,f}$	0	kmoleC m^{-3}
18	$X_{aa,f}$	0	kgCOD m^{-3}	36	$S_{h,ion,f}$	0	kmoleH^+ m^{-3}

4.2.2 Trial simulation results

The ADM1 model was tested with food waste substrate using a range of ammonia inhibitory parameters ($K_{I,nh3}$) to estimate key elements such as gas production, pH, VFA concentration, TAN, *etc.* at a moderate organic loading rate of 3 kg VS m^{-3} day^{-1} and in a steady–state period.

Results from simulations for testing the capability of the original ADM1 model to represent food waste digestion are presented in Table 4.9.

As can be seen from Table 4.9, the decrease in the 50% inhibitory concentration of free ammonia from 0.0045 to 0.00113 kgCODm^{-3} (4 times) leads to a considerable increase in acetic acid from 218.2 to 25000 mg L^{-1} (115 times). Interestingly, however, it can also be seen that within this range, the TAN concentration was quite stable at around 5 g N L^{-1}.

Table 4.9 Original ADM1 simulated results for food waste digestion at steady–state period with different values of $K_{I,nh3}$

$K_{I,nh3}$ kgCODm^{-3}	Acetic mg L^{-1}	Propionic mg L^{-1}	Butyric mg L^{-1}	Valeric mg L^{-1}	pH	TAN mg L^{-1}	CH_4 %	CH_4 Yield m^3 m^{-3}day^{-1}
0.00113	25000	9.205	8.954	4.708	7.66	5057	52.28%	1.397
0.00129	21670	9.205	8.954	4.708	7.72	5048	52.57%	1.413
0.00138$^{(**)}$	**19610**	**9.205**	**8.954**	**4.708**	**7.76**	**5042**	**52.75%**	**1.424**
0.00150	17220	9.205	8.954	4.708	7.79	5035	52.95%	1.436
0.00180$^{(*)}$	11080	9.205	8.954	4.708	7.88	5018	53.47%	4.467
0.00225	3360	9.205	8.954	4.708	7.97	4997	54.11%	1.506
0.00300	610.3	9.205	8.954	4.708	7.99	4989	54.33%	1.52
0.00450	218.2	9.205	8.954	4.708	8	4988	54.36%	1.522

Note: $^{(*)}$ suggested value in original ADM1 model. $^{(**)}$ see section 4.3.3.

Previous investigations have shown that in food waste digesters operated without trace element addition, when the TAN concentration is around 5 gN L^{-1} and the VFA is about 20000 mg L^{-1} the system could fail due to the accumulation of VFA, resulting in a dramatic fall in pH and inhibition of biogas production (Zhang & Walker, 2010; Banks, Chesshire, *et al.*, 2011; Banks *et al.*, 2012; Jiang, 2012; Zhang, Banks, *et al.*, 2012b). The original ADM1 did not seem to replicate the system failure well, however, as even at very high acetic acid concentrations of 25000 mg L^{-1}, TAN concentration of 5.057 gN L^{-1} biogas production still continued with only a slight decline in specific methane yield (about 8%, from 1.522 to 1.397 m^3 CH_4 m^{-3}day^{-1}), along with a gradual decline in pH from 8.0 to 7.66 (see Figure 4.5 and 4.6).

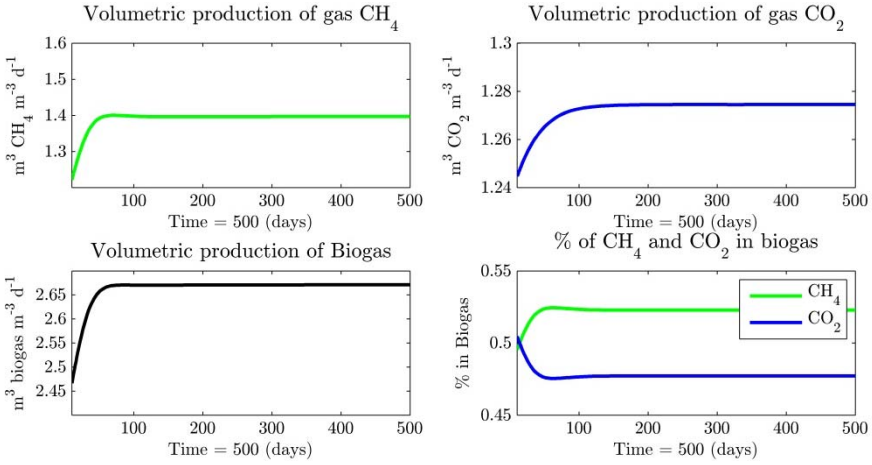

Figure 4.5 Biogas production from trial simulation with $K_{I,nh3} = 0.0113$

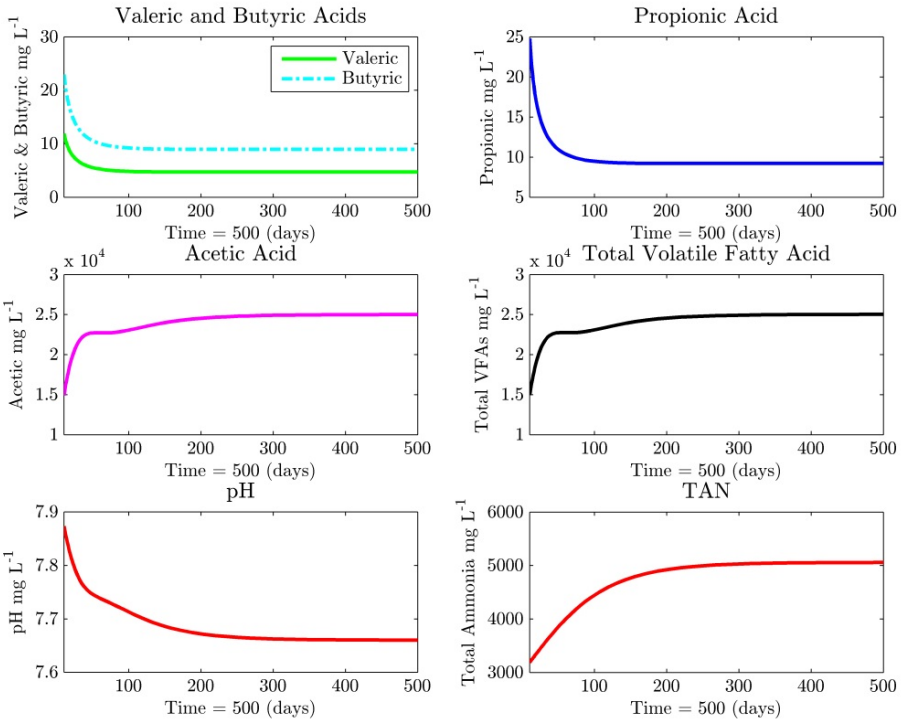

Figure 4.6 pH, TAN and VFAs from trial simulation with $K_{I,nh3} = 0.0113$

The results indicated the weakness of ADM1 in modelling digestion of substrates with a high nitrogen contents like food waste, and confirmed the need to adapt the model to make it adequate for simulating this waste.

It is believed that although mesophilic acetoclastic methanogens are inhibited by TAN concentrations somewhere around 5 g N L^{-1}, food waste digestion still works as the acetate oxidation pathway takes over the acetoclastic pathway and is less sensitive to ammonia (Banks *et al.*, 2012; Wett *et al.*, 2014). As concluded in Chapter 2, the syntrophic acetate oxidation pathway exists in anaerobic digestion of food waste and it represents a second pathway shifted from a conventional acetoclastic route of methane formation. This is indicated by the consumption of acetic acid by micro–organisms in the second pathway, resulting in a very low acetic acid concentration.

In real practice, trace elements have been shown to be an important factor controlling the stability of food waste digesters at such high TAN concentrations (see Chapter 2).

Taking into account all the testing simulations and explanations presented above, it was concluded that there was a need to modify the ADM1 model to accurately simulate real food waste digesters with process failures, acetate oxidation pathway and trace element additions.

4.3 Extending the ADM1 model

4.3.1 ADM1 model with acetate oxidation pathway

The method for extending the ADM1 model with the acetate oxidation pathway was based on the one described in (Shimada *et al.*, 2011). ADM1 was extended to include acetate oxidation by adding two processes into the original model mechanism: acetate degradation by a new biomass group of acetate oxidisers, and the decay of that new biomass group. These two processes are presented in the extended ADM1 Petersen matrix in Appendix A (i.*e.* process 11*b* and 18*b*), and the resulting model has 21 conversion processes and 25 components.

A new state variable was added to the original ADM1, namely acetate oxidiser biomass or acetate oxidation degraders (X_{ac2}). Two new kinetic expressions for the rates of uptake acetate oxidisers and decay of acetate oxidiser biomass were introduced as shown in equations (4.58) and (4.59), respectively.

$$\rho_{11b} = k_{m,ac2} \frac{S_{ac}}{K_{S,ac2} + 1} X_{ac2} I_{11b} \tag{4.58}$$

$$\rho_{18b} = k_{dec,Xac2} X_{ac2} \tag{4.59}$$

Subsequently, the differential equation for the decay of acetate oxidisers can be defined:

$$\frac{dX_{ac2}}{dt} = \frac{q}{V_{liq}}\left(X_{ac2,in} - X_{ac2}\right) + Y_{ac2}\rho_{11b} - \rho_{18b} \tag{4.60}$$

With these additions, some of the original equations were updated:

[1], equation (4.7) was adjusted as:

$$\begin{aligned}\frac{d_{S_{ac}}}{dt} = \frac{q}{V_{liq}}\left(S_{ac,in} - S_{ac}\right) + \left(1 - Y_{su}\right) f_{\mathrm{ac,su}}\rho_5 + \\ \left(1 - Y_{aa}\right) f_{\mathrm{ac},aa}\rho_6 + \left(1 - Y_{fa}\right)0.7\rho_7 + \left(1 - Y_{c4}\right)0.31\rho_8 + \\ \left(1 - Y_{c4}\right)0.8\rho_9 + \left(1 - Y_{pro}\right)0.57\rho_{10} - \rho_{11} - \rho_{11b}\end{aligned}$$

[2], equation (4.8) was adjusted as:

$$\frac{d_{S_{h2}}}{dt} = \frac{q}{V_{liq}}\left(S_{h2,in} - S_{h2}\right) + \left(1 - Y_{su}\right) f_{\mathrm{h2,su}}\rho_5 + \left(1 - Y_{aa}\right) f_{\mathrm{h2},aa}\rho_6 + \left(1 - Y_{fa}\right)0.3\rho_7 + \left(1 - Y_{c4}\right)0.15\rho_8 + \left(1 - Y_{c4}\right)0.2\rho_9 + \left(1 - Y_{pro}\right)0.43\rho_{10} + \left(1 - Y_{ac2}\right)\rho_{11b} - \rho_{12} - \rho_{T,8}$$

[3], the sum in equation (4.10) was adjusted as:

$$\sum_{j=1}^{25}\left(\sum_{i=1-9,11-25} C_i \upsilon_{i,j}\rho_j\right) = \sum_{k=1}^{12} stoich_k\rho_k + stoich_{13}\left(\rho_{13} + \rho_{14} + \rho_{15} + \rho_{16} + \rho_{17} + \rho_{18} + \rho_{18b} + \rho_{19}\right)$$

In which:

$$stoich_{11b} = -C_{ac} + Y_{ac2}C_{bac}$$

[4], equation (4.11) was adjusted as:

$$\frac{d_{S_{IN}}}{dt} = \frac{q}{V_{liq}}\left(S_{IN,in} - S_{IN}\right) - Y_{su}N_{bac}\rho_5 + \left(N_{aa} - Y_{aa}N_{bac}\right)\rho_6 - Y_{fa}N_{bac}\rho_7 - Y_{c4}N_{bac}\rho_8 - Y_{c4}N_{bac}\rho_9 - Y_{pro}N_{bac}\rho_{10} - Y_{ac}N_{bac}\rho_{11} - Y_{ac2}N_{bac}\rho_{11b} - Y_{h2}N_{bac}\rho_{12} + \left(N_{bac} - N_{xc}\right)\sum_{i=13}^{19}\rho_i + \left(N_{xc} - f_{xI,xc}N_I - f_{sI,xc}N_I - f_{pr,xc}N_{aa}\right)\rho_1$$

The inhibition term I_{11b} was defined as:

$$I_{11b} = I_{pH,ac2}I_{IN,\mathrm{lim}}I_{h2,\mathrm{ac2}} \tag{4.61}$$

Where $I_{pH,ac2}$ is the pH inhibition to the uptake of acetate oxidisers; $I_{IN,lim}$ is inorganic nitrogen inhibition, $I_{h2,ac2}$ is hydrogen inhibition to the uptake of acetate oxidisers. These inhibition factors can be calculated from equations (4.62)–(4.65).

$$I_{pH,ac2} = \frac{\left(pH_{Lim,ac2}\right)^{k_{ac2}}}{\left(S_{H^+}\right)^{k_{ac2}} + \left(pH_{Lim,ac2}\right)^{k_{ac2}}} \tag{4.62}$$

$$k_{ac2} = \frac{45}{pH_{UL,ac2} - pH_{LL,ac2}} \tag{4.63}$$

$$I_{IN,\text{lim}} = \frac{1}{1 + \frac{K_{S,IN}}{S_{IN}}} \tag{4.64}$$

$$I_{h2,\text{ac}2} = \frac{1}{1 + \frac{S_{ac}}{K_{Ih2,ac}}} \tag{4.65}$$

In the above equations (4.58)–(4.65), X_{ac2} are the particulate acetate oxidation degraders, kgCOD m^{-3}; other parameters from the original ADM1 expressions can be found from Tables 4.1 and 4.2; the parameters for functioning of the extended pathway are given in Table 4.10.

Table 4.10 Parameters for acetate oxidation pathway

Parameters	Expressions	Units
$k_{m,ac2}$	Maximum uptake rate of acetate oxidisers	day^{-1}
$K_{dec,Xac2}$	Biomass decay of acetate oxidisers	day^{-1}
$K_{S,ac2}$	Half saturation coefficient of acetate oxidisers	kgCOD m^{-3}
Y_{ac2}	Yield uptake acetate oxidisers	kgCOD m^{-3}
$K_{Ih2,ac}$	50% inhibitory concentration of H_2 to acetate uptake	kgCOD m^{-3}
$pH_{UL,ac2}$	Upper pH limit for acetate oxidation	–
$pH_{LL,ac2}$	Lower pH limit for acetate oxidation	–

In order to implement the acetate oxidation extension, kinetic parameters (Table 4.10) needed to be identified. Shimada *et al.* (2011) implemented an AO pathway with the parameters shown in Table 4.11. However, there are errors in the inhibition factors, and also no data for pH inhibiton at the upper and lower pH limits. In addition, a trial simulation based on the provided parameters revealed that the coefficients chosen for maximum uptake rate of acetate oxidisers ($k_{m,ac2}$) and yield uptake acetate oxidisers (Y_{ac2}) do not fit data for food waste. Y_{ac2} appears too high since it is expected to be similar to the yield uptake for acetate (Y_{ac} = 0.05 kgCOD kgCOD^{-1}); whereas $k_{m,ac2}$ is too low as higher values similar to the maximum uptake rate of acetate degraders ($k_{m,ac}$ = 8 day^{-1}) are expected. Notwithstanding this, 50% inhibitory concentration of H_2 to acetate uptake seems reasonable as it was assumed to be the same 50% inhibitory concentration of H_2 to propionate uptake. Therefore, it was used for this modified model.

Table 4.11 Parameters for simulation the AO pathway of extended model

Parameters	Unit	Original ADM1	Shimada *et al.* (2011)	This study
$k_{m,ac2}$	day^{-1}	Not given (NG)	3.9	8
$K_{dec,Xac2}$	day^{-1}	NG	0.02[(a)]	0.02[(a)]
$K_{S,ac2}$	kgCOD m^{-3}	NG	0.15[(a)]	0.15[(a)]
Y_{ac2}	kgCOD m^{-3}	NG	0.1	0.05
$K_{I\!h2,ac}$	kgCOD m^{-3}	NG	3.5E–6	3.5E–6
$pH_{UL,ac2}$	–	NG	NG	7[(b)]
$pH_{LL,ac2}$	–	NG	NG	6[(b)]

Note: [(a)] The same as values provided from (Batstone *et al.*, 2002) for acetate degraders. [(b)] Assumed to be the same values of uptake of acetate (Batstone *et al.*, 2002).

A reference to a recent publication (Wett *et al.*, 2014) also was made to update knowledge. However the paper does not report how the AO mechanism was developed and the set of coefficients for simulation was not provided.

Consequently, after checking recent relevant works (Shimada *et al.*, 2011; Wett *et al.*, 2014) and using the methods indicated in Chapter 3, a set of kinetic parameters for simulating the AO pathway of the extended model was suggested as in Table 4.11.

4.3.2 Inhibition factors for propionic, butyric and valeric degradation to represent the system failure

As noted in section 4.2 above, the original ADM1 is unable to describe digester failure at high concentrations of TAN and VFA. However, a number of studies have indicated the link between system failure and elevated concentrations of TAN (around 5 gN L^{-1}) and VFA (see section 2.3.1). The most favoured solution suggested from previous successful studies is to increase the trace element content in the digester to maintain its stability (Zhang & Walker, 2010; Banks *et al.*, 2012; Jiang, 2012). In other words, without adding trace elements food waste digesters should fail at elevated TAN concentration. Hence, it is necessary to include trace elements in the ADM1 model to represent correctly the failure of the system.

Previous investigations by University of Southampton (published and unpublished) indicated that trace elements play an important role in unblocking the degradation of valeric, butyric and propionic acids. Therefore, two new inhibition factors were introduced in the ADM1 model:

- $I_{te,c4}$: Inhibition factor of trace elements to the valeric and butyric uptake.
- $I_{te,pro}$: Inhibition factor of trace elements to the propionic uptake.

Although trace element addition probably does not promote valeric, butyric or propionic degradation directly, stopping the supplement causes a blockage in conversion of these acids, resulting in the digestion failure corresponding to accumulation of VFA (especially propionic acid) (Banks & Zhang, 2010; Banks *et al.*, 2012). To model this problem fully would require establishing further pathways and equations for relationships that are not yet fully understood; thus introducing these two inhibition factors is a sensible simplification.

As a first attempt the original inhibition functions of parameters for valerate, butyrate and propionate uptake as shown in Table 4.4 were adjusted as in (4.66) and (4.67), respectively.

$$I_{8,9} = I_{pH,aa} I_{IN,\lim} I_{h2,c4} I_{te,c4} \tag{4.66}$$

$$I_{10} = I_{pH,aa} I_{IN,\lim} I_{h2,\mathrm{pro}} I_{te,pro} \tag{4.67}$$

These relationships between inhibition factors and TAN concentration in a digester can be schematised as in Figure 4.7.

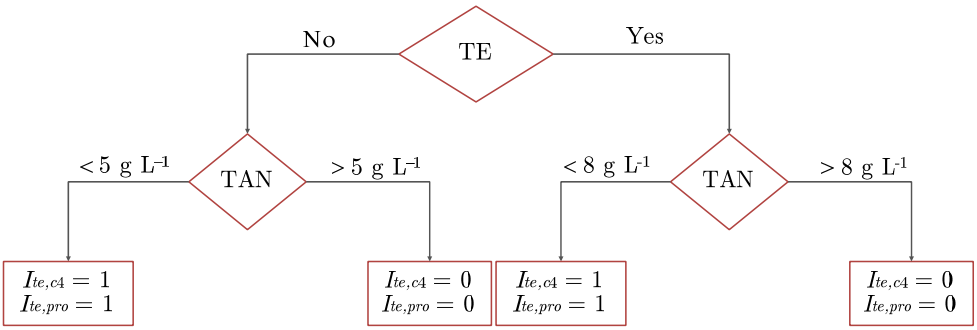

Figure 4.7 Inhibition factors $I_{te,c4}$, $I_{te,pro}$ under different TE and TAN conditions

As can be seen from the schematic, when no trace elements are added and TAN concentration is less than 5 gN L^{-1}, or when trace elements are supplemented and TAN concentration is less than 8 gN L^{-1} the system operates with a healthy degradation of valeric, butyric and propionic acids ($I_{te,c4} = I_{te,pro} = 1$). In contrast, when the TAN concentration is higher than 5 gN L^{-1} and no trace elements are present the degradation of these acids is completely blocked, resulting in significant accumulation of these acids and system failure ($I_{te,c4} = I_{te,pro} = 0$). The same failure scenario is applied when TAN is higher than 8 gN L^{-1} even with presence of trace elements.

4.3.3 Verifying the modified ADM1 model

Verification is necessary to determine whether the extended ADM1 model could overcome the shortcomings of the original ADM1 and be able to represent what is seen in reality. An appropriate set of input data and kinetic parameters as run in section 4.2 was again used for running the modified model with the acetoclastic route only enabled with and without the presence of trace elements. The acetoclastic and acetate oxidation pathways were active, with trace elements added. The set of input data shown by the highlighted line displayed in Table 4.9 was chosen for this purpose. The simulated results of these two scenarios were compared to each other and the degree to which they could reflect real data was assessed.

4.3.3.1. Modified ADM1 with system failure

This verification was carried out to show the role of trace elements together with the system failure at elevated TAN concentrations as indicated in section 4.3.2. In practice, the condition when TAN concentration exceeds 8 g L^{-1} rarely happens with source segregated domestic food waste, thus only the failure caused by the deficiency of trace elements was investigated (Figures 4.8, 4.9).

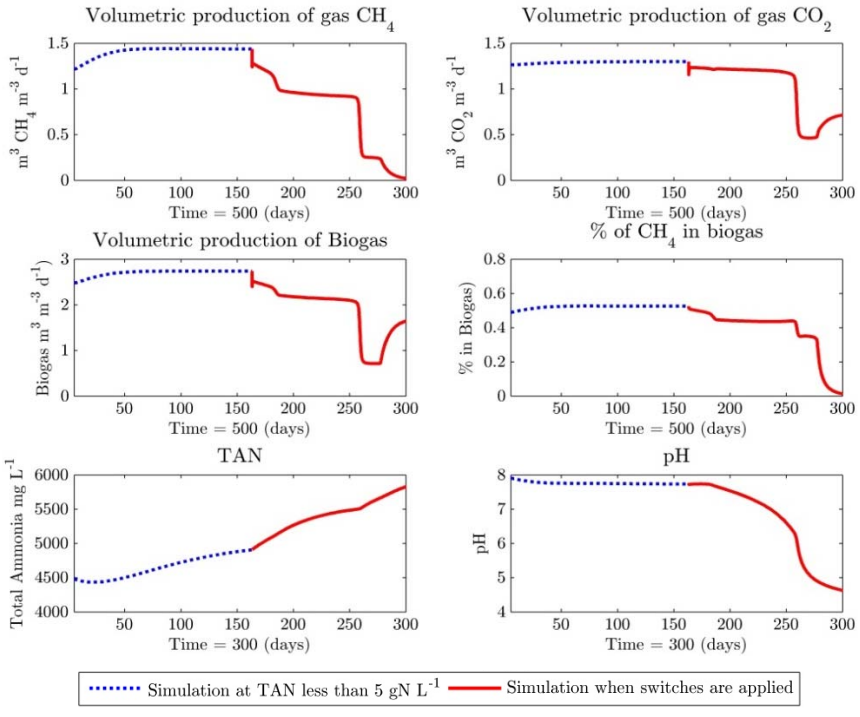

Figure 4.8 Gas production, pH and TAN of the failure simulation without presence of trace elements

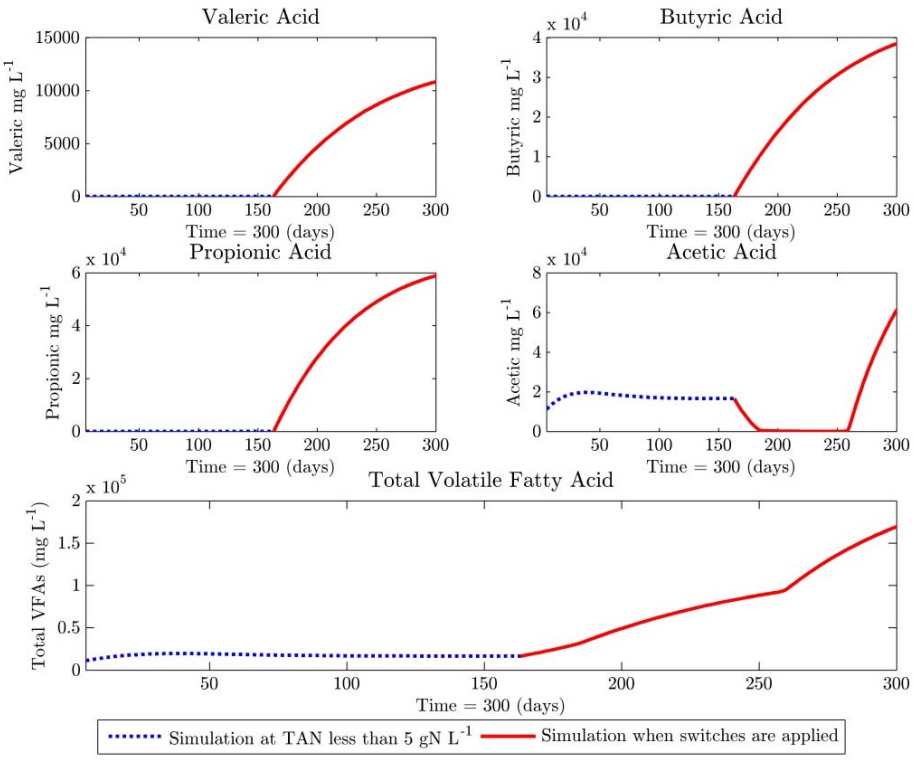

Figure 4.9 VFAs of the failure simulation without presence of trace elements

As can be seen from Figures 4.8 and 4.9, when the TAN concentration is less than 5 gN L^{-1}, the system works properly with no failure. Total VFA of approximately 17000 mg L^{-1}, pH between 7.8–8.0, the gas production is predicted sensibly with methane concentration about 54%. When the TAN concentration exceeds 5 gN L^{-1}, however, the system starts to fail (due to the two new inhibition factors introduced), as indicated by a gradual drop in pH followed by a drastic decline from 7 to about 5. At the same time, methane content in the biogas decreases from more than 50% to about 6%. This failure simulation agreed with the results reported by Zhang and Walker (2010) for a laboratory–scale digester failure test: pH dropped to 5.6 and methane content dropped to less than 10%. In addition, the huge increase in propionic, valeric and butyric acids along with the rapid fall in acetic acid concentrations corresponds to what is seen in reality when the digestion system fails.

Therefore, it was considered that by adding the two inhibiton factors considering the role of trace elements to the degradation of valeric, butyric and propionic acids, the ADM1 model is able to model the failure state of food waste digesters.

4.3.3.2.Modified ADM1 with the role of TE and acetate oxidation pathway

This verification tested the model output when trace elements are added to the digester and the acetate oxidation pathway is present and operational. Results from testing simulations are presented in Figures 4.10, 4.11, 4.12, 4.13, 4.14 and 4.15.

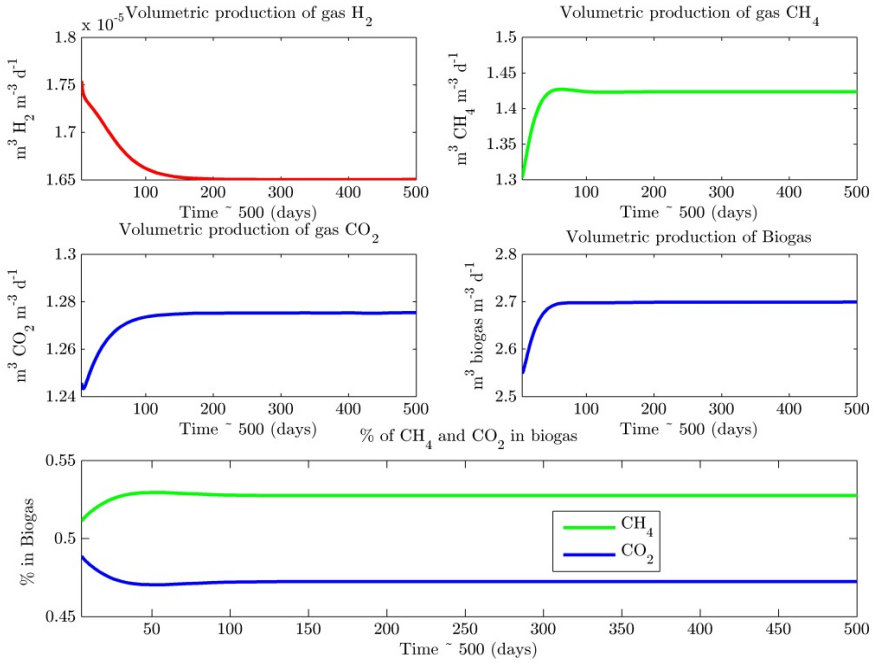

Figure 4.10 Gas production of AC pathway simulation

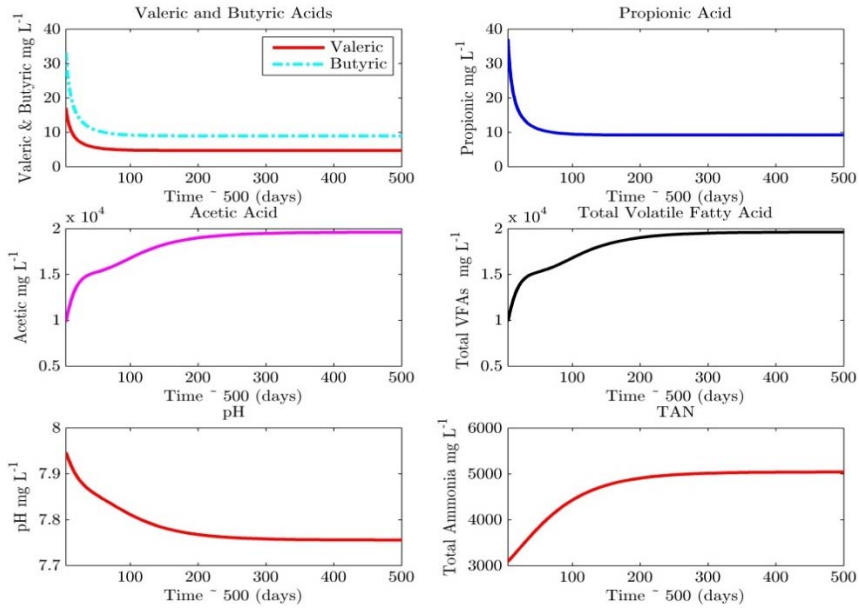

Figure 4.11 VFAs, pH and TAN of AC pathway simulation

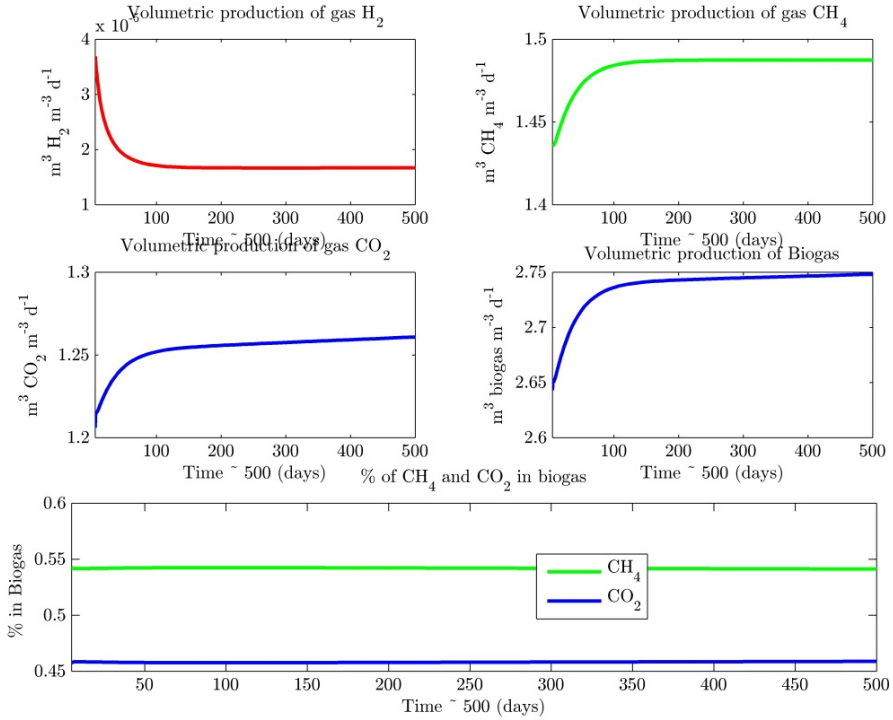

Figure 4.12 Gas production of AC & AO pathway simulation

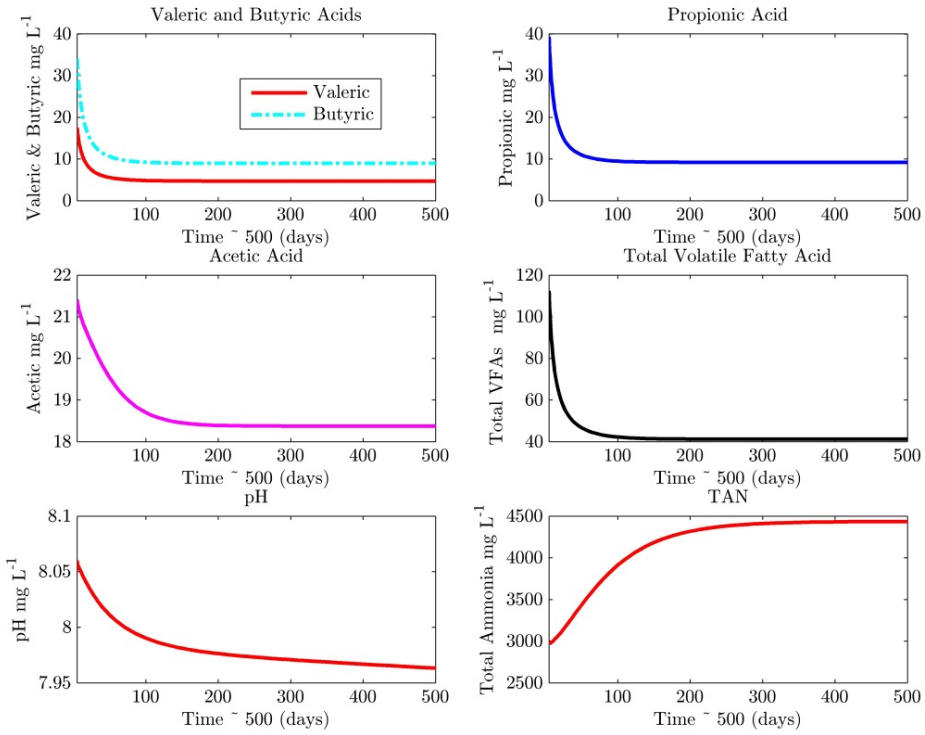

Figure 4.13 VFAs, pH and TAN of AC & AO pathway simulation

The results for the two scenarios give a good representation of what was expected in practice. It can be clearly seen that by adding the AO pathway to the model, the simulated results show almost no acetic accumulation, with concentrations at just above 15 mg L^{-1} (Figure 4.9) compared to 19610 mg L^{-1} in the AC simulation (Figure 4.7). The pH increased slightly from 7.76 in the AC simulation to 7.97 in the AC plus AO simulation. Volumetric methane production was marginally enhanced, from 1.424 m^3 m^{-3} day^{-1} to 1.487 m^3 m^{-3} day^{-1}. In contrast, TAN concentration decreased moderately from 5.042 gN L^{-1} to just above 4.4 gN L^{-1}. This reduction in TAN is perhaps due to an increased uptake by microbial biomass which expanded greatly with the support of trace elements, as suggested in (Jiang, 2012).

The proportion of methane produced by the acetoclastic and acetate oxidation routes is another interesting parameter. It is difficult to estimate exactly how much CH_4 is derived from acetate uptake or acetate oxidiser uptake both in practice and from the ADM1 model. An attempt was made to achieve this in the model by reporting separately on the amount of CH_4 generated from acetate and the amount created from the uptake of hydrogen (Figure 4.14 and Figure 4.15).

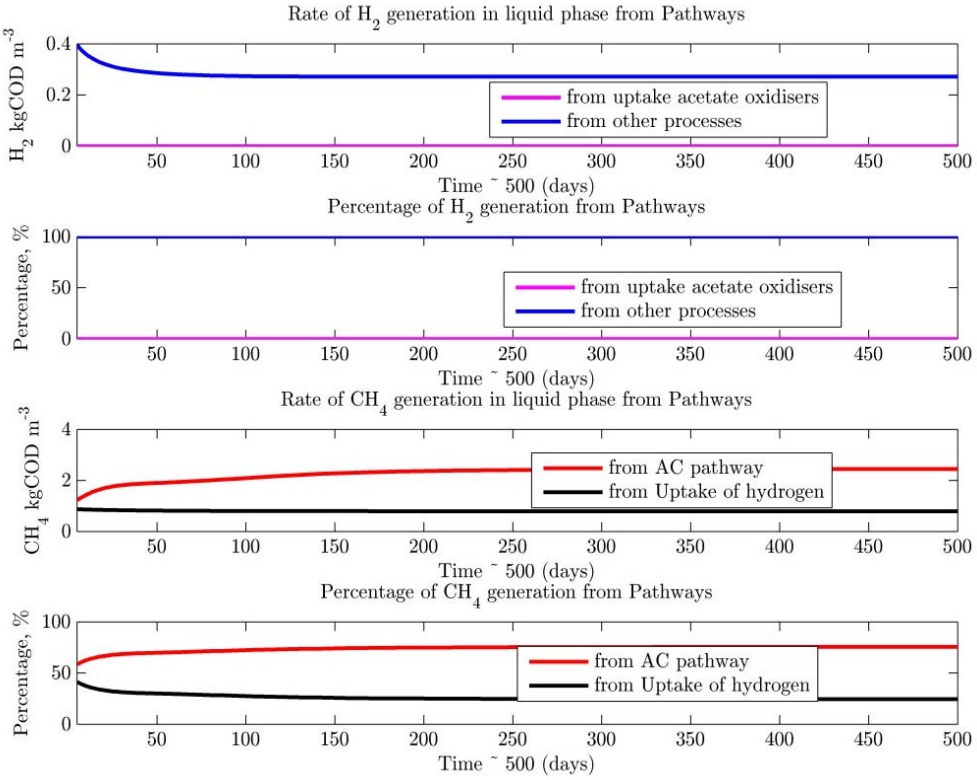

Figure 4.14 Generation of H_2 and CH_4 from pathways (AC simulation)

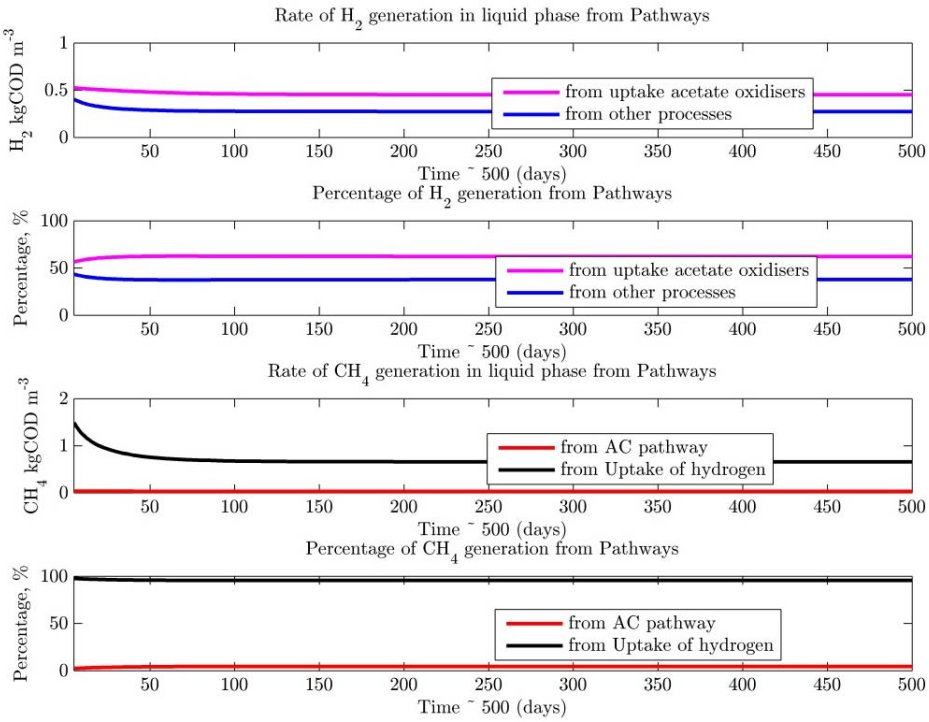

Figure 4.15 Generation of H_2 and CH_4 from pathways (AC & AO simulation)

Results from simulations indicated that with the AC pathway only operating, no hydrogen is generated from the AO route, and all produced H_2 (about 0.3 kgCOD m^{-3}) is derived from the remaining routes (Figure 4.14). However, with the AO route in operation (Figure 4.15), while the same amount of H_2 is produced by other routes, a significant extra amount of H_2 (about 0.5 kgCOD m^{-3}) is obtained from the uptake of acetate oxidisers, with a total hydrogen generation of 0.8 kgCOD m^{-3}.

Consequently, as shown in Figure 4.14, when only the acetoclastic pathway was active, a high proportion of methane was generated from the acetate uptake process, *e.g.* 72%. In contrast to this, less than 5% of methane was derived from the acetoclastic pathway when both routes operated (Figure 4.15). This means that more than 95% of methane was generated by the additional second pathway (AO), similar to the results found in recent research (Jiang, 2012; Wett *et al.*, 2014). Strictly speaking, this amount of methane is not all produced from hydrogen from acetate oxidisers since some other sources also produce hydrogen (degradation of sugars, amino acids and higher VFAs). However, this indicator implies that by adding trace elements, food waste digesters still worked properly at high TAN concentration, but with a shift in the pathway for methane formation, from an orthodox acetoclastic route to the syntrophic acetate oxidation route.

In essence, it could be suggested that in order to replicate properly the anaerobic digestion of food waste substrate, the acetate oxidation route needs to run simultaneously with the acetoclastic route. In this way, the ADM1 model was extended byh the presence of acetate oxidation methanogenesis. For this modified model, the 50% inhibitory concentration of free ammonia is recommended to be 0.00138 kgCOD m^{-3}; disintegration and hydrolysis rates of carbohydrates, proteins and lipids were set for values given in Table 4.6; kinetic parameters for AO pathway were set for values as in Table 4.11. Other stoichiometric and kinetic parameters were taken from original ADM1 as shown in Appendix B.

4.4 Validating the modified ADM1 model

In order to validate the modified model, a direct comparison between the model output and experimental data was made. Experimental results (published and not yet published) from two sets of data of laboratory–scale digesters run at the University of Southampton were used. In the following validation steps, the extended ADM1 model was implemented with the same set of stoichiometric and kinetic parameters as verified previously.

4.4.1 Model input and initial conditions

The initial conditions and food waste inputs used in the following validations are shown in Table 4.7 and Table 4.8, respectively. Since these validations were applied for the extended ADM1 version, however, one input parameter and one initial parameter for particulate acetate oxidation degraders (X_{ac2}) were assumed:

- $X_{ac2,f} = 0$, kgCOD m^{-3}.
- $X_{ac2,ini} = 2.96$, kgCOD m^{-3}.

Other stoichiometric and kinetic parameters used were the same as those specified in section *4.3.3.2*.

4.4.2 Validation

In this validation, data from a set of experimental results acquired from laboratory–based mesophilic CSTR reactors running with and without trace element supplementation was used, as presented in (Zhang & Walker, 2010). The aim of this validation was to judge if the optimised parameters suggested for the modified ADM1 version from previous steps accurately predicted the behaviour of food waste digesters.

4.4.2.1. Experimental setup and description

Details of all food waste digestion trials with trace element supplementation can be found in (Zhang & Walker, 2010). For the purpose of validation in this study, only two digesters among them were chosen and these are described briefly below.

The experimental work was carried out in a set of 5–litre digesters with a 4–litre working volume, constructed of PVC tube with gas–tight top and bottom plates (Figure 4.16). Temperature was controlled at 36±1°C by circulating water from a thermostatically–controlled bath through a heating coil around the digesters. Biogas was measured using tipping bucket gas counters with continuous data logging. Semi–continuous operation was achieved by removing digestate to ensure a constant working capacity in the digesters.

Figure 4.16 5–litre CSTR anaerobic digesters

Firstly, digesters were run at 2 g VS L^{-1} day^{-1} to reach a stable condition. Then one digester was maintained at 2 g VS L^{-1} without trace element additions (D2), while the loading rate on the other was increased to 3 g VS L^{-1} day^{-1} with trace element supplementation (D3). The trace elements consisted of Selenium (Se), Molybdenum (Mo), Cobalt (Co), Tungsten (W), Iron (Fe) and Nickel (Ni). Details of how the trace element supplementation was carried out are given in (Zhang & Walker, 2010). These two digesters were operated for 322 days after the loading rate was raised.

4.4.2.2. Validation results

Simulated and experimental results were compared for several key parameters including biogas production, methane and carbon dioxide contents, VFAs, pH and TAN concentration , as shown in Figures 4.17, 4.18, 4.19 and 4.20.

As can be seen from Figure 4.17, the biogas production, methane yield and methane composition were predicted quite well. Although small over–predictions from the model can be observed, the biggest deviation was only about 12%. The model also replicated the pH quite well, within the range of 7.8–8 for both measured and simulated results. Similar accuracy can be seen from TAN concentration as maximum deviations were only more or less 7%.

With respect to total VFA, although the simulated and measured results were not in perfect agreement for the first 140 days, the simulated results converged with the observed data afterwards. The reasons for this may include errors in setting initial variables, or the slower accumulation of VFA in digesters compared to the expected results caused by inconsistent operational conditions. Furthermore, the '*wash–out*' of inoculum digestate that contains trace elements could also be counted as another reason, although this happens in practical digesters, it was omitted from the model.

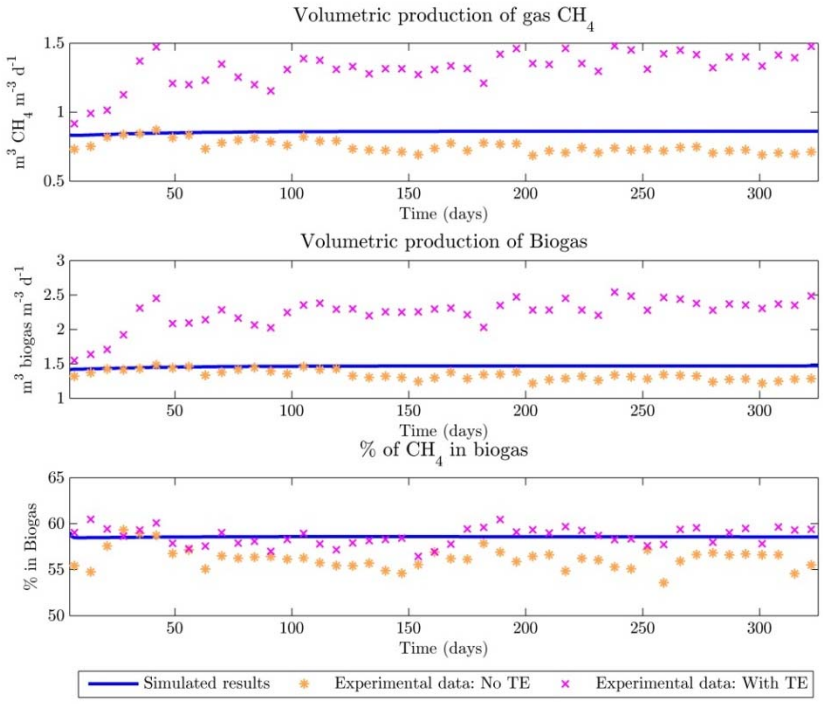

Figure 4.17 Gas production of AC & no TE simulation and experimental data (No TE: D2; With TE: D3)

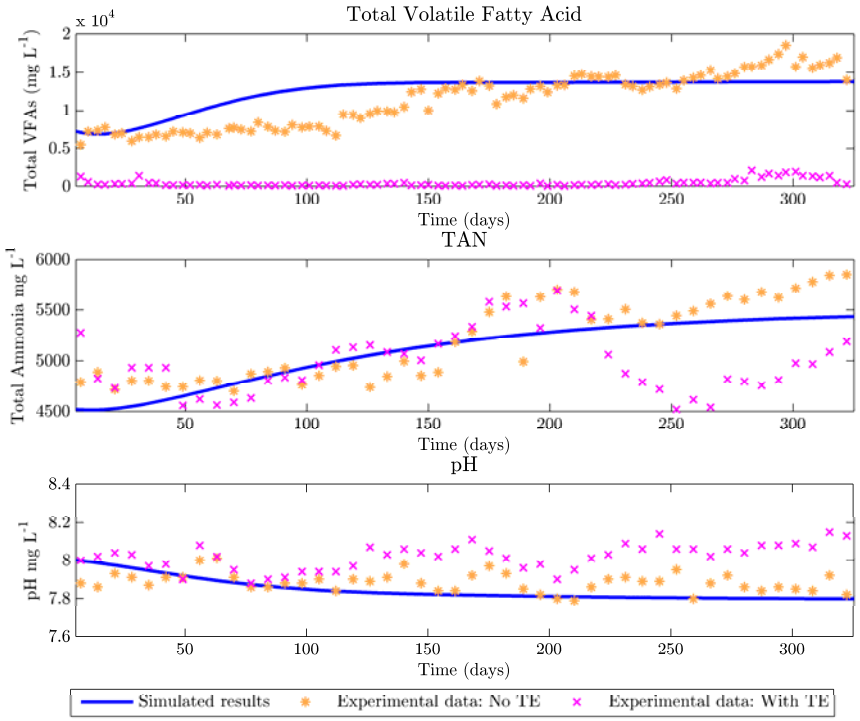

Figure 4.18 VFAs, pH and TAN concentration of AC & no TE simulation and experimental data (No TE: D2; With TE: D3)

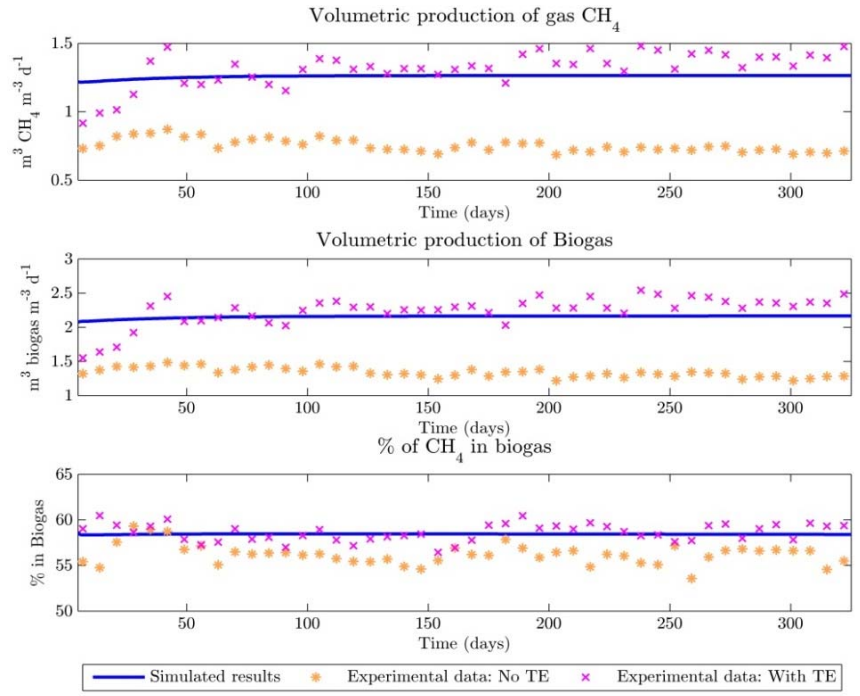

Figure 4.19 Gas production of AC + AO simulation and experimental data (No TE: D2; With TE: D3)

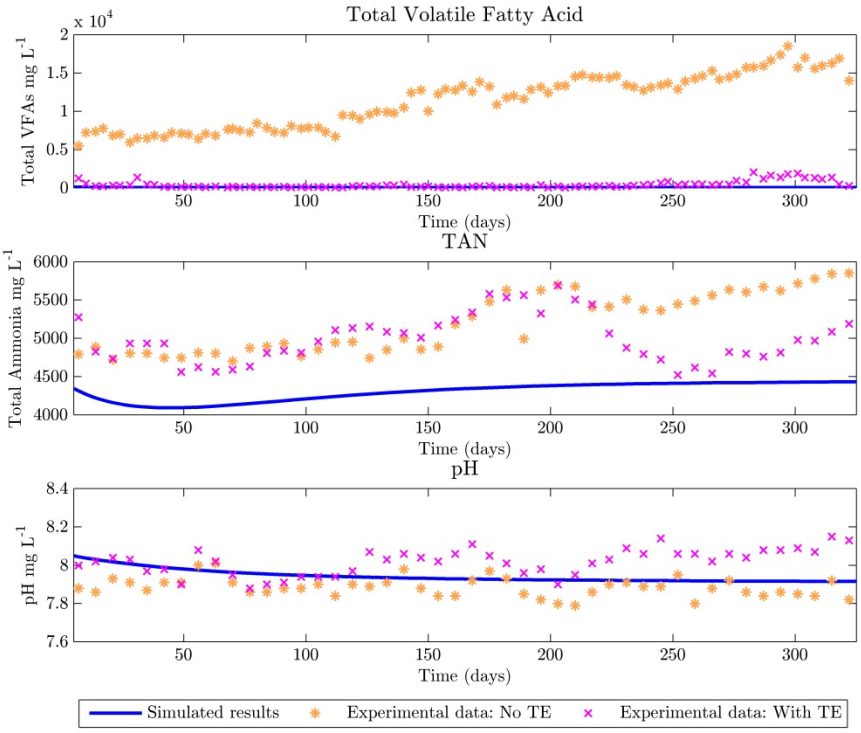

Figure 4.20 VFAs, pH and TAN concentration of AC + AO simulation and experimental data (No TE: D2; With TE: D3)

Comparing the experimental data and the simulation results with both AC and AO pathways activated, it can be clearly seen that the model again represented satisfactorily the measured data. First and foremost, the model replicated accurately the total VFAs measured with only around 100 mg L^{-1} difference observed between experiment and simulation (Figure 4.20). Furthermore, the biogas production and methane composition were predicted quite well for both steady–state and transient–state periods with the maximum deviation less than 15%. However, in the first few weeks (about 24 days) there was a considerable difference between measured and simulated data with a deviation of 25% (Figure 4.19). The reason for this maybe due to miscalculations in setting initial variables as well as limits of previous characterisation. Predicted values for pH and TAN concentration were less accurate, with the maximum deviations for both of these nearly 20%. This may indicate that the model slightly underestimated the TAN and pH measured. This could be linked to the fact that the current model calculates digestate TAN concentration by an '*end–of–pipe*' fix and does not take into account the real changes in its concentration, which may consequently affect other parameters in the digestion process.The model showed good agreement with

experimental measurements for several typical periods, however, including the changing trend where the pH increased slightly when the AO pathway increased and the TAN decreased due to the greater uptake by microbial communities.

Therefore, it was concluded that the modified ADM1 model with the proposed parameters is suitable and sufficient for food waste applications.

This page is intentionally left blank

Chapter 5

Energy model

This chapter presents a broad-based process optimisation tool (also referred to as an energy model) developed using the Aspen Plus platform and the modified ADM1 establised in Chapter 4 to allow determination and optimisation of overall mass and energy balances for different industrial scenarios. Development of specific built–in modules for certain components (CHP plant, upgrading unit, boiler unit, mixing system) which are not included in Aspen Plus, and spreadsheet models for heat loss from digesters are described.

5.1 System description

This section of the work deals with the components of the anaerobic digestion system within the system boundaries as shown in Figure 3.1.

Nine Aspen block types were used to simulate the energy model. These are defined in Table 5.1 as below.

Table 5.1 Description of Aspen Plus unit operation models

Aspen ID	Block ID	Description
RSTOIC	DIGESTER	Models reactions in the digester based on the Buswell equation (current stage) and ADM1 model (future work)
FLASH	SEPARATOR	Separates digester output into gas and digestate
	FLASHTAN	Releases most CH_4 and some CO_2 in liquid coming out of the absorber
HEATER	COOLER1, COOLER2 COOLER3	Cools down the temperature of water streams
	HRSG	Heat Recovery Steam Generator
RADFRAC	STRIPPER1, STRIPPER2	Model of Strippers
	ABSORBER	Model of Absorber
FSPLIT	SPLITTER, SPLITTER2, SPLITTER3	Divides feed based on splits specified for outlet streams
COMPR	COMP1, COMP2, COMP3, COMP4	Changes stream pressure to meet the pressure requirement based on energy demand–related information, such as power requirements
	FAN1, FAN2	Generates enough pressure of gas and air for upgrading system
	GASTURB	Generates electricity as an isentropic turbine
RGIBBS	BURNER1	Equilibrium reactor with Gibbs energy minimisation
PUMP	PUMP1	Changes pressure to meet the pressure requirement

The main components of the platform are shown in Figure 5.1, and the Aspen Plus simulation window is shown in Figure 5.2.

As can be seen from Figure 5.2, food waste is initially fed into a digester for the digestion. Raw biogas produced by the digester may be fed to a CHP unit and/or boiler for generating electricity and/or heat, or to an upgrading

unit for biofuel production. Typically, the overall efficiency of a CHP unit using gas is about 90 % (Seadi *et al.*, 2008). The electrical efficiencies can vary depending upon the CHP unit's configuration and capacities but about 35–43% can be achieved (Weiland, 2010). A CHP unit can also produce heat with an efficiency of around 65%, depending on the type of boiler used (Verougstraete *et al.*, 1985).

Both thermal and electrical energy can be used to meet on–site energy requirements or for off–site purposes. In some cases, when the demand for heat for internal uses exceeds the amount of heat generated by the CHP unit, a boiler is integrated in the biogas plant to make up the deficiency.

A certain amount of raw biogas may also be fed to the upgrading unit to be refined for biofuel purposes. In the upgrading unit, carbon dioxide and unwanted compounds are separated from the raw biogas to make purified biogas with a composition that meets the requisite standard for vehicle fuel or natural gas for grid injection.

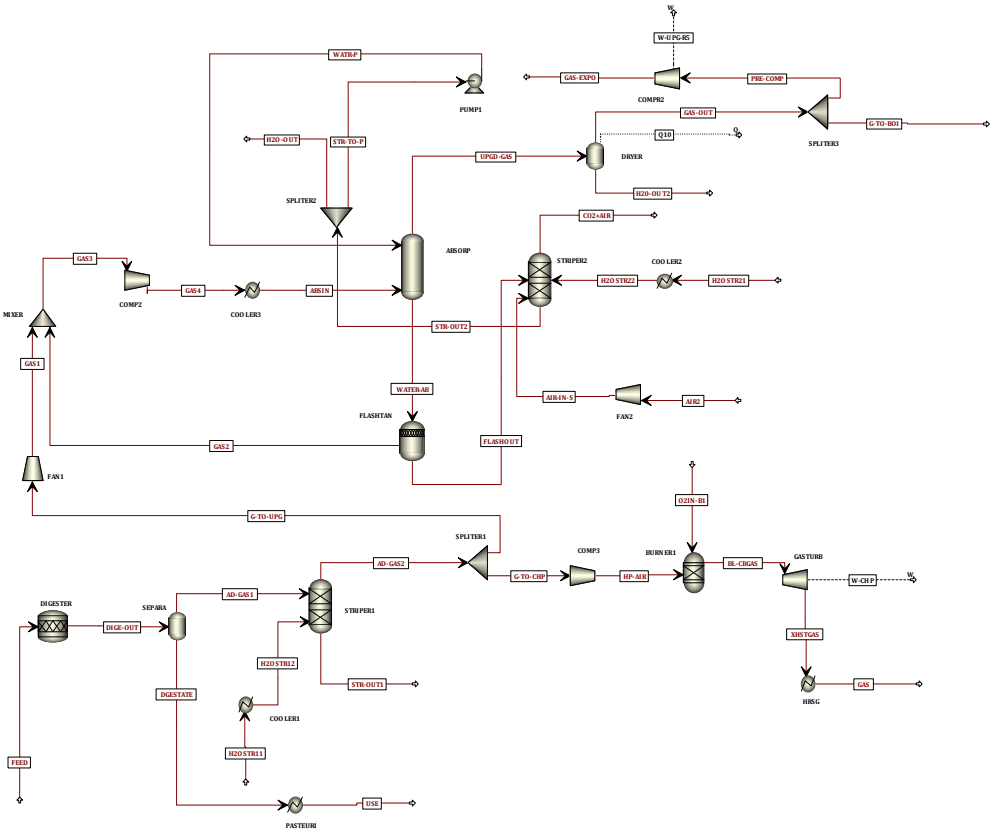

Figure 5.1 Main components of the energy model

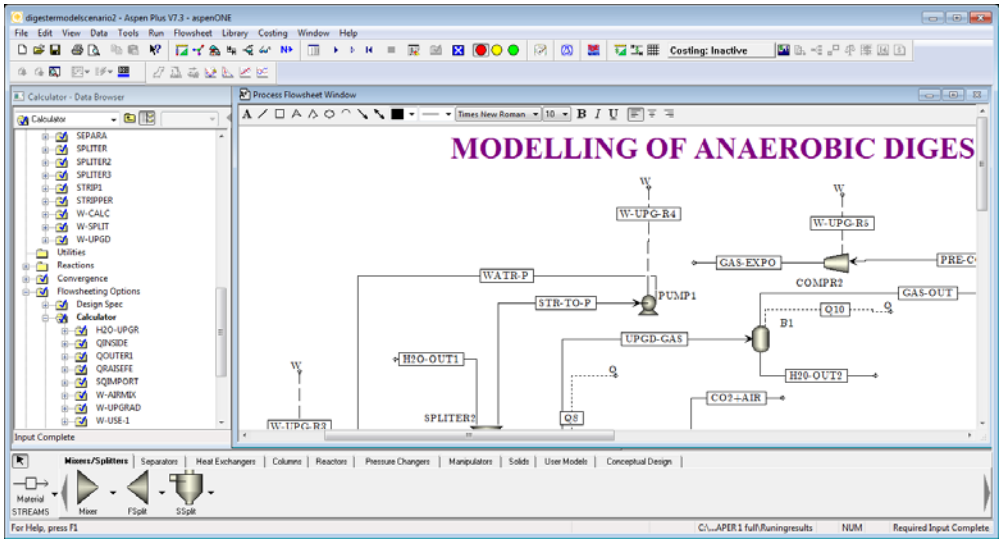

Figure 5.2 Aspen Plus simulation window

The following sections describe how the main components were implemented in the model.

5.2 Digestion unit

The model was implemented with a choice of options for the digestion process: a simple steady–state option based on stoichiometry, and a dynamic version based on ADM1. A simple steady–state digester based on a stoichiometric approach was built in Aspen Plus for two reasons. Firstly, it was used for verification against the dynamic model of ADM1 in terms of biogas production, the most important product of anaerobic digestion technology, as mentioned in Chapter 3. Secondly, it can be used selectively in the whole energy model to size elements of a biogas plant quickly without any concern about the dynamic and kinetics issues of ADM1, which undoubtedly require a lot of information to run.

5.2.1 Theoretical stoichiomentric model

A theoretical stoichiometric method based on the Buswell equation is an easy way to estimate products of the anaerobic digestion process (*e.g.* biogas, digestate). This method has been widely applied in a large number of studies (Sobotka *et al.*, 1983; Shelton & Tiedje, 1984; Hayes *et al.*, 1990; Angelidaki & Ahring, 1992; Salanitro & Diaz, 1995; Sialve *et al.*, 2009), *etc.*

Symons and Buswell (1933) presented an equation for the overall process of anaerobic degradation, known as the '*Buswell equation*':

$$C_cH_hO_oN_nS_s + yH_2O \rightarrow xCH_4 + (c\text{-}x)CO_2 + nNH_3 + sH_2S \quad (5.1)$$

$$\text{where: } x = \frac{1}{8}\left(4c + h - 2o - 3n - 2s\right) \text{ and } y = \frac{1}{4}\left(4c + h - 2o + 3n + 3s\right)$$

The validation of this theoretical approach was made in terms of methane yield and other products for further energy calculation.

5.2.1.1. Estimation of physical properties for food waste simulation

In Aspen Plus, all blocks need property methods to generate results (Schefflan, 2011). The property method used in this work is NRTL (Non–Random–Two–Liquid) as it takes activity coefficients of different compounds into account and also facilitates the liquid and the gas phase in the biogas production (Serrano, 2011; Rajendran *et al.*, 2014). The Henry's component list HC contains O_2, H_2S, CO_2 and CH_4. These components are assumed to obey Henry's law for calculation of their solubility in the liquid phase.

Although the software includes databases on a wide range of chemical compounds to support different types of simulation, food waste is a non–conventional component and is not available in the standard Aspen Plus property databases. Its characteristics therefore need to be estimated using a physical property method (Wooley & Putsche, 1996). Due to the complex composition of food waste, an empirical formula was used in this model at this stage.

The empirical formula of food waste was estimated based on its ultimate analysis as presented in Table 5.2 (Zhang, Banks, *et al.*, 2012a).

Table 5.2 Ultimate analysis of food waste

Component	Elemental composition (*TS basis*)	Atomic weight(*)
C (%)	47.6	12.0116
H (%)	7.67	1.00811
O (%)	35.9	15.99977
N (%)	3.48	14.00728
S (%)	0.16	32.076

Note: (*) Data from (Wieser *et al.*, 2013).

Assuming that food waste is broken down into its elemental composition of carbon, hydrogen, oxygen, nitrogen and sulphur, if 1 mole of food waste (dry basis) is assumed, then the empirical formula for food waste can be expressed as: $C_{3.963}H_{7.608}O_{2.248}N_{0.248}S_{0.005}$.

Physical properties of food waste were estimated based on values for cellulose and biomass in the NREL (National Renewable Energy Laboratory, USA) biofuels databank which is included in Aspen Plus, and these are listed in Table 5.3 (Wooley & Putsche, 1996).

Table 5.3 Food waste physical property using as non–database component

Property	Aspen property	Unit	Food waste
Molecular weight	MW		94.80934
Solid Heat of Formation(*)	DHSFRM	J Kmole^{-1}	–782,931,796
Solid Molar Volume (**)	VSPOLY–1	cum Kmole^{-1}	0.106
	VSPOLY–2		0
	VSPOLY–3		0
	VSPOLY–4		0
	VSPOLY–5		0
	VSPOLY–6		298.15
	VSPOLY–7		1000
Solid Heat Capacity (**)	CPSPO1–1	J Kmole^{-1} K^{-1}	–11704
	CPSPO1–2		672.07
	CPSPO1–3		0
	CPSPO1–4		0
	CPSPO1–5		0
	CPSPO1–6		0
	CPSPO1–7		298.15
	CPSPO1–8		1000

Note: (*) Estimated from Cellulose and Biomass data; (**) estimated from Cellulose data (Wooley & Putsche, 1996).

5.2.2 Stoichiometric model validation

As methane production from anaerobic digestion is the key parameter for the mass and energy balance calculations, this model was validated on methane yield. The validation was carried out using two case studies for digesters with different volumes. Case study 1 was adapted from a small pilot–scale digester

of 1.5 m^3 which ran for 58 weeks (Banks *et al.*, 2008). In contrast, case study 2 is a data set reported from a 900 m^3 digester running for 62 weeks (Banks, Chesshire, *et al.*, 2011).

Table 5.4 shows the modelling results: it can be seen that the model predictions are in good agreement for the two case studies. The methane yields estimated from the model for case study 1 and 2 are 0.2743 and 0.2874 kg CH_4 kg^{-1} VS_{added} which are equal to 0.383 and 0.401 m^3 CH_4 kg^{-1} VS_{added}, respectively. These values are close to methane yield data from previous research: 0.405–0.415 (Cho *et al.*, 1995), 0.44 (Zhang *et al.*, 2007), 0.348–0.435 (Demirel *et al.*, 2010). Therefore, it was concluded that the stoichiometric model is adequate to estimate biogas generation from food waste digestion.

Table 5.4 Case studies results versus model calculation

Parameters	Unit	Case study 1	Case study 2
Case study information			
Volume of Digester	m^3	1.5	900
Duration of study	week	58	61
Average TS (%WW)	%	23	27.7
Average VS (%WW)	%	21.16	24.4
Validation data			
Plant data CH_4 yield	kg kg^{-1} VS_{added}	0.2617	0.2865
Model estimation CH_4 yield	kg kg^{-1} VS_{added}	0.2743	0.2874
Differences		0.0126 (4.8%)	9×10^{-4} (0.31%)

5.2.3 ADM1 model of the digester

As mentioned, one of the aims of this research was to integrate the modified ADM1 model described in Chapter 4 with Aspen Plus to allow accurate simulation of biogas plant operation in terms of mass and energy balance. At the plant level there is no need to simulate the process dynamically as the main purposes of simulation are to predict future mass and energy balances for anaerobic digester inputs, to size elements included in the plant, and to run scenarios under different operating conditions with alternative energy utilisation options. Outputs from running a modified ADM1 model when it reaches steady–state conditions can be used as the inputs for the energy model to achieve the above purposes. Users can also choose a period to estimate the mass and energy balance of the whole system on a daily basis.

5.3 Calculation of energy requirements

5.3.1 Heating calculations

Although the anaerobic digestion process can occur at ambient temperatures, it is slow and therefore anaerobic digesters are normally heated to accelerate the process and enhance biogas production. In mesophilic and thermophilic digestion, heat is required to (*i*) raise the temperature of the feedstock and (*ii*) compensate for heat losses from the digester (*e.g.* roof, walls and base of the digester).

5.3.1.1. Heat to raise the temperature of feedstock

As the digester in this research was assumed to work in mesophilic conditions, the required feedstock temperature was assumed to be 35°C. Initial heating of feedstock is calculated from:

$$H = C_p Q\left(T_{op} - T_f\right) \tag{5.2}$$

Where C_p is specific heat, kJ kg^{-3} K^{-1}; Q is volumetric flowrate m^3 s^{-1}; T_{op} is the operating temperature (37°C); T_f is the feedstock temperature. T_f was assumed to be 5°C.

5.3.1.2. Heat loss calculation

An important element in determining the overall energy balance of the energy model is the heat loss from the digester and to estimate this, heat transfer coefficients are needed. Therefore, an Excel spreadsheet model was constructed to calculate heat loss based on overall heat transfer coefficients of digester components.

In the Excel spreadsheet, the total calculated heat loss by heat transfer through the walls and the roof takes into account the conduction, convection and radiation processes. It also allows a choice of two types of digester construction: steel or concrete, with different layers in the wall structure including water insulation, heat insulation, mortal coating and aluminum plates (see Figure 5.3).

Heat transfer coefficient calculation			
Wall construction			
Number of wall-layers	3		
Layers	**Layer 1**	**Layer 2**	**Layer 3**
Material	water insulation	steel	heat insulation
Heat transfer coefficient	0.6	64	0.03
Thickness (mm)	5	25	5
Roof construction type	**Different from the wall**		
Layers of the roof	3		
Layers	**Layer 1**	**Layer 2**	**Layer 3**
Material	HDPE	air gap	HDPE
Heat transfer coefficient	0.33	1	0.33
Thickness (mm)	1		1
Floor construction			
Number of floor-layers	3		
Layers	**Layer 1**	**Layer 2**	**Layer 3**
Material	water insulation	concrete (stone)	concrete (stone)
Heat transfer coefficient	0.6	1.5	1.5
Thickness (mm)	5	70	
Overall heat transfer coefficient of the digester			
FLOOR	**WALL**	**ROOF**	
0.947	4.114	0.931	

Figure 5.3 Overall heat transfer coefficients tool used to calculate heat losses from digester

Digesters are commonly cylindrical, with the roof often including an air layer in order to reduce heat loss (Qasim, 1998). This configuration was therefore applied in this work. In previous studies, authors have often assumed that the structure of the roof and wall of the digester are similar and there is no air layer in the roof (Zupancic, 2003; Salter & Banks, 2009; Higgins & Kendall, 2012). This may lead to incorrect results, therefore the air layer of the digester roof was included in the calculations. The convective heat transfer coefficient of the air–gap (α_A) was taken as 1 W m^{-2} K^{-1} based on the following assumptions and calculations:

- typical digester layout as shown in Figure 5.4,
- digester roof structure is two layers of HDPE, thickness 0.001 m each, with heat transfer coefficient 0.5 W m^{-1} K^{-1},
- average temperature of air–gap layer is 27°C (300 K). Hence, its heat transfer coefficient is 0.02623 W m^{-1} K^{-1} (Lienhard, 2011),
- temperature on inside of outer HDPE layer (point 3a) is 10°C,
- temperature inside digester T_{inner} (point 1) is 37°C,

- temperature outside digester T_{outer} (point 4) is 5°C,
- convective heat transfer coefficient: α_{inner} = 1000 W m^{-2} K^{-1} (liquid phase) and α_{outer} =15 Wm^{-2} K^{-1} (gas phase) (Lienhard, 2011).

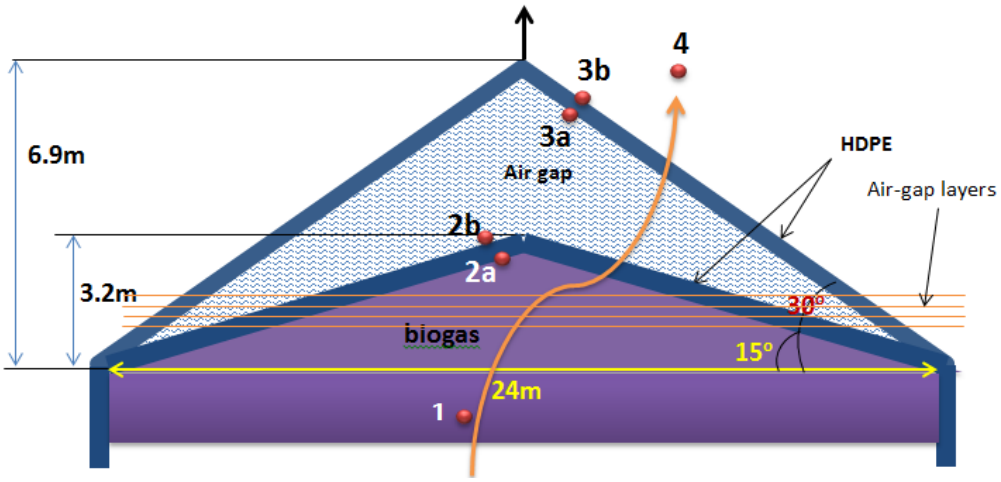

Figure 5.4 Structure of the exemplified digester's roof

Calculation of heat loss (Q)

Heat is transferred through the HDPE layers and the air–gap. The air–gap thickness changes from 0 to $12 \times \left[\tan(30^o) - \tan(15^o)\right] = 3.71$ m. Q can be obtained from the differential equation:

$$dQ = k \cdot dF \cdot \left(T_{inner} - T_{outer}\right) \tag{5.3}$$

Where:

$$k \cdot dF = \frac{r \cdot dr}{A + B + Cr} \tag{5.4}$$

$$\Rightarrow dQ = \frac{\left(T_{inner} - T_{outer}\right) r \cdot dr}{A + B + C \cdot r} \tag{5.5}$$

Where:

$$A = \left(\frac{1}{1000} + \frac{0.001}{0.5}\right) \times \frac{\cos^2(15)}{2\pi} = \frac{\frac{3\sqrt{3}}{8000} + \frac{3}{4000}}{\pi} = 4.455 \times 10^{-4}$$

$$B = \left(\frac{1}{15} + \frac{0.001}{0.5}\right) \times \frac{\cos^2(30)}{2\pi} = \frac{103}{4000\pi} = 8.2 \times 10^{-3}$$

$$C = \frac{1}{0.02623 \times \delta} \times \frac{\cos^2(30) \times \left[\tan(30) - \tan(15)\right]}{2\pi}$$

and δ is an "*adjustment number*" for natural convection in an enclosure which can be calculated as below:

$$\delta = 0.18(Gr \times Pr)^{0.25} \tag{5.6}$$

$$Gr = \frac{g\beta\left(T_1 - T_2\right)D^3}{\upsilon^2} \tag{5.7}$$

Where r is radius of the digester, m; Gr is the *Grashof* number (dimensionless); Pr is *Prandtl* number (dimensionless); g is acceleration due to Earth's gravity = 9.81 m s^{-2}; β is volumetric thermal expansion coefficient (approximately equal to $1/T$ for ideal fluids, where T is absolute temperature); T_{inner} is temperature inside digester (assumed 37°C); T_{outer} is temperature outside digester (assumed 5°C) T_1 is temperature of the air layer near the inner HDPE ($2b$), assumed 37°C; T_2 is temperature of the air layer near the inner HDPE ($3a$), assumed 10°C; D = 1.85m is average thickness of the air gap; υ is the kinematic viscosity of air, $m^2\,s^{-1}$.

As the average temperature of the air gap was assumed to be 27°C, the kinematic viscosity υ = 1.578×10^{-5} m^2 s^{-1} and Pr = 0.713 (Lienhard, 2011). Therefore:

$$Gr = \frac{9.81\frac{1}{300}\left(37 - 10\right)1.85^3}{\left(1.578 \cdot 10^{-5}\right)^2} = 2.245 \times 10^9$$

$$\delta = 0.18\left(2.245 \times 10^9 \times 0.713\right)^{0.25} = 64$$

$$\Rightarrow C = \frac{1}{0.02623 \times 64} \times \frac{\cos^2(30) \times \left[\tan(30) - \tan(15)\right]}{2\pi} = 0.022$$

$$\Rightarrow dQ = \frac{\left(37 - 5\right)r \cdot dr}{8.6455 \times 10^{-3} + 0.022 \cdot r}$$

Because r ranges from 0 to 12, this gives:

$$Q = \int_0^{12} \frac{32}{8.6455 \times 10^{-3} + 0.022 \cdot r} r \cdot dr = 15481\ W$$

Calculation of the overall heat transfer coefficient (U)

The heat transfer through the roof of digester is:

$$Q = U \cdot A \cdot \Delta T \tag{5.8}$$

Where Q is heat loss per unit time, W; A is area of the roof = 522.4 m²; ΔT is temperature difference, °C. As calculated from above, Q = 15481 W.

The overall heat transfer coefficient for the roof can now be calculated as follows:

$$U = \frac{Q}{A \cdot \Delta T} \tag{5.9}$$

$$\Rightarrow U = \frac{15481}{522.4 \times (37 - 5)} \approx 0.93$$

Calculation of the convective heat transfer coefficient of the air–gap

To simplify calculation of the heat loss for different sizes/diameters of the roof, the convective heat transfer coefficient of the air–gap between the 2 HDPE layers is needed.

Conduction takes place in the air gap between two HDPE layers. This process can be considered as transfer through a thin air layer so it is likely to be a convective process with a very small heat transfer coefficient α_A. So the overall heat transfer coefficient should be:

$$\Rightarrow U = \frac{1}{\frac{1}{\alpha_{inner}} + \frac{HDPE\ thickness}{\lambda_{inner}} + \frac{1}{\alpha_A} + \frac{HDPE\ thickness}{\lambda_{inner}} + \frac{1}{\alpha_{outer}}} \tag{5.10}$$

Where α_{inner} is the inner convective heat transfer coefficient; α_{outer} is the outer convective heat transfer coefficient; λ_{inner} is conductive heat transfer

coefficient of the HDPE; and α_A is the heat transfer coefficient of the air layer, W m^{-2} K^{-1}. For the current case:

$$\Rightarrow 0.93 = \frac{1}{\frac{1}{1000} + \frac{0.001}{0.5} + \frac{1}{\alpha_A} + \frac{0.001}{0.5} + \frac{1}{15}}$$

$$\Rightarrow \alpha_A = 0.996$$

Another sample calculation based on the same steps was carried out using data from Zupancic (2003) with an inner heat transfer coefficient of 245 W m^{-2} K^{-1}, and gave $\alpha_A = 0.99$ W m^{-2} K^{-1}.

From these calculations it seems likely that, while the convective heat transfer coefficient of the air–gap will vary depending on the position of the HDPE membranes, the size of digester, structure of digester roof and the nature of the gas layer, a value of $\alpha_A \approx 1$ W m^{-2} K^{-1} is reasonable for a typical digester construction, and is used for simulation purposes in this study.

5.3.2 Digester mixing

As presented in section *2.2.2.4*, this study employed gas mixing and mechanical mixing systems for model implementation.

5.3.2.1. Gas mixing module

Gas mixing is one of the most popular methods of digester mixing in the UK since its key benefit is the absence of moving parts inside the digester (Cumiskey *et al.*, 2003). The design of a gas mixing system is based on generally accepted empirical correlations or '*rules–of–thumb*' using: (*i*) power input per unit volume (W m^{-3}), (*ii*) gas flow rate per unit volume of digestate (m^3 h^{-1} m^{-3}), and (*iii*) gas flow rate per unit cross–sectional area of digester (m^3 h^{-1} m^{-2}).

Two types of gas mixing were implemented in this model: confined (*draft tube*) and unconfined (*free lift*). Schematic diagrams for the gas mixing systems are presented in Figure 5.5.

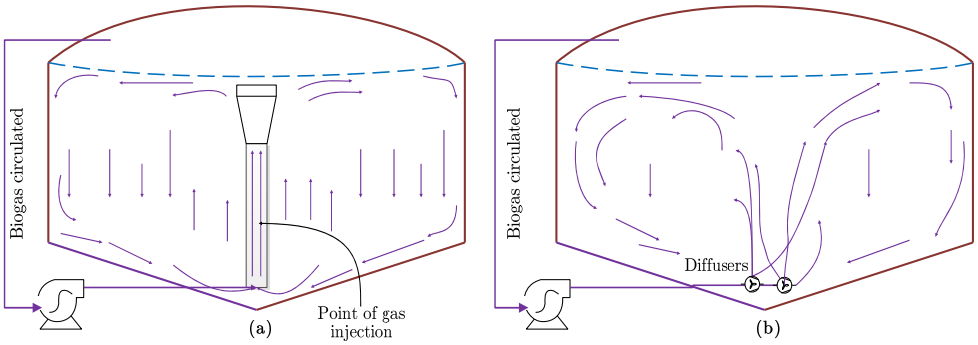

Figure 5.5 Schematic diagrams of gas mixing systems: (*a*) confined (*draft tube*) gas injection, (*b*) unconfined (*free lift*) gas injection. Adapted from (EPA, 1979, 1987)

When gas is discharged into a digester, liquid flow results from the transfer of energy from the gas to the liquid as the gas expands isothermally and rises to the surface (EPA, 1987). Ignoring the kinetic energy of the gas, the rate of power transferred from the gas to the liquid may be expressed as in equation (5.2).

$$E = 2.4 P_1 Q \ln \frac{P_2}{P_1} \tag{5.11}$$

Where E is rate of energy transfer (power), J s^{-1} (or W); Q is gas flow rate, m^3 min^{-1}; P_1 is absolute pressure at liquid surface, atm; P_2 is absolute pressure at the depth of gas injection, atm.

The position of gas injection is assumed to be at the bottom of the digester and it is assumed that pressure at the injector position is 1.05 times higher than the pressure of internal liquid at that depth to generate the necessary pressure for performance.

$$P_2 = P_1 + 1.05 \rho H g \tag{5.12}$$

Where ρ is density of liquid in digester, kg m^{-3}; H is depth of the digester, m; g is the acceleration due to Earth's gravity, m s^{-2}.

The velocity gradient to measure the effectiveness of the gas mixing is given by:

$$G = \sqrt{\frac{W}{\mu}} = \sqrt{\frac{E/V}{\mu}} \tag{5.13}$$

Where G is velocity gradient, s^{-1}; W is power dissipated per unit volume, J m^{-3} s^{-1} (or W m^{-3}); E is rate of energy transfer (power), J s^{-1} (or W); V is volume of reactor, m^3; μ is absolute viscosity of mixed substrate, kg m^{-1} s^{-1}.

The value of μ is assumed to be in the range of 2.12 to 3.27 mPa s^{-1} (Tixier *et al.*, 2003). The velocity gradient for an effective mixing system as suggested by Barggman (1996) is 50–80 s^{-1}.

The unit gas flow rate required to produce a desired velocity gradient can be estimated as:

$$Q = V \frac{G^2 \mu}{2.4 P_1 \ln\left(\frac{P_2}{P_1}\right)} \tag{5.14}$$

Where Q is gas flow rate, m^3 min^{-1}; P_1 is absolute pressure at liquid surface, atm; P_2 is absolute pressure at the depth of gas injection, atm.

Turovskiĭ and Mathai (2006) suggested that the unit gas flow requirement for unconfined circulation is 0.0045–0.005 m^3 m^{-3} min^{-1}. In this study, the average value of 0.00475 m^3 m^{-3} min^{-1} was used. A gas flow rate of 0.006 m^3 m^{-3} min^{-1} was used for the confined (draft tube) mixing type based on the values of 0.005–0.007 m^3 m^{-3} min^{-1} proposed by (Metcalf *et al.*, 2003; Turovskiĭ & Mathai, 2006) for this method.

Since the key target of this study was to produce an energy balance, the purpose of modelling the gas mixing unit is to determine the power consumption per unit volume of digester during gas mixing (W m^{-3}).

The schematic model of gas mixing used in Aspen Plus is shown in Figure 5.6.

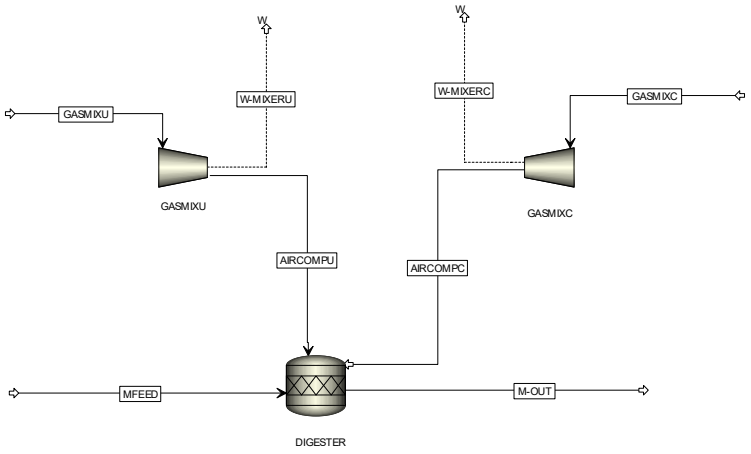

Figure 5.6 Schematic gas mixing model

In order to confirm the validity of the gas mixing model, a verification step was carried out. Data were taken from two case studies of gas–mixing systems for anaerobic digestion of sludge with a dry solids content of 12% (Cumiskey *et al.*, 2003). Model controlling parameters *i.e.* compressor effectiveness were adjusted to get an acceptable value of power consumption during gas mixing.

5.3.2.2. Mechanical mixing module

Mechanical mixing devices consist of three main elements: an impeller, a shaft and a motor or a gear box (Figure 5.7). The power consumption and effectiveness of a mechanical mixing device is determined mainly by the characteristics of its impeller.

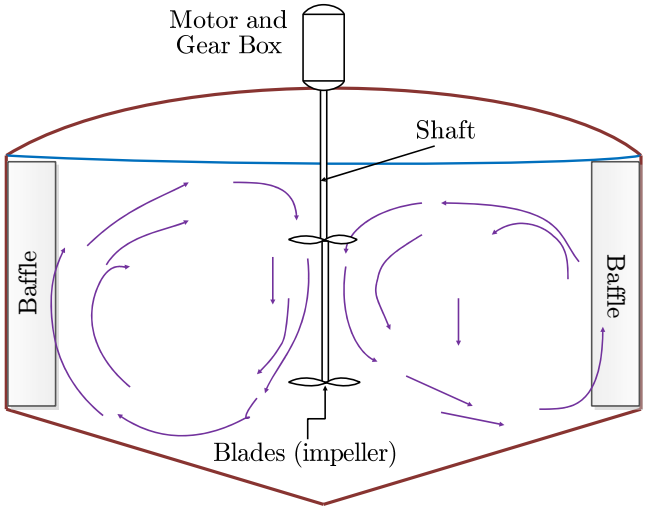

Figure 5.7 Schematic diagram of mechanical mixing system

The three most widely used types, namely, propeller, turbine and paddle mixers (Laoulache, 2011) were implemented in this study. Propeller mixers are used for mixing liquids with viscosities up to 2000 cP, and particle size from 0.1 to 0.5 mm. They are unsuitable for suspending a rapidly settling substance. Turbine mixers are operated at relatively high rotational speeds. Paddle mixers consist of two or more blades mounted on a vertical or inclined shaft. They are used for liquids with viscosities only up to about 1000 cP. Due to the concentration gradient that is often created in the liquid when mixers of this type are used, they are unusable for continuous operation (Cheremisinoff, 2000; Raju, 2011). Several types of these impellers are presented in Figure 5.8 and these were implemented in the mechanical mixing module so that users can

choose suitable ones for the intended purpose. The mechanical mixing module was simulated using an Excel spreadsheet. Power consumption was estimated and then linked to Aspen Plus for the energy balance calculation.

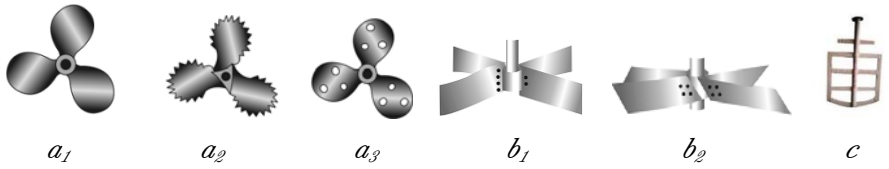

Figure 5.8 Various typical types of impellers: (a_1) Marine propeller, (a_2) Saw–toothed propeller, (a_3) perforated propeller; (b_1) Standard blade turbine, (b_2) Pitched blade turbine, (c) Anchor paddle mixer

The power requirement of an agitator system is a function of the impeller shape, size, speed of rotation, fluid density and viscosity, vessel dimensions and internal attachments *etc.* (Ludwig, 1995). Many authors have reported impeller power characteristics in terms of dimensionless numbers: the power number (N_P) and Reynolds number (N_{Re}) (Raju, 2011; Holloway *et al.*, 2012).

Power number N_P relates impeller power P to operating variables such as liquid density μ, agitator rotational speed N, and impeller diameter D as follows:

$$N_P = \frac{P}{\rho N^3 D^5} \tag{5.15}$$

Where P is power dissipation, kW; N_P is power number, dimensionless; ρ is fluid density at conditions, kg m^{-3}; N is impeller rotational speed, rev s^{-1}; D is impeller diameter, m.

Reynolds number (dimensionless) can be calculated as:

$$N_{\mathrm{Re}} = \frac{\rho N D^2}{\mu} \tag{5.16}$$

In agitation, turbulent conditions exist when $N_{\mathrm{Re}} > 10000$ and laminar conditions exist for $N_{\mathrm{Re}} < 10000$. In most cases, the Reynolds number is ≥ 10000 therefore the flow in the tank is fully turbulent.

The Power and Reynolds numbers for different types of impellers and ratios of impeller diameter to tank diameter are shown in Table 5.5.

Table 5.5 Power number (N_P) and Reynolds number (N_q) of mixers with different impeller patterns and ratio of impeller diameter to tank diameter

N_P at turbulent	D/T = 0.25		D/T = 0.3		D/T = 0.4		D/T = 0.5		Ref.
(Re ≥ 10000)	N_P	N_q	N_P	N_q	N_P	N_q	N_P	N_q	
180 Degree Concave	3.2	0.7	3.2	0.7	3.2	0.7	3.2	0.7	*d*
Anchor	5	0.35	5	0.35	5	0.35	5	0.35	*c*
Chemineer HD3	0.33	0.57	0.32	0.55	0.29	0.53	0.27	0.51	*d*
Curved blade (P–6)	4.8	0.3	4.8	0.3	4.8	0.3	4.8	0.3	*a*
Narrow Hydrofoil	0.31	0.57	0.31	0.55	0.31	0.53	0.31	0.51	*d*
Pitched blade (P–4)	1.37	0.79	1.37	0.79	1.37	0.79	1.37	0.79	*a*
Pitched blade (P–6)	1.7	0.79	1.7	0.79	1.7	0.79	1.7	0.79	*a*
Pitched Blade Turbine	1.37	0.88	1.37	0.8	1.37	0.68	1.37	0.6	*d*
Propeller (3 blade)	0.32	0.6	0.32	0.54	0.32	0.47	0.32	0.4	*a*
Rushton 6 Blade (D–6)	5.5	0.72	5.5	0.72	5.5	0.72	5.5	0.72	*d*
Straight blade (S–4)	3.96	0.62	3.96	0.62	3.96	0.62	3.96	0.62	*b*
Straight blade (S–6)	3.86	0.7	3.86	0.7	3.86	0.7	3.86	0.7	*a*
Straight blade (P–2)	1.7	0.62	1.7	0.62	1.7	0.62	1.7	0.62	*b*
Wide Hydrofoil	1.06	0.8	1.05	0.73	1	0.63	0.98	0.56	*d*

Note: D/T is ratio of impeller diameter to tank diameter. *a*: (Paul *et al.*, 2004), *b*: (Post-Mixing, 2012), *c*: (Doran, 1995), *d*: (Benz, 2011)

In a large digester, there can be more than one mixer. For the mixing purposes mentioned, the speed of rotation is not important, therefore slow rotating mixers are usually applied with rotations as low as 15–50 rpm (Burton & Turner, 2003). Standard geometry utilises only one impeller on the mixer shaft. If the ratio of liquid height to diameter (Z/T) < 1.2 one impeller is needed; if (Z/T) > 1.2 then two impellers are used (Cheremisinoff, 2000).

Figure 5.9 shows a screen–shot of the mechanical mixing calculation integrated with Aspen Plus.

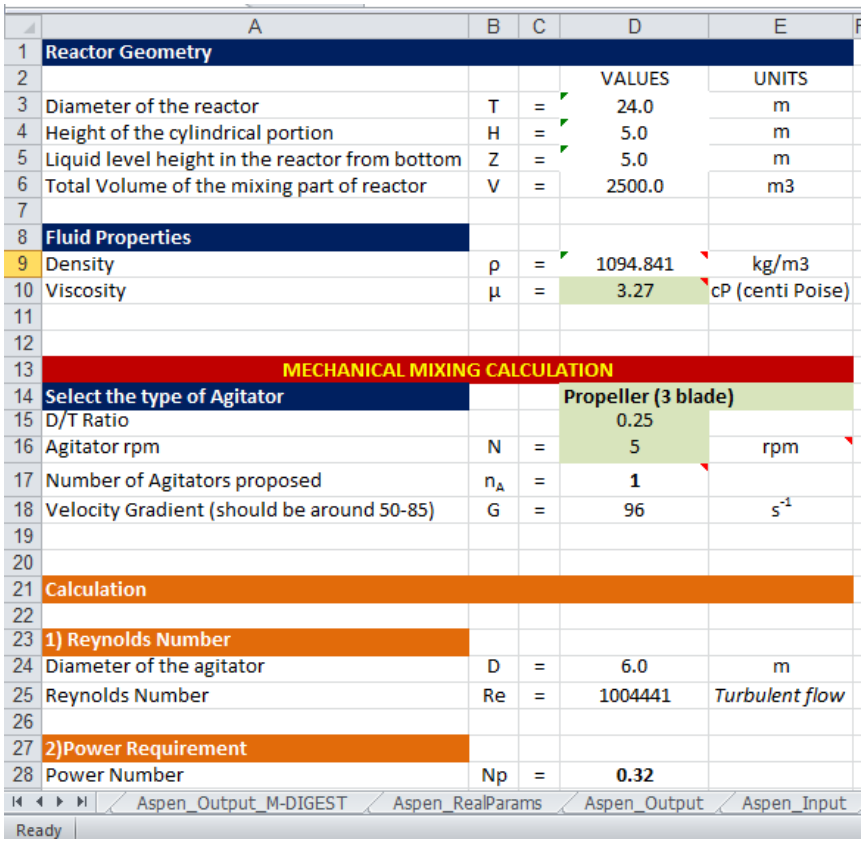

	A	B	C	D	E
1	**Reactor Geometry**				
2				VALUES	UNITS
3	Diameter of the reactor	T	=	24.0	m
4	Height of the cylindrical portion	H	=	5.0	m
5	Liquid level height in the reactor from bottom	Z	=	5.0	m
6	Total Volume of the mixing part of reactor	V	=	2500.0	m3
7					
8	**Fluid Properties**				
9	Density	ρ	=	1094.841	kg/m3
10	Viscosity	μ	=	3.27	cP (centi Poise)
11					
12					
13	**MECHANICAL MIXING CALCULATION**				
14	**Select the type of Agitator**			**Propeller (3 blade)**	
15	D/T Ratio			0.25	
16	Agitator rpm	N	=	5	rpm
17	Number of Agitators proposed	n_A	=	**1**	
18	Velocity Gradient (should be around 50-85)	G	=	96	s^{-1}
19					
20					
21	**Calculation**				
22					
23	**1) Reynolds Number**				
24	Diameter of the agitator	D	=	6.0	m
25	Reynolds Number	Re	=	1004441	*Turbulent flow*
26					
27	**2)Power Requirement**				
28	Power Number	Np	=	**0.32**	

Figure 5.9 Screen–shot of mechanical mixing calculation spreadsheet

Mixing power input per unit of digester volume for mechanical mixing systems has been reported by several sources as 3–4 W m^{-3} (Angelidaki *et al.*, 2003), 5–8 W m^{-3} (Appels *et al.*, 2008) and 5.2 W m^{-3} (Meroney & Colorado, 2009). These ranges reflect the dependency of energy consumption in mechanical mixing on certain parameters *i.e.* capacity of digester, type of impeller, method of setting up agitators in the tank *etc.* They were used in this model to verify the electricity consumption per cubic metre of digester.

5.4 Gas handling and utilisation components

5.4.1 CHP unit

Aspen Plus does not include a CHP unit so it was necessary to construct one. Several CHP technologies have been applied widely such as gas turbine, steam turbine, fuel cell, etc. This study used gas turbine technology because of

its high reliability, low emissions, high–grade heat available and no cooling requirement (Breeze, 2005; Deublein & Steinhauser, 2008b; Spellman, 2013). The developed gas turbine engine system based on the Brayton cycle as presented in (Cengel & Boles, 2011) is shown in Figure 5.10.

The biogas produced from digester is drawn to a compressor, where its temperature and pressure are increased and then sent to a combustion chamber. Subsequently, the high–temperature gases then enter the turbine, where they expand to atmospheric pressure and produce power. The exhaust gases are sent to a heat recovery steam generating unit (HRSG) for heat recovery.

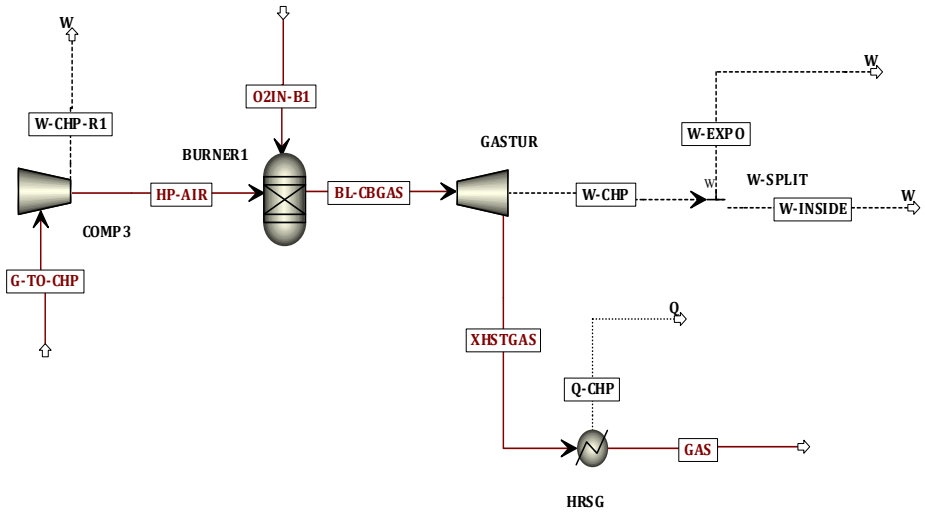

Figure 5.10 The CHP unit

Heat and electricity generated from the CHP unit can be used to supply pumps, mixers, compressors etc in the system. First, the raw gas required for the CHP unit is calculated based on the need for electricity for internal uses. From the amount of gas required, the heat generated that is availabe for on–site heating purposes is calculated. If the total heat requirement of the AD plant exceeds the amount generated by the CHP unit, a boiler unit must be added to the system. An amount of upgraded gas split via a *FSplit* block is fed to the boiler unit for heat generation to make up the shortfall in thermal energy.

The assumed operational parameters for model blocks to simulate the CHP unit are given in Table 5.6 (Ongiro *et al.*, 1995). The overall efficiency was assumed to be in the range 35–43% (Weiland, 2010).

Table 5.6 Design parameters for CHP unit

Parameters	Unit	Value
Air compressor		
isentropic efficiency	–	0.9
mechanical efficiency	–	0.99
discharge pressure	atm	20
Gas turbine		
polytropic efficiency	–	0.92
mechanical efficiency	–	0.99
discharge pressure	atm	1
Heat Recovery Steam Generator (HRSG)		
HRSG Exhaust Temp.	F	300

5.4.2 Upgrading unit

5.4.2.1. Model description

The pressure water scrubbing method was used in the model. Raw gas is compressed to about 10 bar and kept at 20°C before being fed to the absorber. The liquid is pumped from the stripper to the top of the absorber, the CO_2 dissolves in the water and the purified gas exits from the top of the column, where it passes through the absorber and then is dried and compressed into 200 bar for ready utilisation. The isentropic and mechanical efficiencies of fans, air compressors, pumps were assumed to be 0.90 and 0.96, respectively. For the upgraded biogas compressor working at 200 bar, these values were assumed to be slightly lower at 0.90 and 0.85, respectively.

In order to reduce methane lost in the stripping process, the liquid stream from the absorber, containing CO_2 and some methane, is fed to a flash tank where most of the dissolved CH_4 and some of the CO_2 is released and returned to the absorber. In the stripper, air fed via a fan contacts with the liquid which is cooled to low temperature to release CO_2. Water from the stripper containing a small amount of CO_2 and CH_4 is then pumped back to the absorber.

The following variables control the process: water flow rate to the stripper, temperature of water, stripping air flow rate, pressure of the absorber, flash

tank and stripper. To determine the amount of water and air needed for the process, the design specification function in Aspen plus was used to calculate these with an appropriate fraction of CO_2 in the upgraded gas stream. Figure 5.11 illustrates the biogas upgrading unit in the model.

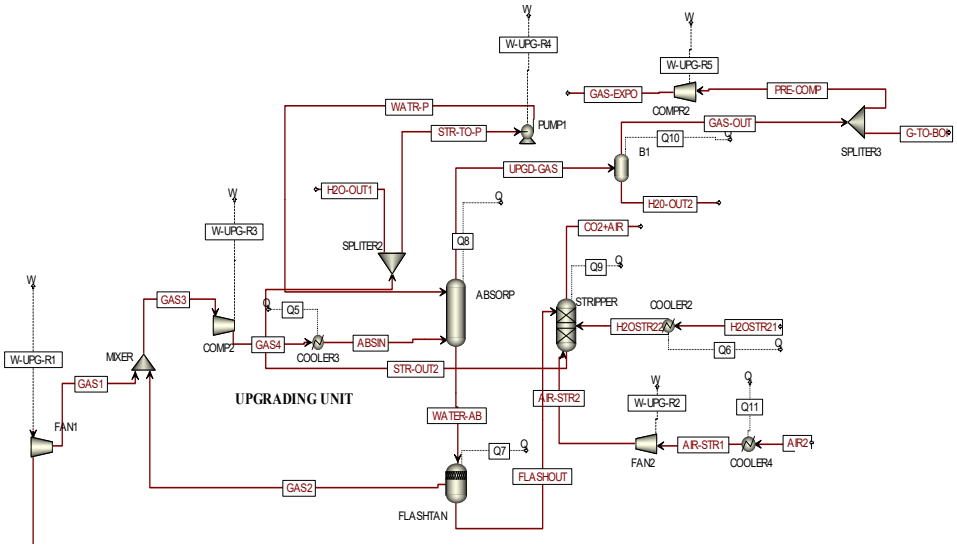

Figure 5.11 Upgrading unit using pressure water scrubbing

5.4.2.2. Upgrading unit validation

The upgrading unit was validated using data from literature and a case study was run based on data provided by the Indian Institute of Technology Delhi (IIT Delhi) as part of the FP7 VALORGAS project (Kapoor & Vijay, 2013).

Results from IIT Delhi using pressure water scrubbing to clean biogas showed that the upgraded gas contained about 95% methane, 3% carbon dioxide and 2% moisture and other trace gases. Operational parameters of elements in IIT Delhi's case study and in this model are shown in Table 5.7.

Table 5.7 Operational parameters of the model

Parameters	Unit	Value
Pressure of Absorber	bar	10
Pressure of Stripper	bar	10
Pressure of Flash tank	bar	2
Temp. of gas to Absorber	°C	10
Temp. of H2O to Stripper	°C	10

Results from the modelling (Table 5.8) show that the electricity required for the upgrading and compression estimated was around 0.415 KW m^{-3} of raw gas (equal to 0.67 KW m^{-3} upgraded biogas) at STP. These values are slightly higher than in the case study, but this is reasonable because in the case study, a stripper has been removed and only a flash tank was used to reduce the electricity requirement.

Table 5.8 Biogas upgrading case study results versus model calculation

Composition	IIT Delhi study			Model estimation		
	Unit	Raw biogas	Upgraded biogas	Unit	Raw biogas	Upgraded biogas
CH4	%	55–60	95	%	60.58	95.61
CO2	%	35–40	3	%	38.57	4.38
Electricity required	KW m^{-3} of	0.413	–	KW m^{-3} of	0.415	0.67

This page is intentionally left blank

Chapter 6

Ammonia removal tool

Chapter 2 indicated the importance of maintaining a suitable concentration of nitrogen in digesters, as well as the potential for an ammonia removal tool to control ammonia concentration in digestate. This chapter describes this ammonia removal tool which combines the modified ADM1 model presented in Chapter 4 and the ammonia removal process using a stripping column created in Aspen Plus.

6.1 Conceptual design and model description

6.1.1 Conceptual design

As mentioned in Chapter 2, the '*side–stream*' method was applied in this study for modelling the removal of ammonia. The systematic steps in running the ammonia stripping model are shown in Figure 6.1.

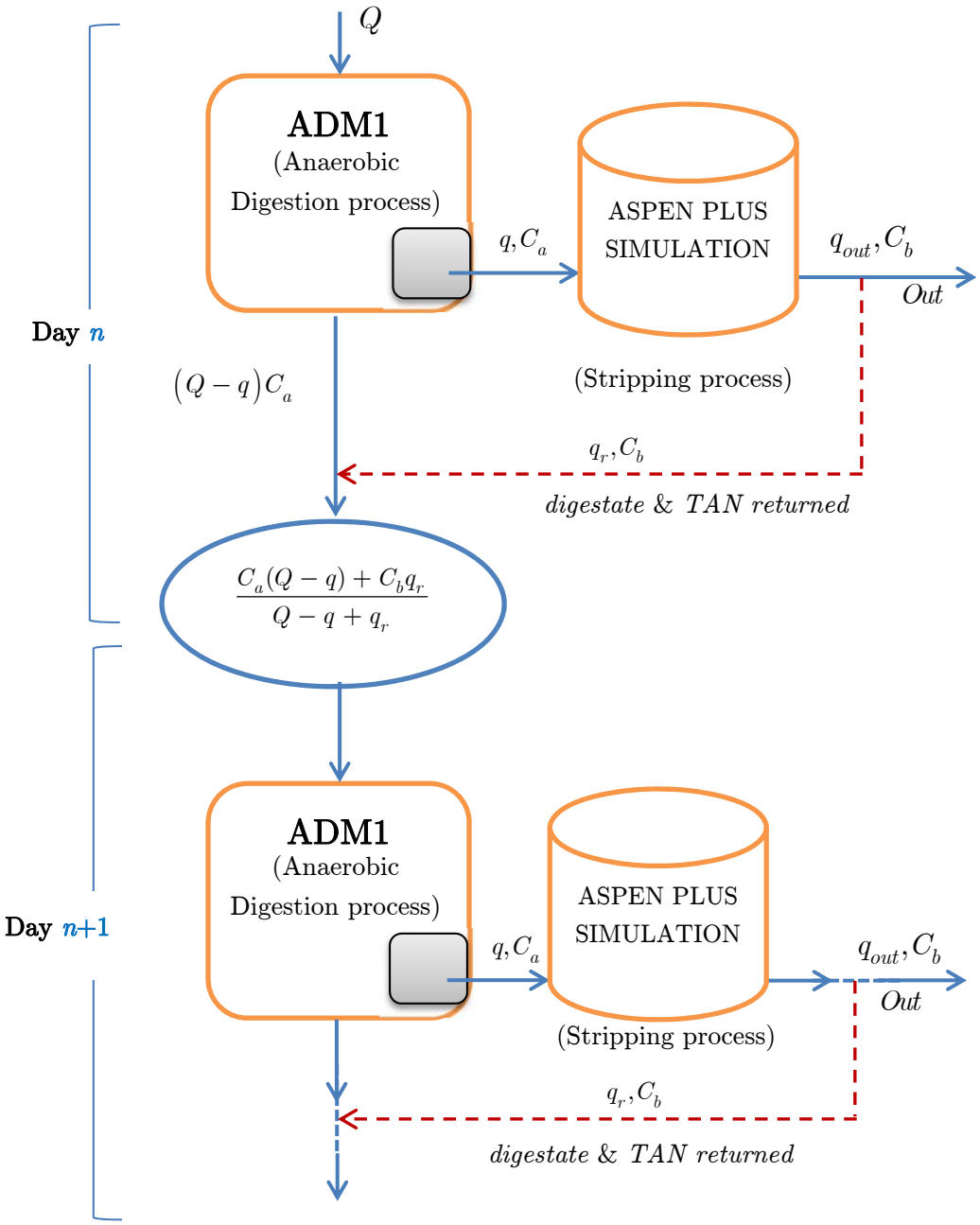

Figure 6.1 Systematic steps in running the ammonia removal tool

At the beginning of a modelling run, the digester can be run without ammonia removal in order to reach suitable starting conditions (*e.g.* a target or stable concentration). During this time the concentration of ammonia in the digestate increases or decreases depending on the relative concentrations in the feedstock and the digestate or initial inoculum. For this process, the ADM1 simulation works without any influence from ammonia removal components.

When the concentration of ammonia in the digester needs to be reduced (day n), a volume of digestate with a high ammonia concentration (q, C_a) is fed to the stripping facilities (Aspen Plus simulation). After stripping, a fraction from that volume (q_r) with lower ammonia concentration (C_b) is recycled back to the digester to continue to work. At the same time, the remaining treated digestate (q_{out}, C_b) is discharged. These steps decrease the concentration of nitrogen in the digester at the end of day n. The day after (day n+1), the same pattern of steps is repeated. In this way, the concentration of nitrogen in the digester will be reduced and then maintained at an appropriate level. This level is determined by the amount of digestate fed to the stripping process and the efficiency of the stripping column.

6.1.2 Model description

The platform for the ammonia removal tool was built in Aspen Plus and is presented in Figure 6.2. Six Aspen block types were implemented: all of these blocks and their descriptions are presented in Table 6.1.

The system can be divided into two main components:

Digester component: the anaerobic digestion process takes place in a digester modelled in MATLAB/Simulink® using the modified ADM1 model developed in this study. Calibration and validation steps were carried out using experimental data from BORRG, University of Southampton.

Stripping component: this element has as a core block of a stripping tower simulated in Aspen Plus only. Some built–in operation blocks were also added to simulate the operating mode used in the experiments.

In order to exchange running results between a digester modelled in MATLAB/Simulink® and a stripping system simulated in Aspen, the Aspen Simulation Workbook (ASW) was used.

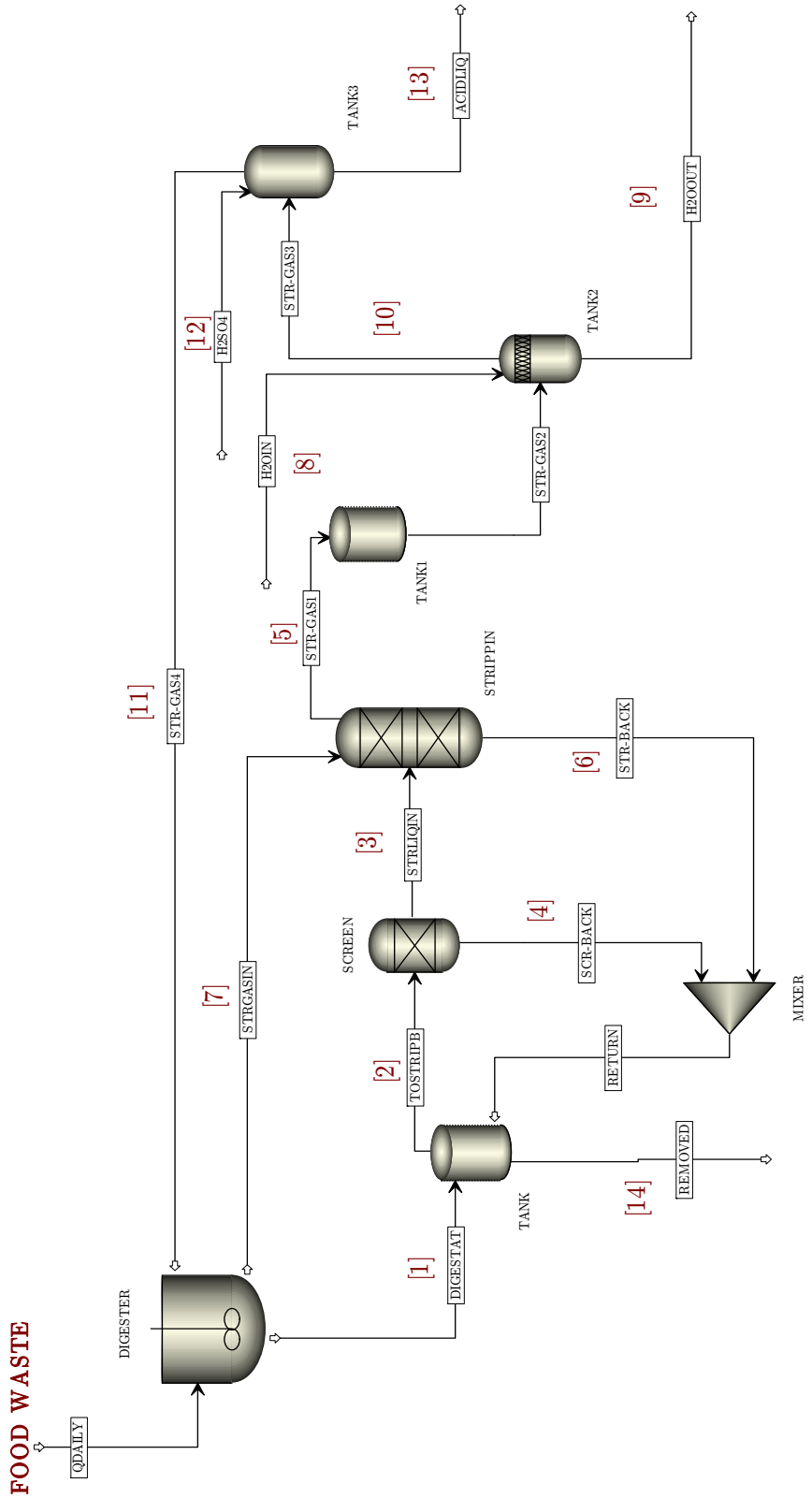

Figure 6.2 The *side-stream* ammonia stripping system in Aspen Plus

Table 6.1 Description of Aspen plus unit operation models

Aspen plus ID	Block/Stream ID	Description
RSTOIC	DIGESTER	Exchanges simulated results between Aspen Plus and ADM1 Matlab model
SEPERATOR	SCREEN	Plays as a solid separator
FLASH	TANK1/2/3	Plays as separators
RADFRAC	STRIPPIN	Model of stripping column
MIXER	TANK	To get the required amount of digestate from Digester to send to stripping tower
MIXER	MIXER	To combine all returned streams back to digester
MATERIAL STREAMS	[1]	Digestate collected to be fed to stripping processes
	[2]	Digestate fed to a screen for liquid/solid separation
	[3]	Digestate liquid to the stripping column
	[4]	Condensed digestate recycled back to digester
	[5]	Stripped gas with high content of ammonia
	[6]	Digestate liquid recycled back to digester
	[7]	Biogas from digester used for stripping process
	[8]	Water used to trap ammonia from tripped gas
	[9]	Water disposal with high ammonia content
	[10]	Gas stream (mainly CO_2, CH_4) to acid tank
	[11]	Gas (mainly CO_2, CH_4) recycled to the digester
	[12]	Acid used to trap remaining ammonia in [10]
	[13]	Acid liquid disposal
	[14]	Digestate removed frequently

6.2 Model formulation

6.2.1 Aspen plus components and assumptions

In order to represent the digestate stream simulated by the ADM1 model, its components had to be defined in Aspen Plus. The *Component ID* of each component was denoted in the same way as in the ADM1 model, and is listed in Table 6.2. These components are represented exactly by the chemical components listed in the '*Component name*' column if they are included in Aspen Plus databanks. In some cases, however, the required components do not exist in Aspen databanks, and therefore assumptions were made when

necessary by using appropriate chemical elements. The assumptions made in this study can be summarised as below:

- Carbohydrates, Sugar, Amino acids were represented by Dextrose,
- Biomass, Inerts and Particulates were assumed to be $C_5H_7ON_2$ (Ethyl–cyanoacetate),
- Valerate and Butyrate were assumed to be in the forms of iso–valerate and iso–butyrate, respectively.

It should be noted that these assumed items were only employed by the Aspen model to represent results from the ADM1 simulation, as there were no kinetic biochemical reactions in the Aspen Plus digester; hence these assumptions were acceptable.

Table 6.2 List of components set in Aspen Plus

Component ID	Type	Component name	Alias
SU	CONVENTIONAL	DEXTROSE	C6H12O6
SAA	CONVENTIONAL	GLYCINE	C2H5NO2–D1
SFA	CONVENTIONAL	OLEIC–ACID	C18H34O2
SVA	CONVENTIONAL	ISOVALERIC–ACID	C5H10O2–D3
SBU	CONVENTIONAL	ISOBUTYRIC–ACID	C4H8O2–4
SPRO	CONVENTIONAL	PROPIONIC–ACID	C3H6O2–1
SAC	CONVENTIONAL	ACETIC–ACID	C2H4O2–1
SH2	CONVENTIONAL	HYDROGEN	H2
SCH4	CONVENTIONAL	METHANE	CH4
SIC	CONVENTIONAL	CARBON–GRAPHITE	C
SIN	CONVENTIONAL	NITROGEN	N2
SI	CONVENTIONAL	ETHYL–CYANOACETATE	C5H7NO2
XC	SOLID	ETHYL–CYANOACETATE	C5H7NO2
XCH	SOLID	DEXTROSE	C6H12O6
XPR	SOLID	LYSINE	C6H14N2O2
XLI	SOLID	GLYCEROL	C3H8O3
XSU	SOLID	DEXTROSE	C6H12O6
XAA	SOLID	DEXTROSE	C6H12O6
XFA	SOLID	OLEIC–ACID	C18H34O2
XC4	SOLID	ISOVALERIC–ACID	C5H10O2–D3
XPRO	SOLID	PROPIONIC–ACID	C3H6O2–1
XAC	SOLID	ACETIC–ACID	C2H4O2–1
XH2	SOLID	HYDROGEN	H2

Table 6.2 List of components set in Aspen Plus (*continued*)

Component ID	Type	Component name	Alias
XI	SOLID	ETHYL–CYANOACETATE	C5H7NO2
SCATION	CONVENTIONAL	H+	H+
SANION	CONVENTIONAL	OH–	OH–
SVAION	CONVENTIONAL	ISOVALERIC–ACID	C5H10O2–D3
SBUION	CONVENTIONAL	ISOBUTYRIC–ACID	C4H8O2–4
SPROION	CONVENTIONAL	PROPIONIC–ACID	C3H6O2–1
SACION	CONVENTIONAL	ACETIC–ACID	C2H4O2–1
SHCO3ION	CONVENTIONAL	HCO3–	HCO_3^-
SNH3	CONVENTIONAL	AMMONIA	H3N
SGASH2	CONVENTIONAL	HYDROGEN	H2
SGASCH4	CONVENTIONAL	METHANE	CH4
SGASCO2	CONVENTIONAL	CARBON–DIOXIDE	CO2
SHION	CONVENTIONAL	H+	H+
SNH4+	CONVENTIONAL	NH4+	NH4+
Q	CONVENTIONAL	WATER	H2O
CH4	CONVENTIONAL	METHANE	CH4
CO2	CONVENTIONAL	CARBON–DIOXIDE	CO2
H2SO4	CONVENTIONAL	SULFURIC–ACID	H2SO4

6.2.2 Stripping column efficiency

In order to calibrate the stripping column, this study used experimental data from work by BORRG researchers at the University of Southampton. Some of these experimental results have been published and can be found in (Zhang & Walker, 2010; Walker *et al.*, 2011; Serna-Maza *et al.*, 2014).

As mentioned in Table 6.1, this study used the RADFRAC in Aspen Plus to model the stripping column, which includes these basic setups as guided by Aspen Technology (2001).

- Condenser = None and Reboiler = None;
- The heat duty is zero for adiabatic operation;
- Algorithm = Sum–Rates;
- Convergence = Standard.

One way to estimate ammonia removed in the stripping tower is to specify the efficiency of removal of this component in the given stripping column configuration. This study assumed the method used to specify efficiencies is for

individual components and the efficiency type is '*vaporisation efficiencies*' which is defined as:

$$Eff_i^v = \frac{y_{i,j}}{K_{i,j}x_{i,j}} \tag{6.1}$$

Where K is the equilibrium K value; x is the liquid mole fraction, y is the vapour mole fraction; i is the component index; j is the stage index.

Previous studies on ammonia removal from source–segregated food waste digestate using *side–stream* stripping suggested that removal could be considered as following first–order kinetics with respect to total ammonia nitrogen concentration (Zhang & Walker, 2010; Walker *et al.*, 2011), and can therefore be expressed as:

$$C = C_0 e^{-\frac{t}{\tau}} \tag{6.2}$$

Where C_0 is the initial ammonia concentration mg L^{-1}; τ is the removal time constant, hour; t is the time of stripping each day, hour.

In equation (6.1), the removal time constant τ varies according to the working conditions of the stripping column, the initial concentration and digestate properties, flow rate of biogas *etc.* Table 6.3 shows some results from batch experimental runs of a *side–stream* ammonia stripping system at 35°C, 55°C and 70°C by BORRG researchers as presented in (Serna-Maza, 2014). As can be clearly seen, the lower the stripping tower operating temperature, the larger the value of τ. Likewise, the lower the pH value and biogas flow rate to the stripping tower, the higher τ.

Table 6.3 Time constant for stripping tower in *side–stream* system

Temp. ^{0}C	Initial pH	Biogas flow L min^{-1} L^{-1}	TAN start mg L^{-1}	TAN end mg L^{-1}	TAN removal %	Time h	τ h
55	8.04	0.125	4732	2440	48.4	836	1111
55	7.9	0.25	4925	3184	35.2	524	1111
55	7.9	0.25	4925	2792	43.2	524	833
70	8.3	0.125	4561	1893	58.5	243	222
70	7.9	0.25	4904	2884	41.2	142	161
70	7.9	0.125	4904	2374	52	234	278

For simplicity, in this study the assumptions below were made:

- Digestate was filled and discharged from the stripping reactor once a day (t = 24 h);
- Ammonia is released into the digester immediately by the incoming food waste;
- pH of digestate is around 8;
- The stripping tower works at 70°C;
- The amount of biogas taken from the digester to feed the stripping column is sufficient to remove the ammonia.

With these assumptions, the removal time constant τ was chosen as about 150 hours (see Table 6.3). This value is very closed to that of 155.1 suggested by Serna-Maza (2014) in a recent continuous trial under the same working conditions. Consequently, the efficiency φ of the stripping reactor is:

$$\varphi = 1 - e^{-\frac{24}{150}} \approx 0.148 \tag{6.3}$$

In other words, for each day of operation, the stripping tower can remove about 15% of the ammonia in the digestate. This value appears to agree well with recent investigations in semi–continuous experiments which show that at 70°C and with unadjusted pH, on average, the TAN concentration decreased by about 15.4% per day (Serna-Maza *et al.*, 2014). Accordingly, this value was assumed in setting the efficiency of the stripping column.

6.3 Model simulation

6.3.1 Simulation procedure

To simulate the stripping process, it is first necessary to run the digester model in the MATLAB environment. Users can set inputs such as the digester volume, volume of waste, OLR, and time of digester operation (days) before digestate is sent to the stripping facilities. In the MATLAB command line, the program allows users to input key parameters including number of days running without stripping.

Once ADM1 is executed in MATLAB, outputs for the digester are automatically sent to an ASW file in MS Excel format. From the ASW file, users can run the model and it will call the Aspen Plus program to simulate

the stripping process. At this step, a certain amount of ammonia will be removed from stripping tower. The amount of ammonia removed depends upon how much digestate is taken from the digester to be stripped and on the efficiency of stripping column: the user can choose a value for the efficiency variable for the stripping tower or use the default value of 0.15. Consequently, an amount of digestate will be removed, and the remaining part (stripped digestate) will be written to an Excel worksheet. All the data from that worksheet together with the digestate that had not been sent to the stripping section is then recalculated and used for the next ADM1 run.

Figure 6.3 provides some screen captures of an example simulation using this tool in ASW.

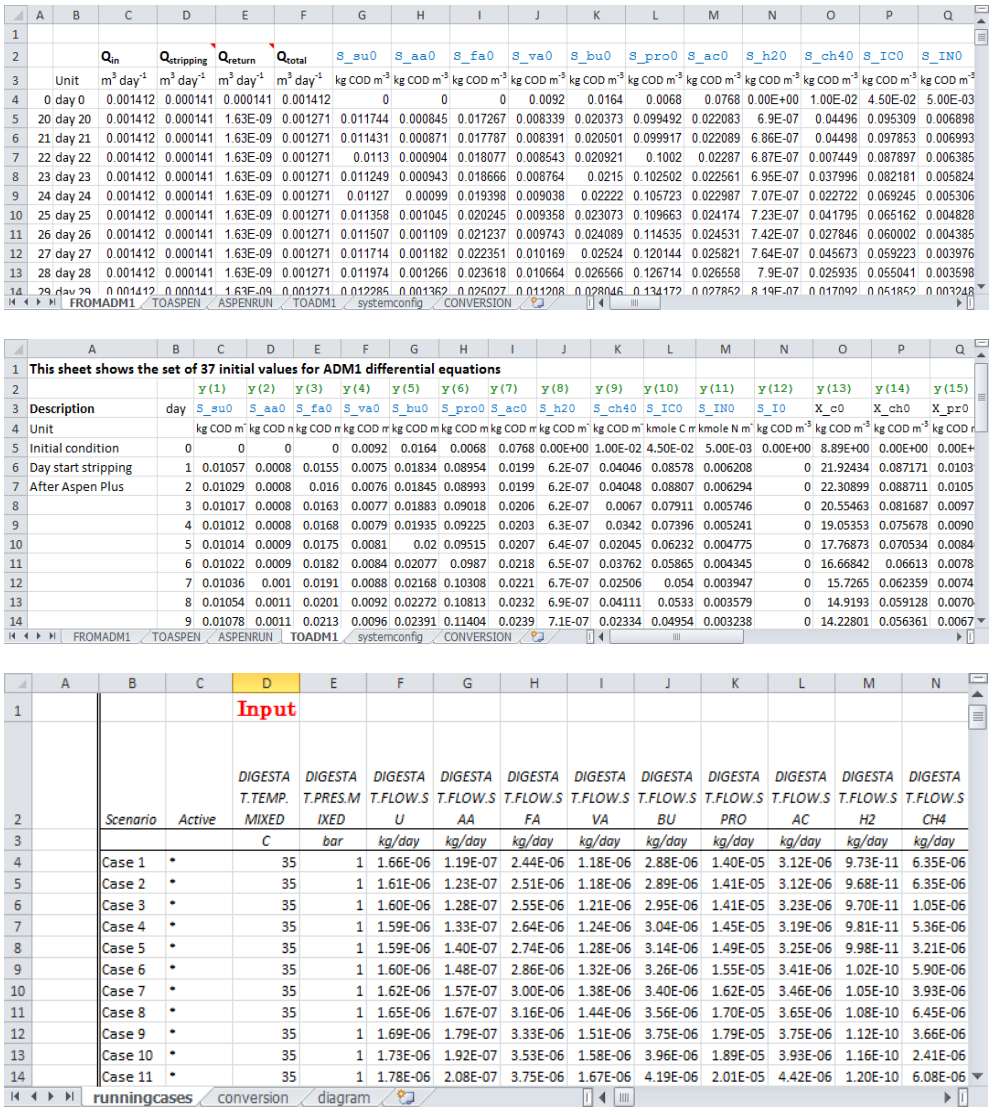

		Q_{in}	$Q_{stripping}$	Q_{return}	Q_{total}	S_su0	S_aa0	S_fa0	S_va0	S_bu0	S_pro0	S_ac0	S_h20	S_ch40	S_IC0	S_IN0
	Unit	$m^3\ day^{-1}$	$m^3\ day^{-1}$	$m^3\ day^{-1}$	$m^3\ day^{-1}$	kg COD m^{-3}	kg COD m^{-3}	kg COD m^{-3}	kg COD m^{-3}	kg COD m^{-3}	kg COD m^{-3}	kg COD m^{-3}	kg COD m^{-3}	kg COD m^{-3}	kg COD m^{-3}	kg COD m^{-3}
0	day 0	0.001412	0.000141	0.000141	0.001412	0	0	0	0.0092	0.0164	0.0068	0.0768	0.00E+00	1.00E-02	4.50E-02	5.00E-03
20	day 20	0.001412	0.000141	1.63E-09	0.001271	0.011744	0.000845	0.017267	0.008339	0.020373	0.099492	0.022083	6.9E-07	0.04496	0.095309	0.006898
21	day 21	0.001412	0.000141	1.63E-09	0.001271	0.011431	0.000871	0.017787	0.008391	0.020501	0.099917	0.022089	6.86E-07	0.04498	0.097853	0.006993
22	day 22	0.001412	0.000141	1.63E-09	0.001271	0.0113	0.000904	0.018077	0.008543	0.020921	0.1002	0.02287	6.87E-07	0.007449	0.087897	0.006385
23	day 23	0.001412	0.000141	1.63E-09	0.001271	0.011249	0.000943	0.018666	0.008764	0.0215	0.102502	0.022561	6.95E-07	0.037996	0.082181	0.005824
24	day 24	0.001412	0.000141	1.63E-09	0.001271	0.01127	0.00099	0.019398	0.009038	0.02222	0.105723	0.022987	7.07E-07	0.022722	0.069245	0.005306
25	day 25	0.001412	0.000141	1.63E-09	0.001271	0.011358	0.001045	0.020245	0.009358	0.023073	0.109663	0.024174	7.23E-07	0.041795	0.065162	0.004828
26	day 26	0.001412	0.000141	1.63E-09	0.001271	0.011507	0.001109	0.021237	0.009743	0.024089	0.114535	0.024531	7.42E-07	0.027846	0.060002	0.004385
27	day 27	0.001412	0.000141	1.63E-09	0.001271	0.011714	0.001182	0.022351	0.010169	0.02524	0.120144	0.025821	7.64E-07	0.045673	0.059223	0.003976
28	day 28	0.001412	0.000141	1.63E-09	0.001271	0.011974	0.001266	0.023618	0.010664	0.026566	0.126714	0.026558	7.9E-07	0.025935	0.055041	0.003598
29	day 29	0.001412	0.000141	1.63E-09	0.001271	0.012285	0.001362	0.025027	0.011208	0.028046	0.134172	0.027852	8.19E-07	0.017092	0.051852	0.003248

FROMADM1 | TOASPEN | ASPENRUN | TOADM1 | systemconfig | CONVERSION

This sheet shows the set of 37 initial values for ADM1 differential equations

			y(1)	y(2)	y(3)	y(4)	y(5)	y(6)	y(7)	y(8)	y(9)	y(10)	y(11)	y(12)	y(13)	y(14)	y(15)
Description		day	S_su0	S_aa0	S_fa0	S_va0	S_bu0	S_pro0	S_ac0	S_h20	S_ch40	S_IC0	S_IN0	S_I0	X_c0	X_ch0	X_pr0
Unit			kg COD m^{-3}	kg COD m^{-3}	kg COD m^{-3}	kg COD m^{-3}	kg COD m^{-3}	kg COD m^{-3}	kg COD m^{-3}	kg COD m^{-3}	kg COD m^{-3}	kmole C m^{-3}	kmole N m^{-3}	kg COD m^{-3}	kg COD m^{-3}	kg COD m^{-3}	kg COD m^{-3}
Initial condition		0	0	0	0	0.0092	0.0164	0.0068	0.0768	0.00E+00	1.00E-02	4.50E-02	5.00E-03	0.00E+00	8.89E+00	0.00E+00	0.00E+
Day start stripping		1	0.01057	0.0008	0.0155	0.0075	0.01834	0.08954	0.0199	6.2E-07	0.04046	0.08578	0.006208	0	21.92434	0.087171	0.0103
After Aspen Plus		2	0.01029	0.0008	0.016	0.0076	0.01845	0.08993	0.0199	6.2E-07	0.04048	0.08807	0.006294	0	22.30899	0.088711	0.0105
		3	0.01017	0.0008	0.0163	0.0077	0.01883	0.09018	0.0206	6.2E-07	0.0067	0.07911	0.005746	0	20.55463	0.081687	0.0097
		4	0.01012	0.0008	0.0168	0.0079	0.01935	0.09225	0.0203	6.3E-07	0.0342	0.07396	0.005241	0	19.05353	0.075678	0.0090
		5	0.01014	0.0009	0.0175	0.0081	0.02	0.09515	0.0207	6.4E-07	0.02045	0.06232	0.004775	0	17.76873	0.070534	0.0084
		6	0.01022	0.0009	0.0182	0.0084	0.02077	0.0987	0.0218	6.5E-07	0.03762	0.05865	0.004345	0	16.66842	0.06613	0.0078
		7	0.01036	0.001	0.0191	0.0088	0.02168	0.10308	0.0221	6.7E-07	0.02506	0.054	0.003947	0	15.7265	0.062359	0.0074
		8	0.01054	0.0011	0.0201	0.0092	0.02272	0.10813	0.0232	6.9E-07	0.04111	0.0533	0.003579	0	14.9193	0.059128	0.0070
		9	0.01078	0.0011	0.0213	0.0096	0.02391	0.11404	0.0239	7.1E-07	0.02334	0.04954	0.003238	0	14.22801	0.056361	0.0067

FROMADM1 | TOASPEN | ASPENRUN | TOADM1 | systemconfig | CONVERSION

Input

	Scenario	Active	DIGESTA T.TEMP. MIXED	DIGESTA T.PRES.MIXED	DIGESTA T.FLOW.SU	DIGESTA T.FLOW.SAA	DIGESTA T.FLOW.SFA	DIGESTA T.FLOW.SVA	DIGESTA T.FLOW.SBU	DIGESTA T.FLOW.SPRO	DIGESTA T.FLOW.SAC	DIGESTA T.FLOW.SH2	DIGESTA T.FLOW.SCH4
			C	bar	kg/day	kg/day	kg/day	kg/day	kg/day	kg/day	kg/day	kg/day	kg/day
Case 1	*		35	1	1.66E-06	1.19E-07	2.44E-06	1.18E-06	2.88E-06	1.40E-05	3.12E-06	9.73E-11	6.35E-06
Case 2	*		35	1	1.61E-06	1.23E-07	2.51E-06	1.18E-06	2.89E-06	1.41E-05	3.12E-06	9.68E-11	6.35E-06
Case 3	*		35	1	1.60E-06	1.28E-07	2.55E-06	1.21E-06	2.95E-06	1.41E-05	3.23E-06	9.70E-11	1.05E-06
Case 4	*		35	1	1.59E-06	1.33E-07	2.64E-06	1.24E-06	3.04E-06	1.45E-05	3.19E-06	9.81E-11	5.36E-06
Case 5	*		35	1	1.59E-06	1.40E-07	2.74E-06	1.28E-06	3.14E-06	1.49E-05	3.25E-06	9.98E-11	3.21E-06
Case 6	*		35	1	1.60E-06	1.48E-07	2.86E-06	1.32E-06	3.26E-06	1.55E-05	3.41E-06	1.02E-10	5.90E-06
Case 7	*		35	1	1.62E-06	1.57E-07	3.00E-06	1.38E-06	3.40E-06	1.62E-05	3.46E-06	1.05E-10	3.93E-06
Case 8	*		35	1	1.65E-06	1.67E-07	3.16E-06	1.44E-06	3.56E-06	1.70E-05	3.65E-06	1.08E-10	6.45E-06
Case 9	*		35	1	1.69E-06	1.79E-07	3.33E-06	1.51E-06	3.75E-06	1.79E-05	3.75E-06	1.12E-10	3.66E-06
Case 10	*		35	1	1.73E-06	1.92E-07	3.53E-06	1.58E-06	3.96E-06	1.89E-05	3.93E-06	1.16E-10	2.41E-06
Case 11	*		35	1	1.78E-06	2.08E-07	3.75E-06	1.67E-06	4.19E-06	2.01E-05	4.42E-06	1.20E-10	6.08E-06

runningcases | conversion | diagram

Figure 6.3 Screen capture of a simulation using ammonia removal tool in ASW

6.3.2 Sample simulation

In order to evaluate the accuracy of the developed ammonia removal model, one simulation was made and compared with a set of experimental data. The extracted experimental data was taken from (Serna-Maza *et al.*, 2014). Measured data for reactor R1 working at 70°C pH from days 131 to 259 was used. Details of the experimental set–up can be found in (Serna-Maza *et al.*, 2014). The initial conditions (*i.e.* volume of digester, OLR *etc.*) for ADM1 simulation were set similar to those presented in (Serna-Maza *et al.*, 2014). The ADM1 model was run to reach a TAN concentration of 5.2 g N L^{-1} before applying the removal steps for 128 days. Results from the model simulation and experiment are presented in Figure 6.4.

As can be seen from the figure, the model predicted the TAN concentration of the examined digester (R1) very well.

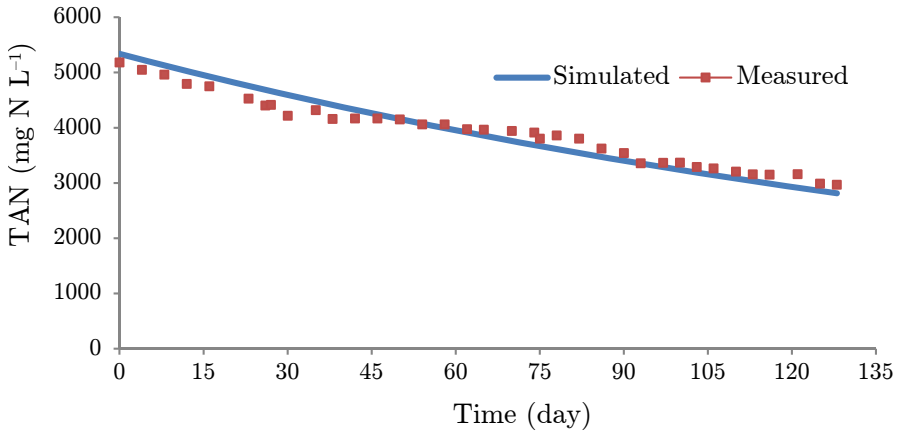

Figure 6.4 Ammonia concentration in digester when stripping applied

6.4 Discussion and conclusions

Results from modelling showed the developed model can be applied to ammonia removal integrated with a digestion process. Although this study only looked at the *side–stream* configuration, any other methods for removing ammonia such as *post* digestion removal, *in situ* removal, *pre–digestion* removal can be modellied in the same way.

When applying the model to real industrial applications of ammonia stripping (laboratory–scale or full–scale plant), it is important to choose an appropriate time constant since it correlates strongly with model outputs. This value can vary depending upon many factors. For example, different food waste

digestates have different values, and even the digestates from food waste digesters running with similar feedstocks may have different time constants due to different operating protocols *e.g.* VFA accumulation (Zhang & Jahng, 2010; Serna-Maza, 2014). Some other factors should also be considered such as pH and temperature of the stripping column (Liao *et al.*, 1995; Zhang & Jahng, 2010; Serna-Maza, 2014), and different storage conditions (*e.g.* fresh digestates versus stored) as indicated in several studies (Walker *et al.*, 2011; Laureni *et al.*, 2013; Serna-Maza, 2014). By adjusting the time constant value, however, the current model can be used to simulate any of these conditions.

Regular discussions were held with other researchers in the BORRG regularly, especially with Miss Serna–Maza, to assess the quality of the developed model. It was concluded that the current model works well and that applying first order kinetics is a reasonably good approach for modelling ammonia stripping.

Chapter 7

Case studies

In order to demonstrate potential applications of the developed tools in dealing with possible problems arising in practice, three case studies were carried out and are presented in this chapter. They are extracted from an accepted paper and manuscripts for submission. The first is to test the ability and flexibility of the developed ADM1 model in applying to anaerobic digestion of another type of substrate: Sugar Beet Pulp. The second case study is an attempt to answer some questions relating to energy and mass balance aspects before building an AD plant for fuel-grade methane production. The third case study is an evaluation of the potential for applying AD as a treatment for food waste in MSW streams in urban areas, which is currently unavailable in Vietnam.

7.1 Modeling of mesophilic anaerobic digestion of Sugar Beet Pulp using ADM1 model

This case study presents an application of ADM1 to replicate the dynamic behaviour of laboratory–scale anaerobic reactors treating sugar beet pulp (SBP) at different organic loading rates (OLR).

This work was carried out as a result of cooperation between the author and Dr Sri Suhartini for a submitted manuscript. All data, information presented in this thesis was extracted from her thesis (Suhartini, 2014) and permitted by her.

7.1.1 Introduction

To date, a number of experimental studies have looked at the anaerobic digestion of SBP under a range of operational conditions, including different OLRs, temperature and pH, and have shown that substrate–to–energy conversion was generally successful (Ghanem *et al.*, 1992; Hutnan *et al.*, 2000; Suhartini *et al.*, 2011; Suhartini *et al.*, 2014). A detailed understanding of the process design, operation and control, however, may help to ensure high efficiency. As noted in Chapter 1, a suitable model capable of representing the system behaviour under different conditions can offer the necessary support for this purpose. Nevertheless, no models of anaerobic digestion have been proposed for SBP as a substrate so far.

This work, therefore, on the one hand attempts to model the anaerobic digestion of SBP using the revised ADM1 model for prediction of important parameters including biogas production, methane and carbon dioxide contents, VFA, pH and total ammonia nitrogen under different loading rate conditions. On the other hand, the findings of this study will expand the application of the ADM1 for various types of solid substrates.

7.1.2 Materials and methods

7.1.2.1. Experimental setup

Substrate and inoculum

Collection and preparation of substrate and inoculum were as described in (Suhartini *et al.*, 2014). The characteristics of sugar beet pulp can be seen in Table 7.1.

Table 7.1 Characteristics of SBP substrate – based on (Suhartini *et al.*, 2014)

Parameters	Units	Values
TS	% of WW	24.2
VS	% of WW	22.6
VS	% of TS	93.2
Biochemical composition		
Hemicellulose	g kg^{-1} WW	70.2
Cellulose	g kg^{-1} WW	32.2
Lignin	g kg^{-1} WW	20.0
Crude protein (TKN × 6.25)	g kg^{-1} WW	21.8
Elemental analysis		
C	% TS	42.64
H	% TS	5.47
N	% TS	1.79
O (by difference)	% TS	42.58
S	% TS	0.46
TKN (N)	3.48	3.48
Phosphorus (P)	0.41	0.41
Potassium (K)	0.84	0.84

Experimental set–up

Experiments on the anaerobic digestion of SBP were carried out in eight digesters of the type described in section 4.4.1, in mesophilic conditions (37°C±0.5°C). The digesters were operated in pairs at OLR of 2, 3, 4 and 5 g VS L^{-1} day^{-1}, corresponding to hydraulic retention times (HRT) of 137.0, 91.3, 68.5 and 54.8 days. All digesters were initially fed at an OLR of 1 g VS L^{-1} day^{-1} which was then steadily raised to the target OLR by day 2, 36, 71 and 162, respectively. For the purposes of ADM1 modelling, the average value for each pair of digesters at a given OLR was used, denoted as R2, R3, R4 and R5.

7.1.2.2. Model implementation

This work used the *transformer* tool as presented in section *2.7.2.3* to generate the concentration of soluble/particulate components in SBP substrate

based on the experimental values for SBP. Table 7.2 shows the values for 11 required characteristics.

Table 7.2 Transformer input or SBP substrate

Components	Unit	Values	Explanations
Total Solids	%WW	24.2	
Volatile Solids	%WW	22.6	VS = 93.4% TS
Density of wet SBP	kg m^{-3}	1000	assumed
(1) Particulate COD (COD_p)	g m^{-3}	307122	= CODt[(a)] – CODs
(2) CODs–VFA	g m^{-3}	3133.9	
(3) Volatile Fatty Acids (VFA)	g m^{-3}	3133.9	1% of CODt (assumed)
(4) Total Organic Carbon (TOC)	gC m^{-3}	101125	= TC – TIC
(5) Total Organic Nitrogen (Norg)	g m^{-3}	3190.8	91.96% TKN[(b)]
(6) Total Ammonia Nitrogen	g m^{-3}	289.2	= TKN – Norg
(7) Organic Phosphorus (TP–orthoP)	gP m^{-3}	382.9	(TS/VS) % of TP
(8) Ortho–Phosphate (orthoP)	gP m^{-3}	27.1	= TP – TP–orthoP
(9) Total Inorganic Carbon (TIC)	moleHCO_3^- m^{-3}	172	= (TC – TOC)/12[(c)]
(10) Total Alkalinity (S_{cat})	equ m^{-3}	25	assumed
(11) Fixed Solids (FS)	g m^{-3}	16000	= TS – VS

Note: [(a)] COD_t estimated with assumption that each g of TS is equal to 1.295 g COD (Hutnan *et al.*, 2000); [(b)] estimation from (Pettersson & Lindgren, 1990); [(c)] assumed that organic carbon accounts for 98% of total carbon.

7.1.2.3. Model calibration and validation

The model was calibrated by comparison between experimental results and the model output. In this study, the experimental data from reactor R2 (OLR of 2 g VS L^{-1} day^{-1}) was used for validation. Experimental results from reactors R3, R4 and R5, corresponding respectively to OLRs of 3, 4 and 5 g VS L^{-1} day^{-1}, were used in the validation.

7.1.3 Results and discussion

7.1.3.1. Experimental results for the laboratory–scale CSTR

The experimental results for gas production and digestion performance characteristics under steady–state conditions are shown in Table 7.3. Overall the results indicated that increasing the OLR influenced process stability parameters such as pH, total VFA as well as slightly reducing organic matter degradation, biogas and methane production: more detailed analysis and discussion is given in (Suhartini, 2014).

Table 7.3 Average steady state values of trial digesters at different OLRs

Parameters	Unit	OLR 2	OLR 3	OLR 4	OLR 5
Specific biogas production	L g^{-1} VS day^{-1}	0.621	0.572	0.565	0.579
Specific CH_4 production	L g^{-1} VS day^{-1}	0.316	0.293	0.286	0.294
Vol. biogas production	L L^{-1} day^{-1}	1.24	1.69	2.17	2.83
Vol. CH_4 production	L L^{-1} day^{-1}	0.63	0.87	1.12	1.44
Digestate TS	g L^{-1}	56.1	63.3	67.6	75.3
Digestate VS	g L^{-1}	38.6	43.0	46.6	54.8
VS destruction	%	90.9	87.9	86.9	83.5
pH	–	7.56	7.45	7.37	7.12
TAN	mg N kg^{-1} WW	2060	1647	1442	1022
Total alkalinity	mg$CaCO_3$ kg^{-1} WW	18909	16355	16007	13357
IA/PA ratio	–	0.28	0.43	0.42	0.57
Total VFA	mg L^{-1}	82	232	219	376

7.1.3.2. Model calibration

Model input and initial conditions

The initial conditions for all simulations at different OLRs were set by simulating reactor R2 for 1000 days, after which steady–state conditions were assumed. This was acceptable, since the OLR on reactors R3, R4 and R5 was steadily increased from 2 to 3, 4 and 5 g VS L^{-1} day^{-1}.

ADM1 input data for the initial conditions and the SBP substrate generated from the *transformer* tool are presented in Table 7.4.

Table 7.4 Model input and initial conditions

Stage	Variable	Unit	Input data	Initial data
1	S_{su}	kgCOD m^{-3}	3.1339	0.0049
2	S_{aa}	kgCOD m^{-3}	–	0.0022
3	S_{fa}	kgCOD m^{-3}	–	0.0357
4	S_{va}	kgCOD m^{-3}	–	0.0018
5	S_{bu}	kgCOD m^{-3}	–	0.0060
6	S_{pro}	kgCOD m^{-3}	–	0.0061
7	S_{ac}	kgCOD m^{-3}	3.1339	0.0285
8	S_{h2}	kgCOD m^{-3}	–	9.7864E–08
9	S_{ch4}	kgCOD m^{-3}	–	0.0477
10	S_{IC}	kgCOD m^{-3}	0.0919	0.1950
11	S_{IN}	kgCOD m^{-3}	0.0207	0.0800
12	S_I	kgCOD m^{-3}	38.3368	44.9001
14	X_{ch}	kgCOD m^{-3}	235.3783	0.2290
15	X_{pr}	kgCOD m^{-3}	15.7445	0.0132
16	X_{li}	kgCOD m^{-3}	1.8127	0.0018
17	X_{su}	kgCOD m^{-3}	–	8.0364
18	X_{aa}	kgCOD m^{-3}	–	0.3662
19	X_{fa}	kgCOD m^{-3}	–	0.0343
20	X_{c4}	kgCOD m^{-3}	–	0.6878
21	X_{pro}	kgCOD m^{-3}	–	0.8091
22	X_{ac}	kgCOD m^{-3}	–	2.5956
23	X_{h2}	kgCOD m^{-3}	–	1.4769
24	X_I	kgCOD m^{-3}	15.85072	17.5749
25	S_{cat}	kmole m^{-3}	2.50E–02	0.0247
26	S_{an}	kmole m^{-3}	7.81E–02	0.0659
27	$S_{va⁻}$	kgCOD m^{-3}	–	0.0018
28	$S_{bu⁻}$	kgCOD m^{-3}	–	0.0060
29	$S_{pro⁻}$	kgCOD m^{-3}	–	0.0061
30	$S_{ac⁻}$	kgCOD m^{-3}	–	0.0285
31	$S_{hco3⁻}$	kmoleC m^{-3}	–	0.4785
32	S_{nh3}	kmoleN m^{-3}	–	0.0650
33	$S_{gas,h2}$	kgCOD m^{-3}	–	3.588E–06
34	$S_{gas,ch4}$	kgCOD m^{-3}	–	1.2507
35	$S_{gas,co2}$	kmoleC m^{-3}	–	0.0178
36	$S_{H^+(*)}$	kmoleH^+ m^{-3}	–	3.1623E–08

Stoichiometric and kinetic parameters

Almost all of the stoichiometric and kinetic parameters used in this work were taken without modification from the original ADM1 model (Batstone *et al.*, 2002) and the study conducted by Rosen *et al.* (2006).

The calibration process allowed identification of parameters that had the greatest influence on the ADM1 output, and in order to reduce complexity, these were chosen for the curve fitting processes. The hydrolysis rate of carbohydrates ($K_{hyd,ch}$) mainly affected gas production and methane content in biogas, while the protein hydrolysis rate ($K_{hyd,pr}$) and the yield uptake for sugars (Y_{su}) were closely linked to TAN concentration. In fact, it was not easy to optimise sensitive kinetic parameters, as adjusting the simulated results to fit the experimental data created differences between the model and measured results of other parameters, since the differential equations in ADM1 are nonlinear and linked together intricately. Hence, the adapted parameters indicated in this study are a usable compromise. The adjusted stoichiometric values were decided in accordance with the inputs for the ADM1 model of SBP derived from *transformer* results. Modified stoichiometric and kinetic parameters from the calibration step are shown in Table 7.5.

Table 7.5 Modified stoichiometric and kinetic parameters

Stoichiometric and kinetic coefficient		Default	Used	Unit
$f_{sI,Xc}$	soluble inerts from composites	0.1	0.1248$^{(a)}$	kgCOD kgCOD^{-1}
$f_{xI,Xc}$	particulate inerts from composites	0.25	0.0516$^{(a)}$	kgCOD kgCOD^{-1}
$f_{ch,Xc}$	carbohydrates from composites	0.2	0.7664$^{(a)}$	kgCOD kgCOD^{-1}
$f_{pr,Xc}$	proteins from composites	0.2	0.0513$^{(a)}$	kgCOD kgCOD^{-1}
$f_{li,Xc}$	lipids from composites	0.25	0.0059$^{(a)}$	kgCOD kgCOD^{-1}
C_{xc}	Carbon content of carbohydrates	0.0313	0.0274$^{(c)}$	kmoleC kgCOD^{-1}
N_{xc}	Nitrogen content of composites	varies	0.000987$^{(c)}$	kmoleN kgCOD^{-1}
N_I	Nitrogen content of inerts	varies	0.000714$^{(b)}$	kmoleN kgCOD^{-1}
N_{bac}	Nitrogen content of biomass	0.00625	0.005$^{(b)}$	kmoleN kgCOD^{-1}
Y_{su}	Yield uptake sugars	0.1	0.02$^{(d)}$	kgCOD kgCOD^{-1}
Y_{c4}	Yield uptake butyrates and valerates	0.06	0.15$^{(d)}$	kgCOD kgCOD^{-1}
Y_{ac}	Yield uptake acetates	0.05	0.015$^{(d)}$	kgCOD kgCOD^{-1}
k_{dis}	disintegration rate (first–order)	5	0.5$^{(d)}$	day^{-1}
$K_{hyd,ch}$	hydrolysis rate of carbohydrates	10	0.03$^{(d)}$	day^{-1}
$K_{hyd,pr}$	hydrolysis rate of proteins	10	0.1$^{(d)}$	day^{-1}
$K_{hyd,li}$	hydrolysis rate of lipids	10	0.1$^{(d)}$	day^{-1}
$K_{I,nh3}$	inhibitory conc. of NH_3 to acetate uptake	0.0018	0.018$^{(d)}$	kgCOD m^{-3}

Note: $^{(a)}$ *transformer* outputs; $^{(b)}$ (Wett *et al.*, 2006); $^{(c)}$ based on SBP ultimate analysis $^{(d)}$ calibrated from best curve fitting method.

7.1.3.3. Calibration results

Figure 7.1 shows the measured and simulated results for biogas production, methane and carbon dioxide content after calibration.

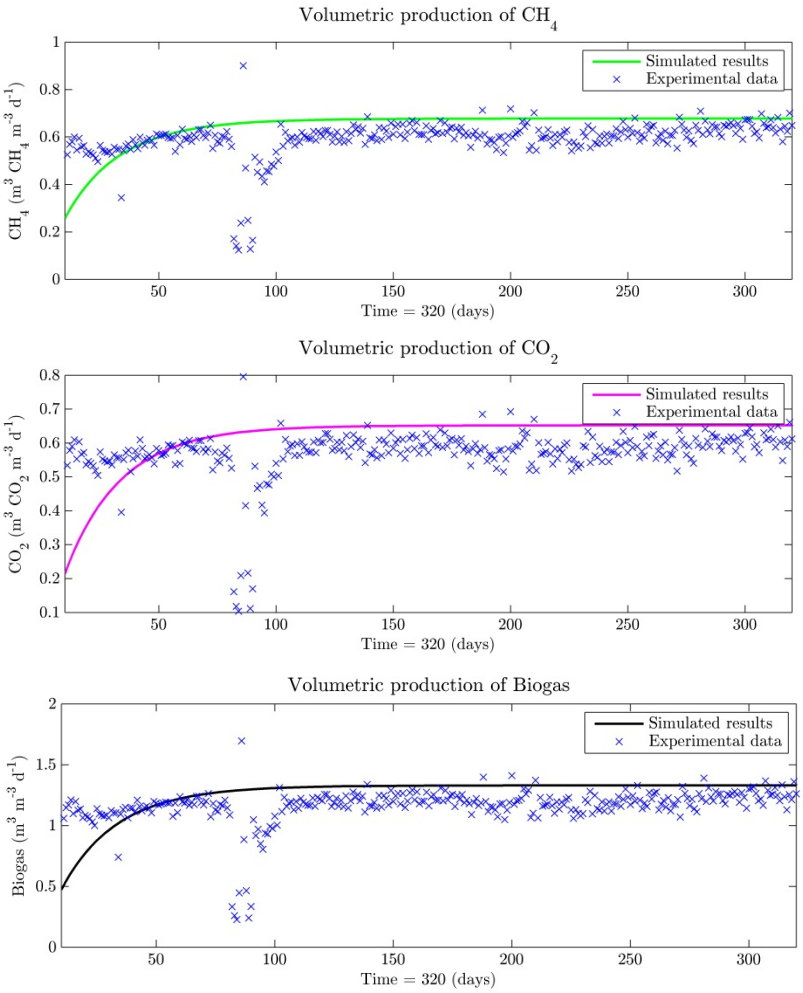

Figure 7.1 Calibration results of gas production for reactor R2 (OLR=2)

As can be seen, the gas production was predicted quite well for the steady–state period; however, good agreement between predicted and experimental data for transient–state periods is only observed after running the model for a couple of weeks (about 25 days). Reasons for this may include incorrect choice of initial conditions and errors in determining the stoichiometric and kinetic parameters for the model run (Table 7.5). In addition, shortcomings in the original ADM1 which have been noted recently in (Batstone & Keller, 2006; Huete *et al.*, 2006; Kleerebezem & Van Loosdrecht, 2006; Yasui *et al.*,

2008) may also contribute to the problem: these include inadequate simplifications in some reactions, lack of some mechanisms or intermediate products, inaccuracies in some stoichiometric coefficients, no restrictions for thermodynamic equilibrium which may control the anaerobic bioconversions *etc.* Figure 7.2 displays the calibration results for pH and TAN concentration.

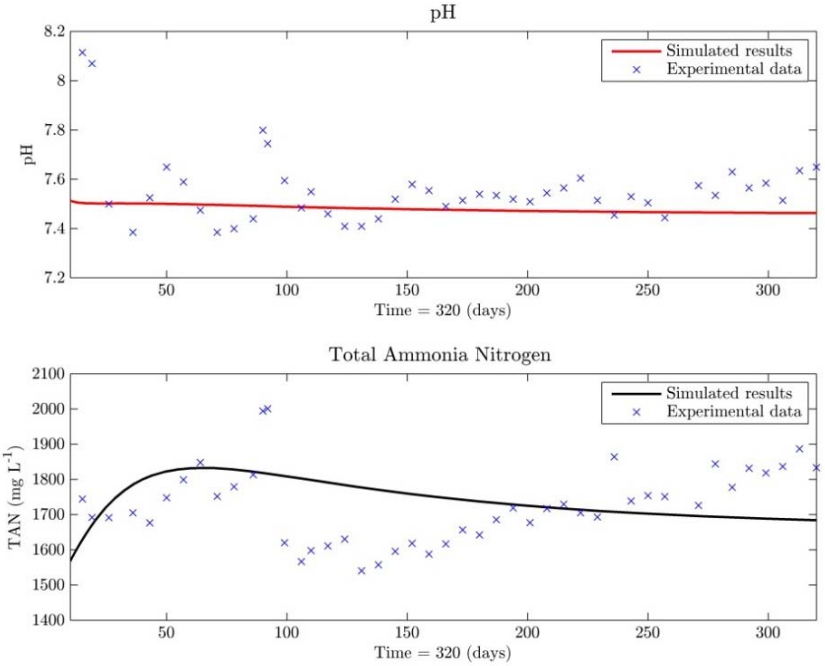

Figure 7.2 Calibration results of pH and TAN concentration of reactor R2 (OLR=2)

Graphs in Figure 7.2 show that the model also appears to replicate the pH and TAN concentration quite well, with variations in the range of approximately 7.4–7.5 and 1.6–1.8 g L^{-1}, respectively.

In terms of VFAs (Figure 7.3), although in general accumulation of VFA was satisfactorily represented, some deviations between simulation and experimental data were observed. This can be explained by operational problems between days 80–90, when a heater failure resulted in a break from feeding during this time. When the heater had been repaired feeding was gradually restored to the previous OLR over a period of 8 days so as not to cause a shock to the digesters. By day 164 all of the digesters had reached their target loading rates, but operational difficulties were apparent in the higher loaded digesters as a stable foam was forming and occupying the head space, causing blockages of the gas outlet with occasional pressurisation and/or loss of digestate.

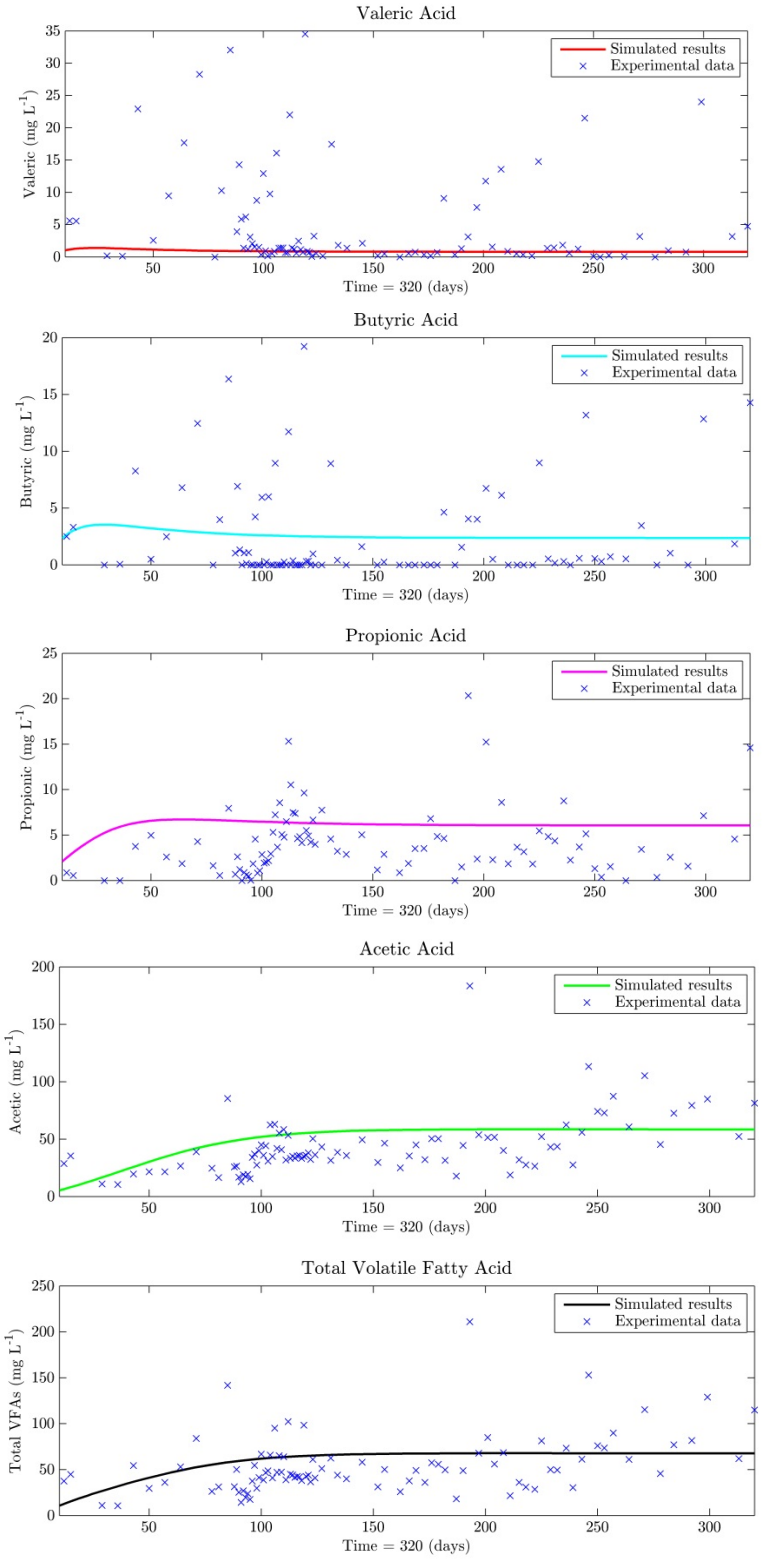

Figure 7.3 Calibration results of VFAs (Valeric,Butyric, Propionic, Acetic, Total VFAs) for reactor R2 (OLR=2)

7.1.3.4. Model validation

Three simulations at OLRs of 3, 4 and 5 g VS L^{-1} day^{-1} (named OLR3, OLR4 and OLR5, respectively) were made using the calibrated model without changing the parameters optimised in the calibration step. Simulated and measured data from reactors R3, R4, R5 were compared to evaluate the applicability of the optimised parameters under different loading rates (see Figures 7.4–7.12).

As with the calibration step, key parameters including biogas production, methane and carbon dioxide contents, VFAs, pH and TAN concentration are presented.

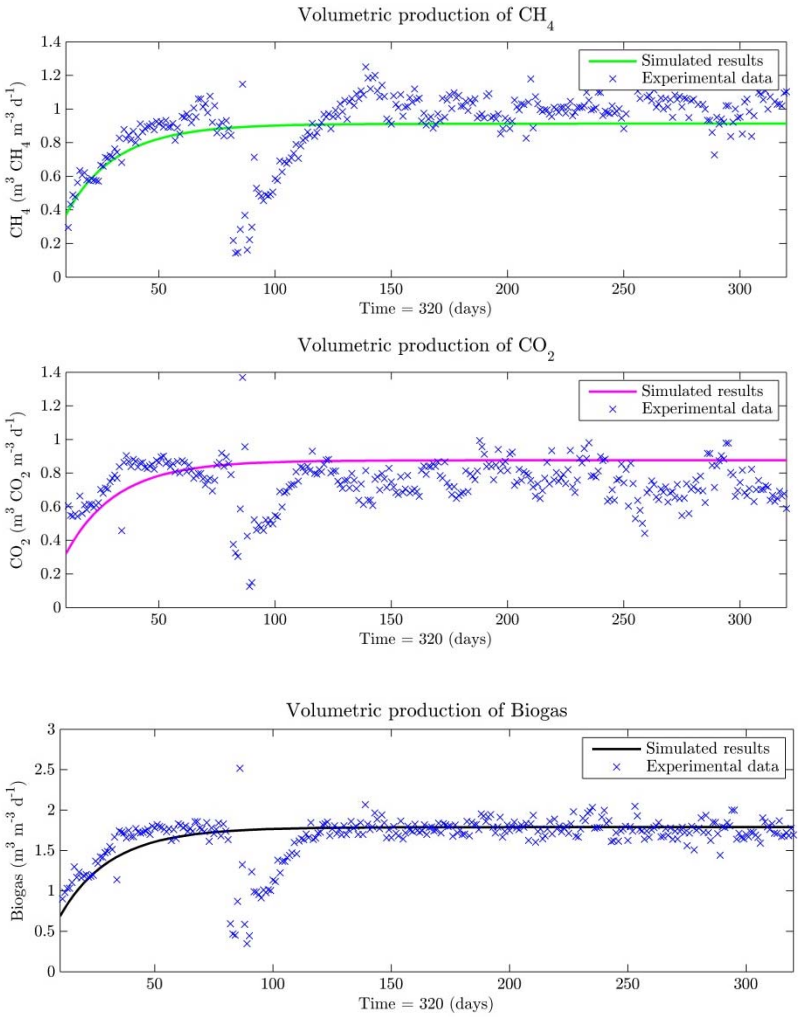

Figure 7.4 Calibration results of gas production for reactor R3 (OLR3)

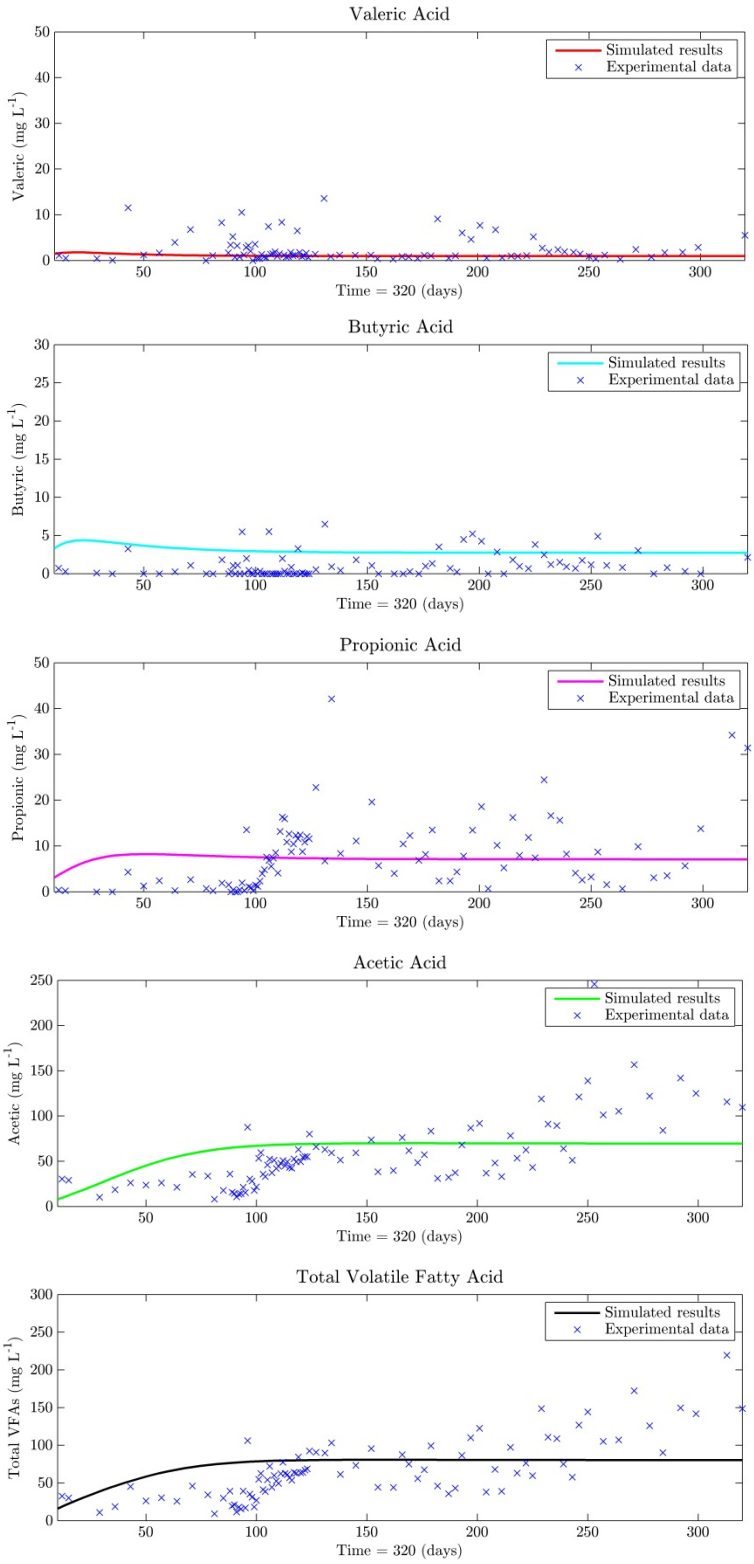

Figure 7.5 Calibration results of VFAs (Valeric, Butyric, Propionic, Acetic, Total VFAs) for reactor R3 (OLR3)

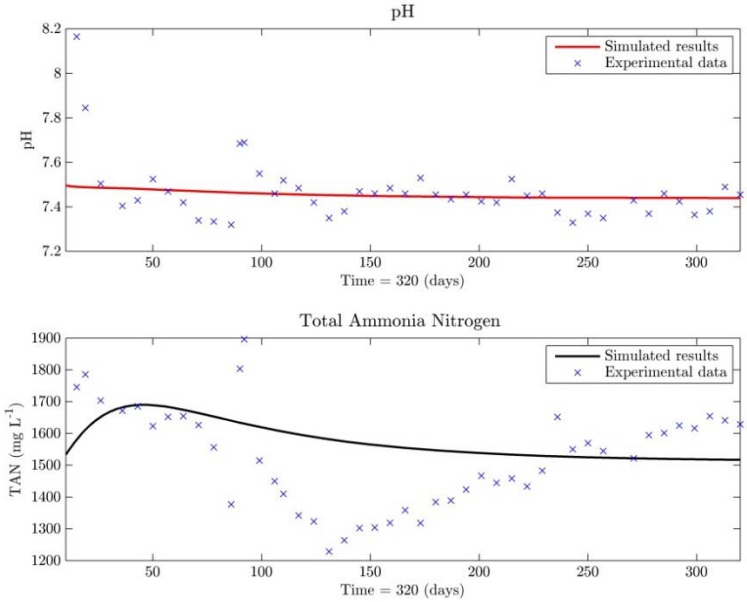

Figure 7.6 Calibration results of pH and TAN for reactor R3 (OLR3)

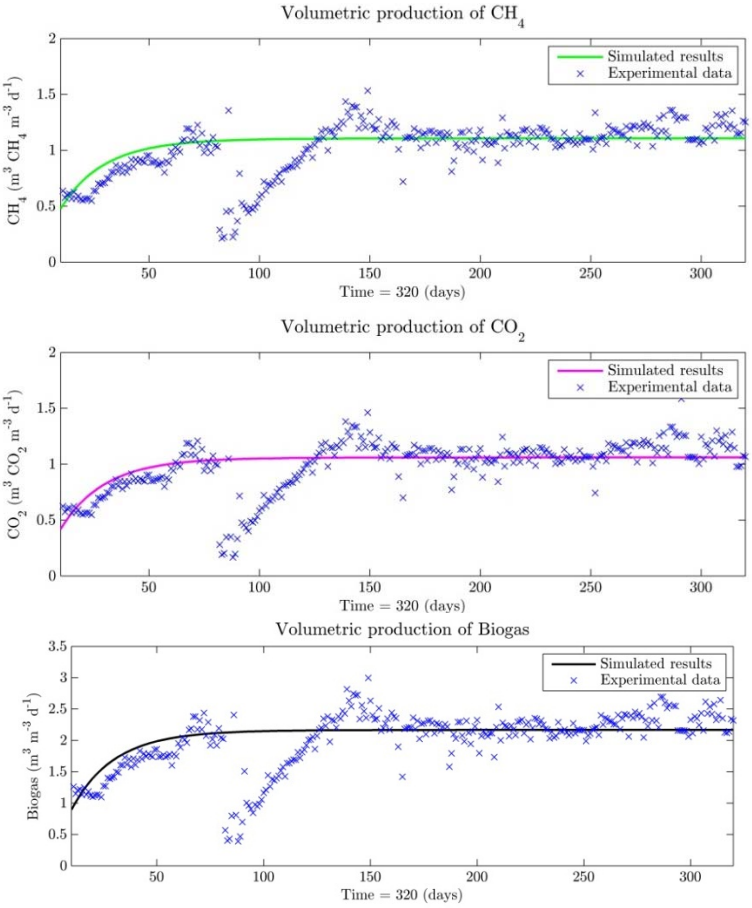

Figure 7.7 Calibration results of gas production for reactor R4 (OLR4)

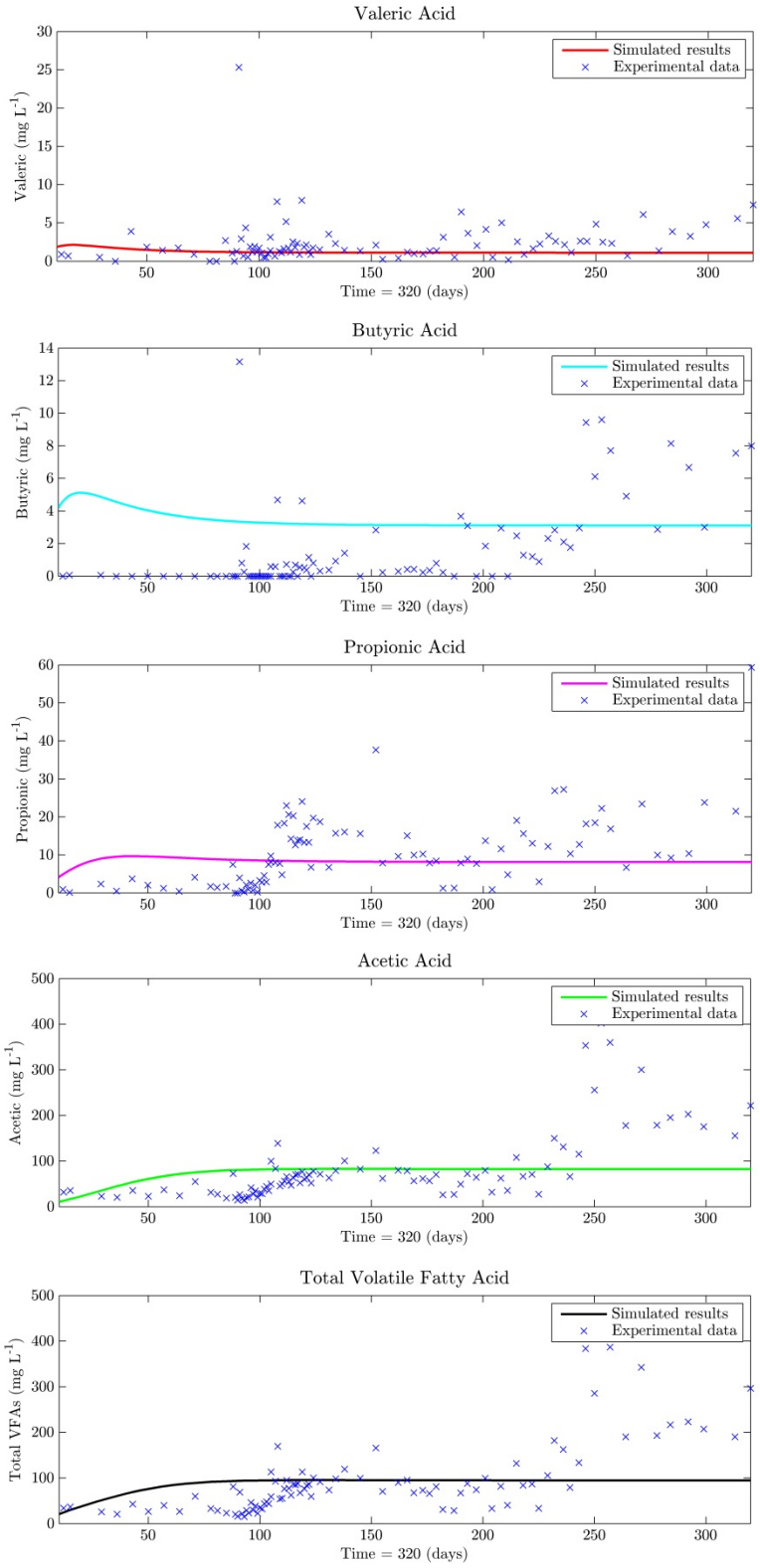

Figure 7.8 Calibration results of VFAs (Valeric,Butyric, Propionic, Acetic, Total VFAs) for reactor R4 (OLR4)

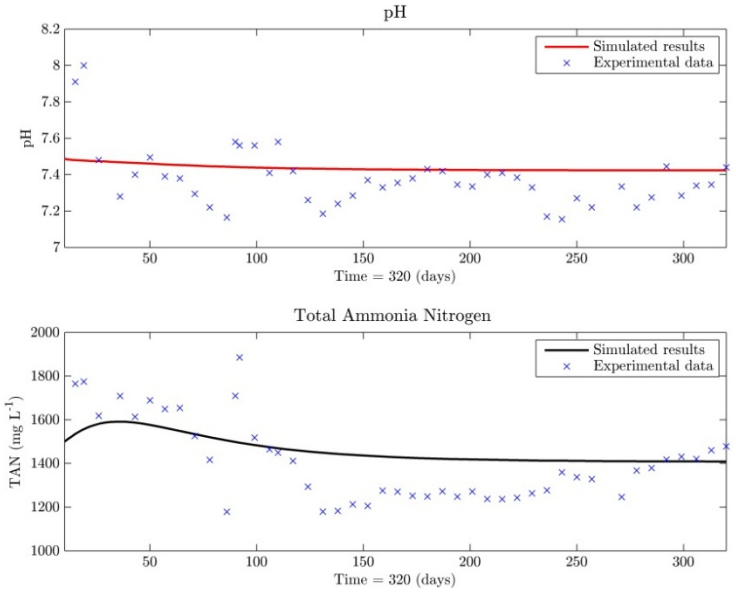

Figure 7.9 Calibration results of pH and TAN for reactor R4 (OLR4)

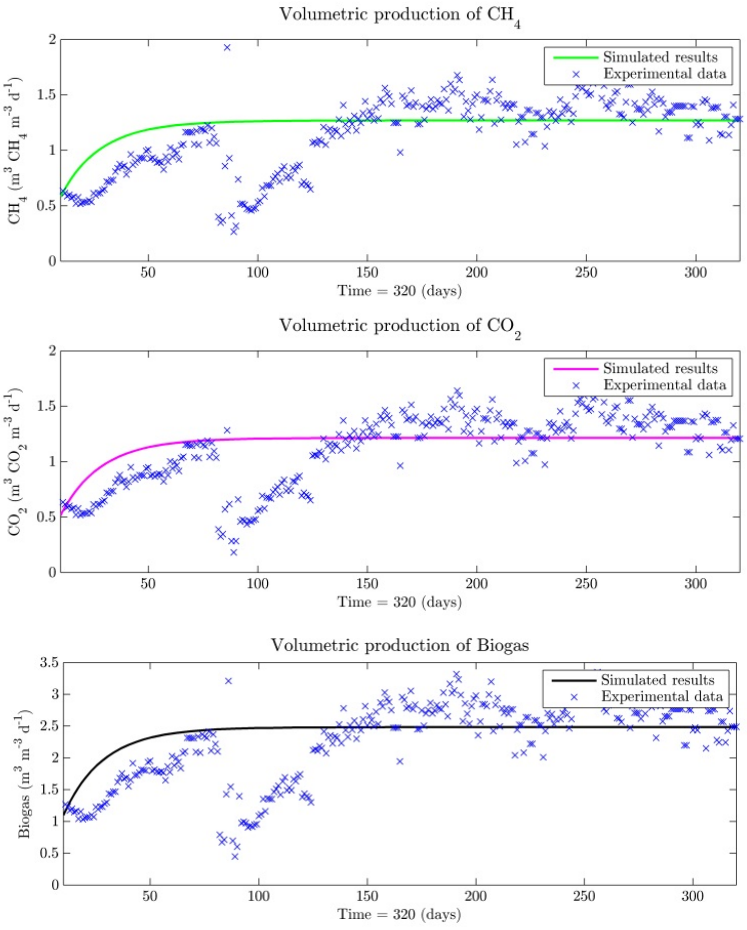

Figure 7.10 Calibration results of gas production for reactor R5 (OLR5)

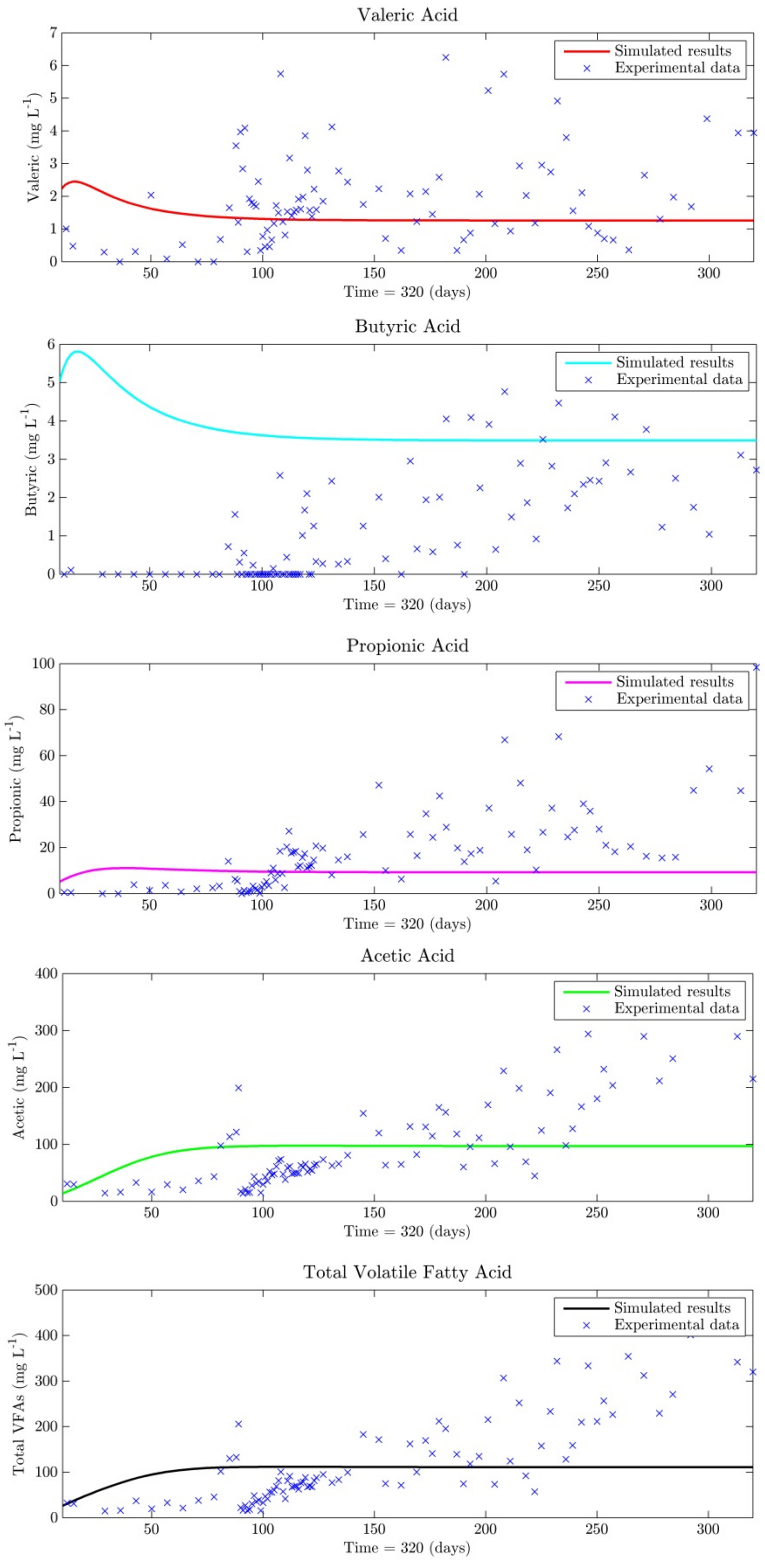

Figure 7.11 Calibration results of VFAs (Valeric,Butyric, Propionic, Acetic, Total VFAs) for reactor R5 (OLR5)

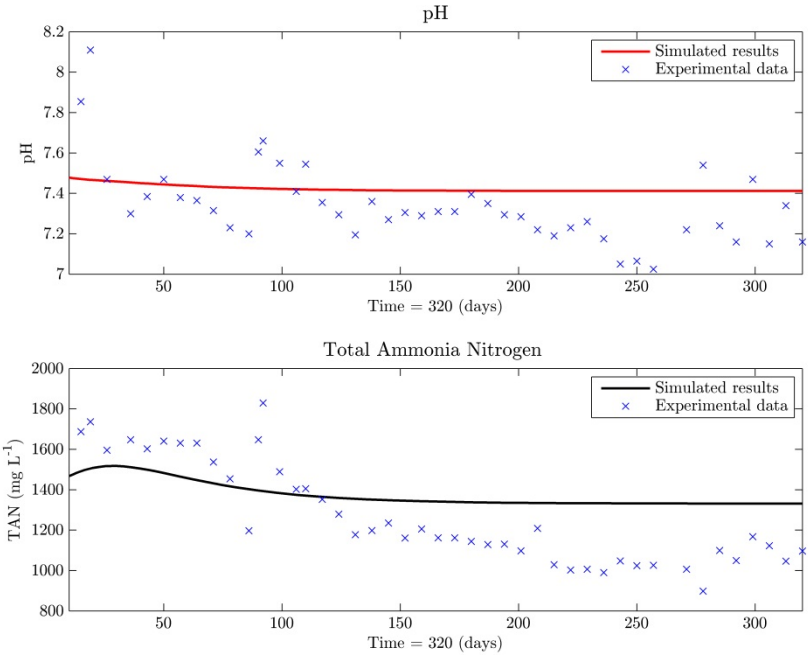

Figure 7.12 Calibration results of pH and TAN for reactor R5 (OLR5)

As can be clearly seen from Figures 7.4, 7.7 and 7.10, the model predicts gas production, methane and carbon dioxide contents with high accuracy in both transient and steady–state periods. The simulated curve fits extremely well with experimental data at moderate OLRs (3 and 4 g VS L^{-1} day^{-1}), while a small increase in deviations at higher OLR (5 g VS L^{-1} day^{-1}) can be recognised. The trend is that gas production is gradually underestimated as the OLR increases. This may be due to the effects of foaming when operating in mesophilic conditions, in particular for digester R5 which was fed at OLR 5 g VS L^{-1} day^{-1}, and experienced severe foaming with a tendency to block the gas outlet line. This led to quite wide variations in values for specific or volumetric biogas and methane production due to uncontrolled '*blow–outs*', resulting in unstable operating conditions. Similar declines in performance after digester '*blow–outs*' have been observed before with various substrates (Rincon *et al.*, 2012; Zhang & Banks, 2013), even when the OLR was maintained by adjustment of the daily amount fed to take account of any loss of digestate (unpublished data, Southampton). This suggests that foaming and/or pressurisation may itself have adverse effects on digestion which are not captured in the model simulation. Additionally, there were differences between measured and simulated results from day 80 to 90 due to the heater failure as previously described.

Overall, it can be seen that total VFAs were accurately predicted at transient state for the first 220 days (Figures 7.5, 7.8 and 7.11). Thereafter, significant differences between model and experimental results were observed with the deviations at steady–state period around 30–55% depending upon OLR. The reason for this is possibly due to the correlation of some sensitive parameters with hydrolysis constants, feed concentration, HRT and reactor configuration (Gavala *et al.*, 2003).

Predicted values for individual volatile fatty acids (valerate, buryrate, propionate and acetate) were in reasonablly good agreement with measured values: acetic acid accounted for the main part of total VFA while valeric and butyric acids made up only a small proportion.

pH and TAN concentration were also well described by the model as can be seen from Figures 7.6, 7.9 and 7.12. Predicted pH was in the range 7.4–7.5 which agreed with the measured values at low OLR; the value was slightly overestimated at higher OLR. Prediction of TAN concentration was reasonably accurate for all simulations. Although the period of the first 80 days and steady–state show a good fit between the modelled and experimental data, some discrepancies can be noted, especially for OLR3 and OLR4. As can be clearly seen from Figure 7.6 and Figure 7.9, measured values of TAN concentration are much lower than predicted between days 80 and 200. This might be due to the fact that the ADM1 model has not taken into account the correlation of hydrolysis constants with OLR and HRT (Gavala et al., 2003), whereas experiments showed that the decrease in TAN concentration in reactors probably happened because of the reduction in protein hydrolysis or due to washout as a result of the shortened HRT and overloading which occurred at higher OLR (Miron *et al.*, 2000; Suhartini *et al.*, 2014). Furthermore, some other limitations of the ADM1 model as previously mentioned also can contribute to the problem. It may also be possible that that the foaming somehow affects the digester performance with respect to VFA, TAN, pH *etc.*

7.1.4 Conclusion

This study has demonstrated that the ADM1 model with the customised stoichiometric and kinetic parameters is capable of satisfactorily predicting biogas, CH_4 and CO_2 contents, VFAs, pH and TAN for both steady–state and

transient periods under different OLRs. However, despite the sufficient predictions of most of the measured data attained, some noticeable deviations between model and experimental results were observed, particularly at higher OLR. This provided evidence for one of the weaknesses of ADM1 model regarding the oversimplification of hydrolysis constants as suggested by several researchers.

Overall, the ADM1 model appears to be a powerful and capable platform for a wide range of organic substrates including SBP. However, further assessment of the model performance, especially under high OLR conditions in accordance with identifying the modelling coefficients is recommended.

7.2 Sizing CHP and direct heating units in an anaerobic digestion plant for fuel–grade methane production

Accurate determination of the size of CHP and direct heating units in an anaerobic digestion plant plays an important role in saving energy when establishing a new plant. It is also useful to know the potentially available energy from running a biogas plant under specific operational conditions. Therefore, this case study was carried out to provide an example of how the model could address these issues.

Different scenarios of energy production were investigated considering the parameters which directly affect the overall energy consumption required to operate an AD plant and the amount of bio–methane produced, such as: ambient temperature, total input food waste, heat loss, *etc.* These possible scenarios were simulated using the energy model from a mass and energy balance point of view.

Assumptions and specification:

- This case study used the energy model integrated with the steady state digester based on a stoichiometric approach;
- Digestate was assumed to be pasteurised at 70^{o}C.

7.2.1 Setting scenarios and input data

Two scenarios were examined in this study. Scenario 1 was intended to provide an overview of the overall energy available in the form of upgraded

biogas and surplus heat generated by a CHP unit under different ambient temperatures and AD plant sizes.

In scenario 1, it was assumed that the digester was operated at mesophilic temperature (35°C); ambient temperature varies from 10–30°C; water and air used for the plant are at ambient temperatures; volume of the digester depends on the total food waste, ranging from 3–30 tonnes per day; digester volume is increased by 10% for gas storage. Other assumptions are as shown in Table 7.6.

Table 7.6 Anaerobic digestion plant operational parameters – Scenario 1

Parameters	Units	Value
Digester temperature	°C	35
Pasteuriser temperature	°C	70
Ambient temperature	°C	10–15–20–25–30
Total food waste (wet)	$\times 10^3$ kg day^{-1}	3–6–12–18–24–30
Time in pasteuriser	hour	1
Loading rate	kg VS m^{-3} day^{-1}	3
TS in food waste	%	27.8
VS in food waste	%	25
Overall heat transfer coefficient of:		
Wall	W m^{-2}K	0.275
Floor	W m^{-2}K	0.823
Roof	W m^{-2}K	0.931

The AD plant operational parameters for scenario 2 are listed in Table 7.7. In this case, it was assumed that the digester operated at 42°C in accordance with common practice at several UK AD plants (Banks, Chesshire, *et al.*, 2011); ambient temperature was 10°C for the different feedstock inputs.

This case study is focused on fuel–grade methane production only, therefore the CHP unit only uses sufficient raw biogas to produce an adequate supply of electricity for internal uses. When the heat generated from the CHP unit by this amount of biogas is lower than the internal heat requirement, a boiler unit is added to the system. One of the aims of the second scenario was to know whether or not a boiler was required under different operational conditions.

Table 7.7 Anaerobic digestion plant operational parameters – Scenario 2

Parameters	Units	Value
Digester temperature	°C	42
Pasteuriser temperature	°C	70
Ambient temperature	°C	10
Total food waste (wet)	$\times 10^3$ kg day^{-1}	3–6–12–18–24–30
Time in pasteuriser	hour	1
Loading rate	kg VS m^{-3} day^{-1}	3
TS in food waste	%	27.8
VS in food waste	%	25
Overall heat transfer coefficient of:		
Wall	W m^{-2}K	4.114
Floor	W m^{-2}K	0.947
Roof	W m^{-2}K	0.931

The gross energy content of methane used in calculations was 55.6 MJ kg^{-1} at standard temperature and pressure (Ali & Basit, 1993; Judd *et al.*, 1999; da Rosa, 2012). In the energy balance calculation, all heating–related units such as digesters, flash tanks, heaters, coolers, absorbers, strippers were taken into account. However, no allowance was made for heat loss in exchanging processes among these units.

7.2.2 Results and discussion

7.2.2.1. Energy balance

Table 7.8 and Figure 7.13 give an overview of the energy consumption of the main elements in the AD plant and the total potential energy produced in the form of surplus heat and upgraded biogas.

As expected, the total available energy increases approximately in proportion to the total amount of food waste digested. For example, at ambient temperature of 30°C, 6 or 18 tonnes of food waste produces about 5457 kWh day^{-1} (4303 and 1154 kWh day^{-1} of upgraded biogas and surplus heat, respectively) or 16402 kWh day^{-1} which is approximately twice and six times the value 2710 kWh day^{-1} derived of 3 tonnes of food waste.

Table 7.8 Energy consumption and energy production from model calculation

Energy (kWh day^{-1})	Total food waste (wet) in different calculations (tonnes day^{-1})					
	3	6	12	18	24	30
CHP electricity produced	210	420	837	1257	1674	2093
Electricity for mixing digester	43	87	174	261	348	435
Electricity for biogas upgrading	103	205	408	613	817	1021
Electricity for biogas compression	64	128	255	383	510	638
Heat loss of digester and pasteuriser	121	192	305	400	485	562
Heat required for raising substrate	191	381	762	1143	1525	1906
Total heat created by CHP unit	369	739	1476	2217	2954	3694
Energy from upgraded biogas	2140	4303	8590	12896	17177	21486
Enery from surplus heat at different ambient temperatures:						
10°C	149	354	786	1240	1698	2169
15°C	254	549	1167	1799	2436	3078
20°C	359	749	1553	2363	3179	4000
25°C	464	951	1940	2927	3927	4929
30°C	570	1154	2329	3506	4682	5863

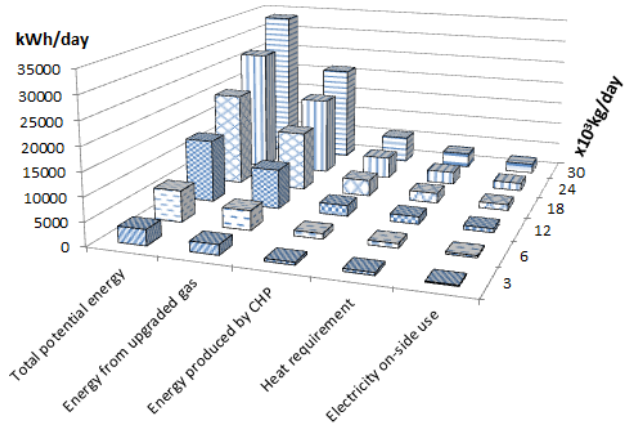

Figure 7.13 Energy balance of the studied AD plant

The input data presented in Table 7.7 (scenario 2) was used to evaluate some cases when the heat produced from the CHP unit may be less than the heat requirement for on–site uses. In these calculations, the heat shortfall was made up by boiler units.

Figure 7.14 shows the decrease in required boiler capacities as the plant size increases when the food waste load increases from 3 tonnes day^{-1} to 12 tonnes day^{-1}.

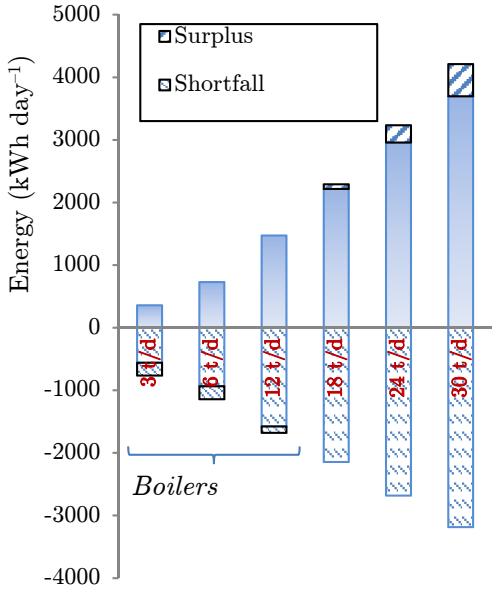

Figure 7.14 The heat balance of CHP unit and boiler capacity requirements

As can be seen from Figure 7.14, when the size of the plant is sufficient, the heat produced from the CHP unit will exceed the on–site heat demands. This is because electricity requirements increase more than heat consumption when plant size increases. Therefore, when CHP units produce adequate electricity for internal use, they also generate a large amount of heat that exceeds the total heat requirement for the AD plant (Figure 7.15).

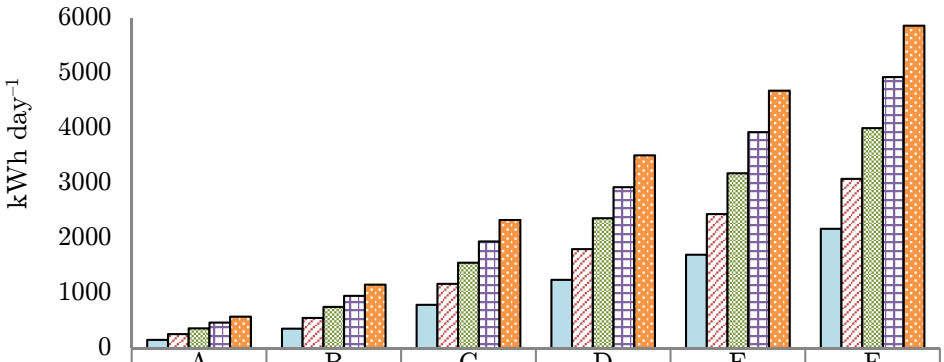

	A	B	C	D	E	F
10 oC	149.43	353.54	786.08	1239.89	1698.38	2169.31
15 oC	254.19	549.37	1166.67	1798.91	2436.01	3078.20
20 oC	358.68	748.77	1552.75	2362.69	3178.88	3999.57
25 oC	463.84	951.10	1939.58	2926.74	3927.00	4928.95
30 oC	570.19	1153.99	2329.41	3505.68	4681.86	5863.22

Figure 7.15 Exportable heat from CHP. (A)–(F) correspond to each value for total daily input food waste (see Table 7.7)

It was estimated that the electricity requirement for all internal uses accounts for about 6% of total energy produced. The electricity requirement for biogas upgrading, biogas compression and digester mixing processes respectively account for 3%, 1.7% and 1.3% of total energy produced.

Figure 7.16 illustrates the results for scenario 2 in terms of the percentages of methane consumed by the CHP and boiler units and the amount of methane loss from the total quantity of biogas to be upgraded.

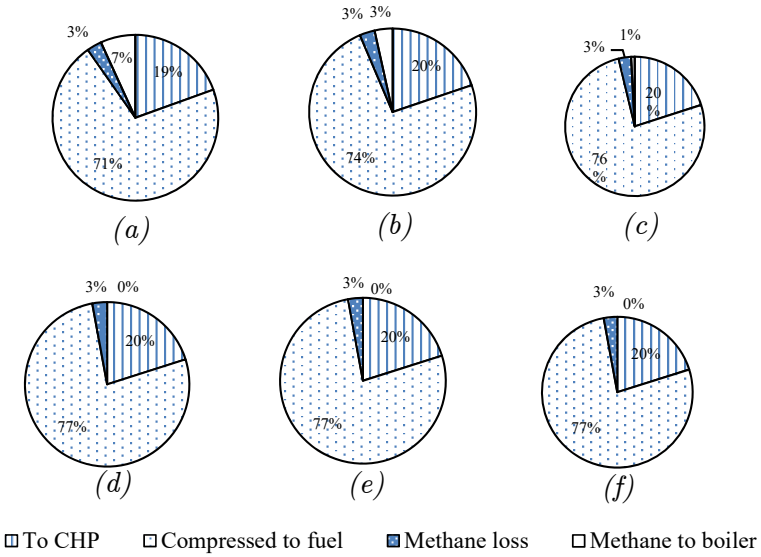

Figure 7.16 Available methane production and consumption
(*a*)–(*f*) correspond to each value for total daily input food waste (see Table 7.7)

Results reported in Figure 7.16 shows that average methane losses accounted for about 3% of total methane to be upgraded. This appears to be in reasonable agreement with what was reported in (Bauer *et al.*, 2013).

About 20% of the total upgraded methane is used in the CHP unit to produce electricity and heat for internal use, including upgrading and compression. When the heat generated from the CHP unit meets internal heat demands, approximately of 77% methane is therefore available for fuel–grade use. In smaller plants with a lower intake of food waste, the heat produced is insufficient and a small amount of methane from refined biogas is used in the boiler to make up the heat deficit (Figures 7.16*a*, 7.16*b*, 7.16*c*).

7.2.2.2. Methane losses through upgrading process

Methane loss is one of the important factors in choosing upgrading techniques (Petersson & Wellinger, 2009; Bauer *et al.*, 2013). In order to know the proportion of methane lost through the upgrading process at different final

methane contents, a simulation using the same data as in section *7.2.2.1* was carried out, and the results are presented in Table 7.9.

Table 7.9 Methane loss through upgrading process

% of CH_4 in biogas	92.17	93.32	95.17	96.64	97.89	98.68	99.35	99.55	99.73	99.85
CH_4 loss	1.68%	1.69%	1.74%	1.81%	2.14%	2.68%	4.05%	4.42%	4.93%	5.15%

As can be seen, methane losses through the upgrading process ranged from below 2% to about 5%, depending on the methane concentration of the upgraded biogas. The higher the methane percentage in the final product gas, the greater the methane loss. This happens because to reach high methane concentrations, larger amounts of water and air need to be supplied. Consequently, more methane is dissolved leading to the increase in methane loss.

In order to reduce the methane loss, one possible method is to use a flash tank working under optimised pressure and temperature to recover the methane lost from the absorber and return it to the compressor. The pressure in the flash tank is suggested to be around 3 atm since under this pressure, the released gas from the liquid phase contains mostly methane (Langerak *et al.*, 2013).

One method to improve the methane concentration in the upgraded biogas while keeping the methane loss at a low level is to raise the temperature of the water supply to the upgrading equipment, because the solubility of methane is inversely proportional to the temperature. However, this also causes a decrease in the solubility of CO_2, and consequently affects the efficiency of the biogas cleaning process. Therefore, choosing a suitable temperature for operation of the upgrading process is an issue that needs to be taken into account and the model can assist in this.

7.2.2.3. Relation between electricity demand and methane content of upgraded gas

The relation between electricity consumption and the methane content of the final upgraded gas was investigated by a simulation according to the parameters below:

- Total input food waste: 12 tonnes day^{-1};
- Ambient temperature: 10°C;
- Methane content of upgraded gas from 92.17% to 99.85%;
- Digester operated at: 42°C.

Figure 7.17 shows the relationship between the power consumption and the methane content of the upgraded biogas. Clearly, energy consumption for both

upgrading and compression increase when the methane content of the upgraded biogas increases. In the range of 92.17–99.85% methane, electricity consumption based on upgraded biogas in standard conditions (0°C and 1 atm) corresponds to 0.379–0.415 kWh Nm^{-3} for upgrading and 0.306–0.313 kWh Nm^{-3} for compression (assuming the upgraded gas is compressed to about 197 atm). This agrees well with results from previous studies: e.g. about 3–6 per cent of the energy content in the upgraded gas (Persson, 2003), and 0.3–0.6 kWh m^{-3} biogas upgraded without compression (or 0.65–1.2275 with both upgrading and compression) (Murphy & McCarthy, 2005; Smyth *et al.*, 2009).

The results also showed that when upgraded biogas is compressed to 197 atm for use in automotive applications, the electricity required for upgrading per unit of upgraded biogas is higher than that required for compression (about 1.24–1.34 times).

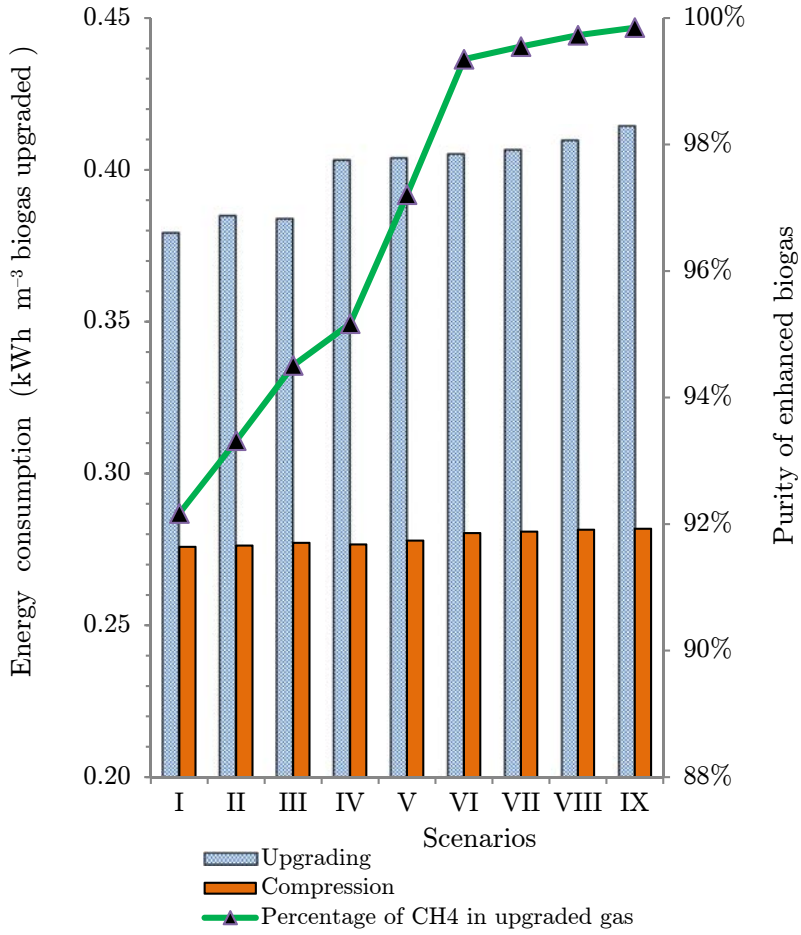

Figure 7.17 Relation between purity of enhanced biogas and electricity consumption

7.2.3 Conclusions for modelling of gas upgrading

Simulations showed that about 20% of the methane produced from anaerobic digestion could be used in a CHP unit to generate heat and electricity for internal use, 3% of the methane lost through biogas upgrading and about 77% of the methane can be available for energy purposes. The methane loss from biogas upgrading using pressurised water scrubbing depends upon the purity of the upgraded gas and can vary from below 2% to about 5% of the total upgraded methane. Electricity consumed for upgrading was estimated at 0.379–0.415 kWh Nm^{-3} and 0.306–0.313 kWh Nm^{-3} upgraded biogas for upgrading and compression, respectively.

7.3 Energy potential from the digestion of food waste in municipal solid waste stream of urban areas in Vietnam

Anaerobic digestion was introduced in Vietnam more than ten years ago, but at a small scale, and due to a lack of information, data and experience it has been somewhat neglected by government when formulating national strategies to deal with MSW problems. Hence, the purpose of this case study is to use the energy model developed in the current work to evaluate the potential of AD as a treatment for food waste in municipal solid waste (MSW) streams from the energy recovery point of view. The outputs provide a useful source of information about the energy potential from food waste using AD technology, which is currently unavailable in urban areas in Vietnam. Furthermore, it can help the Vietnamese government and industry decision–makers to establish more effective and sustainable MSW management strategies.

Assumptions and specification:

- Food waste can be separated from MSW before sending to AD plants in accordance with the national strategy for sustainable development;
- All food waste collected will be treated at centralised plants;
- This case study used the energy model integrated with the modified ADM1. The aim was to establish the ultimate energy from anaerobic digestion, hence steady–state simulation with ADM1 was used before exchanging simulated data with the Aspen Plus platform;
- All AD plants were assumed to work in mesophilic conditions (35°C).

7.3.1 Background

7.3.1.1. Population growth and increased urbanisation in Vietnam

Urbanisation in Vietnam has been increasing rapidly along with the country's economic growth. In 2000, the number of cities and towns in Vietnam was 649 but this has increased to 715 in 2005 and 755 in 2010. The growth in the number of people moving from rural to urban areas is the main driver in the expansion of Vietnam's urban population. As of 2009, the urban population was 25.59 million, accounting for 29.74% of the total population; this expanded to 26.22 million (30.17%) a year later.

According to MONRE (2011), it has been estimated that in 2025 the urban population in Vietnam will double to 52 million, accounting for 50% of Vietnam's total population. This rapid urbanisation has put pressure on the government in dealing with environmental problems, including solid waste management in cities; and this is exacerbated by the limited space for treatment of wastes by traditional methods. For Vietnam to develop sustainably more effort is required to solve this challenge.

7.3.1.2. Quantity and composition of MSW in Vietnam

In Vietnam the generation of MSW is growing rapidly, in parallel with urbanisation. According to recent reports, urban areas currently contain 30% of the country's population but produce about 42–46% of total solid wastes. The waste is mainly generated from households, buildings, commercial activities and other sources similar to households; from commercial enterprises such as offices, hotels, retail, institutions; and from municipal services such as street cleaning, *etc.*

MSW in Vietnams urban areas is mainly composed of food waste, paper, plastic, wood, metal and glass, with some hazardous household waste such as electric light bulbs, batteries, *etc.* (MONRE, 2011). Composition of MSW from some of the main cities in Vietnam between 2009 and 2010 is presented in Table 7.10.

Table 7.10 Composition of MSW from some main cities in Vietnam 2009 – 2010

Components	Hanoi 1	Hanoi 2	Haiphong 1	Haiphong 2	Hue	Danang	HCM city 1	HCM city 2	Bacninh	Average
Food waste (*)	53.81	60.79	55.18	57.56	77.1	68.47	64.50	62.83	56.9	61.9
Paper	6.53	5.38	4.54	5.42	1.92	5.07	8.17	6.05	3.73	5.20
Textile	5.82	1.76	4.57	5.12	2.89	1.55	3.88	2.09	1.07	3.19
Wood	2.51	6.63	4.93	3.70	0.59	2.79	4.59	4.18	–	3.74
Plastic	13.57	8.35	14.34	11.28	12.47	11.36	12.42	15.96	9.65	12.15
Leather& Rubber	0.15	0.22	1.05	1.90	0.28	0.23	0.44	0.93	0.20	0.60
Metal	0.87	0.25	0.47	0.25	0.40	1.45	0.36	0.59	–	0.58
Glass	1.87	5.07	1.69	1.35	0.39	0.14	0.40	0.86	0.58	1.37
porcelain	0.39	1.26	1.27	0.44	0.79	0.79	0.24	1.27	–	0.81
Soil & Sand	6.29	5.44	3.08	2.96	1.70	6.75	1.39	2.28	27.85	6.42
cinder	3.10	2.34	5.70	6.06	–	0.00	0.44	0.39	–	2.58
hazardous waste	0.17	0.82	0.05	0.05	–	0.02	0.12	0.05	0.07	0.17
Sludge	4.34	1.63	2.29	2.75	1.46	1.35	2.92	1.89	–	2.33
Others	0.58	0.05	1.46	1.14	–	0.03	0.14	0.04	–	0.49
Total	100	100	100	100	100	100	100	100	100	

Note: (*) food waste can be considered as the organic fraction of MSW when it does not contain irrecoverable paper residues (Hartmann & Ahring, 2005; Zhu *et al.*, 2008).The data have been adapted from JICA (2011) and MONRE (2011).

As can be seen from Table 7.10, food waste accounts for a very large proportion of the MSW stream, ranging between 54–77 % dependent on the city.

The proportion of food waste can be estimated based on the municipal waste generation rate, population growth in urban areas and the organic fraction. Table 7.11 shows estimates for the predicted generation of food waste in cities for 2015, 2020 and 2025.

Table 7.11 Estimation of MSW and food waste generation in Vietnam for the 2015, 2020 and 2025

Contents	2015	2020	2025
Urban population (million)[(a)]	35	44	52
% of Vietnam's population	38	45	50
Municipal waste generation rate (kg cap^{-1}day^{-1})[(b)]	1.2	1.4	1.6
Total MSW per day (tonnes day^{-1})	42,000	61,600	83,200
Rate of MSW collected (% of total MSW)	85[(c)]	90[(c)]	100[(d)]
Total MSW collected per day (tonnes day^{-1})	35,700	55,440	83,200
Total food waste collected per day (tonnes day^{-1})[(e)]	21,420	33,264	49,920

Note: [(a), (d)] data taken from the GWP (2009); [(b)] according to the MONRE (2011), [(c)] according to the GWP (2011); [(e)] assumed that food waste fraction in MSW stream is 60%.

7.3.1.3. The problems with landfilling

One of the most common treatment methods which is applied widely in cities across Vietnam to deal with almost all types of MSW is landfilling. It is considered the simplest, and in many cases the cheapest, method of disposal. During stabilisation the solid waste produces leachate and landfill gas which can be used for heat and electricity generation. This process has many significant economic and environmental problems, however, including: limited space for landfill sites; cost of waste burial; cost of transporting the waste; risk of contamination of groundwater with pollutants; and the emission of greenhouse gases to the atmosphere (Byrne, 1997; Trzcinski & Stuckey, 2009). Due to space limitations landfill sites will have to be located further from the cities, considerably increasing transportation costs.

There is no simple solution to the waste issue, but it obviously requires alternative methods to shift the paradigm.

7.3.1.4. Development of anaerobic digestion worldwide and in Vietnam

As noted above, biogas production was introduced to Vietnam over 10 years ago. By the end of 2006, more than 18,000 domestic biogas plants had been installed in 10 provinces in Vietnam with support from the Netherlands government. This investment, however, is only to deal with agricultural wastes,

manure, *etc.* at the household or household–group levels (Abbasi *et al.*, 2012). When it comes to MSW, AD has been neglected by the government. The main reason for this is a lack of information, data and experience, as well as economic factors.

Despite its many advantages, AD does not yet make a significant contribution to resolving Vietnam's urban waste issues. The National Environment Report of Vietnam (2011) indicated that strategies from now to 2025 will focus on methods to recover energy and materials from MSW in cities. Recently, the Vietnam Government again emphasised that it is necessary to develop waste management systems in which solid wastes are classified at source, collected, reused, renewed and treated with progressive technologies to boost technological innovation in waste–to–energy processes (GWP, 2012). Thus, waste–to–energy technologies could not only help to provide a solution to this problem but also meet the national energy consumption policy for sustainable development (MONRE, 2011).

7.3.2 Scenarios, results and discussion

7.3.2.1. Setting scenarios

The estimated amounts of food waste generated in 2015, 2020 and 2025 as shown in Table 7.12 were used for modelling.

Table 7.12 AD plant operational parameters

Parameters	Unit	Values
Digester temperature	°C	35
Pasteuriser temperature	°C	70
Ambient temperature	°C	22 / 27
Total food waste (wet)	$\times 10^3$ kg day^{-1}	21420 / 22260 / 49920
Time in pasteuriser	hour	1
Loading rate	kg VS m^{-3} day^{-1}	3
TS in food waste	%	27.8
VS in food waste	%	25
Overall heat transfer coefficient of digesters surroundings		
Wall	W m^{-2} K	0.275
Floor	W m^{-2} K	0.823
Roof	W m^{-2} K	0.931

The seasonal average temperature in Vietnam was taken as 22°C in winter and 27°C in summer (Usa, 2007).

As already mentioned, biogas can be utilised in the forms of heat, electricity, vehicle fuel, natural gas, fuel cells, *etc.* Among these, electricity and vehicle fuel are currently the most suitable for use in Vietnam, and therefore these two were used in the scenarios to estimate the possible energy from food waste. These scenarios consider parameters which directly affect the overall energy consumption in operation of the AD plant, such as: ambient temperature, total input food waste, heat loss, etc. The required digester volume is also increased by 10% for gas storage. Other assumptions made in the model are summarised in Table 7.12.

Scenario 1 was chosen to obtain the maximum possible usable energy in the form of heat and electricity, by sending all of the biogas generated from the digesters to the CHP unit. The surplus heat and electricity after internal uses (for pumps, mixers, compressors, *etc.*) is then sold for commercial purposes.

7.3.2.2. Results and discussion

The amounts of biogas and digestate derived from the AD of food waste for different years are shown in Table 7.13.

Table 7.13 Biogas generated, gas lost and digestate from food waste in years

Contents	Unit	2015	2020	2025
Food waste	tonnes day^{-1}	21420	22260	49920
Gas generated	tonnes day^{-1}	5858	6088	13654
Biogas available	tonnes day^{-1}	4221	4397	9853
Digestate	tonnes day^{-1}	15561	16171	36265

As can be seen from Table 7.13 the biogas generated in 2025 is about 9850 tonnes day^{-1} which is two times greater than in 2015.

Results from running scenario 1 (Table 7.14) show that energy in the form of heat produced from the CHP unit is about two times greater than the electricity generated. This reflects the fact that the efficiency of heat from CHP units is about 65% whereas in electric power it is around 35–43% (Verougstraete *et al.*, 1985; Weiland, 2010; Spellman, 2013).

From these figures electricity generated that can be sent to the grid could contribute between 2.4% to 4.1% of the total electricity demand in Vietnam in

2015 and 2025, respectively. The heat produced can also be used for heating/cooling in buildings (Deng *et al.*, 2011; Choudhury *et al.*, 2013) or other industrial purposes in urban areas.

Table 7.14 Scenario 1: Energy potential in the form of heat and electricity

Contents	Unit	2015		2020		2025	
Ambient temp.		Winter	Summer	Winter	Summer	Winter	Summer
Heat and electricity for off–site use							
Heat	GWh	12.6	13.0	13.1	13.5	28.2	29.0
Electricity	GWh	6.85	6.85	7.10	7.10	14.8	14.8
Annual electricity demands of VN(*)	GWh	241		301		360	

Note: (*) adapted from World Bank (2012)

In the second scenario (Table 7.15), upgraded biogas with a methane content of over 97% (clean gas) can be used as fuel for trucks, buses, *etc.* According to Vietnam's national energy development strategy (2007), it is estimated that the fuel requirement for transportation in 2020 will be 23 million tonnes, increasing to around 30 million tonnes in 2025. Assuming 1 kg fuel (diesel) is equal to 11.5 kWh (Denny, 2013) then upgraded biogas can replace about 2.2% and 4.75% of anticipated daily fuel use for transportation in 2020 and 2025, respectively.

Table 7.15 Scenario 2: Energy potential in the form of upgraded biogas

Contents	**Unit**	**2015**		**2020**		**2025**	
Ambient temp.		Winter	Summer	Winter	Summer	Winter	Summer
Heat and electricity for off–site uses							
Heat	GWh	3.06	3.74	3.23	3.90	7.50	9.09
Energy potential of upgraded biogas	GWh	16.03	16.11	16.85	16.74	37.33	37.36

Because of the high average ambient temperature, the heat requirements for internal uses such as for heating the digester, pasteurising *etc.* are small compared to those in cooler climates (Deublein & Steinhauser, 2008a; Smyth *et al.*, 2009; Pertl *et al.*, 2010). Therefore, use of the surplus biogas for on–site

electricity generation in a CHP plant will produce a large amount of surplus heat. This is potenitally available for export but it is notoriously difficult to find economic uses for it, especially in warm climates where there is little or no demand for domestic heating. Waste heat can, however, be used for cooling and industrial purposes and work on development of these areas is important to ensure effective use of the renewable energy.

The embodied energy in the biogas plants was not included in this study, as it is normally quite small relative to the net energy flows in the operation of the plant (Berglund & Borjesson, 2006). Future work could include the embodied energy, specifically for Vietnam, to give a more comprehensive overall energy balance.

7.3.3 Conclusions from energy balance modelling for food waste in Vietnam

Results from running scenarios in an energy balance model based on Aspen Plus show that if the food waste in the MSW stream from cities in Vietnam could be separated, it could be a significant source of energy in the form of heat, electricity or biofuel. This can potentially be achieved in the future through encouraging changes in people's behaviour and enforcement of environmental laws. The total surplus exportable energy generated from biogas plants working at standard conditions each day in any form of heat, electricity or purified gas, after allowing for plant operating demand is about 19 GWh, 20 GWh and 45 GWh in 2015, 2020 and 2025, respectively.

Results from modelling show that when food waste is separated from the MSW stream and sent to AD plants, it could contribute between 2.4% to 4.1% of the electricity demand of Vietnam, with about two times this energy also in the form of heat. Alternatively, upgrading this biogas could contribute approximately 2.2% to 4.7% of fuel consumption for transportation. This suggests AD is a promising method to treat MSW in cities, especially when considering the problematic aspects of other waste disposal methods such as: landfilling, composting and incineration.

If the organic waste component in the MSW stream of cities in Vietnam could be separated, then AD offers a source of energy generation with many economic benefits. This could provide a contribution towards dealing with the dramatic increases in costs associated with energy supply, waste disposal, space for landfilling and the increasing public concerns with environmental issues.

7.4 Conclusions from case study modelling

Three case studies were conducted to point out possible applications of the developed energy model and its sub–models. The first case study tested the ability and flexibility of the core developed ADM1 model in digestion of SBP. Comparisons between measured and simulated data under four different organic loading rates were made. Results showed that although the ADM1 is a good platform for modelling adequately the anaerobic digestion of SBP, some extra work is needed to overcome the models shortcomings associated with high OLR and foaming issues.

The second case study aimed to answer some questions relating to energy and mass balance aspects before building an AD plant for fuel–grade methane production, by using the energy model integrated with the steady state digester based on a stoichiometric approach. A number of scenarios were carried out under different conditions including ambient temperature, digestion temperature, total input food waste, *etc.* Simulation results indicated that the model is capable of sizing CHP and direct heating units in an anaerobic digestion plant for fuel–grade methane production. It also allows prediction of energy consumption of biogas plant components during the upgrading process, and of likely methane losses.

The third case study was applied to Vietnam to deal with a real problem arising in the management of solid wastes in urban areas: how much energy can be gained from food waste digestion if all food waste from urban areas in Vietnam is collected, classified and digested in the next ten years? The energy model integrated with the modified ADM1 model was used. The results showed total exportable energy from biogas plants in 2015, 2020 and 2025 in the forms of heat, electricity and fuel could be: about 19 GWh, 20 GWh and 45 GWh in 2015, 2020 and 2025. The simulation outputs suggest AD is a promising method to treat MSW in cities in Vietnam as an alternative option besides other waste disposal methods currently applied such as landfilling, composting and incineration.

This page is intentionally left blank

Chapter 8

Conclusions and further work

This chapter draws together the main conclusions and contributions of the whole study and proposes further work.

8.1 Conclusions

Within the general area of modelling, there has been no existing adequate tool for prediction of the behaviour of food waste digesters nor of the mass and energy balance of food waste digestion systems. This work, hence, carried out a number of tasks to produce an integrated modelling platform in which an anaerobic digestion process can be linked to other units of a biogas plant for accurate mass and energy balances. All the objectives of the research were accomplished and the outcomes are briefly presented as below.

8.1.1 General achievements

In order accurately to simulate food waste digestion, three important issues were considered and successfully implemented in this work using the well–known ADM1 platform: firstly, the acetate oxidation route for methanogenesis, which largely replaces the conventional acetoclastic pathway under elevated TAN concentrations, was implemented; secondly, the role of trace elements in nurturing stability during the digestion process was modelled; and finally, an option for the removal of ammonia from digestate was added to provide useful guidance for research on and operation of food waste digesters.

The extended version of ADM1 was integrated with Aspen Plus, which performs rigorous mass and energy balance calculations using detailed models of equipment, to determine the flow rates, composition and energy flows for all streams involved in the process. In addition, a simple steady state digester based on a stoichiometric approach was built in Aspen Plus to provide an alternative option for verification in terms of biogas production compared to the dynamic ADM1 model. This also allows for rapid sizing of the elements of a biogas plant without any concerns over the difficulties in identifying dynamic and kinetic parameters for ADM1.

Ammonia removal from digestate was also included in the generic model of ADM1 and Aspen Plus, with the aim of keeping a suitable concentration of ammonia in the digester to maintain the stability of the anaerobic treatment process.

Finally, the improved digester model was integrated with Aspen Plus to simulate a biogas plant in which water scrubbing is used to model the biogas upgrading.

8.1.2 Specific contributions

The contributions of this work are specified explicitly as below:

1. Development and delivery of a platform (MATLAB/Simulink® and Excel) of the ADM1 model for a CSTR system, which is flexible and adjustable and could also be applied to the anaerobic digestion of other types of organic substrates. Suggestion of optimised stoichiometric and kinetic parameters such as hydrolysis rate, inhibition factors, *etc.* for simulation of the anaerobic digestion of food waste and sugar beet pulp using ADM1.
2. Evaluation of the suitability of the ADM1 model to represent food waste digestion, with the conclusion that the original ADM1 is not able to describe the digestion of food waste at elevated ammonia concentrations without any modifications.
3. Modifications of the original ADM1 model to include the syntrophic acetate oxidation pathway with the revised program codes. Recommendation of a set of kinetic parameters for simulation of acetate oxidation pathway in ADM1 in parallel with the conventional acetoclastic pathway. A clear demonstration that with the dominance of the acetate oxidation pathway, the contribution of the conventional acetoclastic pathway to methane formation is about 5%.
4. Establishment of a biogas system in Aspen Plus which integrates the modified ADM1 model for accurate simulation of biogas plant operations in terms of mass and energy balance.
5. Establishment of an ammonia stripping model in Aspen Plus which integrates the modified ADM1 model and the Aspen Simulation Workbook (ASW) to allow optimisation/control of the ammonia concentration in food waste digesters.
6. A first attempt at introducing new inhibition factors for propionic, butyric and valeric degradation ($I_{te,c4}$, $I_{te,pro}$) to represent system failure without trace elements addition.
7. Specification of an adjustment factor (a_f) to the ADM1 model for accurate estimation concentration of solid compounds. This value for '*typical*' food waste substrate is about 1.2.
8. A value of the convective heat transfer coefficient of the air–gap in the digester roof of 1 W m^{-2} K^{-1}, which has been neglected in previous studies, was proposed for more accurate heat loss calculation.

8.2 Further work

Specific further research arising from this work can be identified as below:

- To optimise the stoichiometric and kinetic parameters to enable the modelling of a wider range of feedstocks.
- To carry out experimental work or update information from the literature on stoichiometric and kinetic parameters, for more accurate prediction such as inhibition factors, yield uptake components, decay rates, etc.
- To further develop the ADM1 model to permit effective modelling of low temperature systems by determining the appropriate kinetic coefficients and input parameters.
- To modify the developed ADM1 model to simulate a digester under unstable loading rates. This can reflect reality since it is often difficult to maintain stable inputs to a digester (due to changes in waste characteristics, loading, *etc.*). This could subsequently be useful for control purposes.
- To extend ADM1 to include other processes and components that are currently omitted from the model to make it more precise such as heterogeneity, bioflocs, H_2S, *etc.*
- To modify the MATLAB code of the extended version to represent transient switches when introducing trace elements instead of the prompt switches of the current model. This would include experimental work or an update of knowledge from the literature to identify specific points controlling the switches between the two pathways of methanogenesis.
- To implement the ADM1 model with use of the Aspen Custom Modeler (ACM) or Excel to make it an easy and flexible '*block*' for integrating with the energy balance platform in Aspen Plus.
- To reform the biogas upgrading system to allow a wider choice of methods such as single stage water scrubbing, pressure adsorption, chemical absorption, *etc.*
- To extend the Aspen Plus platform to include the digestate dewatering process for further quantification by–product streams and nutrient balances of a biogas plant.
- To adapt the current ammonia removal tool to provide more options for users to choose appropriate methods such as post digestion ammonia removal, in situ ammonia removal. To carry out experimental work or an

updated investigation from literature for kinetic parameters of ammonia removal under different conditions such as temperature, pH, organic loading rates, *etc.* to improve capabilities and accuracy of the current ammonia removal model.

This page is intentionally left blank

References

Abatzoglou, N. & Boivin, S. (2009) A review of biogas purification processes. *Biofuels, Bioproducts and Biorefining,* **3**, 42-71.

Abbasi, T., Tauseef, S. M. & Abbasi, S. A. (2012) *Biogas energy*. Springer, New York, NY.

Ahring, B. (1995) Methanogenesis in thermophilic biogas reactors. *Antonie van Leeuwenhoek,* **67**, 91-102.

Ali, I. & Basit, M. (1993) Significance of hydrogen content in fuel combustion. *International journal of hydrogen energy,* **18**, 1009-1011.

Amon, T., Amon, B., Kryvoruchko, V., Bodiroza, V., Pötsch, E. & Zollitsch, W. (2006) Optimising methane yield from anaerobic digestion of manure: Effects of dairy systems and of glycerine supplementation. *International Congress Series,* **1293**, 217-220.

Amon, T., Amon, B., Kryvoruchko, V., Machmüller, A., Hopfner-Sixt, K., Bodiroza, V., *et al.* (2007) Methane production through anaerobic digestion of various energy crops grown in sustainable crop rotations. *Bioresource Technology,* **98**, 3204-3212.

Anderson, G., Sallisp, P. & Uyanik, S. (2003) Anaerobic treatment processes. In *Handbook of Water and Wastewater Microbiology*, pp. 391-426. Academic Press, London; San Diego.

Anderson, G. & Yang, G. (1992) pH control in anaerobic treatment of industrial wastewater. *Journal of environmental engineering,* **118**, 551-567.

Andersson, K. & Johnsson, F. (2006) Process evaluation of an 865MWe lignite fired O2/CO2 power plant. *Energy Conversion and Management,* **47**, 3487-3498.

Andrews, J. F. (1974) Dynamic models and control strategies for wastewater treatment processes. *Water Research,* **8**, 261-289.

Angelidaki, I. & Ahring, B. (1992) Effects of free long-chain fatty acids on thermophilic anaerobic digestion. *Applied Microbiology and Biotechnology,* **37**, 808-812.

Angelidaki, I. & Ahring, B. (1993) Thermophilic anaerobic digestion of livestock waste: the effect of ammonia. *Applied Microbiology and Biotechnology,* **38**, 560-564.

Angelidaki, I., Ellegaard, L. & Ahring, B. (1993) A mathematical model for dynamic simulation of anaerobic digestion of complex substrates: focusing on ammonia inhibition. *Biotechnol Bioeng,* **42**, 159-166.

Angelidaki, I., Ellegaard, L. & Ahring, B. (1999) A comprehensive model of anaerobic bioconversion of complex substrates to biogas. *Biotechnology and Bioengineering,* **63**, 363-372.

Angelidaki, I., Ellegaard, L. & Ahring, B. (2003) Applications of the anaerobic digestion process. In *Biomethanation II*, pp. 1-33. Springer.

Angelidaki, I. & Sanders, W. (2004) Assessment of the anaerobic biodegradability of macropollutants. *Re/Views in Environmental Science & Bio/Technology,* **3**, 117-129.

Angenent, L. & Scott, N. (2010) Practical Aspects of Methane Production from Agricultural Wastes. In *Biofuels from Agricultural Wastes and Byproducts*, pp. 39-66.

Angenent, L., Sung, S. & Raskin, L. (2002) Methanogenic population dynamics during startup of a full-scale anaerobic sequencing batch reactor treating swine waste. *Water Research,* **36**, 4648-4654.

Antonelli, R. & Astolfi, A. (2003) Continuous stirred tank reactors: easy to stabilise? *Automatica,* **39**, 1817-1827.

Appels, L., Baeyens, J., Degreve, J. & Dewil, R. (2008) Principles and potential of the anaerobic digestion of waste-activated sludge. *Progress in Energy and Combustion Science,* **34**, 755-781.

Appels, L., Lauwers, J., Degreve, J., Helsen, L., Lievens, B., Willems, K.*, et al.* (2011) Anaerobic digestion in global bio-energy production: Potential and research challenges. *Renewable and Sustainable Energy Reviews,* **15**, 4295-4301.

Ash, M., Organisation for Economic, C.-o. & Development. (2010) *Taxation, innovation and the environment*. OECD, Paris.

Aspen Technology, I. (2001) *Aspen Plus 11.1 Unit Operation Models*. Aspen Technology, Inc., Cambridge, USA.

AspenTech. (2011) Aspen Plus V7.3; Aspen Technology, Inc., Burlington, MA.

Astals, S., Ariso, M., Gali, A. & Mata-Alvarez, J. (2011) Co-digestion of pig manure and glycerine: experimental and modelling study. *Journal of environmental management,* **92**, 1091-1096.

Badenes, S., Ferreira, F. & Cabral, J. (2013) Membrane Bioreactors for Biofuel Production. In *Separation and Purification Technologies in Biorefineries* (ed. by S. Ramaswamy, H. Huang & B. Ramarao), pp. 377-407.

Baker, R. W. & Lokhandwala, K. (2008) Natural gas processing with membranes: An overview. *Industrial & Engineering Chemistry Research,* **47**, 2109-2121.

Banks, C., Bolzonella, D., Zhang, Y., Jiang, Y. & Cavinato, C. (2013) Description of problems associated with ammonia toxicity and trace metal deficiency in mesophilic and thermophilic digestion of high

nitrogen wastes (VALORGAS Project: Deviverable D4.1). University of Southampton, 48 pp.

Banks, C., Chesshire, M., Heaven, S. & Arnold, R. (2011) Anaerobic digestion of source-segregated domestic food waste: Performance assessment by mass and energy balance. *Bioresource Technology,* **102**, 612-620.

Banks, C., Chesshire, M. & Stringfellow, A. (2008) A pilot-scale comparison of mesophilic and thermophilic digestion of source segregated domestic food waste. *Water Science and Technology,* **58**, 1475-1481.

Banks, C., Salter, A., Heaven, S. & Riley, K. (2011) Energetic and environmental benefits of co-digestion of food waste and cattle slurry: A preliminary assessment. *Resources Conservation and Recycling,* **56**, 71-79.

Banks, C. & Zhang, Y. (2010) Technical Report: Optimising inputs and outputs from anaerobic digestion processes. Defra Project Code WR0212. 2010.

Banks, C., Zhang, Y., Jiang, Y. & Heaven, S. (2012) Trace element requirements for stable food waste digestion at elevated ammonia concentrations. *Bioresource Technology,* **104**, 127-135.

Barggman, R. (1996) Anaerobic sludge digestion-MOP 16. *J Water Pollut Control Fed,* **38**, 717-721.

Barker, D. & Stuckey, D. (2001) Modeling of soluble microbial products in anaerobic digestion: The effect of feed strength and composition. *Water environment research,* **73**, 173-184.

Barker, H. (1936) On the biochemistry of the methane fermentation. *Archiv für Mikrobiologie,* **7**, 404-419.

Barsukov, I. V. (2006) *New carbon based materials for electrochemical energy storage systems : batteries, supercapacitors and fuel cells*. Springer, Dordrecht.

Basu, S., Khan, A. L., Cano-Odena, A., Liu, C. & Vankelecom, I. F. J. (2010) Membrane-based technologies for biogas separations. *Chemical Society Reviews,* **39**, 750-768.

Batstone, D. & Keller, J. (2003) Industrial applications of the IWA anaerobic digestion model No. 1 (ADM1). *Water Science & Technology,* **47**, 199-206.

Batstone, D. & Keller, J. (2006) Anaerobic Digestion Model No 1 - Developments and applications - Selected Papers from the 1(st) International Workshop on the IWA Anaerobic Digestion Model No 1 (ADM1), held in Lyngby, Copenhagen, Denmark, 4-6 September 2005 - Preface. *Water Science and Technology,* **54**, Vii-Vii.

Batstone, D., Keller, J., Angelidaki, I., Kalyuzhnyi, S., Pavlostathis, S., Rozzi, A., *et al.* (2002) *Anaerobic digestion model No. 1 (ADM1). Scientific and Technical report*. International Water Association, London.

Batstone, D., Keller, J. & Steyer, J. (2006) A review of ADM1 extensions, applications, and analysis: 2002-2005. *Water Science and Technology,* **54**, 1-10.

Bauer, F., Hulteberg, C., Persson, T. & Tamm, D. (2013) Biogas upgrading-Review of commercial technologies.

Beam, R. G. (2011) Enhanced biogas production through the optimization of the anaerobic digestion of sewage sludge. The University of Alabama TUSCALOOSA.

Benz, G. (2011) Agitator Design Principles for Pharmaceutical and Biotechnology Applications, Benz Technology International, Inc.

Berglund, M. & Borjesson, P. (2006) Assessment of energy performance in the life-cycle of biogas production. *Biomass and Bioenergy,* **30**, 254-266.

Bjorklund, A. (2000) Environmental System Analysis of Waste Management: Experiences from Applications of the ORWARE Model.

Bjorklund, A., Dalemo, M. & Sonesson, U. (1999) Evaluating a municipal waste management plan using orware. *Journal of Cleaner Production,* **7**, 271-280.

Bjornsson, L. (2000) Intensification of the biogas process by improved process monitoring and biomass retention. [Univ.-bibl.] ;, Lund.

Blumensaat, F. & Keller, J. (2005) Modelling of two-stage anaerobic digestion using the IWA Anaerobic Digestion Model No. 1 (ADM1). *Water Research,* **39**, 171-183.

Bodalo, A., Gomez, J. L., Gomez, E., Leόn, G. & Tejera, M. (2005) Ammonium removal from aqueous solutions by reverse osmosis using cellulose acetate membranes. *Desalination,* **184**, 149-155.

Bogle, I. D. L. & Cameron, D. (2002) CAPE Tools for Off-line Simulation, Design and Analysis. *Computer Aided Chemical Engineering,* **11**, 373-392.

Bonmati, A. & Flotats, X. (2003) Air stripping of ammonia from pig slurry: characterisation and feasibility as a pre-or post-treatment to mesophilic anaerobic digestion. *Waste Management,* **23**, 261-272.

Boone, D. R., Johnson, R. L. & Liu, Y. (1989) Diffusion of the interspecies electron carriers H2 and formate in methanogenic ecosystems and its implications in the measurement of Km for H2 or formate uptake. *Applied and Environmental Microbiology,* **55**, 1735-1741.

Borja, R., Sanchez, E. & Weiland, P. (1996) Influence of ammonia concentration on thermophilic anaerobic digestion of cattle manure in

upflow anaerobic sludge blanket (UASB) reactors. *Process Biochemistry,* **31**, 477-483.

Borole, A., Klasson, K., Ridenour, W., Holland, J., Karim, K. & Al-Dahhan, M. (2006) Methane production in a 100-L upflow bioreactor by anaerobic digestion of farm waste. In *Proceedings of the Twenty-Seventh Symposium on Biotechnology for Fuels and Chemicals*, pp. 887-896. Springer.

Boubaker, F. & Ridha, B. (2008) Modelling of the mesophilic anaerobic co-digestion of olive mill wastewater with olive mill solid waste using anaerobic digestion model No. 1 (ADM1). *Bioresource Technology,* **99**, 6565-6577.

Breeze, P. (2005) *Power generation technologies*. Newnes.

Breverton, T. (2012) *Breverton's encyclopedia of inventions : a compendium of technological leaps, groundbreaking discoveries and scientific breakthroughs that changed the world*. Quercus, London.

Bryers, J. (1985) Structured modeling of the anaerobic digestion of biomass particulates. *Biotechnology and bioengineering,* **27**, 638-649.

Burton, C. H. & Turner, C. (2003) *Manure management: treatment strategies for sustainable agriculture*. Silsoe Research Inst., Silsoe.

Busch, G. (2013) Biogas Technology. In *Bioprocessing technologies in biorefinery for sustainable production of fuels, chemicals, and polymers* (ed. by S.-T. Yang, H. Enshasy & N. Thongchul), pp. 279-292. Wiley ; AIChE, Hoboken, N. J.; [New York].

Byrne, K. (1997) *Environmental science*. Nelson, Walton-On-Thames.

Calli, B., Mertoglu, B. & Inanc, B. (2005) Landfill leachate management in Istanbul: applications and alternatives. *Chemosphere,* **59**, 819-829.

Cecchi, F., Traverso, P., Pavan, P., Bolzonella, D. & Innocenti, L. (2003) Characteristics of the OFMSW and Behavior of the Anaerobic Digestion Process. *ChemInform,* **34**, no-no.

Cengel, Y. & Boles, M. (2011) *Thermodynamics: an engineering approach (7th edition)*. McGraw-Hill New York.

Chae, K., Jang, A., Yim, S. & Kim, I. (2008) The effects of digestion temperature and temperature shock on the biogas yields from the mesophilic anaerobic digestion of swine manure. *Bioresour Technol,* **99**, 1-6.

Chemstations. (2011) *CHEMCAD Version 6 : User manual*. Chemstations, Inc. .

Chen, Y., Cheng, J. & Creamer, K. (2008) Inhibition of anaerobic digestion process: A review. *Bioresource technology,* **99**, 4044-4064.

Chen, Y., Jiang, S., Yuan, H., Zhou, Q. & Gu, G. (2007) Hydrolysis and acidification of waste activated sludge at different pHs. *Water Research,* **41**, 683-689.

Cheremisinoff, N. P. (2000) *Handbook of chemical processing equipment*. Butterworth-Heinemann, Boston.

Cheung, K., Chu, L. & Wong, M. (1997) Ammonia stripping as a pretreatment for landfill leachate. *Water, Air, & Soil Pollution,* **94**, 209-221.

Cho, J., Park, S. & Chang, H. (1995) Biochemical methane potential and solid state anaerobic digestion of Korean food wastes. *Bioresource Technology,* **52**, 245-253.

Choudhury, B., Saha, B., Chatterjee, P. & Sarkar, J. (2013) An overview of developments in adsorption refrigeration systems towards a sustainable way of cooling. *Applied Energy,* **104**, 554-567.

Christ, O., Wilderer, P. & Faulstich, M. (2000) Mathematical modeling of the hydrolysis of anaerobic processes. *Water Science and Technology,* **41**, 61-65.

Chu, C., Li, Y., Xu, K., Ebie, Y., Inamori, Y. & Kong, H. (2008) A pH-and temperature-phased two-stage process for hydrogen and methane production from food waste. *international journal of hydrogen energy,* **33**, 4739-4746.

Chynoweth, D. P., Owens, J. M. & Legrand, R. (2001) Renewable methane from anaerobic digestion of biomass. *Renewable energy,* **22**, 1-8.

Cimini, S., Prisciandaro, M. & Barba, D. (2005) Simulation of a waste incineration process with flue-gas cleaning and heat recovery sections using Aspen Plus. *Waste Management,* **25**, 171-175.

Clark, G., Rossiter, D. & Chung, P. (2000) Intelligent Modelling Interface for Dynamic Process Simulators. *Chemical Engineering Research and Design,* **78**, 823-839.

Climenhaga, A. & Banks, C. (2008) Anaerobic digestion of catering wastes: effect of micronutrients and retention time. *Water Science & Technology,* **57**.

Coker, A. K. L. E. E. (2010) *Ludwig's applied process design for chemical and petrochemical plants. Volume 2 Volume 2*. Elsevier Gulf Professional Pub., Amsterdam; Boston.

COM, E. C. (2010) Communication from the Commission to the Council and the European Parliament on future steps in bio-waste management in the European Union. Brussels, 12 pp.

Conly, H. (2011) Using DDGS as a Feedstock for Bioenergy via Anaerobic Digestion. In *Distillers Grains*, pp. 465-474. AOCS Publishing.

Copp, J. B., Jeppsson, U. & Rosen, C. (2003) Towards an ASM1–ADM1 state variable interface for plant-wide wastewater treatment modeling. *Proceedings of the Water Environment Federation,* **2003**, 498-510.

Cormos, C. C., Imre-Lucaci, A., Cormos, A. M., Tasnadi-Asztalos, Z. & Lazar, M. D. (2013) Conceptual design of hydrogen production process from bioethanol reforming. *COMPUTER AIDED CHEMICAL ENGINEERING*, 19-24.

Cosoli, P., Ferrone, M., Pricl, S. & Fermeglia, M. (2008) Hydrogen sulphide removal from biogas by zeolite adsorption: Part I. GCMC molecular simulations. *Chemical Engineering Journal,* **145**, 86-92.

Costello, D. J., Greenfield, P. F. & Lee, P. L. (1991) Dynamic Modeling of a Single-Stage High-Rate Anaerobic Reactor .1. Model Derivation. *Water Research,* **25**, 847-858.

Cumiskey, A., Harrison, D., Dawson, M. & Jolly, M. (2003) Effective design of gas-mixing systems for thick sludge digestion: Two case studies. *Journal of the Chartered Institution of Water and Environmental Management,* **17**, 29-33.

Curry, N. & Pillay, P. (2012) Biogas prediction and design of a food waste to energy system for the urban environment. *Renewable Energy,* **41**, 200-209.

da Rosa, A. (2012) *Fundamentals of Renewable Energy Processes*. Elsevier Science.

Dalemo, M. (1999) Environmental systems analysis of organic waste management : the ORWARE model and the sewage plant and anaerobic digestion submodels. Swedish University of Agricultural Sciences, Uppsala.

Dalemo, M., Sonesson, U., Bjorklund, A., Mingarini, K., Frostell, B., Jonsson, H.*, et al.* (1997) ORWARE - A simulation model for organic waste handling systems .1. Model description. *Resources Conservation and Recycling,* **21**, 17-37.

Dalemo, M., Sonesson, U., Jonsson, H. & Bjorklund, A. (1998) Effects of including nitrogen emissions from soil in environmental systems analysis of waste management strategies. *Resources Conservation and Recycling,* **24**, 363-381.

Dawson, B. & Spannagle, M. (2009) *The complete guide to climate change*. Routledge, London; New York.

DEFRA. (2010) Accelerating the Uptake of Anaerobic Digestion in England: an Implementation Plan. London.

DEFRA. (2011) Government Review of Waste Policy in England 2011. London.

Demirel, B. & Scherer, P. (2008) The roles of acetotrophic and hydrogenotrophic methanogens during anaerobic conversion of biomass to methane: a review. *Reviews in Environmental Science and Bio/Technology,* **7**, 173-190.

Demirel, B., Scherer, P., Yenigun, O. & Onay, T. (2010) Production of Methane and Hydrogen from Biomass through Conventional and High-Rate Anaerobic Digestion Processes. *Critical Reviews in Environmental Science and Technology,* **40**, 116-146.

Deng, J., Wang, R. & Han, G. (2011) A review of thermally activated cooling technologies for combined cooling, heating and power systems. *Progress in Energy and Combustion Science,* **37**, 172-203.

Deng, L.-W., Zheng, P. & Chen, Z.-A. (2006) Anaerobic digestion and post-treatment of swine wastewater using IC–SBR process with bypass of raw wastewater. *Process Biochemistry,* **41**, 965-969.

Denny, M. (2013) *Lights On!: The Science of Power Generation*. JHU Press.

Derbal, K., Bencheikh-Iehocine, M., Cecchi, F., Meniai, A. H. & Pavan, P. (2009) Application of the IWA ADM1 model to simulate anaerobic co-digestion of organic waste with waste activated sludge in mesophilic condition. *Bioresource Technology,* **100**, 1539-1543.

Descoins, N., Deleris, S., Lestienne, R., Trouve, E. & Marechal, F. (2012) Energy efficiency in waste water treatments plants: Optimization of activated sludge process coupled with anaerobic digestion. *Energy,* **41**, 153-164.

Deublein, D. & Steinhauser, A. (2008a) *Biogas from waste and renewable resources : an introduction*. Wiley-VCH, Weinheim [Germany].

Deublein, D. & Steinhauser, A. (2008b) Utilization of biogas for the generation of electric power and heat. In *Biogas from waste and renewable resources: an introduction*, pp. 361-388. John Wiley & Sons.

Deublein, D. & Steinhauser, A. (2011) Substrates and biogas. In *Biogas from Waste and Renewable Resources: An Introduction*. John Wiley & Sons.

Deutsche, G. f. S. & Ecofys. (2005) *Planning and installing bioenergy systems a guide for installers, architects, and engineers*. Earthscan, Sterling, VA.

Dewil, R., Appels, L. & Baeyens, J. (2006) Energy use of biogas hampered by the presence of siloxanes. *Energy Conversion and Management,* **47**, 1711-1722.

Dewil, R., Appels, L., Baeyens, J., Buczynska, A. & Van Vaeck, L. (2007) The analysis of volatile siloxanes in waste activated sludge. *Talanta,* **74**, 14-19.

Donoso-Bravo, A., Mailier, J., Martin, C., Rodriguez, J., Aceves-Lara, C. & Wouwer, A. (2011) Model selection, identification and validation in anaerobic digestion: A review. *Water Res,* **45**, 5347-5364.

Doran, P. M. (1995) *Bioprocess engineering principles*. Academic Press, San Diego.

Eastman, J. A. & Ferguson, J. F. (1981) Solubilization of particulate organic carbon during the acid phase of anaerobic digestion. *Journal (Water Pollution Control Federation)*, 352-366.

Edelmann, W., Schleiss, K. & Joss, A. (2000) Ecological, energetic and economic comparison of anaerobic digestion with different competing technologies to treat biogenic wastes. *Water Science & Technology,* **41**, 263-273.

El-Mashad, H. & Zhang, R. (2010) Biogas production from co-digestion of dairy manure and food waste. *Bioresource Technology,* **101**, 4021-4028.

Elnekave, M., Tüfekçi, N., Kimchie, S. & Shelef, G. (2006) Tracing the mixing efficiency of a primary mesophilic anaerobic digester in a municipal wastewater treatment plant. In *Proceedings of the 13th International Symposium on Environmental Pollution and its Impact on Life in the Mediterranean Region (MESAEP), Thessaloniki, Greece, 8-12 October 2005.*, pp. 1098-1105. Parlar Scientific Publications.

EPA. (1979) *Process design manual for sludge treatment and disposal*. U.S. Environmental Protection Agency, Municipal Environmental Research Laboratory, Office of Research and Development, Center for Environmental Research Information, Technology Transfer, Cincinnati.

EPA. (1987) Anaerobic digester mixing systems. *Journal of Water Pollution Control Federation,* **59**.

Eriksson, O., Carlsson Reich, M., Frostell, B., Björklund, A., Assefa, G., Sundqvist, J.-O., *et al.* (2005) Municipal solid waste management from a systems perspective. *Journal of Cleaner Production,* **13**, 241-252.

Eriksson, O., Finnveden, G., Ekvall, T. & Björklund, A. (2007) Life cycle assessment of fuels for district heating: A comparison of waste incineration, biomass-and natural gas combustion. *Energy Policy,* **35**, 1346-1362.

Evans, G. (2001) Chapter 6. Anaerobic Digestion (AD). In *Biowaste and biological waste treatment*. James & James, London.

Facchin, V., Cavinato, C., Fatone, F., Pavan, P., Cecchi, F. & Bolzonella, D. (2012) Effect of trace element supplementation on the mesophilic anaerobic digestion of foodwaste in batch trials: the influence of inoculum origin. *Biochemical Engineering Journal*.

Fdez.-Guelfo, L., Alvarez-Gallego, C., Sales Marquez, D. & Romero Garcia, L. (2011) Dry-thermophilic anaerobic digestion of simulated organic fraction of Municipal Solid Waste: Process modeling. *Bioresource Technology,* **102**, 606-611.

Fedorovich, V., Lens, P. & Kalyuzhnyi, S. (2003) Extension of Enaerobic Digestion Model No. 1 with processes of sulfate reduction. *Applied biochemistry and biotechnology,* **109**, 33-45.

Feng, L., Wang, H. P., Chen, Y. & Wang, Q. (2009) Effect of solids retention time and temperature on waste activated sludge hydrolysis and short-chain fatty acids accumulation under alkaline conditions in continuous-flow reactors. *Bioresource technology,* **100**, 44-49.

Feng, X., Karlsson, A., Svensson, B. & Bertilsson, S. (2010) Impact of trace element addition on biogas production from food industrial waste–linking process to microbial communities. *FEMS microbiology ecology,* **74**, 226-240.

Feng, Y., Behrendt, J., Wendland, C. & Otterpohl, R. (2006) Parameter analysis of the IWA Anaerobic Digestion Model No. 1 for the anaerobic digestion of blackwater with kitchen refuse. *Water Science and Technology,* **54**, 139-147.

Fernandez, B., Porrier, P. & Chamy, R. (2001) Effect of inoculum-substrate ratio on the start-up of solid waste anaerobic digesters. *Water Science & Technology,* **44**, 103-108.

Fezzani, B. & Cheikh, R. (2008) Implementation of IWA anaerobic digestion model No. 1 (ADM1) for simulating the thermophilic anaerobic co-digestion of olive mill wastewater with olive mill solid waste in a semi-continuous tubular digester. *Chemical Engineering Journal,* **141**, 75-88.

Fezzani, B. & Cheikh, R. (2009) Extension of the anaerobic digestion model No. 1 (ADM1) to include phenolic compounds biodegradation processes for the simulation of anaerobic co-digestion of olive mill wastes at thermophilic temperature. *Journal of Hazardous Materials,* **162**, 1563-1570.

Finnveden, G., Johansson, J., Lind, P. & Moberg, Å. (2005) Life cycle assessment of energy from solid waste—part 1: general methodology and results. *Journal of Cleaner Production,* **13**, 213-229.

Fischer, M. (2010) *Biogas purification H2S removal using biofiltration*. University of Waterloo, Waterloo, Ont.

Flora, J. R. V., McAnally, A. S. & Petrides, D. (1998) Treatment plant instructional modules based on SuperPro Designerff v.2.7. *Environmental Modelling & Software,* **14**, 69-80.

Ford, A. (2010) *Modeling the environment*. Island Press, Washington, DC.

Francis, J. (2008) *Philosophy of mathematics*. Global Vision Pub. House, New Delhi, India.

Freudenthal, K., Koglatis, J., Otterpohl, R. & Behrendt, J. (2005) Prediction of sulfide formation in sewer pressure mains based on the IWA Anaerobic Digestion Model No. 1 (ADM1). *Water Sci Technol,* **52**, 13-22.

Fricke, K., Santen, H., Wallmann, R., Huttner, A. & Dichtl, N. (2007) Operating problems in anaerobic digestion plants resulting from nitrogen in MSW. *Waste management,* **27**, 30-43.

Fuentes, M., Aguirre, P. A. & Scenna, N. J. (2013) Optimization of bio-hydrogen production and C-N removal in combined anaerobic-aerobic systems. *COMPUTER AIDED CHEMICAL ENGINEERING*, 793-798.

Fujishima, S., Miyahara, T. & Noike, T. (2000) Effect of moisture content on anaerobic digestion of dewatered sludge: ammonia inhibition to carbohydrate removal and methane production. *Water science and technology : a journal of the International Association on Water Pollution Research,* **41**, 119-127.

Fulford, D. (1988) *Running a biogas programme : a handbook*. Intermediate Technology Publications, London.

Gadre, R. V. (1989) Removal of hydrogen sulfide from biogas by chemoautotrophic fixed-film bioreactor. *Biotechnol Bioeng,* **34**, 410-414.

Gali, A., Benabdallah, T., Astals, S. & Mata-Alvarez, J. (2009) Modified version of ADM1 model for agro-waste application. *Bioresource Technology,* **100**, 2783-2790.

Gallert, C., Bauer, S. & Winter, J. (1998) Effect of ammonia on the anaerobic degradation of protein by a mesophilic and thermophilic biowaste population. *Applied Microbiology and Biotechnology,* **50**, 495-501.

Garber, W. F. (1982) Operating Experience with Thermophilic Anaerobic-Digestion. *Journal Water Pollution Control Federation,* **54**, 1170-1175.

Garcia-Heras, J. (2003) Reactor sizing, process kinetics and modelling of anaerobic digestion of complex wastes. In *Biomethanization of the organic fraction of municipal solid wastes*, pp. 31-43.

Gavala, H., Angelidaki, I. & Ahring, B. (2003) Kinetics and Modeling of Anaerobic Digestion Process. In *Biomethanation I* (ed. by B. Ahring, I. Angelidaki, E. de Macario, H. Gavala, J. Hofman-Bang, A. Macario, S. Elferink, L. Raskin, A. Stams, P. Westermann & D. Zheng), pp. 57-93. Springer Berlin / Heidelberg.

Gavala, H., Skiadas, I., Bozinis, N. & Lyberatos, G. (1996) Anaerobic codigestion of agricultural industries' wastewaters. *Water Science and Technology,* **34**, 67-75.

Gawel, R. (2012) Design simulations for a biogas purification process using aqueous amine solutions. *Chemical Papers,* **66**, 1010-1018.

Geankoplis, C. J. (1993) *Transport processes and unit operations*. PTR Prentice Hall, Engelwood Cliffs, N.J.

Gerardi, M. H. (2003) The microbiology of anaerobic digesters. Wiley-Interscience, Hoboken, N.J.

Gernaey, K., Rosen, C. & Jeppsson, U. (2006) WWTP dynamic disturbance modelling - an essential module for long-term benchmarking development. *Water Science and Technology,* **53**, 225-234.

Ghanem, K. M., El-Refai, A. H. & El-Gazaerly, M. A. (1992) Methane production from beet pulp. *J. Resour. Convers. Recycl.,* **6**, 275.

Girault, R., Bridoux, G., Nauleau, F., Poullain, C., Buffet, J., Steyer, J. P., *et al.* (2012) A waste characterisation procedure for ADM1 implementation based on degradation kinetics. *Water Research,* **46**, 4099-4110.

Gosling, I. (2005) Process simulation and modeling for industrial bioprocessing: Tools and techniques. *Industrial Biotechnology Industrial Biotechnology,* **1**, 106-109.

Graef, S. P. & Andrews, J. F. (1973) Mathematical modeling and control of anaerobic digestion. In *Proceedings of the AICHE Symposium Series*, pp. 101-131.

Graef, S. P. & Andrews, J. F. (1974) Stability and Control of Anaerobic Digestion. *Journal Water Pollution Control Federation,* **46**, 666-683.

Gunnerson, C. G. & Stuckey, D. C. (1986) *Anaerobic digestion: Principles and practices for biogas systems*. World Bank.

Gupta, A., Flora, J. R., Sayles, G. D. & Suidan, M. T. (1994) Methanogenesis and sulfate reduction in chemostats—II. Model development and verification. *Water Research,* **28**, 795-803.

Gustin, S. & Marinsek-Logar, R. (2011) Effect of pH, temperature and air flow rate on the continuous ammonia stripping of the anaerobic digestion effluent. *Process Safety and Environmental Protection,* **89**, 61-66.

GWP. (2009) Decision No. 445/QD-TTg dated on April 7th, 2009 on orientations for the development of urban area system in Vietnam up to 2025. Vietnam Government Web Portal.

GWP. (2011) Decision No. 798/QD-TTg dated on May 25th, 2011 on "Approving the investment program for solid waste treatment for the 2011-2020". Vietnam Government Web Portal.

GWP. (2012) Decision No. 432/QD-TTg dated on April 12th, 2012 on "Approving the Vietnam Sustainable Development Strategy for the 2011-2020". Vietnam Government Web Portal.

Haas, M. J., McAloon, A. J., Yee, W. C. & Foglia, T. A. (2006) A process model to estimate biodiesel production costs. *Bioresource Technology,* **97**, 671-678.

Hagen, M. (2001) *Adding gas from biomass to the gas grid*. SGC.

Hagmann, M., Heimbrand, E. & Hentschel, P. (2002) Determination of Siloxanes in Biogas from Landfills and Sewage Treatment Plants. *SOFW JOURNAL,* **128**, 3-7.

Hakansson, A. (2006) Preventing microbial growth on pall-rings when upgrading biogas using absorption with water wash.

Hangos, K. M. & Cameron, I. T. (2001) *Process modelling and model analysis*. Academic Press, San Diego.

Hansen, K., Angelidaki, I. & Ahring, B. (1998) Anaerobic digestion of swine manure: inhibition by ammonia. *Water research,* **32**, 5-12.

Hansen, K., Angelidaki, I. & Ahring, B. (1999) Improving thermophilic anaerobic digestion of swine manure. *Water Research,* **33**, 1805-1810.

Hansen, T., Bhander, G., Christensen, T., Bruun, S. & Jensen, L. (2006) Life cycle modelling of environmental impacts of application of processed organic municipal solid waste on agricultural land (EASEWASTE). *Waste Manag Res,* **24**, 153-166.

Hao, L.-P., Lü, F., He, P.-J., Li, L. & Shao, L.-M. (2010) Predominant contribution of syntrophic acetate oxidation to thermophilic methane formation at high acetate concentrations. *Environmental science & technology,* **45**, 508-513.

Harper, S. R. & Pohland, F. G. (1986) Recent developments in hydrogen management during anaerobic biological wastewater treatment. *Biotechnology and bioengineering,* **28**, 585-602.

Hartmann, H. & Ahring, B. (2005) Anaerobic digestion of the organic fraction of municipal solid waste: influence of co-digestion with manure. *Water research,* **39**, 1543-1552.

Hattori, S. (2008) Syntrophic acetate-oxidizing microbes in methanogenic environments. *Microbes and environments / JSME,* **23**, 118-127.

Hayes, T., Isaacson, H., Pfeffer, J. & Liu, Y. (1990) In situ methane enrichment in anaerobic digestion. *Biotechnology and bioengineering,* **35**, 73-86.

He, P. J. (2010) Anaerobic digestion: An intriguing long history in China. *Waste management,* **30**, 549-550.

Heinzle, E. B. A. P. C. C. L. (2006) Development of sustainable bioprocesses modeling and assessment, pp. 145. John Wiley & Sons, Chichester, England; Hoboken, NJ.

Heyes, R. & Hall, R. (1981) Anaerobic digestion modelling-the role of H2. *Biotechnology Letters,* **3**, 431-436.

Hickey, R. F., Vanderwielen, J. & Switzenbaum, M. S. (1989) The effect of heavy metals on methane production and hydrogen and carbon

monoxide levels during batch anaerobic sludge digestion. *Water Research,* **23**, 207-218.

Higgins, B. T. & Kendall, A. (2012) Life cycle environmental and cost impacts of using an algal turf scrubber to treat dairy wastewater. *Journal of Industrial Ecology,* **16**, 436-447.

Hill, D. & Barth, C. (1977) A dynamic model for simulation of animal waste digestion. *Journal (Water Pollution Control Federation)*, 2129-2143.

Hoffmann, J., Rudra, S., Toor, S. S., Holm-Nielsen, J. B. & Rosendahl, L. A. (2013) Conceptual design of an integrated hydrothermal liquefaction and biogas plant for sustainable bioenergy production. *Bioresource Technology,* **129**, 402-410.

Holloway, M. D., Nwaoha, C. & Onyewuenyi, O. A. (2012) *Process plant equipment operation, control, and reliability*. Wiley, Hoboken, N.J.

Holm-Nielsen, J., Dahl, C. & Esbensen, K. (2006) Representative sampling for process analytical characterization of heterogeneous bioslurry systems—a reference study of sampling issues in PAT. *Chemometrics and intelligent laboratory systems,* **83**, 114-126.

Honeywell. (2011) UniSim Design Suite In *UniSim Design Suite*

Hori, T., Haruta, S., Ueno, Y., Ishii, M. & Igarashi, Y. (2006) Dynamic transition of a methanogenic population in response to the concentration of volatile fatty acids in a thermophilic anaerobic digester. *Applied and Environmental Microbiology,* **72**, 1623-1630.

Huete, E., De Gracia, M., Ayesa, E. & Garcia-Heras, J. (2006) ADM1-based methodology for the characterisation of the influent sludge in anaerobic reactors. *Water Science & Technology,* **54**, 157-166.

Hullu, J., Maassen, J., Van Meel, P., Shazad, S., Vaessen, J., Bini, L., *et al.* (2008) Comparing different biogas upgrading techniques. *Dirkse Milieutechniek, Eindhoven University of Technology, Eindhoven, the Netherlands*.

Huppmann, R., Lohoff, H. W. & Schröder, H. F. (1996) Cyclic siloxanes in the biological waste water treatment process – Determination, quantification and possibilities of elimination. *Fresenius' Journal of Analytical Chemistry,* **354**, 66-71.

Hutnan, M., Drtil, M. & Mrafkova, L. (2000) Anaerobic biodegradation of sugar beet pulp. *Biodegradation,* **11**, 203-211.

Intelligen. (2011) SuperPro Designer. Intelligen, Inc.

Ishida, M., Haga, R. & Odawara, Y. (1982) Anaerobic digestion process. Google Patents.

Ivanov, V. (2009) *Microbiology for Civil and Environmental Engineers*. Taylor & Francis.

Jain, S., Salter, A. & Banks, C. (2011) Calculating the economic cost of mitigating GHG emissions from UK dairy farms by anaerobic digestion of slurry.

Jensen, A. B. & Webb, C. (1995) Treatment of H2S-containing gases: A review of microbiological alternatives. *Enzyme and Microbial Technology,* **17**, 2-10.

Jeong, H., Suh, C., Lim, J., Lee, S. & Shin, H. (2005) Analysis and application of ADM1 for anaerobic methane production. *Bioprocess Biosyst Eng,* **27**, 81-89.

Jeppsson, U., Rosen, C., Alex, J., Copp, J., Gernaey, K. V., Pons, M. N.*, et al.* (2006) Towards a benchmark simulation model for plant-wide control strategy performance evaluation of WWTPs. *Water Sci Technol,* **53**, 287-295.

Jiang, Y. (2012) Anaerobic digestion of food and vegetable waste. University of Southampton, University of Southampton.

JICA. (2011) Study report on Solid waste management in Vietnam.

Johnson, B. & Shang, Y. (2006) Applications and limitations of ADM 1 in municipal wastewater solids treatment. *Water Science & Technology,* **54**, 77-82.

Jones, P. & Salter, A. (2013) Modelling the economics of farm-based anaerobic digestion in a UK whole-farm context. *Energy Policy,* **62**, 215-225.

Judd, M., Kellier, F., Ulyatt, M., Lassey, K., Tate, K., Shelton, I.*, et al.* (1999) Net methane emissions from grazing sheep. *Global Change Biology,* **5**, 647-657.

Julien, C. & Whitford, W. (2007) Bioreactor monitoring modeling and simulation. *BioProcess Int. Suppl,* **5**, 10-17.

JyU. (2013) Evaluation of potential technologies and operational scales reflecting market needs for low-cost gas upgrading systems (VALORGAS Project: Deviverable D5.1). University of Southampton, 30 pp.

Kalfas, H., Skiadas, I., Gavala, H., Stamatelatou, K. & Lyberatos, G. (2006) Application of ADM1 for the simulation of anaerobic digestion of olive pulp under mesophilic and thermophilic conditions. *Water Science and Technology,* **54**, 149-156.

Kaparaju, P., Buendia, I., Ellegaard, L. & Angelidakia, I. (2008) Effects of mixing on methane production during thermophilic anaerobic digestion of manure: Lab-scale and pilot-scale studies. *Bioresource Technology,* **99**, 4919-4928.

Kaparaju, P., Rasi, S. & Rintala, J. (2013) Biogas upgrading and compression. In *Bioenergy Production by Anearobic Digestion*, pp. 152.

Kapdi, S., Vijay, V., Rajesh, S. & Prasad, R. (2005) Biogas scrubbing, compression and storage: perspective and prospectus in Indian context. *Renewable Energy,* **30**, 1195-1202.

Kapoor, R. & Vijay, V. (2013) Evaluation of Existing Low Cost Gas Bottling Systems for Vehicles Use Adaption in Developing Economies (VALORGAS Project: Deviverable D5.2). University of Southampton, 59 pp.

Karakashev, D., Batstone, D., Trably, E. & Angelidaki, I. (2006) Acetate oxidation is the dominant methanogenic pathway from acetate in the absence of Methanosaetaceae. *Applied and environmental microbiology,* **72**, 5138-5141.

Karim, K., Hoffmann, R., Klasson, T. & Al-Dahhan, M. (2005) Anaerobic digestion of animal waste: Waste strength versus impact of mixing. *Bioresource technology,* **96**, 1771-1781.

Kashyap, D., Dadhich, K. & Sharma, S. (2003) Biomethanation under psychrophilic conditions: a review. *Bioresource Technology,* **87**, 147-153.

Kayhanian, M. (1999) Ammonia inhibition in high-solids biogasification: an overview and practical solutions. *Environmental Technology,* **20**, 355-365.

Kell, D., Peck, M., Rodger, G. & Morris, J. (1981) On the permeability to weak acids and bases of the cytoplasmic membrane of Clostridiumpasteurianum. *Biochemical and biophysical research communications,* **99**, 81-88.

Kerroum, D., Mossaab, B. L. & Abdessalam, H. M. (2010) Use of ADM1 model to simulate the anaerobic digestion process used for sludge waste treatment in thermophilic conditions. *Turk. J. Eng. Environ. Sci. Turkish Journal of Engineering and Environmental Sciences,* **34**, 121-129.

Khalid, A., Arshad, M., Anjum, M., Mahmood, T. & Dawson, L. (2011) The anaerobic digestion of solid organic waste. *Waste management,* **31**, 1737-1744.

Khanal, S. (2011) *Anaerobic Biotechnology for Bioenergy Production: Principles and Applications*. John Wiley & Sons.

Kim, D., Choi, E., Yun, Z. & Kim, S. (2004) Nitrogen removal from piggery waste with anaerobic pretreatment. *Water Science & Technology,* **49**, 165-171.

Kirkeby, J., Birgisdottir, H., Hansen, T., Christensen, T., Bhander, G. & Hauschild, M. (2006a) Environmental assessment of solid waste systems and technologies: EASEWASTE. *Waste Management & Research,* **24**, 3-15.

Kirkeby, J., Birgisdottir, H., Hansen, T., Christensen, T., Bhander, G. & Hauschild, M. (2006b) Evaluation of environmental impacts from

municipal solid waste management in the municipality of Aarhus, Denmark (EASEWASTE). *Waste Management & Research,* **24**, 16-26.

Kleerebezem, R. & Loosdrecht, M. (2006) Critical analysis of some concepts proposed in ADM1. *Water Science and Technology,* **54**, 51-57.

Kleerebezem, R. & Van Loosdrecht, M. (2006) Critical analysis of some concepts proposed in ADM 1. *Water Science & Technology,* **54**, 51-57.

Klemes, J. (2011) *Sustainability in the process industry : integration and optimization*. McGraw-Hill Professional, New York.

Koch, K., Lubken, M., Gehring, T., Wichern, M. & Horn, H. (2010) Biogas from grass silage – Measurements and modeling with ADM1. *Bioresource Technology,* **101**, 8158-8165.

Kohl, A. & Nielsen, R. (1997) *Gas purification*. Gulf Pub., Houston.

Kopf, M., Bonnet, D., Artaud, I., Petre, D. & Mansuy, D. (1996) Key Role of Alkanoic Acids on the Spectral Properties, Activity, and Active-Site Stability of Iron-Containing Nitrile Hydratase from Brevibacterium R312. *European Journal of Biochemistry,* **240**, 239-244.

Krakat, N., Westphal, A., Schmidt, S. & Scherer, P. (2010) Anaerobic digestion of renewable biomass: thermophilic temperature governs methanogen population dynamics. *Applied and environmental microbiology,* **76**, 1842-1850.

Kwiatkowski, J. R., McAloon, A. J., Taylor, F. & Johnston, D. B. (2006) Modeling the process and costs of fuel ethanol production by the corn dry-grind process. *Industrial Crops and Products,* **23**, 288-296.

Lackey, J. Q. s. U. D. o. C. E. Q. s. U. (2012) Operation of solid oxide fuel cells on anaerobically derived wastewater treatment plant biogas. [publisher not identified], Kingston, Ont.

Lal, R. & Stewart, B. A. (2012) *Soil water and agronomic productivity*. CRC Press, Boca Raton, FL.

Lam, H. L., Klemeš, J. J., Kravanja, Z. & Varbanov, P. S. (2011) Software tools overview: process integration, modelling and optimisation for energy saving and pollution reduction. *Asia-Pacific Journal of Chemical Engineering,* **6**, 696-712.

Langerak, J., Lems, R. & Dirkse, E. (2013) Full-Scale Biogas Upgrading. In *Air Pollution Prevention and Control: Bioreactors and Bioenergy*, pp. 525-544.

Laoulache, R. N. (2011) Fluid mechanics, heat transfer, and mass transfer: chemical engineering practice. *Choice: Current Reviews for Academic Libraries,* **49**, 339-339.

Laureni, M., Palatsi, J., Llovera, M. & Bonmatí, A. (2013) Influence of pig slurry characteristics on ammonia stripping efficiencies and quality of the recovered ammonium-sulfate solution. *Journal of Chemical Technology and Biotechnology,* **88**, 1654-1662.

Lawrence, A. W. (1971) *Application of process kinetics to design of anaerobic processes*. Water Resources and Environmental Engineering, Department of Civil Engineering, State University of New York at Buffalo.

Lee, M., Suh, C., Ahn, Y. & Shin, H. (2009) Variation of ADM1 by using temperature-phased anaerobic digestion (TPAD) operation. *Bioresource Technology,* **100**, 2816-2822.

Lee, M. & Zinder, S. (1988) Isolation and characterization of a thermophilic bacterium which oxidizes acetate in syntrophic association with a methanogen and which grows acetogenically on H2-CO2. *Applied and environmental microbiology,* **54**, 124-129.

Lee, S., Cho, N. & Maeng, W. (1995) Using the Pressure of Biogas Created during Anaerobic-Digestion as the Source of Mixing Power. *Journal of Fermentation and Bioengineering,* **80**, 415-417.

Lei, X. & Maekawa, T. (2007) Electrochemical treatment of anaerobic digestion effluent using a Ti/Pt–IrO2 electrode. *Bioresource Technology,* **98**, 3521-3525.

Lei, X., Sugiura, N., Feng, C. & Maekawa, T. (2007) Pretreatment of anaerobic digestion effluent with ammonia stripping and biogas purification. *Journal of Hazardous Materials,* **145**, 391-397.

Leineweber, D. B., Schäfer, A., Bock, H. G. & Schlöder, J. P. (2003) An efficient multiple shooting based reduced SQP strategy for large-scale dynamic process optimization: Part II: Software aspects and applications. *Computers & Chemical Engineering,* **27**, 167-174.

Lettinga, G. (1995) Anaerobic digestion and wastewater treatment systems. *Antonie van leeuwenhoek,* **67**, 3-28.

Li, H. & Lam, C. P. (2004) An exchange language for process modelling and model management. In *Proceedings of the Proceedings of the 7th international symposium on dynamics and control of process systems, Boston, US*.

Li, Y., Park, S. Y. & Zhu, J. (2011) Solid-state anaerobic digestion for methane production from organic waste. *Renewable and sustainable energy reviews,* **15**, 821-826.

Liao, P., Chen, A. & Lo, K. (1995) Removal of nitrogen from swine manure wastewaters by ammonia stripping. *Bioresource Technology,* **54**, 17-20.

Lienhard, J. (2011) *A heat transfer textbook*. Courier Dover Publications.

Lier, J., Mahmoud, N. & Zeeman, G. (2008) Anaerobic wastewater treatment. In *Biological wastewater treatment: principles, modelling and design*, pp. 415-456. IWA publishing.

Lier, J. B. v., Rebac, S. & Lettinga, G. (1997) High-rate anaerobic wastewater treatment under psychrophilic and thermophilic conditions. *Water Science and Technology,* **35**, 199-206.

Lim, J. W. & Wang, J.-Y. (2013) Enhanced hydrolysis and methane yield by applying microaeration pretreatment to the anaerobic co-digestion of brown water and food waste. *Waste Management,* **33**, 813-819.

Lin, C. (1993) Effect of heavy metals on acidogenesis in anaerobic digestion. *Water Research,* **27**, 147-152.

Lin, L., Yuan, S., Chen, J., Xu, Z. & Lu, X. (2009) Removal of ammonia nitrogen in wastewater by microwave radiation. *Journal of Hazardous Materials,* **161**, 1063-1068.

Liss, S., Droppo, I., Leppard, G. & Milligan, T. (2004) *Flocculation in natural and engineered environmental systems*. CRC Press.

Lissens, G., Vandevivere, P., De Baere, L., Biey, E. M. & Verstrae, W. (2001) Solid waste digestors: process performance and practice for municipal solid waste digestion. *Water Sci Technol,* **44**, 91-102.

Liu, C., Yuan, X., Zeng, G., Li, W. & Li, J. (2008) Prediction of methane yield at optimum pH for anaerobic digestion of organic fraction of municipal solid waste. *Bioresource technology,* **99**, 882-888.

Liu, G., Zhang, R., El-Mashad, H. & Dong, R. (2009) Effect of feed to inoculum ratios on biogas yields of food and green wastes. *Bioresource technology,* **100**, 5103-5108.

Llabres-Luengo, P. & Mata-Alvarez, J. (1988) The hydrolytic step in a dry digestion system. *Biological wastes,* **23**, 25-37.

Lo, H., Chiang, C., Tsao, H., Pai, T., Liu, M., Kurniawan, T., *et al.* (2012) Effects of spiked metals on the MSW anaerobic digestion. *Waste Management & Research,* **30**, 32-48.

Loeser, M. & Redfern, M. A. (2010) Modelling and simulation of a novel micro-scale combined feedstock biomass generation plant for grid-independent power supply. *International Journal of Energy Research,* **34**, 303-320.

Lopez, I. & Borzacconi, L. (2010) Modelling of slaughterhouse solid waste anaerobic digestion: Determination of parameters and continuous reactor simulation. *Waste Management,* **30**, 1813-1821.

Lopez, M., Rene, E., Veiga, M. & Kennes, C. (2012) Biogas Technologies and Cleaning Techniques. In *Environmental Chemistry for a Sustainable World (Volume 2: Remediation of Air and Water Pollution)* (ed. by E. Lichtfouse, J. Schwarzbauer & D. Robert), pp. 347-377. Springer.

Lubken, M., Wichern, M., Schlattmann, M., Gronauer, A. & Horn, H. (2007) Modelling the energy balance of an anaerobic digester fed with cattle manure and renewable energy crops. *Water Res,* **41**, 4085-4096.

Ludwig, E. E. (1995) *Applied Process Design for Chemical and Petrochemical Plants*. Gulf Publishing Company.

Lyberatos, G. & Pullammanappallil, P. (2010) Anaerobic Digestion in Suspended Growth Bioreactors

Environmental Biotechnology (ed. by L. K. Wang, V. Ivanov & J.-H. Tay), pp. 395-438. Humana Press.

Lyberatos, G. & Skiadas, I. (1999) Modelling of anaerobic digestion-a review. *Global Nest Int J,* **1**, 63-76.

Madigan, M., Martinko, J., Stahl, D. & Clark, D. (2012) *Brock biology of microorganisms (13th edition)*. Pearson Benjamin-Cummings, San Francisco, Calif.; London.

Maier, R. M., Pepper, I. L. & Gerba, C. P. (2000) *Environmental microbiology*. Elsevier, New Delhi.

Mairet, F., Bernard, O., Ras, M., Lardon, L. & Steyer, J. (2011) Modeling anaerobic digestion of microalgae using ADM1. *Bioresource Technology,* **102**, 6823-6829.

Malakahmad, A., Ahmad Basri, N. E. & Md Zain, S. (2012) Design and Process Simulation of a Small Scale Waste-To-Energy Bioreactor. *Journal of Applied Sciences,* **12**.

Maria, F., Sordi, A. & Micale, C. (2012) Optimization of Solid State Anaerobic Digestion by inoculum recirculation: The case of an existing Mechanical Biological Treatment plant. *Applied Energy,* **97**, 462-469.

Martin, A. M. (1998) *Bioconversion of waste materials to industrial products*. Blackie Academic & Professional.

Mata-Alvarez, J. (2001) Biomethanization of the organic fraction of municipal solid wastes, pp. 114. IWA, London.

Mata-Alvarez, J., Dosta, J., Mace, S. & Astals, S. (2011) Codigestion of solid wastes: a review of its uses and perspectives including modeling. *Critical reviews in biotechnology,* **31**, 99-111.

Mata-Alvarez, J., Macé, S. & Llabrés, P. (2000) Anaerobic digestion of organic solid wastes. An overview of research achievements and perspectives. *Bioresource Technology,* **74**, 3-16.

Matteson, G. C. & Jenkins, B. M. (2007) Food and processing residues in California: Resource assessment and potential for power generation. *Bioresource Technology,* **98**, 3098-3105.

Mayumi, D., Mochimaru, H., Yoshioka, H., Sakata, S., Maeda, H., Miyagawa, Y., *et al.* (2011) Evidence for syntrophic acetate oxidation coupled to

hydrogenotrophic methanogenesis in the high-temperature petroleum reservoir of Yabase oil field (Japan). *Environmental microbiology,* **13**, 1995-2006.

McBean, E. (2008) Siloxanes in biogases from landfills and wastewater digesters. *Canadian Journal of Civil Engineering,* **35**, 431-436.

McCarty, P. (1964) Anaerobic waste treatment fundamentals. *Public works,* **95**, 107-112.

McCarty, P. & McKinney, R. (1961a) Salt toxicity in anaerobic digestion. *Journal (Water Pollution Control Federation),* **33**, 399-415.

McCarty, P. & McKinney, R. (1961b) Volatile acid toxicity in anaerobic digestion. *Journal (Water Pollution Control Federation),* **33**, 223-232.

McCarty, P. & Mosey, F. (1991) Modelling of anaerobic digestion processes (a discussion of concepts). *Water Science & Technology,* **24**, 17-33.

McCormick, K. & Kaberger, T. (2005) Exploring a pioneering bioenergy system: The case of Enköping in Sweden. *Journal of Cleaner production,* **13**, 1003-1014.

McDougall, F. R. & White, P. (2001) *Integrated solid waste management : a life cycle inventory*. Blackwell Science, Oxford, UK; Malden, MA.

McFarland, M. J. (2001) *Biosolids engineering*. McGraw-Hill, New York.

Mehrotra, I., Alibhai, K. R. K. & Forster, C. F. (1987) The removal of heavy metals in anaerobic upflow sludge blanket reactors. *Journal of Chemical Technology & Biotechnology,* **37**, 195-202.

Meireles, M. A. A. (2009) Extracting bioactive compounds for food products : theory and applications, pp. 198. CRC Press, Boca Raton.

Meroney, R. N. & Colorado, P. E. (2009) CFD simulation of mechanical draft tube mixing in anaerobic digester tanks. *Water Research,* **43**, 1040-1050.

Metcalf, Eddy, Tchobanoglous, G., Burton, F. L. & Stensel, H. D. (2003) *Wastewater engineering : treatment and reuse*. McGraw-Hill, Boston.

Milledge, J. (2013) Energy balance and techno-economic assessment of algal biofuel production systems. University of Southampton.

Minocha, V. K. & Rao, A. V. S. P. (1988) Ammonia removal and recovery from urea fertilizer plant waste. *Environmental Technology,* **9**, 655-664.

Miron, Y., Zeeman, G., Lier, J. & Lettinga, G. (2000) The role of sludge retention time in the hydrolysis and acidification of lipids, carbohydrates and proteins during digestion of primary sludge in CSTR systems. *Water Research,* **34**, 1705-1713.

Moeller, L., Goersch, K., Neuhaus, J., Zehnsdorf, A. & Mueller, R. (2012) Comparative review of foam formation in biogas plants and ruminant bloat. *Energy, Sustainability and Society,* **2**, 1-9.

Moletta, R., Verrier, D. & Albagnac, G. (1986) Dynamic modelling of anaerobic digestion. *Water Research,* **20**, 427-434.

Molino, A., Migliori, M., Ding, Y., Bikson, B., Giordano, G. & Braccio, G. (2013) Biogas upgrading via membrane process: Modelling of pilot plant scale and the end uses for the grid injection. *Fuel,* **107**, 585-592.

MONRE. (2011) Vietnam's 2011 National Environment Report - Solid waste section.

Moya, J., Huiliñir, C., Peredo, K., Aspé, E. & Roeckel, M. (2012) Modeling of simultaneous denitrification – Anaerobic digestion – Organic matter aerobic oxidation and nitrification in an anoxic–anaerobic–aerobic compact filter reactor. *Journal of Biotechnology,* **160**, 176-188.

Mujtaba, I. (2012) Use of Various Computational Tools and gPROMS for Modelling Simulation Optimisation and Control of Food Processes. In *Handbook of Food Process Design*, pp. 239.

Murphy, J. & McCarthy, K. (2005) The optimal production of biogas for use as a transport fuel in Ireland. *Renewable Energy,* **30**, 2111-2127.

Murray, W. & Van Den Berg, L. (1981) Effects of nickel, cobalt, and molybdenum on performance of methanogenic fixed-film reactors. *Applied and environmental microbiology,* **42**, 502-505.

Murto, M., Bjornsson, L. & Mattiasson, B. (2004) Impact of food industrial waste on anaerobic co-digestion of sewage sludge and pig manure. *Journal of Environmental Management,* **70**, 101-107.

Mussati, M., Aguirre, P. & Scenna, N. J. (1998) Modeling of real biological reactors for the treatment of complex substrates. Dynamic simulation. *Computers & Chemical Engineering,* **22, Supplement 1**, S723-S726.

Nijaguna, B. T. (2006) *Biogas technology*. New Age International, New Delhi.

Nikoo, M. B. & Mahinpey, N. (2008) Simulation of biomass gasification in fluidized bed reactor using ASPEN PLUS. *Biomass and Bioenergy,* **32**, 1245-1254.

Nilsson, L., Pisarek, M., Buriak, J., Oniszk-Poplawska, A., Bucko, P. & Ericsson, K. (2004) Bioenergy policy and strategies for Poland. In *Proceedings of the world conference on biomass for energy, industry and climate protection, Rome*.

Nopens, I., Batstone, D., Copp, J., Jeppsson, U., Volcke, E., Alex, J., *et al.* (2009) An ASM/ADM model interface for dynamic plant-wide simulation. *Water Res,* **43**, 1913-1923.

Novak, J. T. & Carlson, D. A. (1970) The kinetics of anaerobic long chain fatty acid degradation. *Journal (Water Pollution Control Federation)*, 1932-1943.

Oddone, S. & Iribarren, O. A. (2002) A modelling formalism for multiproduct and multiplant batch processes. In *Computer Aided Chemical Engineering* (ed. by G. Johan & S. Jan van), pp. 139-144. Elsevier.

Omil, F., Méndez, R. & Lema, J. M. (1995) Anaerobic treatment of saline wastewaters under high sulphide and ammonia content. *Bioresource Technology,* **54**, 269-278.

Ong'iro, A., Ugursal, V. I., Al Taweel, A. M. & Lajeunesse, G. (1996) Thermodynamic simulation and evaluation of a steam CHP plant using ASPEN Plus. *Applied Thermal Engineering,* **16**, 263-271.

Ongiro, A. O., Ugursal, V. I., Altaweel, A. M. & Blamire, D. K. (1995) Simulation of Combined-Cycle Power-Plants Using the Aspen Plus Shell. *Heat Recovery Systems & Chp,* **15**, 105-113.

Ozkan-Yucel, U. G. & Gokcay, C. F. (2010) Application of ADM1 model to a full-scale anaerobic digester under dynamic organic loading conditions. *Environ Technol,* **31**, 633-640.

Ozkan-Yucel, U. G. & Gokcay, C. F. (2010) Application of ADM1 model to a full-scale anaerobic digester under dynamic organic loading conditions. *Environmental technology,* **31**, 633-640.

Palanichamy, J. & Palani, S. (2014) Simulation of anaerobic digestion processes using stochastic algorithm. *Journal of Environmental Health Science and Engineering,* **12**, 121.

Palmeri, N., Cavallaro, S. & Bart, J. C. J. (2008) Carbon dioxide absorption by MEA - A preliminary evaluation of a bubbling column reactor. *Journal of Thermal Analysis and Calorimetry,* **91**, 87-91.

Pant, D. & Adholeya, A. (2007) Biological approaches for treatment of distillery wastewater: A review. *Bioresource Technology,* **98**, 2321-2334.

Park, C., Lee, C., Kim, S., Chen, Y. & Chase, H. (2005) Upgrading of anaerobic digestion by incorporating two different hydrolysis processes. *Journal of Bioscience and Bioengineering,* **100**, 164-167.

Parker, W. (2005) Application of the ADM1 model to advanced anaerobic digestion. *Bioresource Technology,* **96**, 1832-1842.

Parkin, G. F. & Owen, W. F. (1986) Fundamentals of anaerobic digestion of wastewater sludges. *Journal of Environmental Engineering,* **112**, 867-920.

Patterson, T., Esteves, S., Dinsdale, R. & Guwy, A. (2011) An evaluation of the policy and techno-economic factors affecting the potential for biogas upgrading for transport fuel use in the UK. *Energy Policy,* **39**, 1806-1816.

Paul, E. L., Atiemo-Obeng, V. A. & Kresta, S. M. (2004) *Handbook of industrial mixing: science and practice*. Wiley-Interscience, Hoboken, N.J.

Paviet, F., Chazarenc, F. & Tazerout, M. (2009) Thermo chemical equilibrium modelling of a biomass gasifying process using ASPEN pLUS. *Int. J. Chem. Reactor Eng. International Journal of Chemical Reactor Engineering,* **7**.

Pazdernik, N. & Clark, D. (2012) *Molecular Biology: Understanding the Genetic Revolution*. Elsevier Science, Burlington.

Persson, M. (2003) Evaluation of upgrading techniques for biogas. Lund Institute of Technology.

Persson, M., Jonsson, O. & Wellinger, A. (2006) Biogas upgrading to vehicle fuel standards and grid injection. In *Proceedings of the IEA Bioenergy task*.

Persson, M. & Wellinger, A. (2006) Biogas upgrading and utilisation.

Pertl, A., Mostbauer, P. & Obersteiner, G. (2010) Climate balance of biogas upgrading systems. *Waste Management,* **30**, 92-99.

Pesta, G. (2007) Anaerobic Digestion of Organic Residues and Wastes. In *Utilization of by-products and treatment of waste in the food industry* (ed. by V. R. W. Oreopoulou), pp. 53-72. Springer, New York.

Petersen, S. & Ahring, B. (1991) Acetate oxidation in a thermophilic anaerobic sewage-sludge digestor: the importance of non-aceticlastic methanogenesis from acetate. *FEMS Microbiology Letters,* **86**, 149-152.

Petersson, A. & Wellinger, A. (2009) Biogas upgrading technologies–developments and innovations. *IEA-Task,* **37**, 20.

Pettersson, K. & Lindgren, S. (1990) The influence of the carbohydrate fraction and additives on silage quality. *Grass and Forage Science,* **45**, 223-233.

Picioreanu, C., Katuri, K., Head, I., Loosdrecht, M. & Scott, K. (2008) Mathematical model for microbial fuel cells with anodic biofilms and anaerobic digestion. *Water science and technology,* **57**, 965-972.

Pistikopoulos, E. N., Georgiadis, M. C. & Dua, V. (2010) *Process systems engineering*. *Volume 7, Dynamic process modeling*. Wiley-VCH ; John Wiley [distributor], Weinheim; Chichester.

PM. (2007) Decision on Vietnam National Energy Development Strategy up to 2020 and vision to 2050 (Decision No. 1855/QĐ-TTg).

Poeschl, M., Ward, S. & Owende, P. (2010) Prospects for expanded utilization of biogas in Germany. *Renewable & Sustainable Energy Reviews,* **14**, 1782-1797.

Popat, S. C. & Deshusses, M. A. (2008) Biological removal of siloxanes from landfill and digester gases: Opportunities and challenges. *Environmental science & technology,* **42**, 8510-8515.

Post-Mixing. (2012) Impellers.

PSe. (2011) Advanced Process Modelling platform.

Purich, D. & Allison, R. (1999) *Handbook of Biochemical Kinetics: A Guide to Dynamic Processes in the Molecular Life Sciences*. Academic Press.

Qasim, S. (1998) *Wastewater Treatment Plants: Planning, Design, and Operation, Second Edition*. Taylor & Francis.

Rafiee, A. & Hillestad, M. (2010) Optimal design and operation of a gas-to-liquid process. *Chem. Eng. Trans. Chemical Engineering Transactions,* **21**, 1393-1398.

Rajaram, V., Siddiqui, F. & Khan, M. (2011) Landfill gas treatment technologies In *From Landfill Gas to Energy: Technologies and Challenges* (ed. by V. Rajaram, F. Siddiqui & M. Khan). Crc Press.

Rajendran, K., Kankanala, H., Lundin, M. & Taherzadeh, M. (2014) A novel process simulation model (PSM) for anaerobic digestion using Aspen Plus. *Bioresource Technology*.

Raju, K. S. N. (2011) *Fluid mechanics, heat transfer, and mass transfer : chemical engineering practice*. Wiley, Hoboken, N.J.

Ramachandran, A. (2008) Performance limitations in wide superscalar processors.

Ramasamy, E. & Abbasi, S. (2001) Enhancement in the treatment efficiency and conversion to energy of dairy wastewaters by augmenting CST Reactors with simple biofilm support systems. *Environmental Technology,* **22**, 561-565.

Ramirez, I., Mottet, A., Carrère, H., Déléris, S., Vedrenne, F. & Steyer, J. (2009) Modified ADM1 disintegration/hydrolysis structures for modeling batch thermophilic anaerobic digestion of thermally pretreated waste activated sludge. *Water Research,* **43**, 3479-3492.

Ramirez, I. & Steyer, J. (2008) Modeling microbial diversity in anaerobic digestion. *Water Science & Technology,* **57**.

Rasi, S., Veijanen, A. & Rintala, J. (2007) Trace compounds of biogas from different biogas production plants. *Energy,* **32**, 1375-1380.

Reinhold, G. & Markl, H. (1997) Model-based scale-up and performance of the Biogas Tower Reactor for anaerobic waste-water treatment. *Water Research,* **31**, 2057-2065.

Rincon, B., Heaven, S., Banks, C. & Zhang, Y. (2012) Anaerobic digestion of whole-crop winter wheat silage for renewable energy production. *Energy & Fuels,* **26**, 2357-2364.

Rivero, J. A. C., Suidan, M. T., Ginestet, P. & Audic, J.-M. (2002) Effect of SRT on the anaerobic digestion of excess municipal sludge. *Proceedings of the Water Environment Federation,* **2002**, 857-865.

Rodriguez, J., Lema, J., Loosdrecht, M. & Kleerebezem, R. (2006) Variable stoichiometry with thermodynamic control in ADM1. *Water Science & Technology,* **54**, 101-110.

Rojas, C., Uhlenhut, F., Schlaak, M., Borchert, A. & Steinigeweg, S. (2011) Simulation des anaeroben Prozesses bei der Biogaserzeugung. *Chemie Ingenieur Technik,* **83**, 306-321.

Rosen, C. & Jeppsson, U. (2005) Aspects on ADM1 Implementation within the BSM2 Framework. *TEIE*.

Rosen, C., Vrecko, D., Gernaey, K., Pons, M.-N. & Jeppsson, U. (2006) Implementing ADM 1 for plant-wide benchmark simulations in Matlab/Simulink. *Water Science & Technology,* **54**, 11-19.

Rousseau, P., Steyer, J., Volcke, E., Bernet, N. & Beline, F. (2008) Combined anaerobic digestion and biological nitrogen removal for piggery wastewater treatment: a modelling approach. *Water Science and Technology,* **58**, 133.

Rubia, D., Angeles, M., Walker, M., Heaven, S., Banks, C. & Borja, R. (2010) Preliminary trials of in situ ammonia stripping from source segregated domestic food waste digestate using biogas: Effect of temperature and flow rate. *Bioresource technology,* **101**, 9486-9492.

Rundle, H., Whyley, J. & Lower Trent Div, S. T. W. A. E. (1981) Comparison of gas recirculation systems for mixing of contents of anaerobic digesters. *Water Pollut. Control (Maidstone, Engl.),* **80:4**, 463-480.

Ryan, P., Forbes, C., McHugh, S., O'Reilly, C., Fleming, G. T. A. & Colleran, E. (2010) Enrichment of acetogenic bacteria in high rate anaerobic reactors under mesophilic and thermophilic conditions. *Water Research,* **44**, 4261-4269.

Ryckebosch, E., Drouillon, M. & Vervaeren, H. (2011) Techniques for transformation of biogas to biomethane. *Biomass and Bioenergy,* **35**, 1633-1645.

Salanitro, J. & Diaz, L. (1995) Anaerobic biodegradability testing of surfactants. *Chemosphere,* **30**, 813-830.

Salter, A. & Banks, C. (2009) Establishing an energy balance for crop-based digestion. *Water Science & Technology,* **59**.

Salter, A., Delafield, M., Heaven, S. & Gunton, Z. (2007) Anaerobic digestion of verge cuttings for transport fuel. *Proceedings of the ICE-Waste and Resource Management,* **160**, 105-112.

Salter, A., Wing Chu, T. & Heaven, S. (2013) Output from an energy and carbon footprint model verified against primary data collected as part of

the research (VALORGAS Project: Deviverable D6.3). University of Southampton, 70 pp.

Sasaki, D., Hori, T., Haruta, S., Ueno, Y., Ishii, M. & Igarashi, Y. (2011) Methanogenic pathway and community structure in a thermophilic anaerobic digestion process of organic solid waste. *Journal of bioscience and bioengineering,* **111**, 41-46.

Schaldach, A., Lapola, D., Jessen, U., Thees, M. & Schaldach, R. (2010) Development of a land-use component for an integrated model of the German biogas system. In *2010 International Congress on Environmental Modelling and Software Modelling for Environment's Sake, Fifth Biennial Meeting*, Ottawa, Canada.

Schefflan, R. (2011) *Teach yourself the basics of Aspen plus*. Wiley ; American Institute of Chemical Engineers, Hoboken, N.J.; [New York].

Schink, B. (2002) Synergistic interactions in the microbial world. *Antonie van Leeuwenhoek,* **81**, 257-261.

Schneider, S. H. (1989) The greenhouse effect: science and policy.

Schnurer, A., Frans, A. & BH., S. (1994) Mesophilic syntrophic acetate oxidation during methane formation by a triculture at high ammonium concentration. *Arch. Microbiol. Archives of Microbiology,* **162**, 70-74.

Schnurer, A. & Nordberg, A. (2008) Ammonia, a selective agent for methane production by syntrophic acetate oxidation at mesophilic temperature. *Water science and technology : a journal of the International Association on Water Pollution Research.,* **57**, 735-740.

Schnurer, A., Zellner, G. & Svensson, B. (1999) Mesophilic syntrophic acetate oxidation during methane formation in biogas reactors. *FEMS microbiology ecology,* **29**, 249-261.

Schonheit, P., Moll, J. & Thauer, R. K. (1979) Nickel, cobalt, and molybdenum requirement for growth of Methanobacterium thermoautotrophicum. *Archives of Microbiology,* **123**, 105-107.

Schweigkofler, M. & Niessner, R. (2001) Removal of siloxanes in biogases. *Journal of Hazardous Materials,* **83**, 183-196.

Seadi, T. A., Rutz, D., Prassl, H., Köttner, M., Finsterwalder, T., Volk, S., *et al.* (2008) *Biogas Handbook*. University of Southern Denmark Esbjerg, Niels Bohrs Vej 9-10, DK-6700 Esbjerg, Denmark.

Seely, R. J. (1985) Product and process for stimulating bacterial action in an anaerobic digestion system. Google Patents.

Serna-Maza, A. (2014) Nitrogen control in source segregated domestic food waste anaerobic digestion using stripping technologies. University of Southampton, University of Southampton.

Serna-Maza, A., Heaven, S. & Banks, C. (2014) Ammonia removal in food waste anaerobic digestion using a side-stream stripping process. *Bioresource technology,* **152**, 307-315.

Serrano, R. (2011) Biogas Process Simulation using Aspen Plus. Syddansk Universitet.

Shang, Y., Johnson, B. & Sieger, R. (2005) Application of the IWA Anaerobic Digestion Model (ADM1) for simulating full-scale anaerobic sewage sludge digestion. *Water Science and Technology,* **52**, 487-492.

Shelton, D. & Tiedje, J. (1984) General method for determining anaerobic biodegradation potential. *Applied and Environmental Microbiology,* **47**, 850-857.

Shigematsu, T., Tang, Y., Kobayashi, T., Kawaguchi, H., Morimura, S. & Kida, K. (2004) Effect of dilution rate on metabolic pathway shift between aceticlastic and nonaceticlastic methanogenesis in chemostat cultivation. *Applied and environmental microbiology,* **70**, 4048-4052.

Shimada, T., Morgenroth, E., Tandukar, M., Pavlostathis, S., Smith, A., Raskin, L., *et al.* (2011) Syntrophic acetate oxidation in two-phase (acid—methane) anaerobic digesters. *Water Science & Technology,* **64**.

Sialve, B., Bernet, N. & Bernard, O. (2009) Anaerobic digestion of microalgae as a necessary step to make microalgal biodiesel sustainable. *Biotechnology advances,* **27**, 409-416.

Siegrist, H., Renggli, D. & Gujer, W. (1993) Mathematical modelling of anaerobic mesophilic sewage sludge treatment. *Water Science & Technology,* **27**, 25-36.

Siegrist, H., Vogt, D., Garcia-Heras, J. & Gujer, W. (2002) Mathematical model for meso- and thermophilic anaerobic sewage sludge digestion. *Environmental Science & Technology,* **36**, 1113-1123.

Siles, J., Martín, M., Chica, A. & Martín, A. (2010) Anaerobic co-digestion of glycerol and wastewater derived from biodiesel manufacturing. *Bioresource Technology,* **101**, 6315-6321.

Sivanagaraju, S. (2010) Generation And Utilization Of Electrical Energy. Pearson India.

Smet, E., Lens, P. & Langenhove, H. V. (1998) Treatment of Waste Gases Contaminated with Odorous Sulfur Compounds. *Critical Reviews in Environmental Science and Technology,* **28**, 89-117.

Smith, J. U. & Smith, P. (2007) *Introduction to environmental modelling*. Oxford University Press, Oxford ; New York.

Smyth, B., Murphy, J. & O'Brien, C. (2009) What is the energy balance of grass biomethane in Ireland and other temperate northern European climates? *Renewable and Sustainable Energy Reviews,* **13**, 2349-2360.

Snape, J., Dunn, I., Ingham, J. & Prenosil, J. (2008) *Dynamics of Environmental Bioprocesses: Modelling & Simulation*. John Wiley & Sons.

Sobotka, M., Votruba, J., Havlik, I. & Minkevich, I. (1983) The mass-energy balance of anaerobic methane production. *Folia Microbiologica,* **28**, 195-204.

Sokolowski, J. (2009) Principles of modeling and simulation: a multidisciplinary approach. *Choice: Current Reviews for Academic Libraries,* **47**, 724-724.

Sonesson, U., Dalemo, M., Mingarini, K. & Jönsson, H. (1997) ORWARE – A simulation model for organic waste handling systems. Part 2: Case study and simulation results. *Resources, Conservation and Recycling,* **21**, 39-54.

Souza, T., Carvajal, A., Donoso-Bravo, A., Pena, M. & Fdz-Polanco, F. (2013) ADM1 calibration using BMP tests for modeling the effect of autohydrolysis pretreatment on the performance of continuous sludge digesters. *Water research,* **47**, 3244-3254.

Speece, R. (1983) Anaerobic biotechnology for industrial wastewater treatment. *Environmental science & technology,* **17**, 416-427.

Speece, R. (1996) *Anaerobic biotechnology for industrial wastewaters*. Archae Press, Nashville, Tenn.

Spellman, F. (2013) *Water & Wastewater Infrastructure: Energy Efficiency and Sustainability*. CRC Press.

Spellman, F. R. W. N. E. (2007) *Environmental management of concentrated animal feeding operations (CAFOs)*. CRC Press, Boca Raton.

Spillman, R. W. (1989) Economics of Gas Separation Membranes. *Chemical Engineering Progress,* **85**, 41-62.

Spooner, J. M. (1994) *A Review of Computer Process Simulation in Industrial Pollution Prevention*. Risk Reduction Engineering Laboratory, US Environmental Protection Agency, Office of Research and Development.

Sprott, G. D. & Patel, G. B. (1986) Ammonia toxicity in pure cultures of methanogenic bacteria. *Systematic and Applied Microbiology,* **7**, 358-363.

Sreela-or, C., Plangklang, P., Imai, T. & Reungsang, A. (2011) Co-digestion of food waste and sludge for hydrogen production by anaerobic mixed cultures: Statistical key factors optimization. *International Journal of Hydrogen Energy,* **36**, 14227-14237.

Srinath, E. G. & Loehr, R. C. (1974) Ammonia desorption by diffused aeration. *Journal (Water Pollution Control Federation)*, 1939-1957.

Stafford, D. A. (1982) The Effects of Mixing and Volatile Fatty-Acid Concentrations on Anaerobic Digester Performance. *Biomass,* **2**, 43-55.

Stams, A. M. (1994) Metabolic interactions between anaerobic bacteria in methanogenic environments. *Antonie van Leeuwenhoek,* **66**, 271-294.

Steffen, R., Szolar, O. & Braun, R. (1998) Feedstocks for anaerobic digestion. *Institute for Agrobiotechnology Tulln University of Agricultural Sciences, Viences*.

Straub, A., Conklin, A., Ferguson, J. & Stensel, H. (2006) Use of the ADM1 to investigate the effects of acetoclastic methanogen population dynamics on mesophilic digester stability. *Water Science & Technology,* **54**, 59-66.

Stroot, P. G., McMahon, K. D., Mackie, R. I. & Raskin, L. (2001) Anaerobic codigestion of municipal solid waste and biosolids under various mixing conditions - I. Digester performance. *Water Research,* **35**, 1804-1816.

Stuart, T. (2009) *Waste: uncovering the global food scandal*. WW Norton & Company.

Stuckey, D. (1986) Biogas: a global perspective. In *Biogas Technology, Transfer and Diffusion*, pp. 18-44. Springer.

Su, S. & Agnew, J. (2006) Catalytic combustion of coal mine ventilation air methane. *Fuel,* **85**, 1201-1210.

Subramanian, S., Yan, S., Tyagi, R. & Surampalli, R. (2009) Bioflocculants. In *Sustainable sludge management : production of value added products* (ed. by R. Tyagi), pp. 146-167. Reston, Va. : American Society of Civil Engineers.

Suhartini, S. (2014) The anaerobic digestion of sugar beet pulp. University of Southampton, University of Southampton.

Suhartini, S., Heaven, S. & Banks, C. (2014) Comparison of mesophilic and thermophilic anaerobic digestion of sugar beet pulp: Performance, dewaterability and foam control. *Bioresour. Technol.,* **152**, 202-211.

Suhartini, S., Heaven, S. & Banks, C. J. (2011) Anaerobic digestion of sugar beet pulp: effects of trace element addition on performance and digestate properties. In *the International Symposium on Anaerobic Digestion of Solid Waste & Energy Crops*, Vienna University of Technology, Vienna, Austria.

Sundqvist, J.-O. (2004) System analysis of organic-waste management schemes - experiences of the orware model. In *Resource recovery and reuse in organic solid waste management* (ed. by Piet Lens, Bert Hamelers, H. Hoitink & W. Bidlingmaier). IWA Pub., London.

Sung, S. & Liu, T. (2003) Ammonia inhibition on thermophilic anaerobic digestion. *Chemosphere,* **53**, 43-52.

Swamy, P. M. (2008) *Laboratory manual on biotechnology*. Rastogi Publications, Meerut, India.

Symons, G. & Buswell, A. (1933) The methane fermentation of carbohydrates. *Journal of the American Chemical Society,* **55**, 2028-2036.

Tchobanoglous, G., Burton, F. & Stensel, H. (2003) *Wastewater Engineering: Treatment and Reuse (4th edition)*. McGraw-Hill Education.

Thamsiriroj, T. & Murphy, J. (2011) Modelling mono-digestion of grass silage in a 2-stage CSTR anaerobic digester using ADM1. *Bioresource Technology,* **102**, 948-959.

Thauer, R. K. (1977) Energy conservation in chemotrophic anaerobic bacteria. *Bacteriol. Rev.,* **41**, 100-180.

Tiehm, A., Nickel, K., Zellhorn, M. & Neis, U. (2001) Ultrasonic waste activated sludge disintegration for improving anaerobic stabilization. *Water Research,* **35**, 2003-2009.

Tixier, N., Guibaud, G. & Baudu, M. (2003) Determination of some rheological parameters for the characterization of activated sludge. *Bioresource Technology,* **90**, 215-220.

Tolsma, J. E. & Barton, P. I. (2001) Process simulation and analysis with heterogeneous models. In *Proceedings of the European Symposium on Computer Aided Process Engineering-11: 11th European Symposium of the Working Party on Computer Aided Process Engineering*, pp. 309. Elsevier.

Tomei, M., Braguglia, C., Cento, G. & Mininni, G. (2009) Modeling of anaerobic digestion of sludge. *Critical Reviews in Environmental Science and Technology,* **39**, 1003-1051.

Tomescu, M. (2005) Innovative bioenergy systems in action: the case of the Mureck bioenergy cycle. *International Institute for Industrial Environmental Economics, Lund (Study prepared for the Bioenergy Network of Excellence).*

Treichel, P., Townsend, J. & Kotz, J. *Chemistry and Chemical Reactivity, Volume 2*. Cengage Learning.

Trzcinski, A. & Stuckey, D. (2009) Continuous treatment of the organic fraction of municipal solid waste in an anaerobic two-stage membrane process with liquid recycle. *Water research,* **43**, 2449-2462.

Trzcinski, A. & Stuckey, D. (2012) Determination of the hydrolysis constant in the biochemical methane potential test of municipal solid waste. *Environmental Engineering Science,* **29**, 848-854.

Turker, M. & Celen, I. (2007) Removal of ammonia as struvite from anaerobic digester effluents and recycling of magnesium and phosphate. *Bioresource technology,* **98**, 1529-1534.

Turovskiĭ, I. & Mathai, P. (2006) *Wastewater sludge processing*. Wiley-Interscience, Hoboken, N.J.

Usa, I. (2007) *Vietnam Ecology & Nature Protection Handbook*. International Business Publications USA.

Valcke, D. & Verstraete, W. (1983) A practical method to estimate the acetoclastic methanogenic biomass in anaerobic sludges. *Journal (Water Pollution Control Federation)*, 1191-1195.

VALORGAS. (2010-2013) Valorisation of food waste to biogas: Final report. University of Southampton.

VALORGAS. (2013) Full assessment of the feasibility of ammonia removal from food waste for improved operational stability and gas production (VALORGAS Project: Deliverable D3.6). University of Southampton.

van de Putte, L. B., Brutel de la Riviere, G., van Breda Vriesman, P. J. & de Graeff, J. (1973) Haematuria of renal parenchymal origin in adults with normal renal function. *Proc Eur Dial Transplant Assoc,* **10**, 391-398.

Van Ginkel, S., Sung, S. & Lay, J. J. (2001) Biohydrogen production as a function of pH and substrate concentration. *Environmental science & technology,* **35**, 4726-4730.

Vanrolleghem, P., Rosen, C., Zaher, U., Copp, J., Benedetti, L., Ayesa, E.*, et al.* (2005) Continuity-based interfacing of models for wastewater systems described by Petersen matrices. *Water Science & Technology,* **52**, 493-500.

Varma, P., Kyazze, G., Premier, R., Dinsdale, R., Guwy, A. & Rodriguez, J. (2007) Application of ADM1 with variable stoichiometry to simulate continuous bio-hydrogen production. In *Proceedings of the 11th IWA World congress on anaerobic digestion. Brisbane, Australia.*

Vavilin, V., Fernandez, B., Palatsi, J. & Flotats, X. (2008) Hydrolysis kinetics in anaerobic degradation of particulate organic material: An overview. *Waste Management,* **28**, 939-951.

Vavilin, V., Lokshina, L., Jokela, J. & Rintala, J. (2004) Modeling solid waste decomposition. *Bioresource Technology,* **94**, 69-81.

Vavilin, V., Rytov, S. & Lokshina, L. (1996) A description of hydrolysis kinetics in anaerobic degradation of particulate organic matter. *Bioresource Technology,* **56**, 229-237.

Vavilin, V., Vasiliev, V., Ponomarev, A. & Rytow, S. (1994) Simulation model 'methane' as a tool for effective biogas production during anaerobic conversion of complex organic matter. *Bioresource Technology,* **48**, 1-8.

Veeken, A. & Hamelers, B. (1999) Effect of temperature on hydrolysis rates of selected biowaste components. *Bioresource technology,* **69**, 249-254.

Veeken, A., Kalyuzhnyi, S., Scharff, H. & Hamelers, B. (2000) Effect of pH and VFA on hydrolysis of organic solid waste. *Journal of environmental engineering,* **126**, 1076-1081.

Ventour, L. (2008) The food we waste.

Verhoff, F. H., Tenney, M. W. & Echelber.Wf. (1974) Mixing in Anaerobic Digestion. *Biotechnology and Bioengineering,* **16**, 757-770.

Verougstraete, A., Nyns, E., Naveau, H. & Gasser, J. (1985) Heat recovery from composting and comparison with energy from anaerobic digestion. In *Proceedings of the Composting of agricultural and other wastes. Proceedings of seminar organised by Commission of the European Communities, Directorate-General Science, R and D, Environment Res. Prog., Brasenose College, Oxford, March 19-20, 1984.*, pp. 135-145. Elsevier Applied Science Publishers.

Vijay, V. K., Chandra, R., Subbarao, P. M. V. & Kapdi, S. S. (2006) Biogas purification and bottling into CNG cylinders: producing Bio-CNG from biomass for rural automotive applications. In *Proceedings of the A paper presentation at The 2ndJoint International Conference on Sustainable Energy and Environmetnt (SEE) on*, pp. 21-23.

Walker, M., Iyer, K., Heaven, S. & Banks, C. (2011) Ammonia removal in anaerobic digestion by biogas stripping: An evaluation of process alternatives using a first order rate model based on experimental findings. *Chemical Engineering Journal,* **178**, 138-145.

Wall, J., Harwood, C. & Demain, A. (2008) *Bioenergy*. ASM Press, Washington, D.C.

Walsh, J. L., Georgia Tech Research Institute. Economic Development Laboratory. Engineering Technology, B., Georgia Tech Research Institute. Economic Development Laboratory. Environmental, H., Safety, D. & Southeastern Regional Biomass Energy, P. (1988) *Handbook on biogas utilization*. Environment, Health, and Safety Division, Georgia Tech Research Institute, Atlanta, Ga.

Wang, S., Wu, X., Wang, Y., Li, Q. & Tao, M. (2008) Removal of organic matter and ammonia nitrogen from landfill leachate by ultrasound. *Ultrasonics sonochemistry,* **15**, 933-937.

Wang, Z. & Banks, C. (2003) Evaluation of a two stage anaerobic digester for the treatment of mixed abattoir wastes. *Process Biochemistry,* **38**, 1267-1273.

Weiland, P. (2003) Production and energetic use of biogas from energy crops and wastes in Germany. *Applied Biochemistry and Biotechnology,* **109**, 263-274.

Weiland, P. (2010) Biogas production: current state and perspectives. *Applied microbiology and biotechnology,* **85**, 849-860.

Wellinger, A. (1999) Process design of agricultural digesters. *Nova Energie GmbH, Elggerstrasse,* **36**.

Wellinger, A. & Lindberg, A. (1999) Biogas upgrading and utilisation. In *Proceedings of the IEA Bioenergy. Task*, pp. 18.

Westerholm, M. (2012) Biogas production through the syntrophic acetate-oxidising pathway : characterisation and detection of syntrophic acetate-oxidising bacteria. Swedish University of Agricultural Sciences, Uppsala, Sweden.

Wett, B., Eladawy, A. & Ogurek, M. (2006) Description of nitrogen incorporation and release in ADM1. *Water Science & Technology,* **54**, 67-76.

Wett, B. & Rauch, W. (2003) The role of inorganic carbon limitation in biological nitrogen removal of extremely ammonia concentrated wastewater. *Water Research,* **37**, 1100-1110.

Wett, B., Takacs, I., Batstone, D., Wilson, C. & Murthy, S. (2014) Anaerobic model for high-solids or high-temperature digestion-additional pathway of acetate oxidation. *Water Science & Technology,* **69**.

Wheeler, P., Jaatinen, T., Lindberg, A. & Pettigrew, A. (2000) Biogas upgrading and utilisation. IEA.

Wheless, E. & Pierce, J. (2004) Siloxanes in landfill and digester gas update. In *Proceedings of the Proc. SWANA 27th LFG conference.(Accessed 04/2008). www. scsengineers. com/Papers/Pierce˙2004Siloxanes˙Update˙Paper. pdf.*

Wichern, M., Gehring, T., Fischer, K., Andrade, D., Lübken, M., Koch, K.*, et al.* (2009) Monofermentation of grass silage under mesophilic conditions: measurements and mathematical modeling with ADM 1. *Bioresource technology,* **100**, 1675-1681.

Wiegant, W. M. & Zeeman, G. (1986) The mechanism of ammonia inhibition in the thermophilic digestion of livestock wastes. *Agricultural Wastes,* **16**, 243-253.

Wieser, M., Holden, N., Coplen, T., Böhlke, J., Berglund, M., Brand, W.*, et al.* (2013) Atomic weights of the elements 2011 (IUPAC Technical Report). *Pure & Applied Chemistry,* **85**.

Wilkie, A., Goto, M., Bordeaux, F. & Smith, P. (1986) Enhancement of Anaerobic Methanogenesis from Napiergrass by Addition of Micronutrients. *Biomass,* **11**, 135-146.

Wood, D. K. & Tchobanoglous, G. (1975) Trace elements in biological waste treatment. *Journal (Water Pollution Control Federation)*, 1933-1945.

Wooley, R. J. & Putsche, V. (1996) *Development of an ASPEN PLUS physical property database for biofuels components*. National Renewable Energy Laboratory Golden, CO.

World Bank. (2012) Electric power consumption (kWh per capita) The World Bank.

Xu, S. Y., Lam, H. P., Karthikeyan, O. P. & Wong, J. W. C. (2011) Optimization of food waste hydrolysis in leach bed coupled with

methanogenic reactor: Effect of pH and bulking agent. *Bioresource Technology,* **102**, 3702-3708.

Yabu, H., Sakai, C., Fujiwara, T., Nishio, N. & Nakashimada, Y. (2011) Thermophilic two-stage dry anaerobic digestion of model garbage with ammonia stripping. *Journal of Bioscience and Bioengineering,* **111**, 312-319.

Yang, Q., Luo, K., Li, X.-m., Wang, D.-b., Zheng, W., Zeng, G.-m., *et al.* (2010) Enhanced efficiency of biological excess sludge hydrolysis under anaerobic digestion by additional enzymes. *Bioresource Technology,* **101**, 2924-2930.

Yasui, H., Goel, R., Li, Y. Y. & Noike, T. (2008) Modified ADM1 structure for modelling municipal primary sludge hydrolysis. *Water Research,* **42**, 249-259.

Zahedi, S., Sales, D., Romero, L. I. & Solera, R. (2013) Optimisation of the two-phase dry-thermophilic anaerobic digestion process of sulphate-containing municipal solid waste: Population dynamics. *Bioresource Technology,* **148**, 443-452.

Zaher, U., Buffiere, P., Steyer, J. & Chen, S. (2009) A procedure to estimate proximate analysis of mixed organic wastes. *Water Environment Research,* **81**, 407-415.

Zaher, U. & Chen, S. (2006) Interfacing the IWA Anaerobic Digestion Model No. 1 (ADM1) with manure and solid waste characteristics. *Proceedings of the Water Environment Federation,* **2006**, 3162-3175.

Zaher, U., Grau, P., Benedetti, L., Ayesa, E. & Vanrolleghem, P. (2007) Transformers for interfacing anaerobic digestion models to pre-and post-treatment processes in a plant-wide modelling context. *Environmental Modelling & Software,* **22**, 40-58.

Zaher, U., Li, R., Jeppsson, U., Steyer, J. & Chen, S. (2009) GISCOD: general integrated solid waste co-digestion model. *Water research,* **43**, 2717-2727.

Zeeman, G. & Kujawa, K. (2013) Anaerobic treatment of source-separated domestic wastewater. In *Source separation and decentralization for wastewater treatment* (ed. by T. A. Larsen, U. K. M. & L. Judit), pp. 307-320. IWA Publishing, London.

Zhang, B., Zhang, L., Zhang, S., Shi, H. & Cai, W. (2005) The influence of pH on hydrolysis and acidogenesis of kitchen wastes in two-phase anaerobic digestion. *Environmental technology,* **26**, 329-340.

Zhang, L. & Jahng, D. (2010) Enhanced anaerobic digestion of piggery wastewater by ammonia stripping: Effects of alkali types. *Journal of Hazardous Materials,* **182**, 536-543.

Zhang, L. & Jahng, D. (2012) Long-term anaerobic digestion of food waste stabilized by trace elements. *Waste Management,* **32**, 1509-1515.

Zhang, L., Lee, Y. & Jahng, D. (2011) Anaerobic co-digestion of food waste and piggery wastewater: focusing on the role of trace elements. *Bioresour Technol,* **102**, 5048-5059.

Zhang, L., Lee, Y. & Jahng, D. (2012) Ammonia stripping for enhanced biomethanization of piggery wastewater. *Journal of Hazardous Materials,* **199–200**, 36-42.

Zhang, R., El-Mashad, H., Hartman, K., Wang, F., Liu, G., Choate, C., *et al.* (2007) Characterization of food waste as feedstock for anaerobic digestion. *Bioresource Technology,* **98**, 929-935.

Zhang, Y. & Banks, C. (2013) Impact of different particle size distributions on anaerobic digestion of the organic fraction of municipal solid waste. *Waste Management,* **33**, 297-307.

Zhang, Y., Banks, C. & Heaven, S. (2012a) Anaerobic digestion of two biodegradable municipal waste streams. *Journal of Environmental Management,* **104**, 166-174.

Zhang, Y., Banks, C. & Heaven, S. (2012b) Co-digestion of source segregated domestic food waste to improve process stability. *Bioresource Technology,* **114**, 168-178.

Zhang, Y. & Walker, M. (2010) Technical Report: Optimising Processes for the Stable Operation of Food Waste Digestion. Defra Project Code WR1208. 2010.

Zhao, Q., Leonhardt, E., MacConnell, C., Frear, C. & Chen, S. (2010) Purification technologies for biogas generated by anaerobic digestion. *Climate Friendly Farming. Washington State University's Center for Sustaining Agriculture & Natural Resources Research, Report.*

Zheng, L. & Furimsky, E. (2003) ASPEN simulation of cogeneration plants. *Energy Conversion and Management,* **44**, 1845-1851.

Zhou, H. D., Loffler, D. & Kranert, M. (2011) Model-based predictions of anaerobic digestion of agricultural substrates for biogas production. *Bioresource Technology,* **102**, 10819-10828.

Zhu, H., Parker, W., Basnar, R., Proracki, A., Falletta, P., Beland, M., *et al.* (2008) Biohydrogen production by anaerobic co-digestion of municipal food waste and sewage sludges. *International Journal of Hydrogen Energy,* **33**, 3651-3659.

Zinder, S. & Koch, M. (1984) Non-aceticlastic methanogenesis from acetate: acetate oxidation by a thermophilic syntrophic coculture. *Arch. Microbiol. Archives of Microbiology,* **138**, 263-272.

Zupancic, G. D. R. M. (2003) Heat and energy requirements in thermophilic anaerobic sludge digestion. *Renewable energy,* **28**, 2255-2267.

Appendix A: Extended ADM1 Peterson matrix

	Component i →	1	2	3	4	5	6	7	8	9	10	11	12	13	14	15	16	17	18	19	20	21	22	23	24	25	Process
	j Process ↓	S_{su}	S_{aa}	S_{fa}	S_{va}	S_{bu}	S_{pro}	S_{ac}	S_{h2}	S_{ch4}	S_{IC}	S_{IN}	S_I	X_c	X_{ch}	X_{pr}	X_{li}	X_{su}	X_{aa}	X_{fa}	X_{c4}	X_{pro}	X_{ac}	X_{ac2}	X_{h2}	X_I	Rate ρ_j (kgCOD m^{-3} d^{-1})
Ci	C content	C_{su}	C_{aa}	C_{fa}	C_{va}	C_{bu}	C_{pro}	C_{ac}		C_{ch4}	C_{IC}		C_{SI}	C_{xc}	C_{ch}	C_{pr}	C_{li}	C_{bac}	C_{bac}	C_{bac}	C_{bac}	C_{bac}	C_{bac}	C_{bac}	C_{bac}	C_{bac}	C_{bac}	
Ni	N content		N_{aa}										N_I	N_{Xc}		N_{pr}		N_{bac}	N_{bac}	N_{bac}	N_{bac}	N_{bac}	N_{bac}	N_{bac}	N_{bac}	N_I	
1	Disintegration										$-\sum_{i=1-9,11-25} C_i\nu_{i,1}$	$-\sum_{i=10,12-25} N_i\nu_{i,1}$	$f_{sI,Xc}$	−1.0	$f_{ch,Xc}$	$f_{pr,Xc}$	$f_{li,Xc}$									$f_{xI,Xc}$	ρ_1
2	Hydrolysis of carbohydrates	1.0									$-\sum_{i=1-9,11-25} C_i\nu_{i,2}$				−1.0												ρ_2
3	Hydrolysis of proteins		1.0								$-\sum_{i=1-9,11-25} C_i\nu_{i,3}$					−1.0											ρ_3
4	Hydrolysis of lipids	$(1-f_{fa,li})$		$f_{fa,li}$							$-\sum_{i=1-9,11-25} C_i\nu_{i,4}$						−1.0										ρ_4
5	Uptake of sugars	−1.0				$(1-Y_{su})f_{bu,su}$	$(1-Y_{su})f_{pro,su}$	$(1-Y_{su})f_{ac,su}$	$(1-Y_{su})f_{h2,su}$		$-\sum_{i=1-9,11-25} C_i\nu_{i,5}$	$-Y_{su}N_{bac}$						Y_{su}										ρ_5
6	Uptake of amino acids		−1.0		$(1-Y_{aa})f_{va,aa}$	$(1-Y_{aa})f_{bu,aa}$	$(1-Y_{aa})f_{pro,aa}$	$(1-Y_{aa})f_{ac,aa}$	$(1-Y_{aa})f_{h2,aa}$		$-\sum_{i=1-9,11-25} C_i\nu_{i,6}$	$-\sum_{i=1-10,12-25} N_i\nu_{i,6}$							Y_{aa}									ρ_6
7	Uptake of LCFA			−1.0				$(1-Y_{fa})0.70$	$(1-Y_{fa})0.30$		$-\sum_{i=1-9,11-25} C_i\nu_{i,7}$	$-Y_{fa}N_{bac}$								Y_{fa}							ρ_7
8	Uptake of valerate				−1.0		$(1-Y_{c4})0.54$	$(1-Y_{c4})0.31$	$(1-Y_{c4})0.15$		$-\sum_{i=1-9,11-25} C_i\nu_{i,8}$	$-Y_{c4}N_{bac}$									Y_{c4}						ρ_8
9	Uptake of butyrate					−1.0		$(1-Y_{c4})0.80$	$(1-Y_{c4})0.20$		$-\sum_{i=1-9,11-25} C_i\nu_{i,9}$	$-Y_{c4}N_{bac}$									Y_{c4}						ρ_9
10	Uptake of propionate						−1.0	$(1-Y_{pro})0.57$	$(1-Y_{pro})0.43$		$-\sum_{i=1-9,11-25} C_i\nu_{i,10}$	$-Y_{pro}N_{bac}$										Y_{pro}					ρ_{10}
11	Uptake of acetate							−1.0		$(1-Y_{ac})$	$-\sum_{i=1-9,11-25} C_i\nu_{i,11}$	$-Y_{ac}N_{bac}$											Y_{ac}				ρ_{11}
11b	Uptake acetate oxidisers							−1.0	$(1-Y_{ac2})$		$-\sum_{i=1-9,11-25} C_i\nu_{i,11b}$	$-Y_{ac2}N_{bac}$												Y_{ac2}			ρ_{11b}
12	Uptake of hydrogen								−1.0	$(1-Y_{h2})$	$-\sum_{i=1-9,11-25} C_i\nu_{i,12}$	$-Y_{h2}N_{bac}$													Y_{h2}		ρ_{12}
13	Decay of Xsu										$-\sum_{i=1-9,11-25} C_i\nu_{i,13}$	$-\sum_{i=1-10,12-25} N_i\nu_{i,13}$		1.0				−1.0										ρ_{13}
14	Decay of Xaa										$-\sum_{i=1-9,11-25} C_i\nu_{i,14}$	$-\sum_{i=1-10,12-25} N_i\nu_{i,14}$		1.0					−1.0									ρ_{14}
15	Decay of Xfa										$-\sum_{i=1-9,11-25} C_i\nu_{i,15}$	$-\sum_{i=1-10,12-25} N_i\nu_{i,15}$		1.0						−1.0								ρ_{15}
16	Decay of Xc4										$-\sum_{i=1-9,11-25} C_i\nu_{i,16}$	$-\sum_{i=1-10,12-25} N_i\nu_{i,16}$		1.0							−1.0							ρ_{16}
17	Decay of Xpro										$-\sum_{i=1-9,11-25} C_i\nu_{i,17}$	$-\sum_{i=1-10,12-25} N_i\nu_{i,17}$		1.0								−1.0						ρ_{17}
18	Decay of Xac										$-\sum_{i=1-9,11-25} C_i\nu_{i,18}$	$-\sum_{i=1-10,12-25} N_i\nu_{i,18}$		1.0									−1.0					ρ_{18}
18b	Decay of Xac2										$-\sum_{i=1-9,11-25} C_i\nu_{i,18b}$	$-\sum_{i=1-10,12-25} N_i\nu_{i,18b}$		1.0										−1.0				ρ_{18b}
19	Decay of Xh2										$-\sum_{i=1-9,11-25} C_i\nu_{i,19}$	$-\sum_{i=1-10,12-25} N_i\nu_{i,19}$		1.0											−1.0			ρ_{19}
		Monosacchrides (kgCOD m^{-3})	Amino acids (kgCOD m^{-3})	LCFAs (kgCOD m^{-3})	Total valerate (kgCOD m^{-3})	Total butyrate (kgCOD m^{-3})	Total propionate (kgCOD m^{-3})	Total acetate (kgCOD m^{-3})	Hydrogen gas (kgCOD m^{-3})	Methane gas (kgCOD m^{-3})	Inorganic carbon (M)	Inorganic nitrogen (M)	Soluble inerts (kgCOD m^{-3})	Composites (kgCOD m^{-3})	Carbohydrates (kg COD m^{-3})	Proteins (kg COD m^{-3})	Lipids (kg COD m^{-3})	Sugar degraders (kg COD m^{-3})	Amino acid degraders (kgCOD m^{-3})	LCFA degraders (kgCOD m^{-3})	Valerate and butyrate degraders(kg COD m^{-3})	Propiorate degraders (kgCOD m^{-3})	Acetate degraders (kgCOD m^{-3})	Acetate oxidisers (kgCOD m^{-3})	Hydrogen degraders (kgCOD m^{-3})	Particulate inerts (kgCOD m^{-3})	

This page is intentionally left blank

Appendix B: ADM1 parameters and variables

Table B1 Stoichiometric parameters

Parameter	Value	Unit	Source of data
$f_{sI,xc}$	0.0061	–	(*b*)
$f_{xI,xc}$	0.0861	–	(*b*)
$f_{ch,xc}$	0.7319	–	(*b*)
$f_{pr,xc}$	0.1544	–	(*b*)
$f_{li,xc}$	0.0215	–	(*b*)
$f_{fa,li}$	0.95	–	(*a*)
$f_{h2,su}$	0.19	–	(*a*)
$f_{bu,su}$	0.13	–	(*a*)
$f_{pro,su}$	0.27	–	(*a*)
$f_{ac,su}$	0.41	–	(*a*)
$f_{h2,aa}$	0.06	–	(*a*)
$f_{va,aa}$	0.23	–	(*a*)
$f_{bu,aa}$	0.26	–	(*a*)
$f_{pro,aa}$	0.05	–	(*a*)
$f_{ac,aa}$	0.40	–	(*a*)
C_{xc}	0.0313	kmoleC kgCOD^{-1}	(*b*)
C_{sI}	0.0313	kmoleC kgCOD^{-1}	(*b*)
C_{ch}	0.0313	kmoleC kgCOD^{-1}	(*a*)
C_{pr}	0.03	kmoleC kgCOD^{-1}	(*a*)
C_{li}	0.022	kmoleC kgCOD^{-1}	(*a*)
C_{xI}	0.03	kmoleC kgCOD^{-1}	(*a*)
C_{su}	0.0313	kmoleC kgCOD^{-1}	(*a*)
C_{aa}	0.03	kmoleC kgCOD^{-1}	(*a*)
C_{fa}	0.0217	kmoleC kgCOD^{-1}	(*a*)
C_{bu}	0.025	kmoleC kgCOD^{-1}	(*a*)
C_{pro}	0.0268	kmoleC kgCOD^{-1}	(*a*)
C_{ac}	0.0313	kmoleC kgCOD^{-1}	(*a*)
C_{bac}	0.0313	kmoleC kgCOD^{-1}	(*a*)
C_{va}	0.024	kmoleC kgCOD^{-1}	(*a*)
C_{ch4}	0.0156	kmoleC kgCOD^{-1}	(*a*)
N_{xc}	0.0016	kmoleN kgCOD^{-1}	(*b*)
N_I	0.03/14	kmoleN kgCOD^{-1}	(*b*)
N_{aa}	0.007	kmoleN kgCOD^{-1}	(*a*)
N_{bac}	0.03/14	kmoleN kgCOD^{-1}	(*b*)

Source of data:

(*a*) value suggested in original ADM1 report (Batstone *et al.*, 2002).

(b) estimated value based on food waste substrate used in this study.

Table B2 Biochemical parameters

Parameter	Value	Unit	Source of data
k_{dis}	0.55	day^{-1}	(*c*)
$k_{hyd,ch}$	0.5	day^{-1}	(*b*)
$k_{hyd,pr}$	0.25	day^{-1}	(*b*)
$k_{hyd,li}$	0.1	day^{-1}	(*b*)
$k_{m,su}$	30	day^{-1}	(*a*)
$k_{m,aa}$	50	day^{-1}	(*a*)
$k_{m,fa}$	6	day^{-1}	(*a*)
$k_{m,c4}$	20	day^{-1}	(*a*)
$k_{m,pro}$	13	day^{-1}	(*a*)
$k_{m,ac}$	8	day^{-1}	(*a*)
$k_{m,h2}$	35	day^{-1}	(*a*)
$k_{dec,Xsu}$	0.02	day^{-1}	(*a*)
$k_{dec,Xaa}$	0.02	day^{-1}	(*a*)
$k_{dec,Xfa}$	0.02	day^{-1}	(*a*)
$k_{dec,Xc4}$	0.02	day^{-1}	(*a*)
$k_{dec,Xpro}$	0.02	day^{-1}	(*a*)
$k_{dec,Xac}$	0.02	day^{-1}	(*a*)
$k_{dec,Xh2}$	0.02	day^{-1}	(*a*)
$K_{S,IN}$	1E–4	kmoleN m^{-3}	(*a*)
$K_{S,su}$	0.5	kgCOD m^{-3}	(*a*)
$K_{S,aa}$	0.3	kgCOD m^{-3}	(*a*)
$K_{S,fa}$	0.4	kgCOD m^{-3}	(*a*)
$K_{S,pro}$	0.1	kgCOD m^{-3}	(*a*)
$K_{S,ac}$	0.15	kgCOD m^{-3}	(*a*)
$K_{S,c4}$	0.2	kgCOD m^{-3}	(*a*)
$K_{S,h2}$	7E–6	kgCOD m^{-3}	(*a*)
$K_{I,h2,fa}$	5E–6	kgCOD m^{-3}	(*a*)
$K_{I,h2,pro}$	3.5E–6	kgCOD m^{-3}	(*a*)
$K_{I,h2,c4}$	1E–5	kgCOD m^{-3}	(*a*)
$K_{I,nh3}$	0.0018	kmoleN m^{-3}	(*a*)
$K_{I,h2,ac2}$	1.3E–8	kgCOD m^{-3}	(*a*)
$pH_{UL,aa}$	5.5	–	(*a*)
$pH_{LL,aa}$	4	–	(*a*)
$pH_{UL,ac}$	7	–	(*a*)
$pH_{LL,ac}$	6	–	(*a*)
$pH_{UL,h2}$	6	–	(*a*)
$pH_{LL,h2}$	5	–	(*a*)

Source of data:

(*a*) value suggested in original ADM1 report (Batstone *et al.*, 2002).

(*b*) (Garcia-Heras, 2003).

(*c*) (Vavilin *et al.*, 2004).

Table B3 Physiochemical parameter values

Parameter	Value	Unit	Source of data
k_La	150	day^{-1}	assumed from data in (*f*)
T_{base}	298.15	K	
T_{op}	308.15	K	assumed digester works at 35°C
K_w	$\approx 2.0932\times10^{-14}$	M	
$pK_{w,base}$	13.997	–	(*b*)
$K_{a,va}$	$10^{-pK_{a,va,base}} \approx 1.38\times10^{-5}$	M	
$K_{a,bu}$	$10^{-pK_{a,bu,base}} \approx 1.51\times10^{-5}$	M	
$K_{a,pro}$	$10^{-pK_{a,pro,base}} \approx 1.32\times10^{-5}$	M	
$K_{a,ac}$	$10^{-pK_{a,ac,base}} \approx 1.74\times10^{-5}$	M	
$pK_{a,va,base}$	4.86	–	(*d*)
$pK_{a,bu,base}$	4.82	–	(*c*)
$pK_{a,pro,base}$	4.87	–	(*b*)
$pK_{a,ac,base}$	4.76	–	(*b*)
$pK_{a,co2,base}$	6.35	–	(*b*)
$pK_{a,IN,base}$	9.25	–	(*b*), assumed Ammonium ion
$K_{a,co2}$	$\approx 4.937\times10^{-7}$	M	
$K_{a,IN}$	$\approx 1.1103\times10^{-9}$	M	
$k_{A,Bva}$	1E+10	$M^{-1}\ day^{-1}$	(*e*)
$k_{A,Bbu}$	1E+10	$M^{-1}\ day^{-1}$	(*e*)
$k_{A,Bpro}$	1E+10	$M^{-1}\ day^{-1}$	(*e*)
$k_{A,Bac}$	1E+10	$M^{-1}\ day^{-1}$	(*e*)
$k_{A,Bco2}$	1E+10	$M^{-1}\ day^{-1}$	(*e*)
$k_{A,BIN}$	1E+10	$M^{-1}\ day^{-1}$	(*e*)
P_{atm}	1.013	bar	
$P_{gas,h2o}$	≈ 0.05567	bar	
k_p	10000	$m^3 day^{-1} bar^{-1}$	(*a*)
$K_{H,co2}$	≈ 0.0271467	$M_{liq}\ bar^{-1}$	
$K_{H,ch4}$	≈ 0.0011619	$M_{liq}\ bar^{-1}$	
$K_{H,h2}$	$\approx 7.3846\times10^{-4}$	$M_{liq}\ bar^{-1}$	
$K_{H,h2o,base}$	0.0313	$M_{liq}\ bar^{-1}$	(*h*)
$K_{H,co2,base}$	0.034	$M_{liq}\ bar^{-1}$	(*g*)
$K_{H,ch4,base}$	0.0014	$M_{liq}\ bar^{-1}$	(*a*)
$K_{H,h2,base}$	0.001	$M_{liq}\ bar^{-1}$	(*a*)

Note: M = 1000 mole m^{-3}

Source of data:

(*a*): value suggested in original ADM1 report (Batstone *et al.*, 2002).

(*b*): (Purich & Allison, 1999).

(c): (Kell *et al.*, 1981).
(*d*): (Kopf *et al.*, 1996).
(*e*): (Rosen *et al.*, 2006).
(*f*): (Siegrist *et al.*, 2002).
(*g*): Table 14.2 of (Treichel *et al.*).
(h): (Rosen & Jeppsson, 2005).

$$K_w = 10^{-pK_{w,base}} \cdot \exp\left(\frac{55900}{R \cdot 100} \cdot \left(\frac{1}{T_{base}} - \frac{1}{T_{op}}\right)\right)$$

$$K_{a,co2} = 10^{-pK_{a,co2,base}} \cdot \exp\left(\frac{7646}{R \cdot 100} \cdot \left(\frac{1}{T_{base}} - \frac{1}{T_{op}}\right)\right)$$

$$K_{a,IN} = 10^{-pK_{a,IN,base}} \cdot \exp\left(\frac{51965}{R \cdot 100} \cdot \left(\frac{1}{T_{base}} - \frac{1}{T_{op}}\right)\right)$$

$$P_{gas,h2o} = 0.0313 \cdot \exp\left(5290\left(\frac{1}{T_{base}} - \frac{1}{T_{op}}\right)\right)$$

$$K_{H,co2} = 0.035 \cdot \exp\left(\frac{-19410}{R \cdot 100} \cdot \left(\frac{1}{T_{base}} - \frac{1}{T_{op}}\right)\right)$$

$$K_{H,ch4} = 0.0014 \cdot \exp\left(\frac{-14240}{R \cdot 100} \cdot \left(\frac{1}{T_{base}} - \frac{1}{T_{op}}\right)\right)$$

$$K_{H,h2} = 0.0014 \exp\left(\frac{-14240}{R \cdot 100} \cdot \left(\frac{1}{T_{base}} - \frac{1}{T_{op}}\right)\right)$$

Table B4 Extented parameters for the modified ADM1 model

Parameter	Value	Unit	Expression
Yield uptake component, rates of disintegration, hydrolysis and coefficients			
Y_{ac2}	0.05	–	Yield uptake acetate oxidisers
$k_{m,ac2}$	8	day^{-1}	maximum uptake rate of acetate oxidisers
$k_{dec,Xac2}$	0.02	day^{-1}	biomass decay of acetate oxidisers
Half saturation coefficients and 50% inhibitory concentrations			
$K_{S,ac2}$	0.15	kgCOD m^{-3}	half saturation coefficient of acetate oxidisers
$K_{I\!h2,ac2}$	3.5E–6	kgCOD m^{-3}	50% inhibitory concentration of H_2 to acetate oxidation
Acid and gas parameters			
$pH_{UL,ac2}$	7	–	Upper pH limit for acetate oxidation
$pH_{LL,ac2}$	6	–	Lower pH limit for acetate oxidation

Appendix C: Benchmark parameters and variables

This appendix represents parameter values of the benchmark ADM1 models for verification in Chapter 4.

C.1 Steady–state simulation (Rosen & Jeppsson, 2005)

Table C1 Stoichiometric values of benchmark steady–state simulation

Parameter	Value	Unit
$f_{sI,xc}$	0.1	–
$f_{xI,xc}$	0.2	–
$f_{ch,xc}$	0.2	–
$f_{pr,xc}$	0.2	–
$f_{li,xc}$	0.3	–
$f_{fa,li}$	0.95	–
$f_{h2,su}$	0.19	–
$f_{bu,su}$	0.13	–
$f_{pro,su}$	0.27	–
$f_{ac,su}$	0.41	–
$f_{h2,aa}$	0.06	–
$f_{va,aa}$	0.23	–
$f_{bu,aa}$	0.26	–
$f_{pro,aa}$	0.05	–
$f_{ac,aa}$	0.40	–
C_{xc}	0.02786	kmoleC kgCOD^{-1}
C_{sI}	0.03	kmoleC kgCOD^{-1}
C_{ch}	0.0313	kmoleC kgCOD^{-1}
C_{pr}	0.03	kmoleC kgCOD^{-1}
C_{li}	0.022	kmoleC kgCOD^{-1}
C_{xI}	0.03	kmoleC kgCOD^{-1}
C_{su}	0.0313	kmoleC kgCOD^{-1}
C_{aa}	0.03	kmoleC kgCOD^{-1}
C_{fa}	0.0217	kmoleC kgCOD^{-1}
C_{bu}	0.025	kmoleC kgCOD^{-1}
C_{pro}	0.0268	kmoleC kgCOD^{-1}
C_{ac}	0.0313	kmoleC kgCOD^{-1}
C_{bac}	0.0313	kmoleC kgCOD^{-1}
C_{va}	0.024	kmoleC kgCOD^{-1}
C_{ch4}	0.0156	kmoleC kgCOD^{-1}
N_{xc}	0.0376/14	kmoleN kgCOD^{-1}
N_I	0.06/14	kmoleN kgCOD^{-1}
N_{aa}	0.007	kmoleN kgCOD^{-1}
N_{bac}	0.08/14	kmoleN kgCOD^{-1}

Note that Carbon contents C_{h2} and C_{IN} are equal to zero.

Table C2 Biochemical values of benchmark steady–state simulation

Parameter	Value	Unit
k_{dis}	0.5	day^{-1}
$k_{hyd,ch}$	10	day^{-1}
$k_{hyd,pr}$	10	day^{-1}
$k_{hyd,li}$	10	day^{-1}
$k_{m,su}$	30	day^{-1}
$k_{m,aa}$	50	day^{-1}
$k_{m,fa}$	6	day^{-1}
$k_{m,c4}$	20	day^{-1}
$k_{m,pro}$	13	day^{-1}
$k_{m,ac}$	8	day^{-1}
$k_{m,h2}$	35	day^{-1}
$k_{dec,Xsu}$	0.02	day^{-1}
$k_{dec,Xaa}$	0.02	day^{-1}
$k_{dec,Xfa}$	0.02	day^{-1}
$k_{dec,Xc4}$	0.02	day^{-1}
$k_{dec,Xpro}$	0.02	day^{-1}
$k_{dec,Xac}$	0.02	day^{-1}
$k_{dec,Xh2}$	0.02	day^{-1}
$K_{S,IN}$	1E–4	kmoleN m^{-3}
$K_{S,su}$	0.5	kgCOD m^{-3}
$K_{S,aa}$	0.3	kgCOD m^{-3}
$K_{S,fa}$	0.4	kgCOD m^{-3}
$K_{S,pro}$	0.1	kgCOD m^{-3}
$K_{S,ac}$	0.15	kgCOD m^{-3}
$K_{S,c4}$	0.2	kgCOD m^{-3}
$K_{S,h2}$	7E–6	kgCOD m^{-3}
$K_{I,h2,fa}$	5E–6	kgCOD m^{-3}
$K_{I,h2,pro}$	3.5E–6	kgCOD m^{-3}
$K_{I,h2,c4}$	1E–5	kgCOD m^{-3}
$K_{I,nh3}$	0.0018	kmoleN m^{-3}
$pH_{UL,aa}$	5.5	–
$pH_{LL,aa}$	4	–
$pH_{UL,ac}$	7	–
$pH_{LL,ac}$	6	–
$pH_{UL,h2}$	6	–
$pH_{LL,h2}$	5	–

Table C3 Physiochemical values of benchmark steady–state simulation

Parameter	Value	Unit
$k_L a$	200	day^{-1}
T_{base}	298.15	K
T_{op}	308.15	K
K_w	$\exp\left(\frac{55900}{R \cdot 100} \cdot \left(\frac{1}{T_{base}} - \frac{1}{T_{op}}\right)\right)$	M 10^{-14}
$K_{a,va}$	$10^{-4.86}$	M
$K_{a,bu}$	$10^{-4.82}$	M
$K_{a,pro}$	$10^{-4.88}$	M
$K_{a,ac}$	$10^{-4.76}$	M
$K_{a,co2}$	$10^{-6.35} \exp\left(\frac{7646}{R \cdot 100} \cdot \left(\frac{1}{T_{base}} - \frac{1}{T_{op}}\right)\right)$	M
$K_{a,IN}$	$10^{-9.25} \exp\left(\frac{51965}{R \cdot 100} \cdot \left(\frac{1}{T_{base}} - \frac{1}{T_{op}}\right)\right)$	M
$k_{A,Bva}$	1E+10	M day^{-1}
$k_{A,Bbu}$	1E+10	M day^{-1}
$k_{A,Bpro}$	1E+10	M day^{-1}
$k_{A,Bac}$	1E+10	M day^{-1}
$k_{A,Bco2}$	1E+10	M day^{-1}
$k_{A,BIN}$	1E+10	M day^{-1}
P_{atm}	1.013	bar
$P_{gas,h2o}$	$0.0313 \exp\left(5290\left(\frac{1}{T_{base}} - \frac{1}{T_{op}}\right)\right)$	bar
k_p	5E+4	$m^3 day^{-1} bar^{-1}$
$K_{H,co2}$	$0.035 \exp\left(\frac{51965}{R \cdot 100} \cdot \left(\frac{1}{T_{base}} - \frac{1}{T_{op}}\right)\right)$	M_{liq} bar^{-1}
$K_{H,ch4}$	$0.0014 \exp\left(\frac{-14240}{R \cdot 100} \cdot \left(\frac{1}{T_{base}} - \frac{1}{T_{op}}\right)\right)$	M_{liq} bar^{-1}
$K_{H,h2}$	$0.0014 \exp\left(\frac{-14240}{R \cdot 100} \cdot \left(\frac{1}{T_{base}} - \frac{1}{T_{op}}\right)\right)$	M_{liq} bar^{-1}

Note: M = 1000 mole m^{-3}

Table C4 Model inputs of benchmark steady–state simulation

Stage No.	Variable	Unit	Value
1	$S_{su,f}$	kgCOD m^{-3}	0.01
2	$S_{aa,f}$	kgCOD m^{-3}	0.001
3	$S_{fa,f}$	kgCOD m^{-3}	0.001
4	$S_{va,f}$	kgCOD m^{-3}	0.001
5	$S_{bu,f}$	kgCOD m^{-3}	0.001
6	$S_{pro,f}$	kgCOD m^{-3}	0.001
7	$S_{ac,f}$	kgCOD m^{-3}	0.001
8	$S_{h2,f}$	kgCOD m^{-3}	1E–8
9	$S_{ch4,f}$	kgCOD m^{-3}	1E–5
10	$S_{IC,f}$	kgCOD m^{-3}	0.04
11	$S_{IN,f}$	kgCOD m^{-3}	0.01
12	$S_{I,f}$	kgCOD m^{-3}	0.02
13	$X_{xc,f}$	kgCOD m^{-3}	2.0
14	$X_{ch,f}$	kgCOD m^{-3}	5.0
15	$X_{pr,f}$	kgCOD m^{-3}	20.0
16	$X_{li,f}$	kgCOD m^{-3}	5.0
17	$X_{su,f}$	kgCOD m^{-3}	0.0
18	$X_{aa,f}$	kgCOD m^{-3}	0.01
19	$X_{fa,f}$	kgCOD m^{-3}	0.01
20	$X_{c4,f}$	kgCOD m^{-3}	0.01
21	$X_{pro,f}$	kgCOD m^{-3}	0.01
22	$X_{ac,f}$	kgCOD m^{-3}	0.01
23	$X_{h2,f}$	kgCOD m^{-3}	0.01
24	$X_{I,f}$	kgCOD m^{-3}	25.0
25	$S_{cat,f}$	kmole m^{-3}	0.04
26	$S_{an,f}$	kmole	0.02

Table C5 Inoculum (initial) conditions of benchmark steady–state simulation

No	Component	Value	Unit	No	Component	Value	Unit
1	$S_{su,ini}$	0.011	kgCOD m^{-3}	19	$X_{fa,ini}$	0.200	kgCOD m^{-3}
2	$S_{aa,ini}$	0.005	kgCOD m^{-3}	20	$X_{c4,ini}$	0.400	kgCOD m^{-3}
3	$S_{fa,ini}$	0.099	kgCOD m^{-3}	21	$X_{pro,ini}$	0.100	kgCOD m^{-3}
4	$S_{va,ini}$	0.012	kgCOD m^{-3}	22	$X_{ac,ini}$	0.760	kgCOD m^{-3}
5	$S_{bu,ini}$	0.013	kgCOD m^{-3}	23	$X_{h2,ini}$	0.310	kgCOD m^{-3}
6	$S_{pro,ini}$	0.015	kgCOD m^{-3}	24	$X_{I,ini}$	25.610	kgCOD m^{-3}
7	$S_{ac,ini}$	0.100	kgCOD m^{-3}	25	$S_{cat,ion,ini}$	0.040	kmole m^{-3}
8	$S_{h2,ini}$	2.00E–07	kgCOD m^{-3}	26	$S_{an,ion,ini}$	0.020	kmole m^{-3}
9	$S_{ch4,ini}$	0.050	kgCOD m^{-3}	27	$S_{va,ion,ini}$	0.011	kgCOD m^{-3}
10	$S_{IC,ini}$	0.100	kmoleC m^{-3}	28	$S_{bu,ion,ini}$	0.013	kgCOD m^{-3}
11	$S_{IN,ini}$	0.130	kmoleN m^{-3}	29	$S_{pro,ion,ini}$	0.015	kgCOD m^{-3}
12	$S_{I,ini}$	0.320	kgCOD m^{-3}	30	$S_{ac,ion,ini}$	0.190	kgCOD m^{-3}
13	$X_{c,ini}$	0.300	kgCOD m^{-3}	31	$S_{hco3,ion,ini}$	0.140	kmole m^{-3}
14	$X_{ch,ini}$	0.020	kgCOD m^{-3}	32	$S_{nh3,ion,ini}$	0.004	kmoleN m^{-3}
15	$X_{pr,ini}$	0.102	kgCOD m^{-3}	33	$S_{gas,h2,ini}$	1.02E–05	kgCOD m^{-3}
16	$X_{li,ini}$	0.020	kgCOD m^{-3}	34	$S_{gas,ch4,ini}$	1.625	kgCOD m^{-3}
17	$X_{su,ini}$	0.420	kgCOD m^{-3}	35	$S_{gas,co2,ini}$	0.014	kmoleC m^{-3}
18	$X_{aa,ini}$	1.100	kgCOD m^{-3}	36	$S_{h,ion,ini}$	3.40E–08	kmoleH^+ m^{-3}

C.2 Dynamic simulation (Thamsiriroj & Murphy, 2011)

Table C6 Stoichiometric values of benchmark dynamic simulation

Parameter	Value	Unit	Note
$f_{sI,xc}$	0.00	–	
$f_{xI,xc}$	0.075	–	
$f_{ch,xc}$	0.797	–	
$f_{pr,xc}$	0.095	–	
$f_{li,xc}$	0.033	–	
$f_{fa,li}$	0.950	–	
$f_{h2,su}$	0.190	–	
$f_{bu,su}$	0.130	–	
$f_{pro,su}$	0.270	–	
$f_{ac,su}$	0.410	–	
$f_{h2,aa}$	0.060	–	
$f_{va,aa}$	0.230	–	
$f_{bu,aa}$	0.260	–	
$f_{pro,aa}$	0.050	–	
$f_{ac,aa}$	0.400	–	
C_{xc}	0.0308	kmoleC kgCOD^{-1}	
C_{sI}	0.03	kmoleC kgCOD^{-1}	
C_{ch}	0.0313	kmoleC kgCOD^{-1}	
C_{pr}	0.03	kmoleC kgCOD^{-1}	
C_{li}	0.022	kmoleC kgCOD^{-1}	
C_{xI}	0.03	kmoleC kgCOD^{-1}	
C_{su}	0.0313	kmoleC kgCOD^{-1}	
C_{aa}	0.03	kmoleC kgCOD^{-1}	
C_{fa}	0.0217	kmoleC kgCOD^{-1}	
C_{bu}	0.025	kmoleC kgCOD^{-1}	
C_{pro}	0.0268	kmoleC kgCOD^{-1}	
C_{ac}	0.0313	kmoleC kgCOD^{-1}	
C_{bac}	0.0313	kmoleC kgCOD^{-1}	
C_{va}	0.024	kmoleC kgCOD^{-1}	
C_{ch4}	0.0156	kmoleC kgCOD^{-1}	
N_{xc}	0.00089	kmoleN kgCOD^{-1}	
N_I	0.003	kmoleN kgCOD^{-1}	
N_{aa}	0.007	kmoleN kgCOD^{-1}	
N_{bac}	0.005714	kmoleN kgCOD^{-1}	

Note that Carbon contents C_{h2} and C_{IN} are equal to zero.

Table C7 Biochemical values of benchmark dynamic simulation

Parameter	Value	Unit	Note
k_{dis}	0.05	day^{-1}	
$k_{hyd,ch}$	10	day^{-1}	
$k_{hyd,pr}$	10	day^{-1}	
$k_{hyd,li}$	10	day^{-1}	
$k_{m,su}$	30	day^{-1}	
$k_{m,aa}$	50	day^{-1}	
$k_{m,fa}$	6	day^{-1}	
$k_{m,c4}$	13.7	day^{-1}	
$k_{m,pro}$	5.5	day^{-1}	
$k_{m,ac}$	7.1	day^{-1}	
$k_{m,h2}$	35	day^{-1}	
$k_{dec,Xsu}$	0.02	day^{-1}	
$k_{dec,Xaa}$	0.02	day^{-1}	
$k_{dec,Xfa}$	0.02	day^{-1}	
$k_{dec,Xc4}$	0.02	day^{-1}	
$k_{dec,Xpro}$	0.02	day^{-1}	
$k_{dec,Xac}$	0.02	day^{-1}	
$k_{dec,Xh2}$	0.02	day^{-1}	
$K_{S,IN}$	1E–4	kmoleN m^{-3}	
$K_{S,su}$	0.5	kgCOD m^{-3}	
$K_{S,aa}$	0.3	kgCOD m^{-3}	
$K_{S,fa}$	0.4	kgCOD m^{-3}	
$K_{S,pro}$	0.392	kgCOD m^{-3}	
$K_{S,ac}$	0.15	kgCOD m^{-3}	
$K_{S,c4}$	0.357	kgCOD m^{-3}	
$K_{S,h2}$	3E–5	kgCOD m^{-3}	
$K_{Ih2,fa}$	5E–6	kgCOD m^{-3}	
$K_{Ih2,pro}$	3.5E–6	kgCOD m^{-3}	
$K_{Ih2,c4}$	1E–5	kgCOD m^{-3}	
$K_{I,nh3}$	0.0018	kmoleN m^{-3}	
$pH_{UL,aa}$	5.5	–	
$pH_{LL,aa}$	4	–	
$pH_{UL,ac}$	7	–	
$pH_{LL,ac}$	6	–	
$pH_{UL,h2}$	6	–	
$pH_{LL,h2}$	5	–	

Table C8 Model inputs of benchmark dynamic simulation

Stage No.	Variable	Unit	Value
1	$S_{su,f}$	kgCOD m^{-3}	16.352
2	$S_{aa,f}$	kgCOD m^{-3}	0.00
3	$S_{fa,f}$	kgCOD m^{-3}	0.00
4	$S_{va,f}$	kgCOD m^{-3}	0.5
5	$S_{bu,f}$	kgCOD m^{-3}	0.892
6	$S_{pro,f}$	kgCOD m^{-3}	0.317
7	$S_{ac,f}$	kgCOD m^{-3}	4.185
8	$S_{h2,f}$	kgCOD m^{-3}	0.00
9	$S_{ch4,f}$	kgCOD m^{-3}	0.00
10	$S_{IC,f}$	kgCOD m^{-3}	0.00
11	$S_{IN,f}$	kgCOD m^{-3}	0.00
12	$S_{I,f}$	kgCOD m^{-3}	0.00
13	$X_{xc,f}$	kgCOD m^{-3}	370.682
14	$X_{ch,f}$	kgCOD m^{-3}	0.0
15	$X_{pr,f}$	kgCOD m^{-3}	0.0
16	$X_{li,f}$	kgCOD m^{-3}	0.0
17	$X_{su,f}$	kgCOD m^{-3}	0.01
18	$X_{aa,f}$	kgCOD m^{-3}	0.01
19	$X_{fa,f}$	kgCOD m^{-3}	0.01
20	$X_{c4,f}$	kgCOD m^{-3}	0.01
21	$X_{pro,f}$	kgCOD m^{-3}	0.01
22	$X_{ac,f}$	kgCOD m^{-3}	0.01
23	$X_{h2,f}$	kgCOD m^{-3}	0.01
24	$X_{I,f}$	kgCOD m^{-3}	25.0
25	$S_{cat,f}$	kmole m^{-3}	0.04
26	$S_{an,f}$	kmole	0.02

Table C9 Initial conditons of benchmark dynamic simulation

Stage No.	Variable	Unit	Value
1	$S_{su,ini}$	kgCOD m^{-3}	–
2	$S_{aa,ini}$	kgCOD m^{-3}	–
3	$S_{fa,ini}$	kgCOD m^{-3}	–
4	$S_{va,ini}$	kgCOD m^{-3}	0.0092
5	$S_{bu,ini}$	kgCOD m^{-3}	0.0164
6	$S_{pro,ini}$	kgCOD m^{-3}	0.0068
7	$S_{ac,ini}$	kgCOD m^{-3}	0.0768
8	$S_{h2,ini}$	kgCOD m^{-3}	0
9	$S_{ch4,ini}$	kgCOD m^{-3}	0.01
10	$S_{IC,ini}$	kgCOD m^{-3}	0.045
11	$S_{IN,ini}$	kgCOD m^{-3}	0.005
12	$S_{I,ini}$	kgCOD m^{-3}	0
13	$X_{xc,ini}$	kgCOD m^{-3}	8.889
14	$X_{ch,ini}$	kgCOD m^{-3}	0
15	$X_{pr,ini}$	kgCOD m^{-3}	0
16	$X_{li,ini}$	kgCOD m^{-3}	0
17	$X_{su,ini}$	kgCOD m^{-3}	0.42
18	$X_{aa,ini}$	kgCOD m^{-3}	1.18
19	$X_{fa,ini}$	kgCOD m^{-3}	0.24
20	$X_{c4,ini}$	kgCOD m^{-3}	0.3
21	$X_{pro,ini}$	kgCOD m^{-3}	0.27
22	$X_{ac,ini}$	kgCOD m^{-3}	0.7
23	$X_{h2,ini}$	kgCOD m^{-3}	0.31
24	$X_{I,ini}$	kgCOD m^{-3}	6.595
25	$S_{cat,ini}$	kmole m^{-3}	0.01
26	$S_{an,ini}$	kmole	0.6
27	$S_{h,ion,ini}$	kmoleH^+ m^{-3}	2.24E–7

This page is intentionally left blank

Appendix D: ADM1 source code package

This appendix provides the extended ADM1 model package. Basically, The the package consist of 4 files (3 MATLAB Code files and 1 Excel files):

- ADM1data.xlsx: Stores model input (substrate), model initial conditions as well as all stoichiometric, physiochemical and biochemical kinetic parameters implemented.
- globalvariables.m: Imports all data from ADM1data.xlsx file to the MATLAB environment.
- ADDE.m: Executes calculations, conversions, etc.
- ad.m: Solves the system of differential equations in ADDE.m file and generates graphs (model outputs) plus extra calculations.

D.1 ADM1data.xlsx file

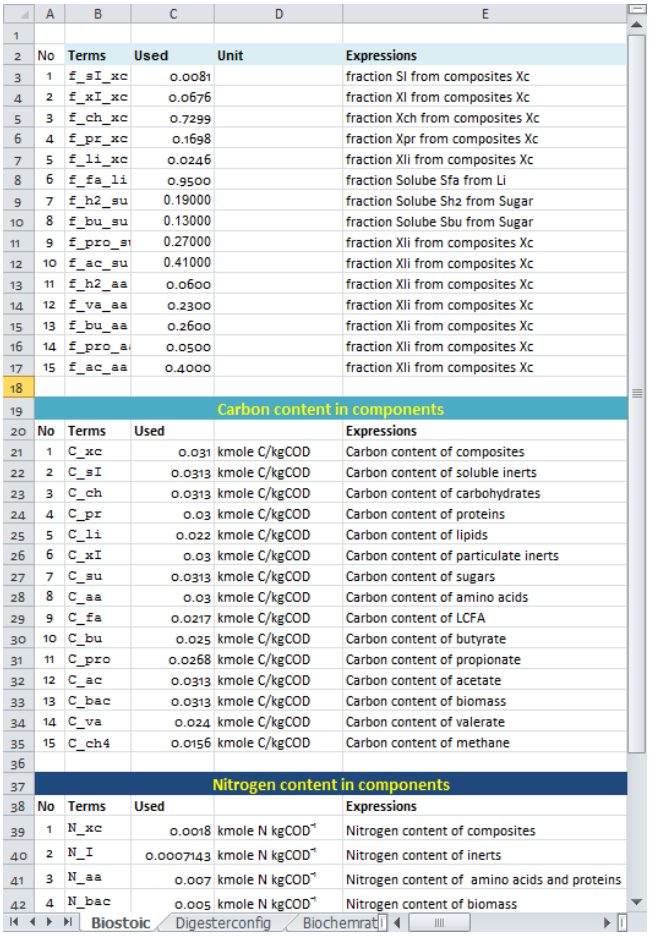

No	Terms	Used	Unit	Expressions
1	f_sI_xc	0.0081		fraction SI from composites Xc
2	f_xI_xc	0.0676		fraction XI from composites Xc
3	f_ch_xc	0.7299		fraction Xch from composites Xc
4	f_pr_xc	0.1698		fraction Xpr from composites Xc
5	f_li_xc	0.0246		fraction Xli from composites Xc
6	f_fa_li	0.9500		fraction Solube Sfa from Li
7	f_h2_su	0.19000		fraction Solube Sh2 from Sugar
8	f_bu_su	0.13000		fraction Solube Sbu from Sugar
9	f_pro_s	0.27000		fraction Xli from composites Xc
10	f_ac_su	0.41000		fraction Xli from composites Xc
11	f_h2_aa	0.0600		fraction Xli from composites Xc
12	f_va_aa	0.2300		fraction Xli from composites Xc
13	f_bu_aa	0.2600		fraction Xli from composites Xc
14	f_pro_a	0.0500		fraction Xli from composites Xc
15	f_ac_aa	0.4000		fraction Xli from composites Xc

Carbon content in components

No	Terms	Used		Expressions
1	C_xc	0.031	kmole C/kgCOD	Carbon content of composites
2	C_sI	0.0313	kmole C/kgCOD	Carbon content of soluble inerts
3	C_ch	0.0313	kmole C/kgCOD	Carbon content of carbohydrates
4	C_pr	0.03	kmole C/kgCOD	Carbon content of proteins
5	C_li	0.022	kmole C/kgCOD	Carbon content of lipids
6	C_xI	0.03	kmole C/kgCOD	Carbon content of particulate inerts
7	C_su	0.0313	kmole C/kgCOD	Carbon content of sugars
8	C_aa	0.03	kmole C/kgCOD	Carbon content of amino acids
9	C_fa	0.0217	kmole C/kgCOD	Carbon content of LCFA
10	C_bu	0.025	kmole C/kgCOD	Carbon content of butyrate
11	C_pro	0.0268	kmole C/kgCOD	Carbon content of propionate
12	C_ac	0.0313	kmole C/kgCOD	Carbon content of acetate
13	C_bac	0.0313	kmole C/kgCOD	Carbon content of biomass
14	C_va	0.024	kmole C/kgCOD	Carbon content of valerate
15	C_ch4	0.0156	kmole C/kgCOD	Carbon content of methane

Nitrogen content in components

No	Terms	Used		Expressions
1	N_xc	0.0018	kmole N kgCOD^{-1}	Nitrogen content of composites
2	N_I	0.0007143	kmole N kgCOD^{-1}	Nitrogen content of inerts
3	N_aa	0.007	kmole N kgCOD^{-1}	Nitrogen content of amino acids and proteins
4	N_bac	0.005	kmole N kgCOD^{-1}	Nitrogen content of biomass

Figure D.1 Stoichiometric parameters in ADM1data.xlsx

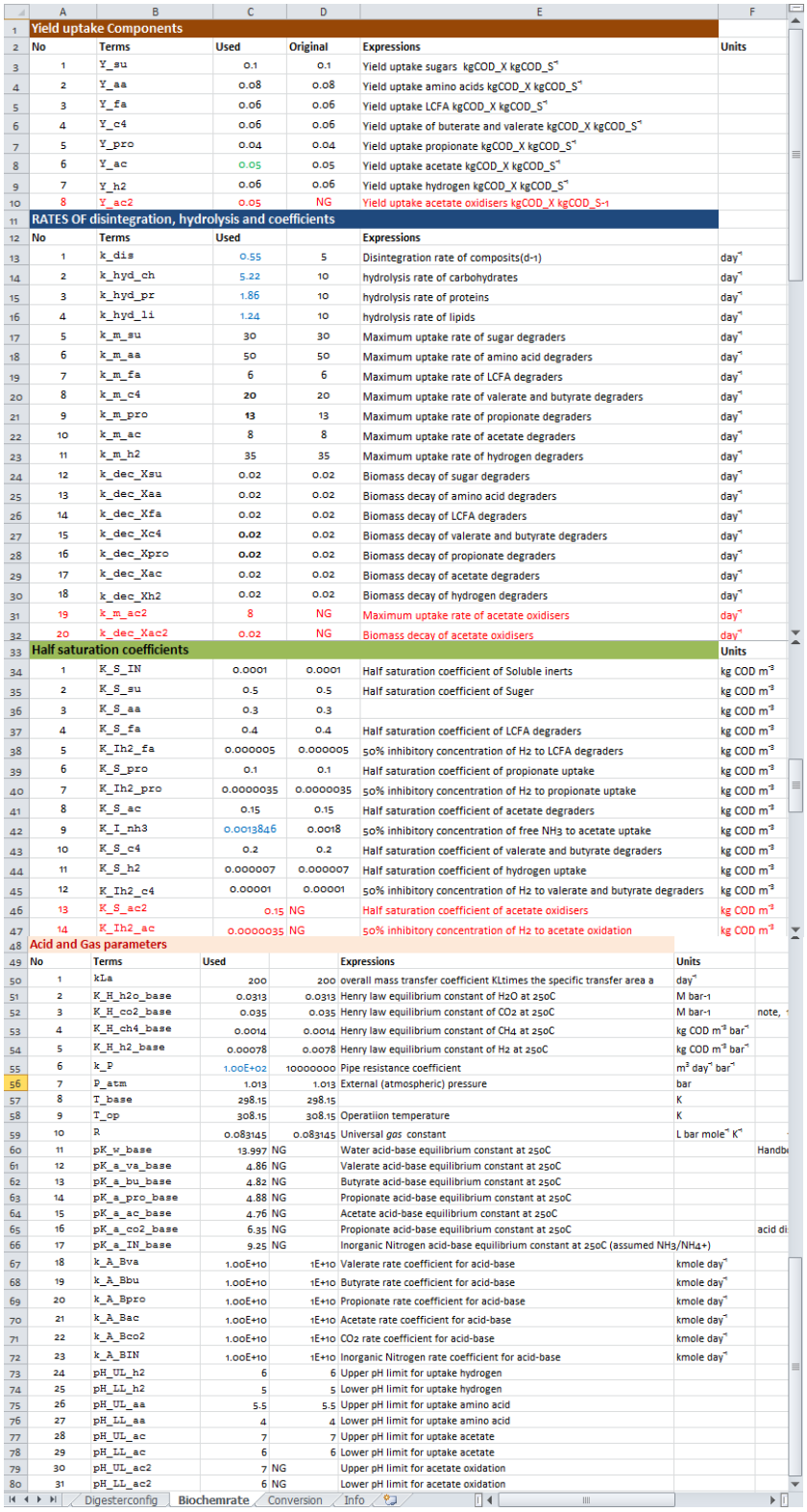

	A	B	C	D	E	F
1	**Yield uptake Components**					
2	**No**	**Terms**	**Used**	**Original**	**Expressions**	**Units**
3	1	Y_su	0.1	0.1	Yield uptake sugars kgCOD_X kgCOD_S^{-1}	
4	2	Y_aa	0.08	0.08	Yield uptake amino acids kgCOD_X kgCOD_S^{-1}	
5	3	Y_fa	0.06	0.06	Yield uptake LCFA kgCOD_X kgCOD_S^{-1}	
6	4	Y_c4	0.06	0.06	Yield uptake of buterate and valerate kgCOD_X kgCOD_S^{-1}	
7	5	Y_pro	0.04	0.04	Yield uptake propionate kgCOD_X kgCOD_S^{-1}	
8	6	Y_ac	0.05	0.05	Yield uptake acetate kgCOD_X kgCOD_S^{-1}	
9	7	Y_h2	0.06	0.06	Yield uptake hydrogen kgCOD_X kgCOD_S^{-1}	
10	8	Y_ac2	0.05	NG	Yield uptake acetate oxidisers kgCOD_X kgCOD_S-1	
11	**RATES OF disintegration, hydrolysis and coefficients**					
12	**No**	**Terms**	**Used**		**Expressions**	
13	1	k_dis	0.55	5	Disintegration rate of composits(d-1)	day^{-1}
14	2	k_hyd_ch	5.22	10	hydrolysis rate of carbohydrates	day^{-1}
15	3	k_hyd_pr	1.86	10	hydrolysis rate of proteins	day^{-1}
16	4	k_hyd_li	1.24	10	hydrolysis rate of lipids	day^{-1}
17	5	k_m_su	30	30	Maximum uptake rate of sugar degraders	day^{-1}
18	6	k_m_aa	50	50	Maximum uptake rate of amino acid degraders	day^{-1}
19	7	k_m_fa	6	6	Maximum uptake rate of LCFA degraders	day^{-1}
20	8	k_m_c4	20	20	Maximum uptake rate of valerate and butyrate degraders	day^{-1}
21	9	k_m_pro	13	13	Maximum uptake rate of propionate degraders	day^{-1}
22	10	k_m_ac	8	8	Maximum uptake rate of acetate degraders	day^{-1}
23	11	k_m_h2	35	35	Maximum uptake rate of hydrogen degraders	day^{-1}
24	12	k_dec_Xsu	0.02	0.02	Biomass decay of sugar degraders	day^{-1}
25	13	k_dec_Xaa	0.02	0.02	Biomass decay of amino acid degraders	day^{-1}
26	14	k_dec_Xfa	0.02	0.02	Biomass decay of LCFA degraders	day^{-1}
27	15	k_dec_Xc4	0.02	0.02	Biomass decay of valerate and butyrate degraders	day^{-1}
28	16	k_dec_Xpro	0.02	0.02	Biomass decay of propionate degraders	day^{-1}
29	17	k_dec_Xac	0.02	0.02	Biomass decay of acetate degraders	day^{-1}
30	18	k_dec_Xh2	0.02	0.02	Biomass decay of hydrogen degraders	day^{-1}
31	19	k_m_ac2	8	NG	Maximum uptake rate of acetate oxidisers	day^{-1}
32	20	k_dec_Xac2	0.02	NG	Biomass decay of acetate oxidisers	day^{-1}
33	**Half saturation coefficients**					**Units**
34	1	K_S_IN	0.0001	0.0001	Half saturation coefficient of Soluble inerts	kg COD m^{-3}
35	2	K_S_su	0.5	0.5	Half saturation coefficient of Suger	kg COD m^{-3}
36	3	K_S_aa	0.3	0.3		kg COD m^{-3}
37	4	K_S_fa	0.4	0.4	Half saturation coefficient of LCFA degraders	kg COD m^{-3}
38	5	K_Ih2_fa	0.000005	0.000005	50% inhibitory concentration of H2 to LCFA degraders	kg COD m^{-3}
39	6	K_S_pro	0.1	0.1	Half saturation coefficient of propionate uptake	kg COD m^{-3}
40	7	K_Ih2_pro	0.0000035	0.0000035	50% inhibitory concentration of H2 to propionate uptake	kg COD m^{-3}
41	8	K_S_ac	0.15	0.15	Half saturation coefficient of acetate degraders	kg COD m^{-3}
42	9	K_I_nh3	0.0013846	0.0018	50% inhibitory concentration of free NH3 to acetate uptake	kg COD m^{-3}
43	10	K_S_c4	0.2	0.2	Half saturation coefficient of valerate and butyrate degraders	kg COD m^{-3}
44	11	K_S_h2	0.000007	0.000007	Half saturation coefficient of hydrogen uptake	kg COD m^{-3}
45	12	K_Ih2_c4	0.00001	0.00001	50% inhibitory concentration of H2 to valerate and butyrate degraders	kg COD m^{-3}
46	13	K_S_ac2	0.15	NG	Half saturation coefficient of acetate oxidisers	kg COD m^{-3}
47	14	K_Ih2_ac	0.0000035	NG	50% inhibitory concentration of H2 to acetate oxidation	kg COD m^{-3}
48	**Acid and Gas parameters**					
49	**No**	**Terms**	**Used**		**Expressions**	**Units**
50	1	kLa	200	200	overall mass transfer coefficient KLtimes the specific transfer area a	day^{-1}
51	2	K_H_h2o_base	0.0313	0.0313	Henry law equilibrium constant of H2O at 250C	M bar-1
52	3	K_H_co2_base	0.035	0.035	Henry law equilibrium constant of CO2 at 250C	M bar-1
53	4	K_H_ch4_base	0.0014	0.0014	Henry law equilibrium constant of CH4 at 250C	kg COD m^{-3} bar^{-1}
54	5	K_H_h2_base	0.00078	0.0078	Henry law equilibrium constant of H2 at 250C	kg COD m^{-3} bar^{-1}
55	6	k_P	1.00E+02	10000000	Pipe resistance coefficient	m^{3} day^{-1} bar^{-1}
56	7	P_atm	1.013	1.013	External (atmospheric) pressure	bar
57	8	T_base	298.15	298.15		K
58	9	T_op	308.15	308.15	Operatiion temperature	K
59	10	R	0.083145	0.083145	Universal *gas* constant	L bar mole^{-1} K^{-1}
60	11	pK_w_base	13.997	NG	Water acid-base equilibrium constant at 250C	
61	12	pK_a_va_base	4.86	NG	Valerate acid-base equilibrium constant at 250C	
62	13	pK_a_bu_base	4.82	NG	Butyrate acid-base equilibrium constant at 250C	
63	14	pK_a_pro_base	4.88	NG	Propionate acid-base equilibrium constant at 250C	
64	15	pK_a_ac_base	4.76	NG	Acetate acid-base equilibrium constant at 250C	
65	16	pK_a_co2_base	6.35	NG	Propionate acid-base equilibrium constant at 250C	
66	17	pK_a_IN_base	9.25	NG	Inorganic Nitrogen acid-base equilibrium constant at 250C (assumed NH3/NH4+)	
67	18	k_A_Bva	1.00E+10	1E+10	Valerate rate coefficient for acid-base	kmole day^{-1}
68	19	k_A_Bbu	1.00E+10	1E+10	Butyrate rate coefficient for acid-base	kmole day^{-1}
69	20	k_A_Bpro	1.00E+10	1E+10	Propionate rate coefficient for acid-base	kmole day^{-1}
70	21	k_A_Bac	1.00E+10	1E+10	Acetate rate coefficient for acid-base	kmole day^{-1}
71	22	k_A_Bco2	1.00E+10	1E+10	CO2 rate coefficient for acid-base	kmole day^{-1}
72	23	k_A_BIN	1.00E+10	1E+10	Inorganic Nitrogen rate coefficient for acid-base	kmole day^{-1}
73	24	pH_UL_h2	6	6	Upper pH limit for uptake hydrogen	
74	25	pH_LL_h2	5	5	Lower pH limit for uptake hydrogen	
75	26	pH_UL_aa	5.5	5.5	Upper pH limit for uptake amino acid	
76	27	pH_LL_aa	4	4	Lower pH limit for uptake amino acid	
77	28	pH_UL_ac	7	7	Upper pH limit for uptake acetate	
78	29	pH_LL_ac	6	6	Lower pH limit for uptake acetate	
79	30	pH_UL_ac2	7	NG	Upper pH limit for acetate oxidation	
80	31	pH_LL_ac2	6	NG	Lower pH limit for acetate oxidation	

Digesterconfig | Biochemrate | Conversion | Info

Figure D.2 Physiochemical and biochemical kinetic parameters in ADM1data.xlsx

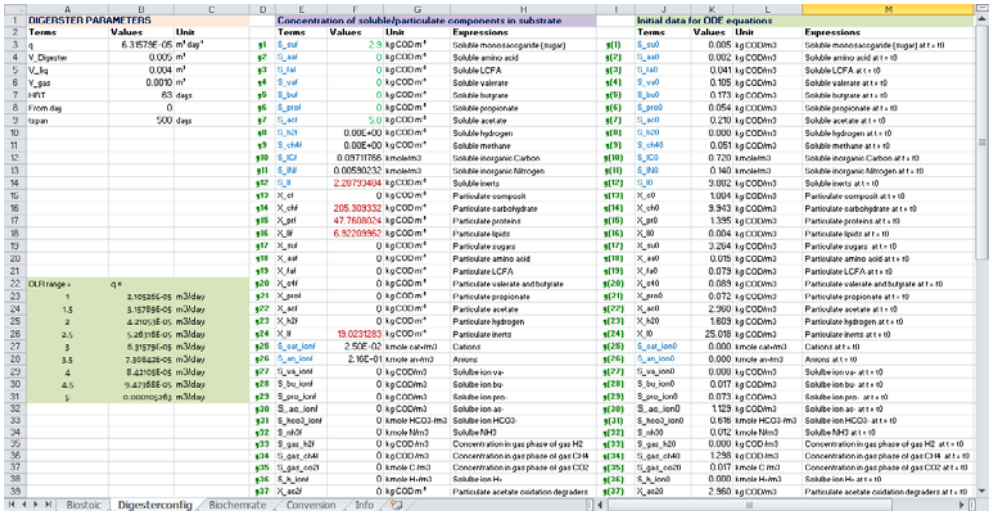

Figure D.3 Inputs and inoculum conditions in ADM1data.xlsx

D.2 MATLAB Code for Extended ADM1 model

globalvariables.m file

```
% ------------------------------------------------------------------------|
% Copyright (2014)by Hoa Huu Nguyen (a,b)                                 |
% (a)Water and Environmental Engineering Group                            |
%    Faculty of Engineering and the Environment                           |
%    University of Southampton, Southampton, United Kingdom.              |
%    Website: http://www.southampton.ac.uk                                |
% b) National University of Civil Engineering, Vietnam                    |
%    Website: http://nuce.edu.vn/index.php?lg=2                           |
% This work had accomplished as parts of the thesis:                      |
% MODELLING OF FOOD WASTE DIGESTION USING ADM1 INTEGRATED WITH ASPEN PLUS|
% This extended ADM1 platform was developed based on original ADM1 report|
% conducted by Batstone et al. 2002 and updates as specified in the thesis.|
% Sources of knowledge, data used (where relevant) were stated in the thesis.|
% ------------------------------------------------------------------------|
% NOTE:                                                                   |
% This Extended ADM1 model is published for OPEN ACCESS                   |
% This package of model consists of 3 MATLAB Code and 1 MS Excel file.    |
% Please make sure all the notations, file names, parameters are as in    |
% original version to avoid errors.                                       |
% Please refer to the above thesis when you use any parts this work.      |
% THANK YOU !                                                             |
% ------------------------------------------------------------------------|
%                          GUIDE TO RUN THE MODEL                         |
% 1. The set of stoichiometric and physico/biochemical parameters provided |
% are for "typical" food waste. You can change any of them for other types |
% of substrate as well as other operational condtions. However, all tables |
```

```
% MUST be kept in their forms.                                              |
% 2. MATLAB command line, type in: globalvariables (enter)                  |
% 3. MATLAB command line, type in: ad(tspan,u) (enter)                      |
% Note: To run model as original (NO acetate oxidation pathway), indicate |
% inhibition factors: I11b =  I18b = 0 before doing step (3) above.        |
% ---------------------------------------------------------------------------|

format long
clear all

%^^^^^^^^^^^^^^^^^^^^^^^^^^^^^^^^^
%---------------------------------
% Digester configurations and tspan

global q
global V_dig
global V_liq
global V_gas
global tspan
global u
global maxx

%^^^^^^^^^^^^^^^^^^^^^^^^^^^^^^^^^^^^^^^^^^^^^^^^^^^^^^^^^^^^^^^^^^^^^^^^
%-------------------------------------------------------------------------
% Variables of soluble and particulate components come in digester

global S_suf
global S_aaf
global S_faf
global S_vaf
global S_buf
global S_prof
global S_acf
global S_h2f
global S_ch4f
global S_ICf
global S_INf
global S_If
global X_cf
global X_chf
global X_prf
global X_lif
global X_suf
global X_aaf
global X_faf
global X_c4f
```

```
global X_prof
global X_acf
global X_ac2f
global X_h2f
global X_If
global S_cat_ionf
global S_an_ionf
global S_va_ionf
global S_bu_ionf
global S_pro_ionf
global S_ac_ionf
global S_hco3_ionf
global S_nh3f
global S_gas_h2f
global S_gas_ch4f
global S_gas_co2f
global S_h_ionf



%^^^^^^^^^^^^^^^^^^^^^^^^^^^^^^^^^
%---------------------------------
%Fraction of each components in Xc

global f_sI_xc
global f_xI_xc
global f_ch_xc
global f_pr_xc
global f_li_xc
global f_fa_li
global f_h2_su
global f_bu_su
global f_pro_su
global f_ac_su
global f_h2_aa
global f_va_aa
global f_bu_aa
global f_pro_aa
global f_ac_aa

%^^^^^^^^^^^^^^^^^^^^^^^^^^^^^^^^^^^^^^^^^^^^^^^^
% -----------------------------------------------
% Carbon and Nitrogen concentration in components

global C_xc
global C_sI
```

```
global C_ch
global C_pr
global C_li
global C_xI
global C_su
global C_aa
global C_fa
global C_bu
global C_pro
global C_ac
global C_bac
global C_va
global C_ch4
global N_xc
global N_I
global N_aa
global N_bac

%^^^^^^^^^^^^^^^^^^^^^^^^
%------------------------
% Yield uptake Components

global Y_su
global Y_aa
global Y_fa
global Y_c4
global Y_pro
global Y_ac
global Y_ac2
global Y_h2




%^^^^^^^^^^^^^^^^^^^^^^^^^^^^^^^^^^^^^^^^^^^^^^^^^^^^^^^^^^^^^^^^
%----------------------------------------------------------------
% RATES OF disintegration, hydrolysis and coefficients

global k_dis
global k_hyd_ch
global k_hyd_pr
global k_hyd_li
global k_m_su
global k_m_aa
global k_m_fa
global k_m_c4
global k_m_pro
```

```
global k_m_ac
global k_m_ac2
global k_m_h2
global k_dec_Xsu
global k_dec_Xaa
global k_dec_Xfa
global k_dec_Xc4
global k_dec_Xpro
global k_dec_Xac
global k_dec_Xac2
global k_dec_Xh2

%^^^^^^^^^^^^^^^^^^^^^^^^^^^^
%----------------------------
% Half saturation coefficients

global K_S_IN
global K_S_su
global K_S_aa
global K_S_fa
global K_Ih2_fa
global K_S_pro
global K_Ih2_pro
global K_S_ac
global K_S_ac2
global K_I_nh3
global K_S_c4
global K_S_h2
global K_Ih2_c4

%^^^^^^^^^^^^^^^^^^^^^^^^
%------------------------
% Acid and Gas parameters

global kLa
global K_H_h2o_base
global K_H_co2_base
global K_H_ch4_base
global K_H_h2_base
global k_P
global P_atm
global T_base
global T_op
global R
global pK_w_base
global pK_a_va_base
global pK_a_bu_base
```

```
global pK_a_pro_base
global pK_a_ac_base
global pK_a_co2_base
global pK_a_IN_base
global k_A_Bva
global k_A_Bbu
global k_A_Bpro
global k_A_Bac
global k_A_Bco2
global k_A_BIN
global pH_UL_h2
global pH_LL_h2
global pH_UL_aa
global pH_LL_aa
global pH_UL_ac
global pH_LL_ac
global pH_UL_ac2
global pH_LL_ac2
global K_Ih2_ac

%^^^^^^^^^^^^^^^^^^^^^^^^
%------------------------
% Inhibition factors

global pHLim_aa
global pHLim_ac
global pHLim_ac2
global pHLim_h2
global k_aa
global k_ac
global k_ac2
global k_h2
global I11a;
global I11b;
global I18a;
global I18b;

%
%

u = xlsread('ADM1data','Digesterconfig','K3:K39'); % Initial conditions
for DEs
Inputs = xlsread('ADM1data','Digesterconfig','F3:F39');
Digesterconfig = xlsread('ADM1data','Digesterconfig','B3:B9');
Fraction = xlsread('ADM1data','Biostoic','C3 : C17');
Carbonstoichiometries = xlsread('ADM1data','Biostoic','C21 : C35');
Nitrogenstoichiometries = xlsread('ADM1data','Biostoic','C39 : C42');
```

```
Yielduptakecomponents = xlsread('ADM1data','Biochemrate','C3:C10');
Dishydcoefficients = xlsread('ADM1data','Biochemrate','C13:C32');
Halfsaturatecoefficients = xlsread('ADM1data','Biochemrate','C34:C47');
Acidgasparameters = xlsread('ADM1data','Biochemrate','C50:C80');

%
%
q = Digesterconfig(1);
V_dig = Digesterconfig(2);
V_liq = Digesterconfig(3);
V_gas = Digesterconfig(4);
tspan = [Digesterconfig(6) Digesterconfig(7)];
maxx = Digesterconfig(7);
%
%

S_suf  =  Inputs(1);
S_aaf  =  Inputs(2);
S_faf  =  Inputs(3);
S_vaf  =  Inputs(4);
S_buf  =  Inputs(5);
S_prof =  Inputs(6);
S_acf  =  Inputs(7);
S_h2f  =  Inputs(8);
S_ch4f =  Inputs(9);
S_ICf  =  Inputs(10);
S_INf  =  Inputs(11);
S_If   =  Inputs(12);
X_cf   =  Inputs(13);
X_chf  =  Inputs(14);
X_prf  =  Inputs(15);
X_lif  =  Inputs(16);
X_suf  =  Inputs(17);
X_aaf  =  Inputs(18);
X_faf  =  Inputs(19);
X_c4f  =  Inputs(20);
X_prof =  Inputs(21);
X_acf  =  Inputs(22);
X_h2f  =  Inputs(23);
X_If   =  Inputs(24);
S_cat_ionf  =  Inputs(25);
S_an_ionf   =  Inputs(26);
S_va_ionf   =  Inputs(27);
S_bu_ionf   =  Inputs(28);
S_pro_ionf  =  Inputs(29);
S_ac_ionf   =  Inputs(30);
S_hco3_ionf =  Inputs(31);
```

```
S_nh3f      =  Inputs(32);
S_gas_h2f   =  Inputs(33);
S_gas_ch4f  =  Inputs(34);
S_gas_co2f  =  Inputs(35);
S_h_ionf    =  Inputs(36);
X_ac2f      =  Inputs(37);

%
%
f_sI_xc   = Fraction (1,1);
f_xI_xc   = Fraction (2,1);
f_ch_xc   = Fraction (3,1);
f_pr_xc   = Fraction (4,1);
f_li_xc   = Fraction (5,1);
f_fa_li   = Fraction (6,1);
f_h2_su   = Fraction (7,1);
f_bu_su   = Fraction (8,1);
f_pro_su  = Fraction (9,1);
f_ac_su   = Fraction (10,1);
f_h2_aa   = Fraction (11,1);
f_va_aa   = Fraction (12,1);
f_bu_aa   = Fraction (13,1);
f_pro_aa  = Fraction (14,1);
f_ac_aa   = Fraction (15,1);


%
%
C_xc  = Carbonstoichiometries (1);
C_sI  = Carbonstoichiometries (2);
C_ch  = Carbonstoichiometries (3);
C_pr  = Carbonstoichiometries (4);
C_li  = Carbonstoichiometries (5);
C_xI  = Carbonstoichiometries (6);
C_su  = Carbonstoichiometries (7);
C_aa  = Carbonstoichiometries (8);
C_fa  = Carbonstoichiometries (9);
C_bu  = Carbonstoichiometries (10);
C_pro = Carbonstoichiometries (11);
C_ac  = Carbonstoichiometries (12);
C_bac = Carbonstoichiometries (13);
C_va  = Carbonstoichiometries (14);
C_ch4 = Carbonstoichiometries (15);

%
%
```

```
N_xc   = Nitrogenstoichiometries (1);
N_I    = Nitrogenstoichiometries (2);
N_aa   = Nitrogenstoichiometries (3);
N_bac  = Nitrogenstoichiometries (4);

%
%

Y_su  = Yielduptakecomponents (1);
Y_aa  = Yielduptakecomponents (2);
Y_fa  = Yielduptakecomponents (3);
Y_c4  = Yielduptakecomponents (4);
Y_pro = Yielduptakecomponents (5);
Y_ac  = Yielduptakecomponents (6);
Y_h2  = Yielduptakecomponents (7);
Y_ac2 = Yielduptakecomponents (8);

%
%

k_dis      = Dishydcoefficients (1);
k_hyd_ch   = Dishydcoefficients (2);
k_hyd_pr   = Dishydcoefficients (3);
k_hyd_li   = Dishydcoefficients (4);
k_m_su     = Dishydcoefficients (5);
k_m_aa     = Dishydcoefficients (6);
k_m_fa     = Dishydcoefficients (7);
k_m_c4     = Dishydcoefficients (8);
k_m_pro    = Dishydcoefficients (9);
k_m_ac     = Dishydcoefficients (10);
k_m_h2     = Dishydcoefficients (11);
k_dec_Xsu  = Dishydcoefficients (12);
k_dec_Xaa  = Dishydcoefficients (13);
k_dec_Xfa  = Dishydcoefficients (14);
k_dec_Xc4  = Dishydcoefficients (15);
k_dec_Xpro = Dishydcoefficients (16);
k_dec_Xac  = Dishydcoefficients (17);
k_dec_Xh2  = Dishydcoefficients (18);
k_m_ac2    = Dishydcoefficients (19);
k_dec_Xac2 = Dishydcoefficients (20);

%
%

K_S_IN    = Halfsaturatecoefficients (1);
K_S_su    = Halfsaturatecoefficients (2);
K_S_aa    = Halfsaturatecoefficients (3);
K_S_fa    = Halfsaturatecoefficients (4);
```

```
K_Ih2_fa  = Halfsaturatecoefficients (5);
K_S_pro   = Halfsaturatecoefficients (6);
K_Ih2_pro = Halfsaturatecoefficients (7);
K_S_ac    = Halfsaturatecoefficients (8);
K_I_nh3   = Halfsaturatecoefficients (9);
K_S_c4    = Halfsaturatecoefficients (10);
K_S_h2    = Halfsaturatecoefficients (11);
K_Ih2_c4  = Halfsaturatecoefficients (12);
K_S_ac2   = Halfsaturatecoefficients (13);
K_Ih2_ac  = Halfsaturatecoefficients (14);

%
%

kLa             = Acidgasparameters (1);
K_H_h2o_base    = Acidgasparameters (2);
K_H_co2_base    = Acidgasparameters (3);
K_H_ch4_base    = Acidgasparameters (4);
K_H_h2_base     = Acidgasparameters (5);
k_P             = Acidgasparameters (6);
P_atm           = Acidgasparameters (7);
T_base          = Acidgasparameters (8);
T_op            = Acidgasparameters (9);
R               = Acidgasparameters (10);
pK_w_base       = Acidgasparameters (11);
pK_a_va_base    = Acidgasparameters (12);
pK_a_bu_base    = Acidgasparameters (13);
pK_a_pro_base   = Acidgasparameters (14);
pK_a_ac_base    = Acidgasparameters (15);
pK_a_co2_base   = Acidgasparameters (16);
pK_a_IN_base    = Acidgasparameters (17);
k_A_Bva         = Acidgasparameters (18);
k_A_Bbu         = Acidgasparameters (19);
k_A_Bpro        = Acidgasparameters (20);
k_A_Bac         = Acidgasparameters (21);
k_A_Bco2        = Acidgasparameters (22);
k_A_BIN         = Acidgasparameters (23);
pH_UL_h2        = Acidgasparameters (24);
pH_LL_h2        = Acidgasparameters (25);
pH_UL_aa        = Acidgasparameters (26);
pH_LL_aa        = Acidgasparameters (27);
pH_UL_ac        = Acidgasparameters (28);
pH_LL_ac        = Acidgasparameters (29);
pH_UL_ac2       = Acidgasparameters (30);
pH_LL_ac2       = Acidgasparameters (31);

%^^^^^^^^^^^^^^^^^^^^^^^^^^^^^^^^^^^^^^^^^^^^^^^^^^^^^^^^^^^^^^^^^^^^^^^^^^^^^^^^
```

```
%-------------------------------------------------------------------------
% The method suggested by Siegrist et al. (2002) used a Hill inhibition
% function based on the hydrogen ion concentration instead to calculate
% inhibition factors.

pHLim_aa = 10^(-(pH_UL_aa + pH_LL_aa)/2.0);
pHLim_ac = 10^(-(pH_UL_ac + pH_LL_ac)/2.0);
pHLim_ac2 = 10^(-(pH_UL_ac2 + pH_LL_ac2)/2.0);
pHLim_h2 = 10^(-(pH_UL_h2 + pH_LL_h2)/2.0);
k_aa = 3.0/(pH_UL_aa-pH_LL_aa);
k_ac = 3.0/(pH_UL_ac-pH_LL_ac);
k_ac2 = 3.0/(pH_UL_ac2-pH_LL_ac2);
k_h2 = 3.0/(pH_UL_h2-pH_LL_h2);

%^^^^^^^^^^^^^^^^^^^^^^^^^^^^^^^^^^^^^^^^^^^^^^^^^^^^^^^^^^^^^^^^^^^^^^^^
%-------------------------------------------------------------
% Setup initial condition for running both pathways AC & AO

I11a = 1;
I11b = 1;
I18a = 1;
I18b = 1;

%^^^^^^^^^^^^^^^^^^^^^^^^^^^^^^^^^^^^
%--------------------------------
% Delete all the temporary variables
clear Inputs;
clear Digesterconfig;
clear Fraction;
clear Carbonstoichiometries;
clear Nitrogenstoichiometries;
clear Yielduptakecomponents;
clear Dishydcoefficients;
clear Halfsaturatecoefficients;
clear Acidgasparameters;
save  saveddata
```

ADDE.m file

```
function [y1] = ADDE(t,y)
y1 = zeros(size(y));


format long

%^^^^^^^^^^^^^^^^^^^^^^^^^^^^^^^^^^
%----------------------------------
% Digester configurations and tspan

global q
global V_liq % Volume of liquid part
global V_gas % Volume of gas space


%^^^^^^^^^^^^^^^^^^^^^^^^^^^^^^^^^^^^^^^^^^^^^^^^^^^^^^^^^^^^^^^^^^^^^^^^^^^^
%-------------------------------------------------------------------------
% Variables of soluble and particulate components come in digester

global S_suf
global S_aaf
global S_faf
global S_vaf
global S_buf
global S_prof
global S_acf
global S_h2f
global S_ch4f
global S_ICf
global S_INf
global S_If
global X_cf
global X_chf
global X_prf
global X_lif
global X_suf
global X_aaf
global X_faf
global X_c4f
global X_prof
global X_acf
global X_ac2f
global X_h2f
```

```
global X_If
global S_cat_ionf
global S_an_ionf

%^^^^^^^^^^^^^^^^^^^^^^^^^^^^^^^^^
%---------------------------------
%Fraction of each components in Xc

global f_sI_xc
global f_xI_xc
global f_ch_xc
global f_pr_xc
global f_li_xc
global f_fa_li
global f_h2_su
global f_bu_su
global f_pro_su
global f_ac_su
global f_h2_aa
global f_va_aa
global f_bu_aa
global f_pro_aa
global f_ac_aa

%^^^^^^^^^^^^^^^^^^^^^^^^^^^^^^^^^^^^^^^^^^^^^^^^^^^^^^^^^^^^^^^^
% ------------------------------------------------
% Carbon and Nitrogen concentration in components

global C_xc
global C_sI
global C_ch
global C_pr
global C_li
global C_xI
global C_su
global C_aa
global C_fa
global C_bu
global C_pro
global C_ac
global C_bac
global C_va
global C_ch4
global N_xc
global N_I
global N_aa
global N_bac
```

```
%^^^^^^^^^^^^^^^^^^^^^^^^
%------------------------
% Yield uptake Components

global Y_su
global Y_aa
global Y_fa
global Y_c4
global Y_pro
global Y_ac
global Y_ac2
global Y_h2

%^^^^^^^^^^^^^^^^^^^^^^^^^^^^^^^^^^^^^^^^^^^^^^^^^^^^^^^^^^^^^^^^
%----------------------------------------------------------------
% RATES OF disintegration, hydrolysis and coefficients

global k_dis
global k_hyd_ch
global k_hyd_pr
global k_hyd_li
global k_m_su
global k_m_aa
global k_m_fa
global k_m_c4
global k_m_pro
global k_m_ac
global k_m_ac2
global k_m_h2
global k_dec_Xsu
global k_dec_Xaa
global k_dec_Xfa
global k_dec_Xc4
global k_dec_Xpro
global k_dec_Xac
global k_dec_Xac2
global k_dec_Xh2

%^^^^^^^^^^^^^^^^^^^^^^^^^^^^^^^
%-------------------------------
% Half saturation coefficients

global K_S_IN
global K_S_su
global K_S_aa
```

```
global K_S_fa
global K_Ih2_fa
global K_S_pro
global K_Ih2_pro
global K_S_ac
global K_S_ac2
global K_I_nh3
global K_S_c4
global K_S_h2
global K_Ih2_c4
global K_Ih2_ac

%^^^^^^^^^^^^^^^^^^^^^^^^
%------------------------
% Acid and Gas parameters

global kLa
global K_H_h2o_base
global K_H_co2_base
global K_H_ch4_base
global K_H_h2_base
global k_P
global P_atm
global T_base
global T_op
global R
global pK_w_base
global pK_a_va_base
global pK_a_bu_base
global pK_a_pro_base
global pK_a_ac_base
global pK_a_co2_base
global pK_a_IN_base
global k_A_Bva
global k_A_Bbu
global k_A_Bpro
global k_A_Bac
global k_A_Bco2
global k_A_BIN
global pHLim_aa;
global pHLim_ac;
global pHLim_ac2;
global pHLim_h2;
global k_aa;
global k_ac;
global k_ac2;
global k_h2;
```

```
%^^^^^^^^^^^^^^^^^^^^^^^^
%------------------------
% Inhibition factors

global I11a;
global I11b;
global I18a;
global I18b;
global inhib11b;
global inhib56;
global inhib7;
global inhib89;
global inhib10;
global inhib11;
global inhib12;
global Itec4;
global Itepro;

%^^^^^^^^^^^^^^^^^^^^^^^^^^^^^^^^^^^^
%------------------------------------
% Parameters for gas-phase calculations

global K_a_va
global K_a_bu
global K_a_pro
global K_a_ac
global K_a_co2
global K_a_IN
global K_w
global K_H_h2
global K_H_ch4
global K_H_co2
global p_gas_h2o
global factor

%^^^^^^^^^^^^^^^^^^^^^^^^^^^^^^^^^^^^^^^^^^^^^^^^^^^^^^^^^^^^^^^^^^^^^^^^
%------------------------------------------------------------------------
% Variables for calculation of q_gas according to Batstone

global P_gas
global p_gas_h2
global p_gas_ch4
global p_gas_co2
global q_gas
```

```
%/-----------------------------------------------/
%/              CALCULATIONS SECTION             /
%/-----------------------------------------------/

%-------------------------------------------
%CALCULATION WITHOUT ANY ADJUSTMENT FOR K_H_I
%-------------------------------------------
factor = (1.0/T_base - 1.0/T_op)/(100*R);
K_a_va =10^(-pK_a_va_base);
K_a_bu = 10^(-pK_a_bu_base);
K_a_pro = 10^(-pK_a_pro_base);
K_a_ac = 10^(-pK_a_ac_base);
K_a_co2 = (10^(-pK_a_co2_base))*exp(7646.0*factor); %T adjustment for
K_a_co2
K_a_IN = 10^(-pK_a_IN_base)*exp(51965.0*factor); % T adjustment for
K_a_IN
K_w = 10^(-pK_w_base)*exp(55900.0*factor); % T adjustment for K_w
K_H_h2 = K_H_h2_base*exp(-4180.0*factor);  %/* T adjustment for K_H_h2
K_H_ch4 =  K_H_ch4_base*exp(-14240.0*factor);
K_H_co2 =  K_H_co2_base*exp(-19410.0*factor);
r_A_4 = (    k_A_Bva*(y(27)*(K_a_va + y(36)) - K_a_va*y(4))    );
r_A_5 = (    k_A_Bbu*(y(28)*(K_a_bu + y(36)) - K_a_bu*y(5))    );
r_A_6 = (    k_A_Bpro*(y(29)*(K_a_pro + y(36))- K_a_pro*y(6))    );
r_A_7 = (    k_A_Bac*(y(30)*(K_a_ac + y(36)) - K_a_ac*y(7))    );
r_A_10 =(    k_A_Bco2*(y(31)*(K_a_co2 + y(36)) - K_a_co2*y(10))    ); %
This equation is orriginate from (*) reference
r_A_11 =(    k_A_BIN*(y(32)*(K_a_IN + y(36))  - K_a_IN*y(11))    );   %
Note: S_nh4_ion = S_IN - S_nh3, S_nh4_ion is not S_IN
r_T_8 = (    kLa*(y(8)-16*K_H_h2*(    y(33)*R*T_op/16.0    ))    );
r_T_9 = (    kLa*(y(9)-64*K_H_ch4*(    y(34)*R*T_op/64.0    ))    );
r_T_10 =(    kLa*(y(10)-y(31)-K_H_co2*(    y(35)*R*T_op    ))    );
%--------------- DONE -----------------

%------------------------
% Stoich (i) calculations
%------------------------
stoich1 = -
C_xc+f_sI_xc*C_sI+f_ch_xc*C_ch+f_pr_xc*C_pr+f_li_xc*C_li+f_xI_xc*C_xI;
stoich2 = -C_ch+C_su;
stoich3 = -C_pr+C_aa;
stoich4 = -C_li+(1.0-f_fa_li)*C_su+f_fa_li*C_fa;
```

```
stoich5 = -C_su+(1.0-
Y_su)*(f_bu_su*C_bu+f_pro_su*C_pro+f_ac_su*C_ac)+Y_su*C_bac;
stoich6 = -C_aa+(1.0-
Y_aa)*(f_va_aa*C_va+f_bu_aa*C_bu+f_pro_aa*C_pro+f_ac_aa*C_ac)+Y_aa*C_bac;
stoich7 = -C_fa+(1.0-Y_fa)*0.7*C_ac+Y_fa*C_bac;
stoich8 = -C_va+(1.0-Y_c4)*0.54*C_pro+(1.0-Y_c4)*0.31*C_ac+Y_c4*C_bac;
stoich9 = -C_bu+(1.0-Y_c4)*0.8*C_ac+Y_c4*C_bac;
stoich10 = -C_pro+(1.0-Y_pro)*0.57*C_ac+Y_pro*C_bac;
stoich11 = -C_ac+(1.0-Y_ac)*C_ch4+Y_ac*C_bac;
stoich11b = -C_ac+Y_ac2*C_bac;
stoich12 = (1.0-Y_h2)*C_ch4+Y_h2*C_bac;
stoich13 = -C_bac+C_xc;
%--------------- DONE -----------------

%-------------------------
% Inhibition calculations
%-------------------------
I_pH_aa = pHLim_aa^k_aa /(y(36)^k_aa + pHLim_aa^k_aa);
I_pH_ac = pHLim_ac^k_ac /(y(36)^k_ac + pHLim_ac^k_ac);
I_pH_ac2 = pHLim_ac2^k_ac2 /(y(36)^k_ac2 + pHLim_ac2^k_ac2);
I_pH_h2 = pHLim_h2^k_h2 /(y(36)^k_h2 + pHLim_h2^k_h2);
I_IN_lim = 1.0/(1.0+K_S_IN/y(11));
I_h2_fa = 1.0/(1.0+y(8)/K_Ih2_fa);
I_h2_c4 = 1.0/(1.0+y(8)/K_Ih2_c4);
I_h2_pro = 1.0/(1.0+y(8)/K_Ih2_pro);
I_h2_ac = 1.0/(1.0+y(8)/K_Ih2_ac);
I_nh3 = 1.0/(1.0+y(32)/K_I_nh3);
Itec4 = 1;
Itepro = 1;
inhib56 = I_pH_aa*I_IN_lim;
inhib7 = inhib56*I_h2_fa;
inhib89 = inhib56*I_h2_c4*Itec4;
inhib10 = inhib56*I_h2_pro*Itepro;
inhib11 = I_pH_ac*I_IN_lim*I_nh3*I11a;
inhib11b = I_pH_ac2*I_IN_lim*I_h2_ac*I11b;
inhib12 = I_pH_h2*I_IN_lim;
%--------------- DONE -----------------

%-----------------------------------------------
% Calculate reaction rates ro(1-19) of processes
%-----------------------------------------------
ro1 = k_dis*y(13);
ro2 = k_hyd_ch*y(14);
ro3 = k_hyd_pr*y(15);
ro4 = k_hyd_li*y(16);
ro5 = k_m_su*(y(1)/(y(1)+K_S_su))*y(17)*inhib56;
ro6 = k_m_aa*(y(2)/(K_S_aa+y(2)))*y(18)*inhib56;
```

```
ro7 = k_m_fa*(y(3)/(K_S_fa+y(3)))*y(19)*inhib7;
ro8 = k_m_c4*(y(4)/(K_S_c4+y(4)))*y(20)*(y(4)/(y(5)+y(4)+1e-6))*inhib89;
ro9 = k_m_c4*(y(5)/(K_S_c4+y(5)))*y(20)*(y(5)/(y(4)+y(5)+1e-6))*inhib89;
ro10 = k_m_pro*(y(6)/(K_S_pro+y(6)))*y(21)*inhib10;
ro11 = k_m_ac*(y(7)/(K_S_ac+y(7)))*y(22)*inhib11;
ro11b = k_m_ac2*(y(7)/(K_S_ac2+y(7)))*y(37)*inhib11b; % Acetate Oxidation
ro12 = k_m_h2*(y(8)/(K_S_h2+y(8)))*y(23)*inhib12;
ro13 = k_dec_Xsu*y(17);
ro14 = k_dec_Xaa*y(18);
ro15 = k_dec_Xfa*y(19);
ro16 = k_dec_Xc4*y(20);
ro17 = k_dec_Xpro*y(21);
ro18 = k_dec_Xac*y(22)*I18a;
ro18b = k_dec_Xac2*y(37)*I18b; % Acetate Oxidation
ro19 = k_dec_Xh2*y(23);
%--------------- DONE -----------------

%----------------------
% gas flow calculations
%----------------------
p_gas_h2 = (    y(33)*R*T_op/16.0    );     % p_gas_h2
p_gas_ch4 =(    y(34)*R*T_op/64.0    );    % p_gas_ch4
p_gas_co2 =(    y(35)*R*T_op    );          % p_gas_co2
p_gas_h2o = (K_H_h2o_base*exp(5290.0*(1.0/T_base - 1.0/T_op))    );  % T
adjustement for water vapour saturation pressure
P_gas = (    p_gas_h2+p_gas_ch4+p_gas_co2+p_gas_h2o    );
q_gas = k_P*(P_gas-P_atm)*P_gas/P_atm;
if q_gas <0
   q_gas = 0;
end
%--------------- DONE -----------------


%----------------------
% Differential equations
%----------------------
% S_Su
y1(1) = (q/V_liq)*(S_suf - y(1)) + ro2 +(1-f_fa_li)*ro4  - ro5 ;
% S_aa
y1(2) = (q/V_liq)*(S_aaf - y(2)) + ro3 - ro6;
% S_fa
y1(3) = (q/V_liq)*(S_faf - y(3)) + f_fa_li*ro4 - ro7;
% S_va
y1(4) = (    (q/V_liq)*(S_vaf - y(4)) + (1-Y_aa)*f_va_aa*ro6 - ro8    );
% S_bu
y1(5) = (    (q/V_liq)*(S_buf - y(5)) + (1-Y_su)*f_bu_su*ro5 + (1-
Y_aa)*f_bu_aa*ro6 - ro9    );
```

```
% S_pro
y1(6) = (    (q/V_liq)*(S_prof - y(6)) + (1-Y_su)*f_pro_su*ro5 + (1-
Y_aa)*f_pro_aa*ro6+(1-Y_c4)*0.54*ro8 - ro10    );
% S_ac
y1(7) = (    (q/V_liq)*(S_acf - y(7)) + (1-Y_su)*f_ac_su*ro5 + (1-
Y_aa)*f_ac_aa*ro6 + (1-Y_fa)*0.7*ro7 + (1-Y_c4)*0.31*ro8 + (1-
Y_c4)*0.8*ro9 + (1-Y_pro)*0.57*ro10 - ro11 -ro11b   );
% S_h2
y1(8) = (q/V_liq)*(S_h2f - y(8)) + (1-Y_su)*f_h2_su*ro5 + (1-
Y_aa)*f_h2_aa*ro6 + (1-Y_fa)*0.3*ro7 + (1-Y_c4)*0.15*ro8 + (1-
Y_c4)*0.2*ro9 +(1-Y_pro)*0.43*ro10 + (1-Y_ac2)*ro11b - ro12 -
(    kLa*(y(8)-16*K_H_h2*(y(33)*R*T_op/16))    );
% S_ch4
y1(9) =  (q/V_liq)*(S_ch4f - y(9)) + (1-Y_ac)*ro11 + (1-Y_h2)*ro12 -
(    kLa*(y(9)-64*K_H_ch4*(y(34)*R*T_op/64))    );
% S_IC
y1(10) =  (    (q/V_liq)*(S_ICf - y(10)) - stoich1*ro1-stoich2*ro2-
stoich3*ro3-stoich4*ro4-stoich5*ro5-stoich6*ro6-stoich7*ro7-stoich8*ro8-
stoich9*ro9-stoich10*ro10-stoich11*ro11-stoich11b*ro11b-stoich12*ro12-
stoich13*ro13-stoich13*ro14-stoich13*ro15-stoich13*ro16-stoich13*ro17-
stoich13*ro18-stoich13*ro18b-stoich13*ro19- (    kLa*(y(10)-y(31)-
K_H_co2*(y(35)*R*T_op))    )    );
% S_IN
y1(11) =  (    (q/V_liq)*(S_INf - y(11))-Y_su*N_bac*ro5+(N_aa-
Y_aa*N_bac)*ro6-Y_fa*N_bac*ro7-Y_c4*N_bac*ro8-Y_c4*N_bac*ro9-
Y_pro*N_bac*ro10-Y_ac*N_bac*ro11-Y_ac2*N_bac*ro11b-
Y_h2*N_bac*ro12+(N_bac-
N_xc)*(ro13+ro14+ro15+ro16+ro17+ro18+ro18b+ro19)+(N_xc-f_xI_xc*N_I-
f_sI_xc*N_I-f_pr_xc*N_aa)*ro1    );
% S_I
y1(12) =  (q/V_liq)*(S_If - y(12))+f_sI_xc*ro1;
% X_c
y1(13) =  (q/V_liq)*(X_cf - y(13))- ro1 + ro13 + ro14 + ro15 + ro16 +
ro17 + ro18 + ro18b + ro19;
% X_ch
y1(14) =  (q/V_liq)*(X_chf - y(14)) + f_ch_xc*ro1 - ro2;
% X_pr
y1(15) =  (q/V_liq)*(X_prf - y(15)) + f_pr_xc*ro1 - ro3;
% X_li
y1(16) =  (q/V_liq)*(X_lif - y(16))+ f_li_xc*ro1 - ro4;
% X_su
y1(17) =  (q/V_liq)*(X_suf - y(17)) + Y_su*ro5 - ro13;
% X_aa
y1(18) =  (q/V_liq)*(X_aaf - y(18))+ Y_aa*ro6 - ro14;
% X_fa
y1(19) =  (q/V_liq)*(X_faf - y(19)) + Y_fa*ro7 - ro15;
% X_c4
```

```
y1(20) =  (q/V_liq)*(X_c4f - y(20)) + Y_c4*ro8 + Y_c4*ro9 - ro16;
% X_pro
y1(21) =  (q/V_liq)*(X_prof - y(21)) + Y_pro*ro10 - ro17;
% X_ac
y1(22) =  (q/V_liq)*(X_acf - y(22)) + Y_ac*ro11 - ro18;
% X_h2
y1(23) =  (q/V_liq)*(X_h2f - y(23)) + Y_h2*ro12 - ro19;
% X_I
y1(24) =  (q/V_liq)*(X_If - y(24)) + f_xI_xc*ro1;
% S_cat_ion
y1(25) =  (    (q/V_liq)*(S_cat_ionf - y(25))    );
% S_an_ion
y1(26) =  (    (q/V_liq)*(S_an_ionf - y(26))    );
% S_va_ion
y1(27) =  - r_A_4;
% S_bu_ion
y1(28) =  - r_A_5;
% S_pro_ion
y1(29) =  - r_A_6;
% S_ac_ion
y1(30) =  - r_A_7;
% S_hco3_ion
y1(31) =  - r_A_10;
% S_nh3_ion
y1(32) =  - r_A_11;
% S_gas_h2
y1(33) =  - y(33)*(q_gas/V_gas) +r_T_8*(V_liq/V_gas);
% S_gas_ch4
y1(34) =  - y(34)*(q_gas/V_gas) + r_T_9*(V_liq/V_gas);
% S_gas_co2
y1(35) =  - y(35)*(q_gas/V_gas)+ r_T_10*(V_liq/V_gas);
% S_h_ion
%-----------------------------------------------------------
% Calculation of dS_H+ in the Thamsiriroj and Murphy, 2011
%-----------------------------------------------------------
A1 = (    (q/V_liq)*(S_an_ionf - y(26))    ); % dSan-/dt
A2 =  (    (q/V_liq)*(S_INf - y(11))-Y_su*N_bac*ro5+(N_aa-
Y_aa*N_bac)*ro6-Y_fa*N_bac*ro7-Y_c4*N_bac*ro8-Y_c4*N_bac*ro9-
Y_pro*N_bac*ro10-Y_ac*N_bac*ro11-Y_h2*N_bac*ro12+(N_bac-
N_xc)*(ro13+ro14+ro15+ro16+ro17+ro18+ro19)+(N_xc-f_xI_xc*N_I-f_sI_xc*N_I-
f_pr_xc*N_aa)*ro1    );  % dSIN/dt
A3 = (    (q/V_liq)*(S_ICf - y(10)) - stoich1*ro1-stoich2*ro2-
stoich3*ro3-stoich4*ro4-stoich5*ro5-stoich6*ro6-stoich7*ro7-stoich8*ro8-
stoich9*ro9-stoich10*ro10-stoich11*ro11-stoich11b*ro11b-stoich12*ro12-
stoich13*ro13-stoich13*ro14-stoich13*ro15-stoich13*ro16-stoich13*ro17-
stoich13*ro18-stoich13*ro18b-stoich13*ro19- (    kLa*(y(10)-y(31)-
K_H_co2*(y(35)*R*T_op))    )    );
```

```
A4=(    (q/V_liq)*(S_acf - y(7)) + (1-Y_su)*f_ac_su*ro5 + (1-
Y_aa)*f_ac_aa*ro6 + (1-Y_fa)*0.7*ro7 + (1-Y_c4)*0.31*ro8 + (1-
Y_c4)*0.8*ro9 + (1-Y_pro)*0.57*ro10 - ro11 -ro11b   );
A5 = (    (q/V_liq)*(S_prof - y(6)) + (1-Y_su)*f_pro_su*ro5 + (1-
Y_aa)*f_pro_aa*ro6+(1-Y_c4)*0.54*ro8 - ro10    );
A6 = (    (q/V_liq)*(S_buf - y(5)) + (1-Y_su)*f_bu_su*ro5 + (1-
Y_aa)*f_bu_aa*ro6 - ro9    );
A7 = (    (q/V_liq)*(S_vaf - y(4)) + (1-Y_aa)*f_va_aa*ro6 - ro8    );
A8 = (    (q/V_liq)*(S_INf - y(11))-Y_su*N_bac*ro5+(N_aa-Y_aa*N_bac)*ro6-
Y_fa*N_bac*ro7-Y_c4*N_bac*ro8-Y_c4*N_bac*ro9-Y_pro*N_bac*ro10-
Y_ac*N_bac*ro11-Y_ac2*N_bac*ro11b-Y_h2*N_bac*ro12+(N_bac-
N_xc)*(ro13+ro14+ro15+ro16+ro17+ro18+ro18b+ro19)+(N_xc-f_xI_xc*N_I-
f_sI_xc*N_I-f_pr_xc*N_aa)*ro1    );
A9= (    (q/V_liq)*(S_cat_ionf - y(25))    );
A =
A1+A2*K_a_IN/(K_a_IN+y(36))+A3*K_a_co2/(K_a_co2+y(36))+(1/64)*A4*K_a_ac/(
K_a_ac+y(36))   +  (1/112)*A5*K_a_pro/(K_a_pro+y(36))  +
(1/160)*A6*K_a_bu/(K_a_bu+y(36))  +  (1/208)*A7*K_a_va/(K_a_va+y(36))   -
A8 - A9;
B = 1 + y(11)*K_a_IN/((K_a_IN+y(36))^2)  +
y(10)*K_a_co2/((K_a_co2+y(36))^2)   +
(1/64)*y(7)*K_a_ac/((K_a_ac+y(36))^2)   +
(1/112)*y(6)*K_a_pro/((K_a_pro+y(36))^2)  +
(1/160)*y(5)*K_a_bu/((K_a_bu+y(36))^2)  +
(1/208)*y(4)*K_a_va/((K_a_va+y(36))^2) + K_w/(y(36)^2);
y1(36) = A/B;   % dS_H+ / dt
% X_ac2 decay of ac oxidisers
y1(37) = (q/V_liq)*(X_ac2f - y(37)) + Y_ac2*ro11b - ro18b;

clear q_gas
```

ad.m file

```
% ------------------------------------------------------------------------|
% This file contains codes for solving DEs and examples of output graphs  |
% ------------------------------------------------------------------------|

function ad(tspan,u)
format long
[t,y] = ode15s('ADDE',tspan,u);

%^^^^^^^^^^^^^^^^^^^^^^^^^^^^^
%-----------------------------
% Global Varialbes

global Y_ac2;
global k_m_ac2
global k_m_su;
global K_S_su;
global k_m_aa;
global K_S_aa;
global k_m_fa;
global K_S_fa;
global k_m_c4;
global K_S_c4;
global k_m_pro;
global K_S_pro;
global k_m_ac;
global K_S_ac;
global k_m_h2;
global K_S_h2;
global inhib11b;
global inhib11;
global inhib12;
global inhib56;
global inhib7;
global inhib89;
global inhib10;
global Y_su;
global f_h2_su;
global Y_aa;
global f_h2_aa;
global Y_fa;
global Y_c4;
global Y_pro;
global Y_ac;
global Y_h2;
```

```
global minx
global R
global T_op
global K_H_ch4
global K_H_co2
global K_H_h2
global kLa
global maxx
global K_S_ac2
global af
af = 1.2; % adjustment factor for accurate concentration prediction
minx = 0;


figure (1)
set(gcf, 'color', [1 1 1])
subplot(3,2,1);
plot(t,(T_op/273.15)*1.4*(    kLa*(y(:,8)-
16*K_H_h2*(y(:,33)*R*T_op/16))    ),'Linewidth',2,
'color','r','LineStyle','-');
title('Volumetric production of gas H_2','FontSize',10,
'Fontname','cmr10');
xlabel(['Time ~ ',num2str(tspan(1,2),'%5.4g'),' (days)'],...
    'FontSize',10,'Fontname','cmr10'), ylabel('m^3 H_2 m^-^3 d^-
^1','Rotation',90,'FontSize',10,'Fontname','cmr10'),
xlim([minx maxx])
set(gca,'fontsize',10,'Fontname','cmr10');

subplot(3,2,2);
plot(t,(T_op/273.15)*0.35*(    kLa*(y(:,9)-
64*K_H_ch4*(y(:,34)*R*T_op/64))    ),'Linewidth',2,
'color','g','LineStyle','-');
title('Volumetric production of gas CH_4','FontSize',10,
'Fontname','cmr10');
xlabel(['Time ~ ',num2str(tspan(1,2),'%5.4g'),' (days)'],...
    'FontSize',10,'Fontname','cmr10'), ylabel('m^3 CH_4 m^-^3 d^-
^1','Rotation',90,'FontSize',10, 'Fontname','cmr10'),
xlim([minx maxx])
set(gca,'fontsize',10,'Fontname','cmr10');

subplot(3,2,3);
plot(t,(T_op/273.15)*22.4*(    kLa*(y(:,10)-y(:,31)-
K_H_co2*(y(:,35)*R*T_op))    ) ,'Linewidth',2, 'color','b','LineStyle','-
');
title('Volumetric production of gas CO_2','FontSize',10,
'Fontname','cmr10');
xlabel(['Time ~ ',num2str(tspan(1,2),'%5.4g'),' (days)'],...
```

```
    'FontSize',10,'Fontname','cmr10'), ylabel('m^3 CO_2 m^-^3 d^-
^1','Rotation',90,'FontSize',10,'Fontname','cmr10'),
xlim([minx maxx])
set(gca,'fontsize',10,'Fontname','cmr10');

subplot(3,2,4);
plot(t,(T_op/273.15)*1.4*(    kLa*(y(:,8)-
16*K_H_h2*(y(:,33)*R*T_op/16))    )+(T_op/273.15)*0.35*(    kLa*(y(:,9)-
64*K_H_ch4*(y(:,34)*R*T_op/64))    )+(T_op/273.15)*22.4*(    kLa*(y(:,10)
-y(:,31)-K_H_co2*(y(:,35)*R*T_op))    ) ,'Linewidth',2,
'color','b','LineStyle','-');
xlim([minx maxx])
title('Volumetric production of Biogas','FontSize',10,
'Fontname','cmr10');
xlabel(['Time ~ ',num2str(tspan(1,2),'%5.4g'),' (days)'],...
    'FontSize',10,'Fontname','cmr10'), ylabel('m^3 biogas m^-^3 d^-
^1','Rotation',90,'FontSize',10,'Fontname','cmr10'),
set(gca,'fontsize',10,'Fontname','cmr10');

subplot(3,1,3);
plot(t,  (  T_op/273.15)*0.35*(    kLa*(y(:,9)-
64*K_H_ch4*(y(:,34)*R*T_op/64))    ) ./
(    (T_op/273.15)*1.4*( kLa*(y(:,8)-
16*K_H_h2*(y(:,33)*R*T_op/16))    )+(T_op/273.15)*0.35*( kLa*(y(:,9)-
64*K_H_ch4*(y(:,34)*R*T_op/64))    )+(T_op/273.15)*22.4*( kLa*(y(:,10)-
y(:,31)-K_H_co2*(y(:,35)*R*T_op))    )    )    ,'Linewidth',2,
'color','g','LineStyle','-');
hold on
plot(t,  (T_op/273.15)*22.4*(    kLa*(y(:,10)-y(:,31)-
K_H_co2*(y(:,35)*R*T_op))    ) ./  (    (T_op/273.15)*1.4*( kLa*(y(:,8)-
16*K_H_h2*(y(:,33)*R*T_op/16))    )+(T_op/273.15)*0.35*( kLa*(y(:,9)-
64*K_H_ch4*(y(:,34)*R*T_op/64))    )+(T_op/273.15)*22.4*( kLa*(y(:,10)-
y(:,31)-K_H_co2*(y(:,35)*R*T_op))    )    )    ,'Linewidth',2,
'color','b','LineStyle','-');
xlim([minx maxx])
title('% of CH_4 and CO_2 in biogas','FontSize',10, 'Fontname','cmr10');
xlabel(['Time ~ ',num2str(tspan(1,2),'%5.4g'),' (days)'],...
    'FontSize',10,'Fontname','cmr10'), ylabel('% in
Biogas)','Rotation',90,'FontSize',10,'Fontname','cmr10'),
hold off
set(gca,'fontsize',10,'Fontname','cmr10');
legend('CH_4','CO_2')



figure(2)
set(gcf, 'color', [1 1 1])
subplot(3,2,1);
```

```
plot(t,af*(1000*y(:,4)),'Linewidth',2, 'color','r','LineStyle','-');
title('Valeric and Butyric Acids','FontSize',10, 'Fontname','cmr10');
xlabel([ 'Time =  ',num2str(maxx,'%5.4g'),' (days)'],...
    'FontSize',10,'Fontname','cmr10'), ylabel('Valeric & Butyric mg L^-
^1','Rotation',90,'FontSize',10,'Fontname','cmr10'),
xlim([minx maxx])

hold on
plot(t,af*(1000*y(:,5)),'Linewidth',2, 'color','c','LineStyle','-.');
xlim([minx maxx])
hold off
legend('Valeric','Butyric')
set(gca,'fontsize',10,'Fontname','cmr10');

subplot(3,2,2);
plot(t,af*(1000*y(:,6)),'Linewidth',2, 'color','b','LineStyle','-');
title('Propionic Acid','FontSize',10, 'Fontname','cmr10');
xlabel([ 'Time =  ',num2str(maxx,'%5.4g'),' (days)'],...
    'FontSize',10,'Fontname','cmr10'), ylabel('Propionic mg L^-
^1','Rotation',90,'FontSize',10,'Fontname','cmr10'),
xlim([minx maxx])
set(gca,'fontsize',10,'Fontname','cmr10');

subplot(3,2,3);
plot(t,af*(1000*y(:,7)),'Linewidth',2, 'color','m','LineStyle','-');
title('Acetic Acid','FontSize',10, 'Fontname','cmr10');
xlabel([ 'Time =  ',num2str(maxx,'%5.4g'),' (days)'],...
    'FontSize',10,'Fontname','cmr10'), ylabel('Acetic mg L^-
^1','Rotation',90,'FontSize',10,'Fontname','cmr10'),
xlim([minx maxx])
set(gca,'fontsize',10,'Fontname','cmr10');



subplot(3,2,4);
% convert kg COD/ m3 to mg /L
plot(t,af*(1000*(y(:,4)+y(:,5)+y(:,6)+y(:,7))),'Linewidth',2,
'color','k','LineStyle','-');
title('Total Volatile Fatty Acid','FontSize',10, 'Fontname','cmr10');
xlabel([ 'Time =  ',num2str(maxx,'%5.4g'),' (days)'],...
    'FontSize',10,'Fontname','cmr10'), ylabel('Total VFAs (mg L^-
^1)','Rotation',90,'FontSize',10,'Fontname','cmr10'),
xlim([minx maxx])
set(gca,'fontsize',10,'Fontname','cmr10');
```

Appendix E: Packages on accompanying CD

Three packages referred to this thesis are put in the accompanying CD as below.

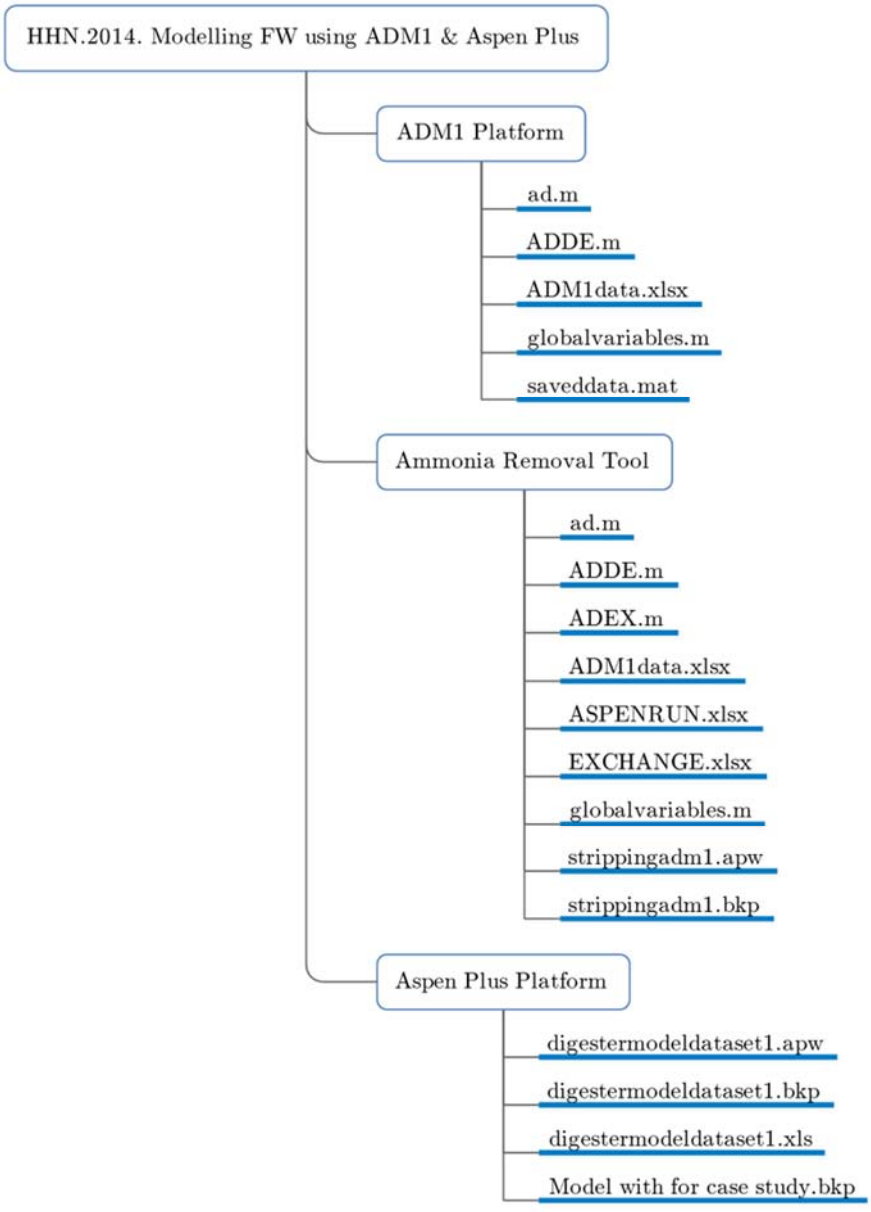

This page is intentionally left blank

Index

A

B

C

D

E

F

G

H

I

K

L

M

N

O

P

R

S

T

U

V

W